



**NAVAL
POSTGRADUATE
SCHOOL**

MONTEREY, CALIFORNIA

DISSERTATION

**RESILIENCE ASSESSMENT OF ISLANDED
RENEWABLE ENERGY MICROGRIDS**

by

William W. Anderson, Jr.

December 2020

Dissertation Supervisor:

Ronald E. Giachetti

Approved for public release. Distribution is unlimited.

THIS PAGE INTENTIONALLY LEFT BLANK

REPORT DOCUMENTATION PAGE			<i>Form Approved OMB No. 0704-0188</i>
Public reporting burden for this collection of information is estimated to average 1 hour per response, including the time for reviewing instruction, searching existing data sources, gathering and maintaining the data needed, and completing and reviewing the collection of information. Send comments regarding this burden estimate or any other aspect of this collection of information, including suggestions for reducing this burden, to Washington headquarters Services, Directorate for Information Operations and Reports, 1215 Jefferson Davis Highway, Suite 1204, Arlington, VA 22202-4302, and to the Office of Management and Budget, Paperwork Reduction Project (0704-0188) Washington, DC 20503.			
1. AGENCY USE ONLY (Leave blank)	2. REPORT DATE December 2020	3. REPORT TYPE AND DATES COVERED Dissertation	
4. TITLE AND SUBTITLE RESILIENCE ASSESSMENT OF ISLANDED RENEWABLE ENERGY MICROGRIDS		5. FUNDING NUMBERS	
6. AUTHOR(S) William W. Anderson, Jr.			
7. PERFORMING ORGANIZATION NAME(S) AND ADDRESS(ES) Naval Postgraduate School Monterey, CA 93943-5000		8. PERFORMING ORGANIZATION REPORT NUMBER	
9. SPONSORING / MONITORING AGENCY NAME(S) AND ADDRESS(ES) N/A		10. SPONSORING / MONITORING AGENCY REPORT NUMBER	
11. SUPPLEMENTARY NOTES The views expressed in this thesis are those of the author and do not reflect the official policy or position of the Department of Defense or the U.S. Government.			
12a. DISTRIBUTION / AVAILABILITY STATEMENT Approved for public release. Distribution is unlimited.		12b. DISTRIBUTION CODE A	
13. ABSTRACT (maximum 200 words) The military's installations on remote islands have the highest power costs and demand resilient and reliable power for mission assurance. These installations have no electrical connection to an external utility provider and encounter numerous challenges in incorporating renewable energy, and there is a pronounced gap in both defining resilience and measuring it for off-grid islanded microgrids at islanded naval installations (INIs). This work's research objective was to develop a methodology to choose renewable energy microgrid designs that maximize resilience and minimize costs on remote islands with applications for INIs. The deliverable is a tool that incorporates the methodology to identify the cost of resilience using a measure that captures the area under the resilience curve. The tool uses the models developed in this research to create the resilience and cost trade-off curves for different microgrid design and maintenance options to enable decision makers to choose an optimal microgrid design primarily for remote islanded military installations like San Nicolas Island. The research concluded that resilience can be improved by using optimal power capacity ratios for a renewable energy microgrids, that redundancy improves resilience for less costs, and that more maintenance only improves resilience when the generation capacity is closer to the demand and for microgrids with less redundancy.			
14. SUBJECT TERMS resilience, renewable energy, microgrid, island, islanded, costs, naval installation, trade-off, off-grid, redundancy, trade space, measures, islanded naval installation		15. NUMBER OF PAGES 297	
		16. PRICE CODE	
17. SECURITY CLASSIFICATION OF REPORT Unclassified	18. SECURITY CLASSIFICATION OF THIS PAGE Unclassified	19. SECURITY CLASSIFICATION OF ABSTRACT Unclassified	20. LIMITATION OF ABSTRACT UU

THIS PAGE INTENTIONALLY LEFT BLANK

Approved for public release. Distribution is unlimited.

**RESILIENCE ASSESSMENT OF ISLANDED RENEWABLE ENERGY
MICROGRIDS**

William W. Anderson, Jr.
Civilian, Department of the Navy
BS, Virginia Military Institute, 1986
MS, University of California, Berkeley, 1993
EMBA, Claremont Graduate University, 2002
MS, University of Southern California, 2015

Submitted in partial fulfillment of the
requirements for the degree of

DOCTOR OF PHILOSOPHY IN SYSTEMS ENGINEERING

from the

**NAVAL POSTGRADUATE SCHOOL
December 2020**

Approved by:	Ronald E. Giachetti Department of Systems Engineering Dissertation Supervisor and Chair	Giovanna Oriti Department of Electrical and Computer Engineering
	Fotis A. Papoulias Department of Systems Engineering	Douglas L. Van Bossuyt Department of Systems Engineering
	Richard Carlin, Office of Naval Research	

Approved by:	Ronald E. Giachetti Chair, Department of Systems Engineering
	Orrin D. Moses Vice Provost of Academic Affairs

THIS PAGE INTENTIONALLY LEFT BLANK

ABSTRACT

The military's installations on remote islands have the highest power costs and demand resilient and reliable power for mission assurance. These installations have no electrical connection to an external utility provider and encounter numerous challenges in incorporating renewable energy, and there is a pronounced gap in both defining resilience and measuring it for off-grid islanded microgrids at islanded naval installations (INIs). This work's research objective was to develop a methodology to choose renewable energy microgrid designs that maximize resilience and minimize costs on remote islands with applications for INIs. The deliverable is a tool that incorporates the methodology to identify the cost of resilience using a measure that captures the area under the resilience curve. The tool uses the models developed in this research to create the resilience and cost trade-off curves for different microgrid design and maintenance options to enable decision makers to choose an optimal microgrid design primarily for remote islanded military installations like San Nicolas Island. The research concluded that resilience can be improved by using optimal power capacity ratios for a renewable energy microgrids, that redundancy improves resilience for less costs, and that more maintenance only improves resilience when the generation capacity is closer to the demand and for microgrids with less redundancy.

THIS PAGE INTENTIONALLY LEFT BLANK

TABLE OF CONTENTS

I.	INTRODUCTION.....	1
A.	MOTIVATION	1
	1. Proposed INI RE Microgrid Definition	4
	2. What Does It Mean to Be Islanded?.....	6
	3. Disturbances for INI Microgrids.....	9
B.	PROBLEM STATEMENT	10
C.	RESEARCH OBJECTIVE	12
D.	CONTRIBUTIONS.....	12
E.	INTENDED USERS OF THIS METHOD	13
	1. Relevance to Island Communities	14
F.	ORGANIZATION OF DISSERTATION	15
II.	LITERATURE REVIEW	17
A.	RESILIENCE.....	17
	1. Resilience States and Dimensions	20
	2. Resilience Definitions.....	24
B.	MEASURING RESILIENCE	28
	1. Inventory of Measures.....	29
	2. Nonquantitative Measures	38
C.	ASSESSING RESILIENCE.....	40
	1. Energy Resilience Assessment (ERA) Tools	41
	2. Energy Security Assessment Tool (ESAT)	43
	3. Incorporating Costs	48
	4. Other Tools to Assess Resilience.....	48
D.	MODELING RESILIENCE	49
	1. Optimized Off-Grid RE.....	50
	2. Optimization Models	50
	3. Simulation Models	52
	4. Fuzzy Logic Models	53
E.	MEASURING COSTS.....	53
F.	DISCUSSION AND CONCLUSION	54
III.	INI RE MICROGRID RESILIENCE AND COST METHOD.....	61
A.	METHOD	61
	1. Gather Data	61
	2. Select Disturbance Scenario.....	62
	3. Establish Resilience and Cost Baseline	62

4.	Simulate Microgrid System.....	64
5.	Select Design	65
B.	COST MODEL.....	67
1.	Nomenclature	67
2.	Problem Formulation	69
C.	RESILIENCE MODEL.....	74
1.	Nomenclature	74
2.	Model Outline and Problem Formulation	77
D.	DISCUSSION AND CONCLUSION	94
IV.	EXPERIMENTS	97
A.	PARAMETERS.....	97
B.	SENSITIVITY ANALYSIS	101
1.	Sensitivity of Resilience Measures to Resilience Input Variables.....	103
2.	Sensitivity of Resilience Measures to Time to Repair λ	105
3.	Sensitivity of Resilience Measures to Battery Discharge Efficiency.	106
4.	Sensitivity of Resilience Measures to WT's Capacity and Availability Factors.....	107
5.	Sensitivity of Time to Recover to Time of Disturbance.....	109
6.	Sensitivity of <i>LCOED</i> Cost Measure to Cost Input Variables	110
C.	VALIDATION.....	111
1.	Framework	111
2.	Assumptions	112
3.	Reproducibility.....	112
D.	EXCESS POWER GENERATION RATING.....	118
1.	Ratio of Microgrid Nominal Power Generation Rating to Demand, and Maintenance Level with Constant DER Nominal Power Rating Impacts on Resilience and Costs.....	119
2.	Ratio of Microgrid Nominal Power Generation Rating to Demand, and Maintenance Level with Constant Number of DER Impact on Resilience and Costs	124
3.	Ratio of RE Nominal Power to DG Nominal Power with Constant DER Nominal Power Rating Impact on Resilience and Costs.....	129
4.	Ratio of RE Nominal Power to DG Nominal Power with Constant Microgrid Nominal Power Generation Rating Impact on Resilience and Costs	132

5.	Ratio of WT Nominal Power to DG Nominal Power with Constant Microgrid Nominal Power Generation Rating Impact on Resilience and Costs	135
6.	Ratio of BAT Nominal Power Rating to Microgrid Nominal Power Rating with Constant Microgrid Nominal Power Generation Rating Impact on Resilience and Costs ...	138
E.	ALTERING REDUNDANCY LEVELS.....	142
1.	Redundancy and Maintenance Levels Impact on Resilience and Costs.....	144
2.	Functional Redundancy and Maintenance Levels Impact on Resilience and Costs	147
3.	RE Redundancy and Maintenance Levels Impact on Resilience and Costs.....	151
F.	VALUE OF INVESTING FOR <i>INVULNERABILITY VS. RECOVERY</i>	153
G.	FUEL COSTS IMPACT ON DG-PARITY FOR PV	157
H.	COMPARISON OF REDUNDANCY ARCHITECTURES.....	159
I.	DISCUSSION AND CONCLUSION	160
V.	DEMONSTRATION	163
A.	ROTA'S ENERGY SYSTEM.....	163
1.	Parameters.....	164
2.	Base Case Impact of Redundancy, and Maintenance on Resilience and Costs.....	167
3.	Optimized Microgrid's Impact of Redundancy, and Maintenance on Resilience and Costs for a Morning Tsunami	170
4.	Optimized Microgrid's Impact of Redundancy, and Maintenance on Resilience and Costs for a Midnight Tsunami	178
5.	Design Options	179
B.	SCI, SNI, AND GTMO MICROGRIDS.....	179
1.	Comparison of Resilience and Costs	184
C.	COMPARATIVE ANALYSIS OF MODELS.....	190
D.	DISCUSSION AND CONCLUSION	191
VI.	CONCLUSION	192
A.	FINDINGS.....	193
B.	RECOMMENDATIONS.....	195
1.	Designing a Microgrid	195
2.	Maintaining a Microgrid.....	196

3.	Limitations.....	196
4.	Future Work.....	197
APPENDIX A. RESILIENCE MEASURES VS. COSTS FIGURES		201
A.	EXCESS POWER GENERATION RATING.....	201
1.	Ratio of Microgrid Nominal Power Generation Rating to Demand, and Maintenance Level with Constant DER Nominal Power Rating Impact on Resilience and Costs	201
2.	Ratio of Microgrid Nominal Power Generation Rating to Demand with Constant Number of DER, and Maintenance Level Impact on Resilience and Costs.....	203
3.	Ratio of Nominal RE Power to Nominal DG Power and Maintenance Level with Constant DER Nominal Power Rating Impact on Resilience and Costs.....	205
4.	Ratio of Nominal RE Power to Nominal DG Power and Maintenance Level with Constant Microgrid Nominal Power Generation Impact on Resilience and Costs	207
5.	Ratio of WT Power to DG Power, and Maintenance Level with Constant Microgrid Power Generation Rating Impact on Resilience and Costs	209
6.	Ratio of BAT Power Rating to Microgrid Power Rating, and Maintenance Level Impact on Resilience and Costs	211
B.	ALTERING REDUNDANCY LEVELS.....	212
1.	Redundancy and Maintenance Levels Impact on Resilience and Costs.....	213
2.	Functional Redundancy and Maintenance Levels Impact on Resilience and Costs	215
3.	RE Redundancy and Maintenance Levels Impact on Resilience and Costs.....	218
C.	ALTERING REDUNDANCY LEVELS AT ROTA.....	220
1.	Base Case Impact of Redundancy, and Maintenance on Resilience and Costs.....	221
2.	Optimized Microgrid’s Impact of Redundancy, and Maintenance on Resilience and Costs for a Morning Tsunami	224
3.	Optimized Microgrid’s Impact of Redundancy, and Maintenance on Resilience and Costs for a Midnight Tsunami	226
APPENDIX B. MICROSOFT EXCEL TOOL DEVELOPED FOR MODELS.....		229
A.	RESILIENCE MODEL.....	229
1.	Input Variables.....	229

2.	Variables	230
3.	Decision Variables.....	230
B.	COST MODEL.....	231
C.	MACRO.....	231
APPENDIX C. CONFIDENCE INTERVAL CALCULATIONS.....		233
LIST OF REFERENCES.....		235
INITIAL DISTRIBUTION LIST		257

THIS PAGE INTENTIONALLY LEFT BLANK

LIST OF FIGURES

Figure 1.	Remote islanded naval installations.....	5
Figure 2.	Microgrid core components. Source: Walsh (2014).....	8
Figure 3.	Microgrid overview diagram. Source: Peterson (2019).....	9
Figure 4.	Bruneau’s 2003 <i>resilience</i> triangle. Source: D’Lima and Medda (2015).....	17
Figure 5.	Microgrid <i>resilience</i> function’s states and <i>resilience</i> measures.	19
Figure 6.	Five specific dimensions of <i>resilience</i> . Source: Yodo and Wang (2016).....	32
Figure 7.	OSD’s Energy <i>Resilience</i> Assessment Tool emphasizing reliability. Adapted from Judson, Pina, and Whitehead (2018); Baxter (2018).....	42
Figure 8.	ESAT <i>resilience</i> score for SNI suggests SNI has poor <i>resilience</i> . Adapted from Department of the Navy (2017a).....	46
Figure 9.	Energy Security Assessment Reporting tool highlights emphasis on backup generation. Source: Department of the Navy (2017a).....	47
Figure 10.	Steps to establish <i>resilience</i> and cost baseline.....	63
Figure 11.	Steps to simulate the microgrid system	65
Figure 12.	Microgrid method process to explore <i>resilience</i> and costs trade space to choose microgrid architecture design.	66
Figure 13.	Data flow: Inputs and outputs for both models.....	67
Figure 14.	Microgrid <i>resilience</i> function relates performance and time to <i>resilience</i> measures.	79
Figure 15.	Daily demand profile portraying typical increase and decrease in consumption throughout the day.....	102
Figure 16.	The sensitivity of time to recover to varying the WTs’ probability of damage 50% and maintenance level.	103
Figure 17.	The sensitivity of <i>recovery</i> to <i>resilience</i> input variables.	104
Figure 18.	The sensitivity of <i>invulnerability</i> to <i>resilience</i> input variables.....	104

Figure 19.	The sensitivity of time to recover to <i>resilience</i> input variables.	104
Figure 20.	The sensitivity of time to recover to each DER's time to repair λ input variables.	105
Figure 21.	The sensitivity of <i>invulnerability</i> to λ for no maintenance.	106
Figure 22.	The sensitivity of <i>invulnerability</i> to λ for reduced maintenance.	106
Figure 23.	The sensitivity of time to recover to battery discharge efficiency.	107
Figure 24.	The sensitivity of <i>recovery</i> to C^{WT}	108
Figure 25.	The sensitivity of <i>recovery</i> to A^{WT}	108
Figure 26.	The sensitivity of time to recover to the time of disturbance.	109
Figure 27.	The sensitivity of time to recover to the time of disturbance and ratio of P^{WT}/P and P^{PV}/P	110
Figure 28.	The sensitivity of <i>LCOED</i> to cost input variables.	110
Figure 29.	Microgrid architecture with three of each DER at 350 kW and 3.15 MW overall power generation rating.	121
Figure 30.	The effects of maintenance level on <i>LCOED</i> and time to recover.	122
Figure 31.	Linear increase in costs and nonlinear increase in <i>resilience</i> as power rating ratio increases.	123
Figure 32.	The sensitivity of time to recover to each microgrid ratio of power rating to demand and redundancy level.	125
Figure 33.	Power generation rating to demand ratio as viewed from a power rating perspective.	126
Figure 34.	The effects of microgrid power rating to demand ratio on <i>LCOED</i> and time to recover.	127
Figure 35.	Exponential increase in <i>resilience</i> as costs linearly increase.	128
Figure 36.	Exponential increase in <i>recovery</i> and <i>invulnerability</i> as the power rating ratio increases.	128
Figure 37.	Microgrid architecture with RE/DG = 2 employing three of each DER at 1,500 kW and 13.5MW overall power generation rating.	130

Figure 38.	The effects of RE proportion to DG on <i>LCOED</i> and time to recover. RE/DG = 4 is at bottom because it has the least power rating.....	131
Figure 39.	Microgrid architecture with RE/DG = 2 employing three of each DER at 778 kW and 7 MW overall nominal power generation rating. ...	133
Figure 40.	The effects of RE proportion on <i>LCOED</i> and time to recover.	134
Figure 41.	<i>Resilience</i> and costs decrease as RE to DG power rating ratio increases.....	135
Figure 42.	The effects of maintenance level and WT proportion on <i>LCOED</i> and time to recover.	137
Figure 43.	<i>Resilience</i> and <i>LCOED</i> decrease as WT to DG power rating ratio increases.....	138
Figure 44.	The effects of storage on <i>LCOED</i> and time to recover.....	140
Figure 45.	Costs and <i>resilience</i> increase as power rating ratio increases.....	141
Figure 46.	<i>Recovery</i> increases but <i>invulnerability</i> stays constant.	141
Figure 47.	Wind turbines provide least costs for similar <i>resilience</i> ; darker datapoints are with no maintenance, brighter are medium maintenance.	143
Figure 48.	Microgrid architecture with no redundancy employing one of each DER at 2,000 kW and 6 MW overall power generation rating.	145
Figure 49.	The effects of redundancy levels on <i>LCOED</i> and time to recover.	146
Figure 50.	<i>Resilience</i> and <i>LCOED</i> vs. redundancy.....	147
Figure 51.	<i>Resilience</i> and <i>LCOED</i> vs. functional redundancy.....	149
Figure 52.	<i>Recovery</i> and <i>invulnerability</i> vs. functional redundancy.....	149
Figure 53.	The effects of functional redundancy on <i>LCOED</i> and time to recover.....	150
Figure 54.	The effects of RE redundancy on <i>LCOED</i> and time to recover.	152
Figure 55.	<i>Resilience</i> and <i>LCOED</i> vs. RE redundancy.....	153
Figure 56.	The effects of investing in power rating or maintenance on <i>LCOED</i> and <i>recovery</i>	155

Figure 57.	The effects of investing in power rating or maintenance on <i>LCOED</i> and <i>invulnerability</i>	156
Figure 58.	The effects of investing in power rating or maintenance on <i>LCOED</i> and <i>resilience</i>	156
Figure 59.	The effects of investing in power rating or maintenance on <i>LCOED</i> and time to recover.....	157
Figure 60.	The effects of fuel costs on DG-parity for PV.....	158
Figure 61.	Microgrid architecture with one 1,250 kW DG.....	168
Figure 62.	Redundancy’s impact on time to recover and <i>LCOED</i> for base case.	169
Figure 63.	Microgrid architecture with no redundancy employing 516 kW overall microgrid power generation rating.	171
Figure 64.	Demand, power rating and delivered power.	172
Figure 65.	Battery energy level.	173
Figure 66.	Diesel genset fuel consumption.	174
Figure 67.	The effects of redundancy on <i>LCOED</i> and time to recover.....	175
Figure 68.	Optimized and base case microgrid’s resilience, and costs as a function of redundancy during a morning tsunami.....	176
Figure 69.	Optimized and base case microgrids’ <i>resilience</i> , and costs as a function of redundancy.	177
Figure 70.	Optimized and base case microgrids’ <i>recovery</i> , and <i>invulnerability</i> as a function of redundancy.	177
Figure 71.	The effects of redundancy and maintenance level on <i>LCOED</i> and time to recover.	178
Figure 72.	SCI’s RE microgrid.....	180
Figure 73.	SNI’s adapted RE microgrid.....	180
Figure 74.	GTMO’s adapted RE microgrid.....	181
Figure 75.	GTMO, SNI, and SCI demand profiles.	181
Figure 76.	<i>LCOED</i> vs. <i>recovery</i> for SNI, SCI, and GTMO.....	182

Figure 77.	<i>LCOED vs. invulnerability</i> for SNI, SCI, and GTMO.	183
Figure 78.	<i>LCOED vs. resilience</i> for SNI, SCI, and GTMO.	183
Figure 79.	<i>LCOED vs. time to recover</i> for SNI, SCI, and GTMO.....	184
Figure 80.	<i>LCOED vs. # of WTs and DGs</i> for SCI, SNI, and GTMO.....	185
Figure 81.	<i>LCOED vs. # of WTs and DGs</i> for GTMO.	186
Figure 82.	<i>LCOED vs. # of WTs and DGs</i> for SNI.....	187
Figure 83.	<i>LCOED vs. # of WTs and DGs</i> for SCI.....	187
Figure 84.	<i>Resilience vs. # of WTs and DGs</i> for SCI, SNI, and GTMO.	188
Figure 85.	<i>Resilience vs. # of WTs and DGs</i> for GTMO.....	189
Figure 86.	<i>Resilience vs. # of WTs and DGs</i> for SNI.	189
Figure 87.	<i>Resilience vs. # of WTs and DGs</i> for SCI.	190
Figure 88.	The effects of maintenance level on <i>LCOED</i> and <i>recovery</i>	201
Figure 89.	The effects of maintenance level on <i>LCOED</i> and <i>invulnerability</i>	202
Figure 90.	The effects of maintenance level on <i>LCOED</i> and <i>resilience</i>	202
Figure 91.	The effects of microgrid power rating to demand ratio on <i>LCOED</i> and <i>recovery</i>	203
Figure 92.	The effects of microgrid power rating to demand ratio on <i>LCOED</i> and <i>invulnerability</i>	204
Figure 93.	The effects of microgrid power rating to demand ratio on <i>LCOED</i> and <i>resilience</i>	204
Figure 94.	The effects of maintenance level and RE proportion on <i>LCOED</i> and <i>recovery</i>	205
Figure 95.	The effects of maintenance level and RE proportion on <i>LCOED</i> and <i>invulnerability</i>	206
Figure 96.	The effects of maintenance level and RE proportion on <i>LCOED</i> and <i>resilience</i>	206
Figure 97.	The effects of maintenance level and RE proportion on <i>LCOED</i> and <i>recovery</i>	207

Figure 98.	The effects of maintenance level and RE proportion on <i>LCOED</i> and <i>invulnerability</i> .	208
Figure 99.	The effects of maintenance level and RE proportion on <i>LCOED</i> and <i>resilience</i> .	208
Figure 100.	The effects of maintenance level and WT proportion on <i>LCOED</i> and <i>recovery</i> .	209
Figure 101.	The effects of maintenance level and WT proportion on <i>LCOED</i> and <i>invulnerability</i> .	210
Figure 102.	The effects of maintenance level and WT proportion on <i>LCOED</i> and <i>resilience</i> .	210
Figure 103.	The effects of storage on <i>LCOED</i> and <i>recovery</i> .	211
Figure 104.	The effects of storage on <i>LCOED</i> and <i>invulnerability</i> .	211
Figure 105.	The effects of storage on <i>LCOED</i> and <i>resilience</i> .	212
Figure 106.	The effects of maintenance level and redundancy on <i>LCOED</i> and <i>recovery</i> .	213
Figure 107.	The effects of maintenance level and redundancy on <i>LCOED</i> and <i>invulnerability</i> .	214
Figure 108.	The effects of maintenance level and redundancy on <i>LCOED</i> and <i>resilience</i> .	214
Figure 109.	The effects of functional redundancy on <i>LCOED</i> and <i>recovery</i> .	215
Figure 110.	The effects of functional redundancy on <i>LCOED</i> and <i>invulnerability</i> .	216
Figure 111.	The effects of functional redundancy on <i>LCOED</i> and <i>resilience</i> .	217
Figure 112.	The effects of PV and WT redundancy on <i>LCOED</i> and <i>recovery</i> .	218
Figure 113.	The effects of PV and WT redundancy on <i>LCOED</i> and <i>invulnerability</i> .	219
Figure 114.	The effects of PV and WT redundancy on <i>LCOED</i> and <i>resilience</i> .	220
Figure 115.	The effects of redundancy level on <i>LCOED</i> and <i>recovery</i> .	221
Figure 116.	The effects of redundancy level on <i>LCOED</i> and <i>invulnerability</i> .	222
Figure 117.	The effects of redundancy level on <i>LCOED</i> and <i>resilience</i> .	223

Figure 118.	The effects of redundancy level on <i>LCOED</i> and <i>recovery</i>	224
Figure 119.	The effects of redundancy level on <i>LCOED</i> and <i>invulnerability</i>	224
Figure 120.	The effects of redundancy level on <i>LCOED</i> and <i>resilience</i>	225
Figure 121.	The effects of redundancy and maintenance level on <i>LCOED</i> and <i>recovery</i>	226
Figure 122.	The effects of redundancy and maintenance level on <i>LCOED</i> and <i>invulnerability</i>	227
Figure 123.	The effects of redundancy and maintenance level on <i>LCOED</i> and <i>resilience</i>	227
Figure 124.	<i>Resilience</i> model variables. Measures are in red.	229
Figure 125.	Cost model variables. Measures are in red.	231

THIS PAGE INTENTIONALLY LEFT BLANK

LIST OF TABLES

Table 1.	INIs’ extreme energy costs. Adapted from Department of the Navy (2018); Kandt (2008).	2
Table 2.	Categories and relevant attributes of resiliency and cost measures per risk. Adapted from Teague et al. (2015).	28
Table 3.	Five specific dimensions of resilience and their measures. Adapted from Yodo and Wang (2016).	33
Table 4.	Differences in measures for resilience, resiliency, reliability, and robustness.	39
Table 5.	Tools to assess microgrid resilience.	48
Table 6.	Differences in cost measures for various microgrid architectures having a total power generation rating of 7 MW.	74
Table 7.	Relationships between time step and time of day for critical infrastructure demand at time t	74
Table 8.	Probability of damage given disturbance S_k occurs for scenario k	98
Table 9.	Mean values of time to repair for each DER. Input variable values are designated with yellow cells.	99
Table 10.	Resilience model input parameters used in simulations.	100
Table 11.	Cost model parameters used in simulations. All values are input parameters.	101
Table 12.	Microgrid architecture validated for $LCOE$	113
Table 13.	Contribution factors for microgrid architecture with decreased DG power.	114
Table 14.	DER’s $LCOE$ after increasing share of PV.	114
Table 15.	Microgrid $LCOE$ after increasing each DER’s $LCOE$ by 10%.	115
Table 16.	Parameters for Faraji et al.’s (2019) DG, and PV microgrids.	116
Table 17.	Simulation results for Faraji et al.’s (2019) DG, and PV microgrid.	118
Table 18.	Microgrid architectures with same power rating for each DER.	120

Table 19.	Microgrid architectures for different ratios of $\frac{P^{WT} + P^{PV} + P^{DG}}{D_t}$.	125
Table 20.	Microgrid architectures for proportion of DER with constant DER power rating.	129
Table 21.	Ratio of RE nominal power rating to DG nominal power rating.	133
Table 22.	Microgrid architectures for proportion of DER with constant microgrid power generation rating.	136
Table 23.	Microgrid architectures for storage relationships. $P^{WT} + P^{PV} + P^{DG} = 6$ MW in all instances.	139
Table 24.	Legend for Figure 47. Colors designate the microgrid architecture for each experiment.	143
Table 25.	Microgrid architectures for redundancy.	144
Table 26.	Microgrid architectures for functional redundancy. Architecture color corresponds to that shown in architectures illustrated in Figure 47.	148
Table 27.	Microgrid architectures for PV and WT combinations. Architecture color corresponds to the architecture illustrated in Figure 47.	151
Table 28.	Microgrid architectures for power rating or maintenance investments.	154
Table 29.	Best architectures compared for experiments, all quintuple and no maintenance, except IV.E.1 which is quadruple. Colors correspond to functions shown in Figure 47.	159
Table 30.	Probability of damage given disturbance S_k occurs for a cyberattack, and a tsunami.	164
Table 31.	Parameters used in simulations.	165
Table 32.	Air terminal demand at time t .	166
Table 33.	Microgrid architectures for impact of redundancy and maintenance.	167
Table 34.	Microgrid architectures for redundancy.	170
Table 35.	Design options for Rota compared; optimized architecture provides 30% higher resilience for only 30% of the base case's costs.	179

Table 36.	Demand profile for each time step.....	229
Table 37.	Power to charge each battery and fuel consumption parameters.....	230
Table 38.	Parameters for DER.....	230
Table 39.	Decision variables for optimization.....	230

THIS PAGE INTENTIONALLY LEFT BLANK

LIST OF ACRONYMS AND ABBREVIATIONS

2D	Two-dimensional
3D	Three-dimensional
4D	Four-dimensional
AEMR	Annual Energy Management Report
Amp	Ampere
ASME	American Society of Mechanical Engineers
AUTEC	Atlantic Undersea Test and Evaluation Center
B	Billion
BESS	Battery Energy Storage System
bg	Backup Generation
BIOT	British Indian Ocean Territory
Capex	Capital Expenses
CLDJ	Camp Lemonnier Djibouti
DER	Distributed Energy Resource
DESC	Defense Energy Supply Center
DG	Diesel Genset
DGAR	Diego Garcia
DHS	Department of Homeland Security
DNI	Direct Normal Irradiance
DOD	Department of Defense
DOE	Department of Energy
DON	Department of the Navy
DR	Dynamic Resilience
EMS	Energy Management Strategy
ERA	Energy Resilience Assessment
ERCIP	Energy Resilience and Conservation Investment Program
ESAT	Energy Security Assessment Tool
EXWC	Engineering and Expeditionary Warfare Center
FERC	Federal Energy Regulatory Commission
FOM	Figure-of-Merit
GTMO	Guantanamo Bay, Cuba
GUI	Graphical User Interface
HEMS	Home Energy Management System

HESS	High Energy Storage System
HILP	High Impact Low Probability
HOMER	Hybrid Optimization of Multiple Energy Resources
HP	Hydropower
IESM	Integrated Energy Systems Model
IHOGA	Improved Hybrid Optimization by Genetic Algorithms
INCOSE	International Council on Systems Engineering
INI	Islanded Naval Installation
IRENA	International Renewable Energy Agency
IST	Infrastructure Survey Tool
JP-5	Jet Propulsion-5
kW	Kilowatt
kWh	Kilowatt-hour
<i>LCCA</i>	Life Cycle Cost Analysis
<i>LCOE</i>	Life cycle Cost of Energy
<i>LCOED</i>	Life cycle Cost of Energy for Demand
LIHP	Low Impact High Probability
LT	London Tube
M	Million
m/s	Meters/Second
MPPT	Maximum-Power-Point-Trackers
MS	Microsoft
<i>MTTR</i>	Mean Time to Repair
MW	Megawatt
MWh	Megawatt-hour
NAVFAC	Naval Facilities Engineering Systems Command
NBVC	Naval Base Ventura County
NIAC	National Infrastructure Advisory Council
NPV	Net Present Value
NREL	National Renewable Energy Laboratory
NSRDB	National Solar Radiation Database
O&M	Operating and Maintenance
OECD	Organization for Economic Co-Operation and Development
Opex	Operating Expenses
PPA	Power Purchase Agreement

PV	Photovoltaic
RAP	Resilience Analysis Process
RE	Renewable Energy
RL	Resilience Loss
RMI	Rocky Mountain Institute
SAIDI	System Average Interruption Duration Index
SAIFI	System Average Interruption Frequency Index
SCI	San Clemente Island
SE	Systems Engineering
SIDS	Small Island Developing States
SLA	Service Level Agreement
SLC	Secondary Load Control
SNI	San Nicolas Island
SODAR	Sonic Detection and Ranging
SWOT	Strengths, Weaknesses, Opportunities, Threats
TJ	Terajoule
U.S.	United States
UFC	Unified Facility Criteria
UK	United Kingdom
UKERC	United Kingdom's Energy Research Center
UMC	Universal Microgrid Controller
UN-ISDR	United Nations-International Strategy for Disaster Reduction
UPS	Uninterruptable Power System
V	Volt
<i>VoLL</i>	Value of Lost Load
WACC	Weighted Average Cost of Capital
WT	Wind Turbine

THIS PAGE INTENTIONALLY LEFT BLANK

EXECUTIVE SUMMARY

Islanded naval installations (INI) are powered by microgrids, and the resilience of these microgrids is crucial to their operational mission. Currently, INIs pay between \$0.21 and \$0.54/kWh for their mostly diesel-based energy supply, (i.e., two to five times the Navy's average). Not only do INIs have the highest costs of power generation for naval installations, they also have the greatest requirements for resilience. However, no method exists to determine the cost-effectiveness of resilience at INIs, therefore the decision makers need a tool in order to assess renewable energy (RE) microgrid designs. In this research, resilience as defined for INIs is *the microgrid's invulnerability and rapid and full recoverability from an improbable and severe disturbance*. This research assesses resilience and costs of RE microgrid designs at INIs, with the objective of identifying how design and maintenance decisions that incorporate renewable energy influence the resilience and costs trade-space.

A. KEY FINDINGS

This research's contributions facilitate microgrid design investments that increase resilience, and cost effectively. A recurring finding is that greater power capacity and redundancy increase resilience. This research's primary contribution addresses the gaps in the literature by developing cost and resilience measures for RE microgrids at INIs. The second contribution is a decision-making tool for the islanded locations to assess resilience of RE microgrids to disturbances, using the resilience and cost measures. The third contribution to systems engineering design is the application of this tool to create the resilience and costs trade space to visualize and choose a RE microgrid design through the system architecture design phase. This third contribution enables smarter investment decisions in power capacity, redundancy, and energy storage, as well as identifies the fuel cost for diesel gensets (DG) to be cost competitive with solar photovoltaic panels (PV) for a microgrid architecture.

General takeaways on the tradeoffs in resilience and costs confirm that microgrids should be designed with redundancy, DG generation should be diversified with RE, and

the microgrid's power rating more than four times the average demand does not improve resilience any further. Finally fuel costs have to drop below \$1.00/gal for PV to be more cost competitive than DG.

B. METHOD AND CONCLUSIONS

This work first assesses the RE microgrids, incorporating wind turbines, solar photovoltaic panels, diesel gensets and batteries. These microgrids are evaluated for their *invulnerability* and *recovery* to hurricanes, tsunamis, and cyberattacks via a method for assessing resilience at INIs. The assessment uses a decision-making tool developed using the method, to generate the resilience and cost measures. The resilience and cost measures are then used to graph resilience and cost trade-off functions. These measures include a cost measure, *LCOED*, and the resilience measures *invulnerability*, *recovery*, and *resilience*. Through design exploration using these trade-off functions, findings are made to improve how a base commander can understand how RE microgrid design and maintenance decisions affect resilience and costs.

A method is developed to create a model to conduct a resilience assessment for a RE microgrid subjected to a High-Impact-Low-Probability (HILP) disturbance. This method uses demand profile data and distributed energy resources (DER) design parameters to calculate the resilience and cost measures simulated by the model for different microgrid design and maintenance levels. These measures are then used to generate the resilience and costs design trade-space.

Specifically, the microgrid's performance behavior is portrayed in Figure 1. The behavior of a microgrid subjected to a HILP disturbance is broken down into five distinct states: pre-disturbance, degradation, stabilization, recovery, and post-disturbance. The three states: degradation, stabilization, and recovery, are represented by *invulnerability* and *recovery*.

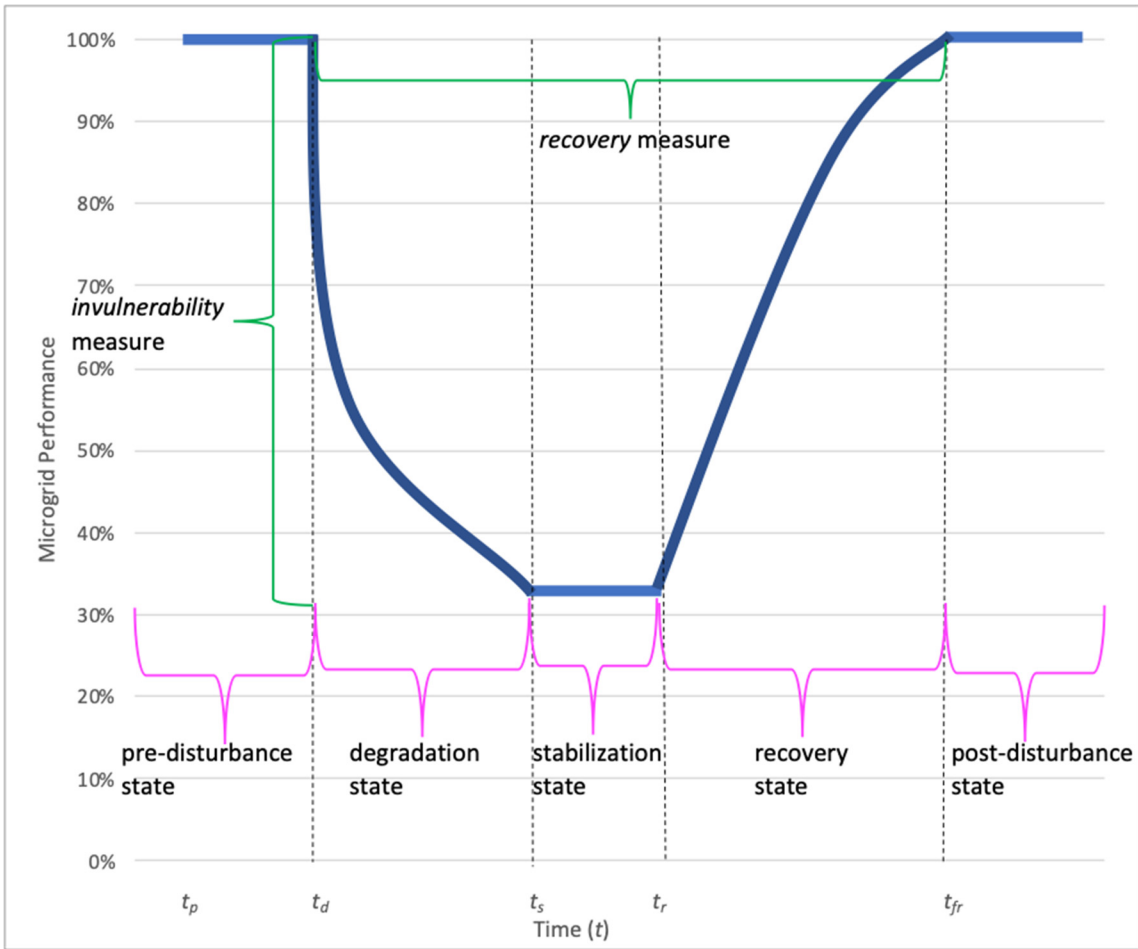


Figure 1. Microgrid Resilience Function's two measures and five states

Figure 2 shows how *resilience* increases at a diminishing rate as redundancy improves while costs do not change.

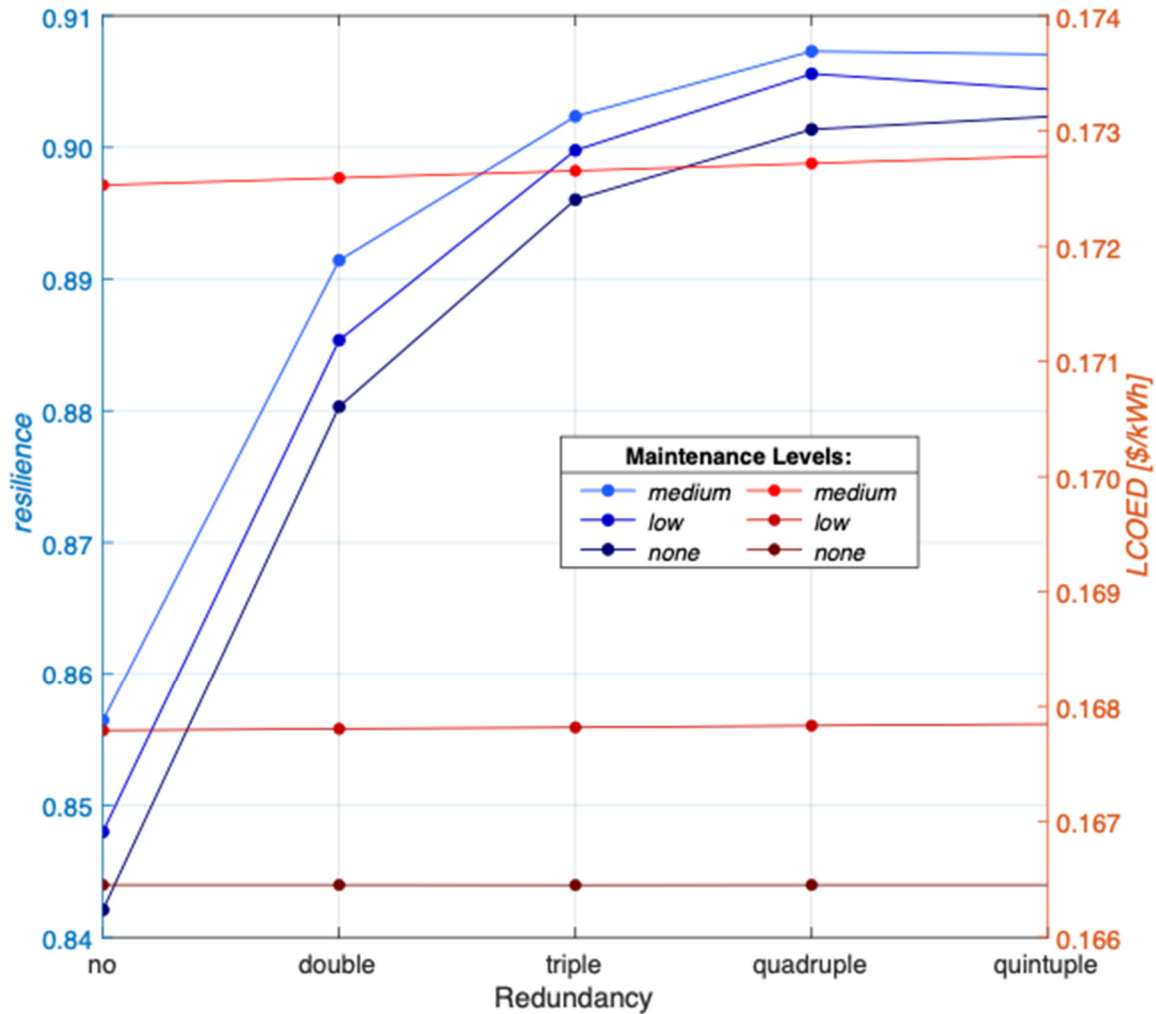


Figure 2. Increasing microgrid’s redundancy increases *resilience* exponentially while costs remain unchanged.

A demonstration of the model’s applicability is conducted for Naval Station Rota’s microgrid as well as the RE microgrids at San Nicolas Island (SNI), San Clemente Island (SCI), and Guantanamo Bay, Cuba (GTMO). Figure 3 exhibits how increasing from one to two DGs improves resilience much more than any additional increments in DGs. We also observe very little contribution in improving *resilience* with WTs when there are more than two DGs. Finally, there is a significant increase in the costs, *LCOED*, for a microgrid with more than three DGs.

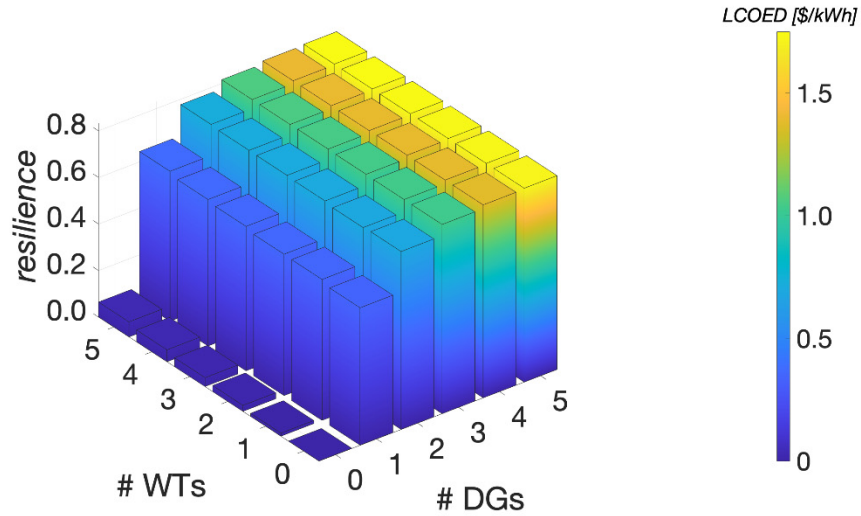


Figure 3. Relationship between *resilience*, number of wind turbines, and number of diesel gensets at SNI. The color changes from blue to yellow as *LCOED* increases.

C. RECOMMENDATIONS

The research finds redundant microgrids provide greater resilience for little added costs. Additionally, we identify and present the power capacity ratios for designing the most beneficial amount and type of power generation. These ratios include excess power that does not exceed the demand by more than 50%. Finally, maintenance has less impact as the power capacity ratio increasingly exceeds the demand profile as observed by the impact of maintenance investments on resilience. These findings can have immediate benefit to ensuring future investments in RE microgrids will provide greater resilience for less costs than alternative designs. Overall, this method creates the resilience and costs trade space to explore design and maintenance options.

Therefore, we recommend the following for future research and application: we can improve our assumptions. Assuming that the microgrid's demand following a disturbance will mimic its historical demand oversimplifies reality. In fact, we would expect a reduced demand that we should be using to assess resilience. We should also not assume that the microgrid's demand will not drop below the microgrid's post-disturbance power rating.

Disturbances and their damage can be made more realistic. The expected damage could incorporate the independent probability of the disturbance with the independent probability of damage. Additionally, we can introduce stochastic behavior to better handle the complexity of common cause failures. Damage can be reassessed at each time step as opposed to an instantaneous point-in-time by extending the disturbance over time. And finally, we can introduce variability in the intensity of the disturbance at each time step to assess damage until the microgrid is recovered with damage that is not limited to a binary outcome. The cost and resilience improvement when varying the $P(d|S_k)$ should generate meaningful and useful findings to make DERs have more *invulnerability*.

Further work can be done to more clearly articulate how threat dependent resilience is. The design differences that provide the most resilience for the most threats should be highlighted by greater analysis of resilience assessments for different threats.

Obvious extensions of this research involve data analytics to generate more meaningful findings. Recommendations for a design option will be possible simply by matching an architecture's resilience function shape to a shape from previously assessed architectures. There is much more we can be done to identify relationships between the experimental results through more complex graphing tools.

More granular time series data will improve the accuracy of the results. Increasing the number of 4D surface plots' datapoints as well as increasing the number of architectures will enable more extensive comparisons between the measures and the design and maintenance choices.

Common cause failures are an obvious avenue for research. Much further can be done to study how decisions on microgrid architectures relate to common cause failures and the resultant impact on resilience and costs.

The models can incorporate multi-objective optimization to more accurately identify the optimal solutions by maximizing resilience and minimizing costs. The optimization model's architecture can be directly input into the resilience model.

Finally, we can more completely investigate the financial aspects of resilience. Specifically, researchers can do more extensive and comparative analysis of the findings

in the comparison of optimal points. Financial tools that more completely value the future energy that has been stored, as well as the unintended complexity costs that are introduced with redundancy, should provide more accurate recommendations.

THIS PAGE INTENTIONALLY LEFT BLANK

ACKNOWLEDGMENTS

None of this work would be possible without the many professional, smart, and caring individuals that have helped guide my way. I am forever humbled and indebted to each of you.

My dissertation committee has provided me meaningful, realistic, and productive guidance. I am particularly grateful to my chair, Professor Ron Giachetti. Your patient, articulate, insightful, timely and thorough feedback exceeds expectations. Thank you for helping me reach my goal, *sans non sequiturs*.

I would like to thank my dedicated and supportive wife for her encouragement and commitment to ensuring both the late nights researching as well as numerous and extended travels could be possible. And of course, Sebastian the cat for his frustrating but well-needed distractions while inserting himself on my keyboard.

To my family, I am blessed to have had your patience and never ending support. I trust you will give me the opportunity to reconnect with you. And to my late father, Professor William W. Anderson, Sr., I trust you are able to delight in my achievement that you inspired.

I would like to thank the Office of Naval Research for supporting this effort, specifically Dr. Rich Carlin. Dr. Philip Vitale is due great credit for being so supportive and instrumental in creating this opportunity. I would also like to thank Jan Jantzen of Denmark's Energy Academy at Samsø Island; Jon Booth, Eddie Scott and Christie Booth of Eigg Electric at Isle of Eigg; Alberto Castañeda of Gorona del Viento in El Hierro; Agustín Marrero of The Canary Island Technology Institute; René Suárez of Red Eléctrica de España; and Pedro Jesús Cabrera Santana of University of Las Palmas for the thorough overview of their power systems and warm welcome to their beautiful island communities.

Lastly, but not least, I would like to pay tribute to a most impressive and promising intern that has helped me immensely: Christopher Baboghli. You always delivered more than expected, this dissertation benefited greatly from your intellect and attention to detail. I would be delighted to read your dissertation one day.

THIS PAGE INTENTIONALLY LEFT BLANK

I. INTRODUCTION

Islanded naval installations (INIs) despite having the highest power costs of all naval installations, also have the greatest exigency for improving resilience. This research contributes to the problem definition, design, and decision-making phases of systems engineering (SE) for INI renewable energy (RE) microgrids by defining resilience with a measure, building a resilience and cost model, and creating trade space of resilience vs. cost to inform decision makers. The models inform the decision-making phase for different microgrid designs subjected to high-impact low-probability (HILP) disturbances.

This introductory chapter discusses the motivation for the research and the problem formulation guiding this research. Specifically, this chapter provides the research objective, contributions, and research method. Additionally, this chapter furnishes the background to impart an understanding and appreciation of other RE microgrids on remote islands.

A. MOTIVATION

Islanded naval installations today almost universally depend upon diesel gensets (DG) for power; historically, most INIs relied on diesel gensets. Islanded naval installations inherently have power supply challenges foremost of which is their isolated location creating greater logistical challenges to resupply fuel to the diesel gensets. This dependence on diesel fuel makes the INIs vulnerable to meeting their mission when resupply challenges arise.

DGs provide power while operating within their loading parameters of 30%–80%. These constraints safeguard the DG from being extremely inefficient at less than 30% loading or having insufficient capacity to meet demand when there are spikes in the load. Having insufficient capacity requires bringing another DG online. Because an INI's DGs operate in an islanded environment, not exceeding 80% loading is considered more seriously than would be for a grid-connected DG; an INI will therefore want to ensure they have adequate spinning reserves (a DG on idle standby) if needed.

Islanded naval installations have unmatched microgrid design challenges due to their remoteness, weather, and uncertainty in demand. For instance, it may take a week to ship fuel to Diego Garcia, British Indian Ocean Territory (DGAR). Harsh and variable weather conditions can threaten all INIs. Extreme heat, winds, dust and dirt routinely threaten Camp Lemonnier, Djibouti (CLDJ). Finally, the INIs due to their high-priority mission have a wide uncertainty in their demand profile.

Islanded naval installations pay between \$0.21 and \$0.54/kWh for their mostly diesel-based energy supply, (i.e., two to five times the Navy’s average) as indicated in Table 1. Islanded naval installations have close to zero RE penetration as compared to 30% for the Navy’s average. With escalating fossil fuel costs, logistical challenges in shipping fuels, and the need to maintain resilience during outages caused by weather or cyberattacks, RE microgrid solutions could greatly enhance mission assurance for these installations and do so more cost-effectively.

Table 1. INIs’ extreme energy costs. Adapted from Department of the Navy (2018); Kandt (2008).

Naval installation	Net Annual Energy Produced [MWh]	RE produced [%]	Annual Demand [MWh]	Annual Generation Costs [\$M]	Cost [\$ kWh]
DGAR	69,813	0.0	62,672	29.67	0.43
SCI	9,545	8.1 (wind)	6,448	5.15	0.54
SNI	5,119	14.0 (wind)	4,588	1.28	0.23
GTMO	128,363	TBD	106,082	28.97	0.22
CLDJ	100,860	0.0	no metering	21.30	0.21
Atlantic Undersea Test and Evaluation Center (AUTEK), Andros Island, Bahamas	44,304	0.7 (wind)	no metering	TBD	TBD

This research explores the design space for microgrids assuming that more power capacity is better, if redundancy and diversification are also introduced. More power

capacity by itself is not assumed to be better with respect to resilience. What however is not understood is the relationship between power capacity, redundancy, diversification, resilience and costs. By being able to plot these relationships as resilience and costs trade-off functions for different microgrid architectures, it is expected that some ratios of power capacity, and both amount and type of diversification will be more desirable to an INI's situation than others.

Although literature is identified on assessing resilience with an operational lenses, very little relevant literature could be found on design based resilience assessments. Mishra et al. (2020) identify microgrid design measures to increase resilience that specifically include adding RE generation on islands, diversification of generation, redundant backup systems to include storage and uninterruptable power supplies (UPS), and spare parts on hand. This research explores how design and maintenance decisions influence the resilience and costs trade-space. Mishra et al. (2020) although identifying measures to harden a microgrid against resilience, do not create a method to interactively evaluate how changes in these decisions (e.g., altering power capacity ratios, diversification combinations, or redundancy levels affect the resilience and costs trade-space).

Anderson et al. (2020) did quantify how many days a grid outage can be reduced by comparing the costs of DG to DG, PV and BAT. This research more clearly articulates these choices to help decision makers in that they show how a \$415K investment could reduce the outage by 1.8 days. However, the trade-space is lacking to provide the interactive and more meaningful analysis that will ensure better design choices can be made. This research squarely is tackling the excess power capacity, diversification, redundancy levels so as to connect these design factors with the corresponding architectures to generate a powerful and meaningful resilience and costs trade-space. It is this contribution that is the most useful and distinct from any of the other research, and despite being tailored for INIs, it is also most relevant to any remote island community employing off-grid microgrids.

1. Proposed INI RE Microgrid Definition

Islanded naval installations present a compelling case for RE microgrid designs. Not only are INIs rich in RE resources, they also have the challenge of an unpredictable demand profile combined with much higher operating and maintenance (O&M) costs primarily due to their remoteness. DGAR is arguably the most remote island on earth having a demand profile equivalent to a small city.

Islanded naval installations are all required to maintain a much higher level of mission assurance due to the unique operational nature of their activities. The need to ensure mission assurance is directly linked to the ability to deliver power to the INI's electrical loads. The INI's mission creates a stochastic and higher demand at the installation compared to daily operations without conducting mission specific operations.

Each INI has an operational military mission to support, and without power, the support cannot be provided. Resilience is critical to ensuring mission assurance. Although base commanders embrace the need to ensure mission assurance, they have thus far been unable to either understand or quantify the INI's power costs to deliver a sufficient level of resilience.

“Energy Security is defined as having assured access to reliable supplies of energy and the ability to protect and deliver sufficient energy to meet mission requirements” according to 10 USC 2924, U.S. Code of Definitions, Department of the Navy (2017b, 9). The Navy has designated the three pillars of Energy Security as Reliability, Resiliency and Efficiency. The Department of the Navy's defines their terms in the Naval Facilities Engineering Command (NAVFAC) P-602 as:

Reliability: the percentage of time energy delivery systems (utilities) can serve customers at acceptable regulatory standards. Reliability can be measured by the frequency and duration of service disruptions to customers.

Resiliency: the ability of a system to anticipate, resist, absorb, respond, adapt and recover from a disturbance.

Efficiency: the use of the minimal energy required to achieve the desired level of service Department of the Navy's (2017b, 9–11).

The U.S. Navy relies on INIs to launch operational missions that are dependent upon reliable and resilient microgrids. Figure 1 identifies the location of all U.S. Naval Installations without external utility grid connections.



Figure 1. Remote islanded naval installations.

To meet the research objectives to analyze cost and resilience of microgrids on military islands, one must first define resilience for the Navy’s RE INI microgrids. The resilience definition for this research into the Navy’s INI RE microgrids refines the Navy’s resilience definition by emphasizing the speed of recovery:

The microgrid’s invulnerability and rapid and full recoverability from an improbable and severe disturbance.

The definition reflects the American Society of Mechanical Engineers’ (ASME) emphasis on recovery as stated by Hosseini, Barker and Ramirez-Marquez (2016) as well as the DOD’s emphasis on invulnerability as indicated by Baxter (2018, 5).

The Navy’s definition includes the ability to anticipate and adapt from a disturbance. Although adaptation is important, it occurs over a longer time and therefore this is not considered in this research.

The resilience definition focuses on INIs and RE microgrids that must be resilient to disturbances other than a loss of power from the utility provider. This research propounds that a properly designed microgrid should have sufficient invulnerability to absorb the disturbance's impact and ensure a rapid recovery to its pre-disturbance performance level.

Although the Navy has made reliability and resiliency their highest energy security priorities, "resiliency" (the Navy's term) is the least understood.¹ It is important to note that increasing resilience may lead to trade-offs in reliability and efficiency. Keogh and Cody (2013) argue that underground power lines although more robust to weather damage have greater recovery time due to being less accessible and taking longer to institute the repair. Easily accessible instrumentation decreases recovery time at the expense of reduced robustness. Choosing between where and how much to invest requires a better understanding of the trade-offs in availability, robustness and recovery.

Islanded naval installations are unique, and therefore enhancing resilience through microgrids requires specially adapted tools. INIs are not only expected to have more reliable power, but they must do so at a geographic location that requires an understanding of the unusual engineering and climate-driven differences that impact the design and operation of the microgrid. We must know how an INI is different not simply by being islanded geographically and within a more arduous climate zone, but also due to the unpredictability of the demand that is a unique byproduct of the military mission, in order to design cost-effective resilience solutions using microgrids.

2. What Does It Mean to Be Islanded?

Wattjes and Slootweg (2013) use islanded in the context of power systems as a term that means there is no external utility provider. In some situations, being islanded for the electrical loads is also geographically indicative. At INIs the loads are islanded both due to the power and geographic criteria. Although a microgrid can be islanded for either reason,

¹ Although the Navy initially used the term "resiliency," they are moving toward using the term "resilience" instead, which will be used throughout this dissertation and generally meaning the same as resiliency.

at all but one of the INIs it is for both. INIs that are not on an island such as Camp Lemonnier, Djibouti have similar challenges to being on an island. INIs are U.S. Naval Installations without external utility grid connections.

By the very nature of INIs' missions being unique and typically erratic in their operational tempo, the power demand is also extremely unpredictable. This is an important distinction for INIs in that not only is the RE generation stochastic, but the stochastic demand is much more extreme in terms of its peak power due to being an operational military installation.

Microgrids are indispensable when there is a need to generate power independent of an external utility provider. A microgrid can introduce greater diversity of generation much closer to the load. While neither the diversity of generation nor proximity to the load are financially compelling either can provide significant energy security enhancements.

Ton and Smith (2012, 84) adopt the U.S. Department of Energy Microgrid Exchange Group's microgrid definition as "a group of interconnected loads and distributed energy resources within clearly defined electrical boundaries that acts as a single controllable entity with respect to the grid. A microgrid can connect and disconnect from the grid to enable it to operate in both grid-connected or island-mode." Microgrids have four core components that include power generation, controls, energy storage and a load with all power being coordinated through controls as indicated in Figure 2.

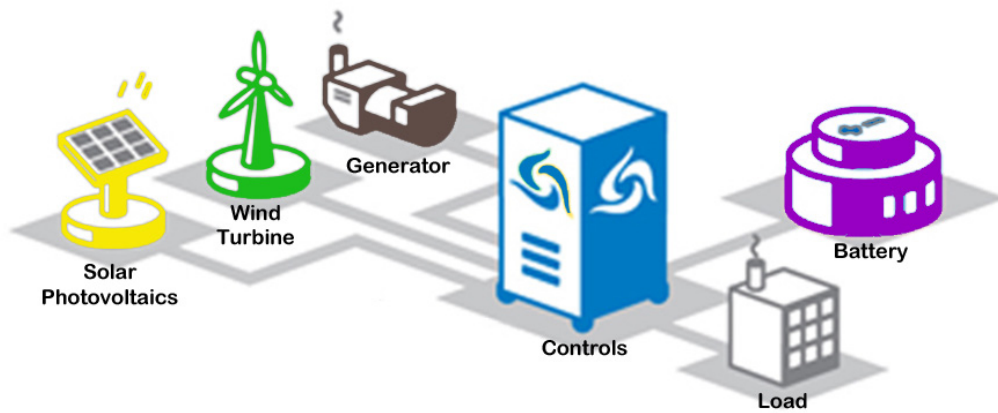


Figure 2. Microgrid core components. Source: Walsh (2014).

The controls component is critical to operating in islanded mode. At SNI the DG control strategy is to always have the gensets on-line and in grid forming mode. SNI's universal microgrid controller (UMC) is automated to dispatch the most efficient combination of gensets to meet the demand and provide overhead through spinning reserves. The wind turbine control strategy is such that the microgrid controller will automatically engage the wind turbines one at a time when the wind exceeds 3.5 m/s. If there is too much wind power for the demand, the UMC will reduce the number of wind turbines.

In contrast to an off-grid islanded microgrid, Peterson (2019) presents an overview diagram of a grid-connected microgrid system with typical components and distribution voltages as seen in Figure 3. Peterson (2019) made this distinction between a grid-connected and an off-grid microgrid before he evaluated what happens when the microgrid is disconnected from the grid.

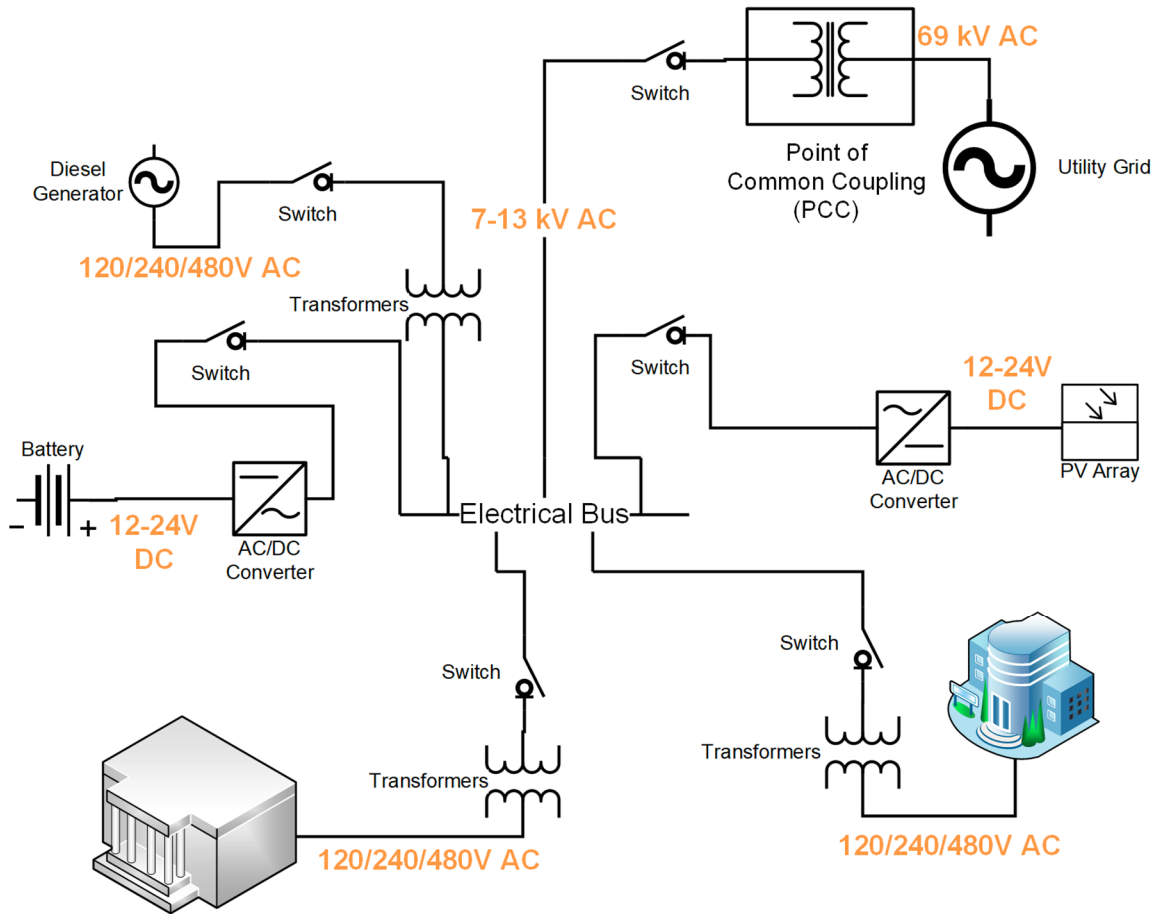


Figure 3. Microgrid overview diagram. Source: Peterson (2019).

3. Disturbances for INI Microgrids

INI microgrids experience degradation of generation due to disturbances that are both extreme and unexpected (e.g., tsunami or cyberattack). Deliberate attacks can be either physical or cyberattacks. Peterson (2019) argues that military installations are a more attractive and likely target due to the mission and higher relative value of the infrastructure.

INIs are not grid connected and accordingly the disturbances explored are not from a loss of utility provided power. Rather, the disturbances are mostly weather-related. Despite INIs being vulnerable to other disturbances such as cyberattacks, the assumption for this research will be that the preponderance of disturbances is weather-related. Using this assumption, the author models four weather related disturbance scenarios and one cyberattack disturbance scenario. Disturbances will be limited to HILP events upon the

INI's microgrid because this is what resilience is intended to address. Only one disturbance is used to disrupt the microgrid. Disturbances included in this research are hurricanes, wildfires, earthquakes, tsunamis and cyberattacks. Also, although other combinations of impact and probability could be introduced, such as high-impact high-probability or medium-impact low-probability we do not explore these within the scope of this research.

B. PROBLEM STATEMENT

The literature on microgrid resilience neither incorporates costs nor investigates off-grid microgrids on remote islands. This gap in understanding both the cost of resilience as well as its application to off-grid microgrids is particularly relevant to the Department of Defense (DOD). Not being able to put a price tag on resilience at INIs prohibits the DOD from investing in microgrids that will provide the desired resilience and costs for the situation.

Currently, DOD microgrids on islands are either 100% DG generation or, they employ RE at a small fraction of the overall microgrid's power capacity. The DOD incurs significant costs and a logistical burden to transport fuel to these INIs, which makes the DOD more vulnerable to ensuring fuel can be supplied. Although using RE for the DOD is not driven by a need to be green, the DOD does want to become more resilient and RE can do this by diversifying the power generation portfolio at INIs. An added benefit of RE at INIs is more energy independence from off-island fuels. The need to understand the interrelationships between the DG and RE generation is essential when adapting conventional diesel genset-based approaches to meeting electrical demand by ensuring supply equals the demand. A RE microgrid with supply unequal to demand requires a design solution addressing the intermittency of the RE. This intermittency can best be addressed by one of the following:

- diverse portfolio of generation
- deferrable/adjustable loads
- backup/highly responsive generation

- energy storage
- extremely high levels of RE generation and “spill” excess capacity (Islam 2017)

Islanded naval installations are much more vulnerable to the cost and engineering’s indirect impacts on their ability to generate power and therefore there is more opportunity to address the gap in the literature at INIs. Islanded naval installations are subject to the volatility and ever-increasing costs of diesel fuels when operating the gensets for power generation. Additionally, there have historically been fuel shortages placing islanded microgrids at significant risk given their dependence upon diesel fuel. Islanded naval installations also suffer damage from cyclones and tsunamis and a properly designed microgrid can reduce their vulnerability to the damage caused by these extreme weather events. Overall, INIs are more vulnerable to costs, engineering challenges, and extreme weather than mainland based installations.

Current state-of-the-art microgrid designs only aim to minimize the cost of energy with the constraint of stable operation and do not optimize for resilience, which is the Navy’s emphasis. Microgrid optimizations mostly focus on costs or RE penetration. Despite resilience being the Navy’s priority, there has been no attempt or ability to incorporate resilience into microgrid designs. Rather, it is unclear what the Navy’s resilience goals are despite having defined resilience. This problem is exacerbated by the lack of microgrid design methodologies in the literature that might offer the Navy the ability to grasp the cost and resilience trade-offs.

The research problem is: ***How can RE microgrid designs at INIs be assessed in order to maximize resilience and minimize cost?*** It is also expected that this problem is equally relevant, for different reasons, and has applications on remote islands other than INIs.

C. RESEARCH OBJECTIVE

The research objective is to develop a method and model to analyze the cost and resilience of RE microgrids on military islands. The base commander can then choose the microgrid design with an acceptable combination of resilience and cost.

We first define resilience for INIs so that we can distinguish its dimensions in order to generate the appropriate resilience measures. The resilience measures are used in a resilience model constrained by an INI microgrid energy balance equation.

The resilience model is used to measure a microgrid's resilience to a disturbance. The measures created assess resilience of a microgrid's design at different maintenance levels.

A cost model calculates a microgrid architecture's costs for a chosen maintenance level. The cost model is adapted from other researchers' efforts so as to be applicable to an INI and communicate meaningful financial information to the INI's base commander.

Trade spaces articulate conflicting performance indices (efficiency, cost, resilience) created using the cost and resilience models. These trade-off functions help answer design and maintenance level questions so as to better inform an INI base commander how to invest for resilience. Finally, these same models are used to assess resilience of a case study for Naval Station Rota, Spain.

The deliverable is a tool that incorporates the method to identify the cost of resilience. This tool uses the models developed in this research to create the trade-off analysis to inform decision makers how their microgrid investments can increase resilience.

D. CONTRIBUTIONS

The contributions address the gaps in the literature that do not examine costs and off-grid microgrids on remote islands in the resilience research. Three primary contributions address these gaps with the first contribution developing cost and resilience measures for RE microgrids at INIs. The second contribution is a decision-making tool for the islanded locations to assess resilience, using the resilience and cost measures, of RE

microgrids to disturbances. The third contribution to SE design and optimization of complex systems is the application of this tool to create the resilience and costs trade analysis that will influence RE microgrid design through the system architecture design phase. This third contribution will enable investment decisions in energy storage, power capacity ratios, and redundancy levels, as well as identify the fuel cost for DG to be cost competitive with PV for a microgrid architecture. This contribution is presented through three-dimensional (3D and 4D) heat maps to better assess the trade analysis.

It is also expected that this research will influence the integration of SE principles into microgrid designs. This research helps identify significant design factors, to include power capacity ratios and redundancy levels.

Contributions include a novel tool to evaluate resilience for remote naval installations. Creating a decision support method for the base commander to select the microgrid design that provides the desired combination of resilience and costs for remote and isolated RE microgrids will also be a significant and useful contribution.

There is also the specific application that is anticipated for the Navy to incorporate this method both into the NAVFAC P-601 Microgrid Design Guide as well as the NAVFAC P-602 3 Pillars of Energy Security. Additionally, the new DOD Microgrid Unified Facility Criteria being developed could leverage this method.

E. INTENDED USERS OF THIS METHOD

People that might also benefit from this work beyond the primary beneficiary (the Navy) include those living in isolated islands that include Small Island Developing States (SIDS) that are showing a growing interest in using RE for economic and environmental reasons. Islanded naval installations could also exploit RE microgrids for energy security (resilience). Three islands were studied and visited to better understand the opportunities for INIs to leverage the success demonstrated at Isle of Eigg, Samsø Island, and El Hierro.

Remote islands that approach 100% RE power generation for an appreciably lower cost than INIs creates a compelling argument for the Navy to rely on smarter designs. The INI's energy security will improve if the Navy's microgrid designs come closer to attaining

these islands' results. As a result, the INIs could deliver better and less costly mission assurance.

Finally, there are two compelling opportunities for the U.S. Navy and National Science Foundation to enhance resilience by implementing an effective method at SNI and McMurdo Antarctica. Although only SNI is an INI, both locations are islanded and remote, have extremely high costs of power generation and have decided to develop and apply a method to assess and improve resilience at these locations.

1. Relevance to Island Communities

A recent study by Rocky Mountain Institute (RMI) evaluated ten islands and remote communities representing various worldwide microgrids Bunker, Hawley and Morris (2015). The locations studied include: Bonaire, The Netherlands; Kodiak, Alaska, U.S.; El Hierro, Canary Islands, Spain; Falkland Islands, U.K.; King Island, Tasmania, Australia; Marble Bar and Nullagine, Australia; Coral Bay, Australia; Isle of Eigg, Scotland, U.K.; Necker Island, British Virgin Islands; Mawson Station, Antarctica.

Despite the higher costs of island electricity (being on the average three times higher than that of oil-based mainland) the RMI study still claims that island-based communities are enjoying the benefits of alternatives to oil-based electricity systems. Bunker, Hawley and Morris (2015) claim these communities realize “operational cost savings, reliable and stable power, long term energy price stability, and reduced dependence upon oil.”

Several islands have demonstrated success in powering their communities with RE microgrid solutions. Each of these islands has its unique solution, relying heavily upon available resources, such as wind, hydro or solar power. For example, El Hierro in the Canary Islands has attained 100% RE generation on-island and is one such island that generates its primary power from pumped hydropower using wind turbines to power the pumps and provide backup power to an island of approximately 11,000 residents. Tetiaroa Island in French Polynesia provides power through a combination of solar PV and gensets using coconut oil for fuel to power to a seven-star resort.

The shallow waters of Kattegat Sea, 15 km off the Jutland peninsula surround Samsø Island, an “inner” island of Denmark. Samsø Island has 3,700 inhabitants and its annual energy consumption is approximately 600 TJ. Spear (2014) observes that Samsø Island’s electricity is entirely from wind power. The electric system is comprised of 11 1 MW onshore wind turbines, and ten 2.3 MW offshore wind turbines. The islanders funded all but four of the wind turbines. The distribution system features 300–400 Amp underground capacity and 200 Amp above-ground capacity.

F. ORGANIZATION OF DISSERTATION

Chapter II reviews the literature to highlight the gaps in the research. Chapter III presents the method to convey how the cost and resilience models both function and are linked. Chapter IV provides the validation of the cost model and questions to which the results of the experiments are analyzed to identify useful implications. Chapter V applies the decision-making tool to assess resilience for Naval Station Rota, Spain’s microgrid to disturbances and compares resilience and costs at three RE INIs. Finally, Chapter VI presents the conclusions and recommendations.

THIS PAGE INTENTIONALLY LEFT BLANK

II. LITERATURE REVIEW

This chapter identifies what other researchers have done to measure resilience in order to adapt and create a method that is appropriate for INIs. The focus of this literature review is on resilience and cost modeling of RE microgrids.

We evaluate interdisciplinary and earlier works on resilience as well as several military and government documents given their applicability to this research's focus on INIs. However, there is no literature on resilience of off-grid RE microgrids.

A. RESILIENCE

Researchers portray resilience as a function of performance over time. D'Lima and Medda (2015) consider Bruneau in 2003 as making one of the first known attempts to plot resilience to better evaluate, demonstrate, and communicate resilience using a resilience triangle for seismic resilience of communities as illustrated in Figure 4. The resilience triangle conveys how performance instantly degrades when a disturbance strikes, before recovering over time to a restored performance level. The seismic resilience used by Bruneau et al. (2003) emphasizes the ability of the community's infrastructure system to perform following an earthquake. Following Bruneau et al. (2003), Yodo and Wang (2016), Panteli et al. (2017), Zhang et al. (2018), Zobel (2011), and Rose (2007) have used either the resilience triangle, trapezoid or curve.

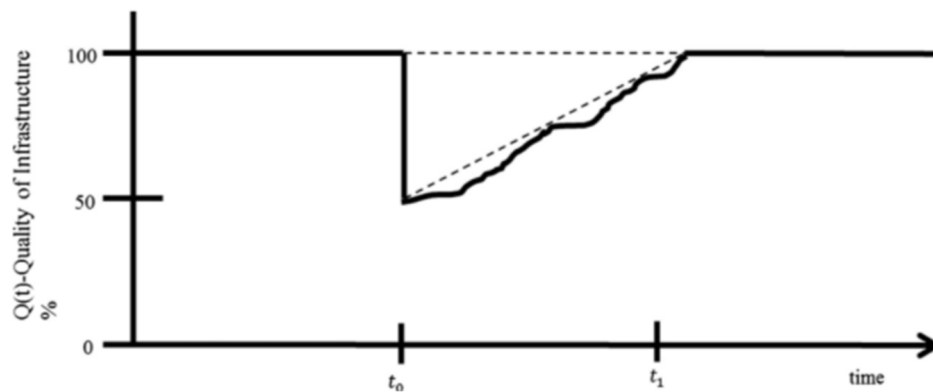


Figure 4. Bruneau's 2003 *resilience* triangle. Source: D'Lima and Medda (2015).

Willis and Loa (2015) helped influence our understanding of resilience and microgrid designs by observing that the resilience function's shape varies for different designs and approaches to operating the energy distribution system, that different responses will result in different costs, and resilience is dependent upon the timescale. The timescale is integral to the shape of the function due to repeated and new disturbances such as those from climate change impacting the energy distribution system if the recovery timeframe is over many years.

Willis and Loa (2015) observe that the resilience function's shape depends upon the energy distribution system's architecture design. The architecture can influence the impact measured by the y-axis and the time to recover measured by the x-axis. It is possible that similar shapes among resilience functions will be useful in ultimately assessing resilience. If an architecture's resilience function portrays the same shape as another previously assessed architecture's shape that is considered preferred by the decision maker, then it is likely that this architecture that has not yet been assessed will also have similar resilience behavior.

D'Lima and Medda (2015) define static resilience as the ability to maintain existing function, as being portrayed by a reduced and smaller triangular area bounded by the three points $(t_0, 100)$, $(t_0, Q(t_0))$ and $(t_1, 100)$ over the same recovery time t_l in Bruneau's resilience triangle shown in Figure 4. And when the recovery is faster, D'Lima and Medda (2015) designate the reduced triangular area due to full recovery and occurring before t_1 as dynamic resilience, a measure of efficiency. They later applied their dynamic and static components to modeling the resilience of the London Underground transport system, aka London Tube (LT), and proposed that recovery from a more volatile disturbance portrays greater resilience than recovery from less volatile disturbances.

The microgrid's behavior as demonstrated by its performance over time is important and useful to understand when defining and ultimately measuring resilience. Panteli and Mancarella (2015; 2017) identify a limitation of Bruneau's resilience triangle in its inability to capture the distinct states (Disturbance, Degraded, and Restorative) beyond the single recovery phase assessment. Additionally, the resilience triangle is threat specific due to its sharp and immediate degradation. Although the resilience triangle is

unable to capture the evolution of a disturbance over time, it may be unfair to criticize this model too harshly in that it, like all models, is a simplification of reality.

The microgrid resilience function in Figure 5 illustrates a disturbance impacting the microgrid at time t_d . A disturbance is any HILP event degrading the microgrid's performance. Microgrid performance is defined as the percentage of demand being met by the microgrid. The resilience measures *recovery* and *invulnerability* are shown and will be explained in more detail in Chapter III. *Recovery* the resilience measure is different than recovery, one of five states. *Invulnerability* is an adaptation of Francis and Bekera's (2014) vulnerability measure that relates the absorptive capacity to the proportion of original system performance retained immediately following the disruption.

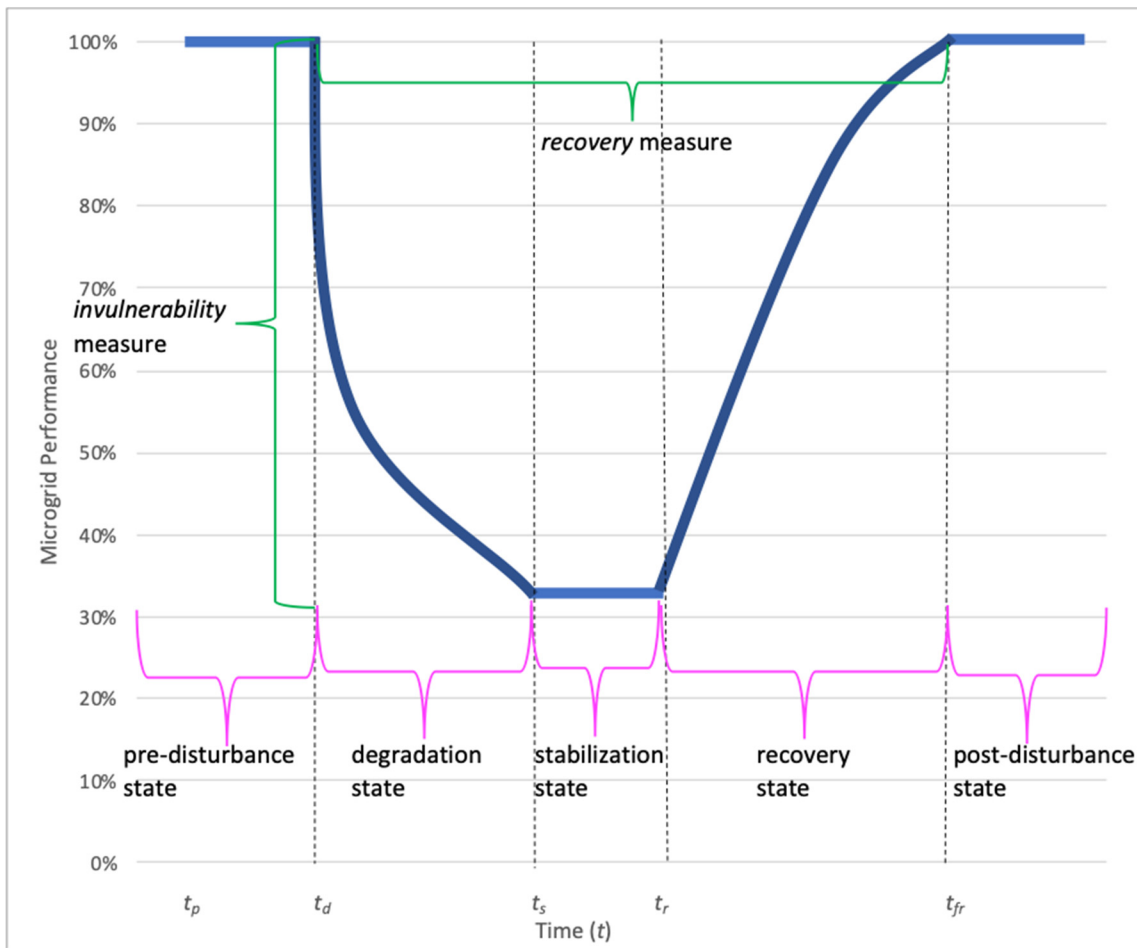


Figure 5. Microgrid *resilience* function's states and *resilience* measures.

Five distinct states partition the resilience function between t_p - t_d , t_d - t_s , t_s - t_r , t_r - t_{fr} , and after t_{fr} . The pre-disturbance state occurs before the disturbance from t_p to t_d . In the degradation state, the microgrid degrades to a minimum level of performance commencing at time t_d up until t_s . During the stabilization state from t_s to t_r the microgrid will continue to perform at diminished level with no recovery. Starting at t_r when the disturbance is no longer present and/or the microgrid is altered either in architecture or operation the microgrid will start to recover its performance until time t_{fr} during the recovery state. Finally, the microgrid attains its post-disturbance state upon full recovery of its pre-disturbance performance at time t_{fr} .

1. Resilience States and Dimensions

Resilience is defined in the literature with as many as five and as few as three dimensions. The National Renewable Energy Laboratory (2019a, 2) identified the “Five Rs” of energy system resilience. These five dimensions include Robustness, Redundancy, Resourcefulness, Response and Recovery.

Bruneau et al. (2003, 738) posit that resilience has only four dimensions: Robustness, Redundancy, Resourcefulness, and Rapidity, defining rapidity as “the capacity to meet priorities and achieve goals in a timely manner in order to contain losses and avoid future disruption.” Li et al. (2017) also define four dimensions of power system resilience: continuous situational awareness, robustness and preparedness, responsiveness and survivability, and recoverability and rapidity. Finally, Madni and Jackson (2009,187) characterize resilience as a “multi-faceted capability of a complex system that encompasses avoiding, absorbing, adapting to, and recovering from disruptions.”

Henry and Ramirez-Marquez (2012) designate $F(t)$ as the value of the delivery function resulting from each of the five states following a disruptive event and the corresponding resilience action for the respective system. Although $F(t)$ represents an important distinction from the performance of the system, this research finds it to be equivalent to performance for microgrids because both $F(t)$ and a microgrid’s performance, or power capacity, are byproducts of all the states following a disruptive event and represent value of the system’s output.

However, Henry and Ramirez-Marquez (2012) argue that disruption and recovery are transitional and therefore not states. They therefore determine that resilience has just three states: Stable Original, Disrupted and Stable Recovered. Whether one believes disruption and recovery as transitional or a state is not important, rather being able to measure each of these is more essential for assessing resilience than whether or not disruption and recovery are transitional or states. Baroud et al. (2014), Hosseini et al. (2016), Panteli and Mancarella (2015), Ouyang, Dueñas-Osorio and Min (2012) also use this three-state view for their research.

Willis and Loa (2015) admit that although these dimensions are relevant, they are inconsistently used. Willis and Loa (2015, 6) argue that synthesizing the competing definitions is neither productive nor worthwhile and instead believe it is more important to evaluate the “service delivery, system design, system operations, disruptions, costs, and timescale” aspects of resilience. Despite conceding that there are many competing definitions, synthesizing these definitions is worthwhile in revealing common themes taken by several scholars.

Other proposed resilience dimensions include prepare and anticipate, resist, response and recover Zhang et al. (2018;) and anticipation, absorption, recovery and adaptability Mohamed et al. (2019,) which is a distilled outcome of over fourteen other organizations. Mohamed et al. (2019) identify the main resilience dimensions as: tolerance, resistance, robustness, anticipation, adaptation, absorption, recovery, learning lessons, and alternative service.

Haines (2018) concludes in evaluating the numerous attempts to define resilience that resilience is both multidimensional and threat dependent. The resilience of a system, such as a microgrid, is different for a wildfire versus a tsunami. A microgrid designed to be more resilient to wildfires should employ less DER that have higher probability of damage to a wildfire but in so doing these DER could be more vulnerable to a tsunami. Most definitions proposed by others include more than one dimension—for example, reliability, restoration, adaptability, anticipation, or absorption—and many use different terms that are mostly synonymous. Many threats are weather-related, however military microgrids must also consider the intentional acts of an adversary such as cyberattacks,

sabotage, and direct attacks on the energy infrastructure. Regardless, of the potential for adversary action, the more likely threats to INIs remain weather related.

Increasing resilience to a specific threat could make it less reliable to other threats. The classic example offered is underground vs. above ground utility lines. Above ground lines tend to be less reliable in conditions such as high winds and ice storms that are Low-Impact-High-Probability disturbances, but more resilient due to being faster to repair. Li et al. (2017, 3) stipulate that “reliability can be evaluated without specifying the threats; but resilience is always relative to a particular threat.”

Lawton et al. (2003), Wang et al. (2016), and Panteli and Mancarella (2015) defined resilience based upon the nature of the attack. Panteli et al. (2017) argue that resilience can differ dramatically for an earthquake that only lasts a few seconds vs. a typhoon that can last many hours or days. Chanda and Mohanpurkar (2018) find each of these approaches to be insufficient due to the omission of the duration of the disturbance in their definition. One could argue that not fully capturing the entire area under the resilience function creates an incomplete and inaccurate measure of the system’s resilience due to the inadequate consideration of the full duration of recovery or full extent of vulnerability.

Although it could be argued that resilience is multidimensional and not captured by just a single measure, other researchers have not reached a consensus on any one measure that is exhaustive in capturing all known resilience dimensions. The numerous approaches to measuring resilience attempt to measure one or multiple aspects of the area under the resilience function. Any or all of the resilience measures suggest that resilience is directly related to the area under the entire resilience function.

Recovery is a key component of resilience but has been approached in different ways by researchers. Resilience has been defined by some to only be preparedness and not recovery whereas Hosseini, Barker and Ramirez-Marquez (2016) emphasize both. Most definitions do incorporate the capability of the system to absorb and adapt from a disruption with recovery as an integral component of resilience. Some definitions dictate full recovery whereas others do not expect a return to pre-disruption state. The United Nations International Strategy for Disaster Reduction (2005) does not dictate full recovery by

defining resilience for the United Nations-International Strategy for Disaster Reduction (UN-ISDR) as a system's ability to retain reasonable performance once exposed to changing conditions.

The Arctic Council (2016) defines resilience for the Stockholm Research Center as the ability to continually change and adapt while operating within critical thresholds. Overbye, Vittal and Dobson (2012) define resilience as how “gracefully” a system deteriorates, that is the capability to gradually deteriorate under increasing disturbances and rapidly recover to its pre-disturbance state. Haines (2018) defines resilience as the capacity to sustain a noteworthy disturbance within “acceptable degradation parameters” and recoup within a worthy time. Both recovery and vulnerability will be incorporated in this dissertation as two dimensions to measure resilience.

Power systems and critical infrastructure usually use capability-based definitions to define resilience. Chaudry et al. (2009) define a power system's resilience for The United Kingdom's Energy Research Center (UKERC) as the capability to endure turbulence while still providing power to subscribers and recuperating quickly from a disturbance by having alternatives to provide energy. This definition, although pragmatic, does not mandate that the microgrid or power system by itself can recover, rather that alternatives to obtaining the energy are available. This solution is not practical or even feasible for an INI due to being off-grid and so remote.

The U.K. Cabinet Office (2011, 14) defines critical infrastructure's resilience for the United Kingdom (UK) Cabinet Office as a capability “to anticipate, absorb, adapt to and / or rapidly recover quickly from a disruptive event.” This definition expands upon and quantifies the desired dynamic behavior.

Field et al. (2012) devised another capability-based definition equating resilience to being able to anticipate, absorb and recover from a disturbance conveniently and successfully. This definition could be argued to fall short in that it has not defined any criteria for success. After reviewing multiple definitions, Mohamed and Su (2019) determined that a resilient power system must have four capabilities in response to a

disturbance: anticipation, absorption, recovery, and adaptability. All of these capabilities-based definitions also support a multi-dimensional approach to resilience.

Resilience for off-grid RE microgrids introduces different disturbances that have risks of damage. The disturbance is not due to a power loss from the grid and there is no interconnection to any generation or storage. Although scholars have researched off-grid microgrids, the literature reviewed did not identify any attempts to define resilience for off-grid RE microgrids. Rather, the research tends to be mostly broad and analytical overviews without providing detailed frameworks for evaluating a microgrid's resilience.

The reviewed literature is limited to resilience in remote off-grid locations that excluded power systems Arctic Council (2016), off-grid RE systems excluding resilience (Akikur et al. 2013; Arriaga 2016; Mandelli et al. 2016; Markovic et al. 2016; Singh et al. 2015; Won et al. 2017), and efficiency of diesel gensets in remote locations excluding resilience Wheeler (2017). Chatterjee et al. (2019) briefly discusses resilience for off-grid RE but fails to demonstrate how others will measure resilience or costs. The extremely limited literature addressing this specific topic suggests that there is little-to-no understanding of design components most useful to enhancing resilience for off-grid microgrids.

2. Resilience Definitions

The Resilience Engineering Institute (2019, 1) states, “resilience is a word found in nearly a dozen academic disciplines, yet there is no consistent definition or approach shared among them.” Most define resilience as a system's ability to recover from a disruptive event. Hosseini, Barker and Ramirez-Marquez (2016) conclude that more general definitions not focused on any particular application consider resilience to be an attribute associated with returning to a normal condition following a disruptive event. Research Assistant Professor Eisenberg of the Naval Postgraduate School in discussion with the author, (August 26, 2019), described resilience as a verb to emphasize the dynamic and temporal characteristics.

a. Vulnerability-focused definitions

Aven (2011) take a less specific approach defining resilience as simply the vulnerability and seriousness of the outcomes for any event. D’Lima and Medda (2015, 36) offered one definition proposed by Holling in 1973 as “a measure of the persistence of systems and of their ability to absorb change and disturbance and still maintain the same relationships between populations or state variables.”

Baxter (2018, 5) defines resilience using the DOD’S definition for “Energy Resilience” as “the ability to avoid, prepare for, minimize, adapt to, and recover from anticipated and unanticipated energy disruptions to ensure energy availability and reliability sufficient to provide for mission assurance and readiness, including task critical assets and other mission essential operations related to readiness, and to execute or rapidly reestablish mission essential requirements” as stipulated in 10 U.S.C. §101. This definition intentionally creates its interpretation of what is included as task critical and mission essential.

Robustness is an element of resilience when evaluating the power system’s performance over time. Li (2017) classifies robustness as an element of resilience in extreme events that is measured before the disturbance. This predisturbance view of an element of resilience is inconsistent with most of the literature that does not study resilience any time before the disturbance.

Robustness in resilience has been defined as the ability to withstand a stress to the system. D’Lima and Medda (2015, 37) define resilience as “strength, or the ability of elements, systems, and other units of analysis to withstand a given level of stress or demand without suffering degradation or loss of function.” Arghandeh et al. (2016, 8) identify specific techniques to assure robustness that include designing distribution poles to withstand wind speeds and earthquakes and “replacing overhead lines with underground cables.”

Arghandeh et al. (2016, 2–3 and 7) state that “resilience hinges on flexibility and survivability in the face of unexpected events, while robustness implies resistance to change.... Robustness is concerned with strength, whereas resilience is concerned with

flexibility.” Certainly, resilience favors flexibility; however, robustness and resilience should not be viewed as mutually exclusive.

b. Recovery-focused definitions

D’Lima and Medda (2015, 35) define resilience as “how fast a variable that has been displaced from equilibrium returns to it” in their study of delays or disruptions to the LT service. Hosseini, Barker, and Ramirez-Marquez (2016,49) define resilience using the ASME’s 2009 definition “as the ability of a system to sustain external and internal disruptions without discontinuity of performing the system’s function or, if the function is disconnected, to fully recover the function rapidly.” The National Infrastructure Advisory Council (2009, 8) defines infrastructure systems’ resilience as the ability to “anticipate, absorb, adapt to, and/or rapidly recover from a potentially disruptive event.”

Several researchers include reliability with recovery in defining resilience. Youn and Chao (2011) sum reliability and recovery rates. Ayyub’s (2013) comprehensive measure incorporates both recovery and reliability.

c. Definitions emphasizing disturbances

The literature on resilience of power systems is mostly in agreement that resilience is in response to HILP events. The nature of the disturbance is what differentiates resilience from reliability that is typically well understood to be in response to LIHP events. This differentiation tends to suggest that resilience is much more attributable and requisite for more severe and unpredictable disturbances than reliability.

Li et al. (2017, 2) simply define resilience of a microgrid as the ability “to withstand disruptions pertaining to severe weather and climate changes (e.g., hurricanes, tornados), catastrophic man-made incidents (e.g., malicious attacks, human operator missteps), and a combination of such incidents.” This definition fails to stipulate any desired dimensions in the recovery of the microgrid.

The Department of Energy’s (DOE) definition follows Presidential Policy Direction 21 as “the ability to prepare for and adapt to changing conditions and withstand and recover rapidly from disruptions.” “Resilience includes the ability to withstand and

recover from deliberate attacks, accidents, or naturally occurring threats or incidents,” according to Energy Infrastructure Resilience (2015, 3). The DOE has incorporated variability of the severity level of the disruption despite DOD not doing so.

The Department of the Navy’s (DON) definition for Resilience is “the ability of a system to anticipate, resist, absorb, respond, adapt and recover from a disturbance.” The Department of the Navy (2017, 10) stipulates that each of these six dimensions are an important resilience attribute for the DON. The DON does not include a requirement to recover rapidly. “Resiliency is what happens when you lose reliability,” as claimed by Michael Partyka (NAVFAC’s Energy Security Program Director) in discussion with the author August 13, 2019.

Although most studies focus on disturbances, very few vary the disturbance levels as the LT study did in a way that others could perceive as useful. Varying weather-related disturbances impacting INI RE is an unnecessary complexity for this research’s resilience model.

d. Operational vs. design approach

Hollnagel, Woods and Leveson (2006) define resilience as the ability of a system to modify its functionality during a disturbance and unpredicted change, emphasizing the operational nature of controlling resilience over design. Berkeley and Wallace (2010) has a broader resilience definition for The National Infrastructure Advisory Council (NIAC) as the capability to learn lessons through subversive events and then modify operations and critical infrastructure framework to “restrain or alleviate” the impact of these same events in the future.

Stamp (Microgrid and Energy Surety expert, Sandia National Laboratories) discussed the operational character of the microgrid immediately following worst case scenarios in discussion with the author July 29, 2019. Stamp suggested that immediate recovery is much more significant in enhancing resilience than the longer-term performance of unserved critical loads. And given this focus on worst case scenarios, that it is not so much how the system is controlled minute-to-minute rather how it shifts from the Uninterruptable Power Systems (UPS) seconds after the disturbance, switches lines or

starts a generator, curtails less important loads, and manages storage considering forecast RE. This perspective could be argued as supporting the greater value to improving resilience in the microgrid’s design vs. its operations in that mostly all the behavior in the first few seconds following a disturbance should be automated and inherent with its design.

Arghandeh et al. (2016) use a resilience definition more focused on cybersecurity of networked power systems that confuses resilience and robustness as they relate to the value proposition; robustness, not resilience, is typically achieved through controls and operations.

An energy investment decision-making model developed for the Navy determined the attributes for resiliency (see Table 2). Teague et al. (2015) provide the attributes to define the category and represent the volatility and factors over the project’s life cycle. Teague et al. (2015) argue these attributes are more focused on operations of the power system vice design and appear to qualify as reliability more than resilience as it provides an indication of desired attributes for this economically driven approach. And although this model does assess multiple attributes it fails to include recoverability.

Table 2. Categories and relevant attributes of resiliency and cost measures per risk. Adapted from Teague et al. (2015).

Category	RISK	RESILIENCY	COST	POLICY
Attributes:	Natural disasters	Localized generation	NPV/TC	DOD
	Terrorist attack	Conservation		DON
	Commercial Grid Reliance	Priority Distribution		
	Fossil Fuel Consumption	Storage Ability		
		Repairability		
		Adaptability		

B. MEASURING RESILIENCE

Willis and Loa (2015) review resilience definitions from various perspectives to filter out those terms inconsistent in describing system characteristics. In this study, Willis

and Loa (2015) generated four main findings foundational to a common resilience definition and integral to measurements:

1. Resilience is a system's attribute in response to a disruption
2. The system's state is dependent upon both design and operation
3. The response to the disruption influences the costs to rebuild the electricity grid
4. Resilience is dependent upon the timescale

Hosseini, Barker and Ramirez-Marquez (2016) conclude that the literature on evaluating resilience is either qualitative or quantitative. Quantitative literature reviewed generated the deterministic and probabilistic measures that were evaluated for this research's models. A qualitative literature analysis is not incorporated in this research since a quantitative analysis is used instead.

Reliability measures, not to be used or confused with resilience measures, incorporate the System Average Interruption Duration Index (*SAIDI*) and System Average Interruption Frequency Index (*SAIFI*) of outages. *SAIDI* and *SAIFI* measures for reliability are described in Keogh et al. (2013) as

$$SAIDI = \text{total number of customer interruptions} / \text{total number of customers served} \quad (2.1)$$

$$SAIFI = \text{sum of all customer interruptions} / \text{total number of customers served} \quad (2.2)$$

Both are typically measured over a year, and despite having much less significance for an INI, are still measured and reported by NAVFAC. Reliability measures performance against potential low-impact high-probability (LIHP) events; resilience applies to HILP extreme events.

1. Inventory of Measures

In measurement theory there are five scale types that can be used for measurements: nominal, ordinal, interval, ratio and absolute. Each of these scales becomes more sophisticated proceeding from nominal to absolute. Giachetti (2003, 49) states that

measurement starts with defining the empirical system followed by defining a representative model.

Willis and Loa (2015) conclude that the only relevant measure is their resilience index derived from robustness, resourcefulness and recovery. There is no consideration of off-grid island microgrids. Despite being able to adapt these measures for an INI, they do not include disturbances other than loss of power from the utility provider. As such, this gap in having measures for off-grid microgrids remains. Despite not knowing how resilience measures would differ for an off-grid island, recoverability from a disturbance is constrained by the resources on the island. Local resources are not a constraint for an on-grid microgrid and therefore we argue has much greater significance for INIs.

Hosseini, Barker and Ramirez-Marquez (2016) group quantitative resilience measures into either generic or structural-based. The generic measures are either deterministic or probabilistic. The structural-based modeling can be either optimization, simulation, or fuzzy logic and will be discussed in Section D, Modeling Resilience.

a. Deterministic

Bruneau et al. (2003) create a deterministic measure derived from the resilience triangle to measure resilience loss (R).

$$R = \int_{t_0}^{t_1} [100 - Q(t)] dt \tag{2.3}$$

where $Q(t)$ is a measure of the quality of infrastructure to the community. This measure is rather unrealistic because it assumes that the system is always operating at 100% performance when the disturbance starts and in a microgrid typically the performance level is less than 100%, the capacity level, to have a cushion to absorb further increases in demand. Zobel (2011) also adopts this same measure and despite this measure being useful for the resilience triangle, it still fails to distinguish the states in the resilience function.

Rose (2007) calculates Dynamic Resilience (DR) as recovery without hastened (faster recovery due to more funding) conditions, SO_{WR} and recovery under hastened

conditions SO_{HR} . SO_{HR} is greater than SO_{WR} due to “hastening repair and reconstructing capital stock.” This resilience measure is more of an economic measure of resilience attempting to capture the resilience improvement resulting from greater investments.

$$DR = \sum_{i=1}^N (SO_{HR}(t_i) - SO_{WR}(t_i)) \quad (2.4)$$

N is the number of time steps. Hastening the repair is assumed to be made possible through investments and reconstructing capital. Although this is not a design decision, it still has relevance to this research given the relationships between investing in more maintenance and its improvement in repair times to be discussed further in Chapter III.

Francis and Bekera (2014) calculate resilience using a measure incorporating recovery speed S_p , performance level at the recovered state F_r , performance level at the original state F_o , and performance level immediately following the disturbance F_d .

$$\rho_i = S_p \frac{F_r}{F_o} \frac{F_d}{F_o} \quad (2.5)$$

The applicability of speedy growth in the S_p term to a RE microgrid is unknown given the example they created for a fictional electric power network wherein the assumed $S_p = 1$ but without any further explanation.

Henry and Ramirez-Marquez (2012) calculate resilience of the system state transition by taking a ratio of the recovery up to time t over the total loss of performance φ due to disruption e_j .

$$R = \frac{\varphi(t_r | e_j) - \varphi(t_d | e_j)}{\varphi(t_0) - \varphi(t_d | e_j)} \quad (2.6)$$

$(t | e_j)$ represents the proportion of performance that has been recovered from the disrupted state. This measure assumes recovery up to time t in the numerator, and the denominator is the total loss due to incorporating vulnerability and recoverability separately.

Orwin and Wardle (2004) calculate resilience by evaluating instantaneous and maximum disturbances using E_{max} as the maximum intensity of the force that can be taken

without disrupting the system's function, E_j is the magnitude of the disturbance's impact on safety at time T_j . R at time T_j can be between 0 and 1.

$$R = \left(\frac{2|E_{\max}|}{|E_{\max}| + |E_j|} \right) - 1 \quad (2.7)$$

This measure fails to incorporate any dynamic components of resilience by virtue of not incorporating time.

As argued by Henry and Ramirez-Marquez (2012), resilience dimensions characterize the state in relation to the disturbance event. An effective resilience measure therefore should rely on measures that capture these states. The use of the five dimensions that include recovery period, impact, performance loss, profile length, and weighted-sum as portrayed in Figure 6 to generate a measure as shown in Table 3 were more comprehensive in more completely characterizing performance than most of the other researchers in the literature.

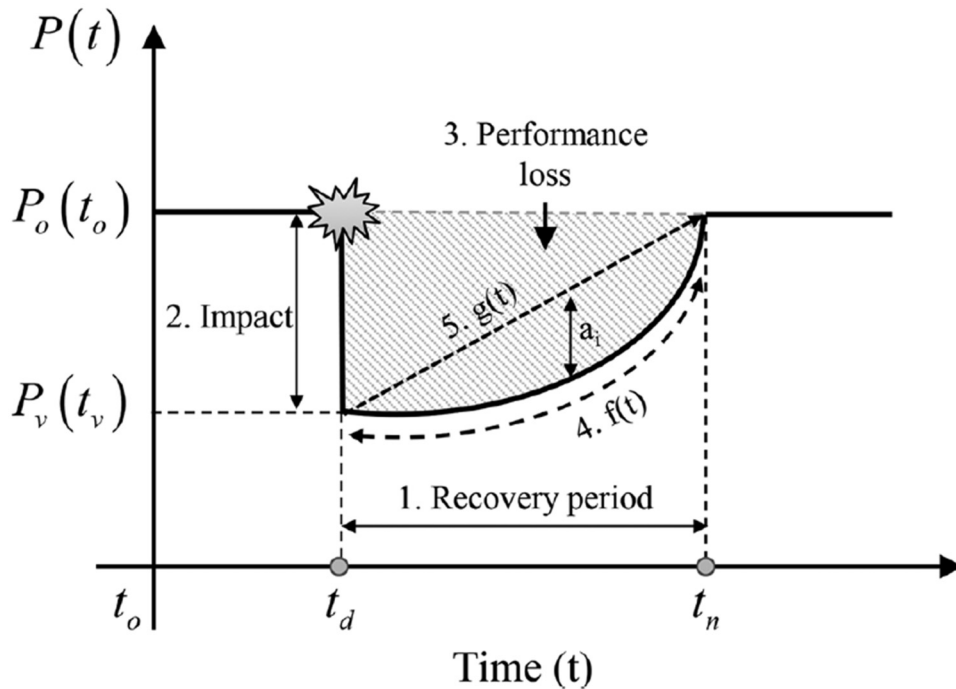


Figure 6. Five specific dimensions of *resilience*. Source: Yodo and Wang (2016).

Table 3. Five specific dimensions of resilience and their measures. Adapted from Yodo and Wang (2016).

Resilience dimension	Description	Equation
Recovery	Time required to return to the acceptable performance range	$t_n - t_d$
Impact	The severity impact on performance	$P_0(t_0) - P_V(t_V)$
Performance loss	Total performance loss in the area above the function $P(t)$ between t_n and t_d	$(t_n - t_d)P_0(t_0) - \int_{t_d}^{t_n} P(t)dt$
Profile length $f(t)$	The length of the recovery profile as it reaches the acceptable performance level	$\int_{t_d}^{t_n} \sqrt{1 + \left(\frac{dp}{dt}\right)^2} dt$
Weighted-sum $g(t)$	A time-dependent deviation weighted sum to capture the speed and shape of the recovery response	$\sum_{i=1}^n a_i [g(a_i) - p(a_i)]$

Munoz and Dunbar (2015), laid out an effective path starting with states, to corresponding dimensions with weighted measures to generate a resilience score:

$$\psi = w_1(\text{Recovery}) + w_2(\text{Impact}) + w_3(\text{Performance Loss}) + w_4(\text{Profile Length}) + w_5(\text{Weighted-sum}) \quad (2.8)$$

Zobel and Khansa (2014) determined that a shorter profile length is characteristic of a more resilient system. Munoz and Dunbar (2015) calculated optimized weights of each dimension using the path modelling process to maximize the model's variance. Munoz and Dunbar (2015) optimized weighting to avoid measures with arbitrary or equal weighting so as to decrease any risk of inappropriate aggregation.

Panteli et al. (2015) created the $\Phi A E I I$ (pronounced FLEP) measure, which segregates the resilience function into infrastructure resilience and operational resilience. Infrastructure resilience occurs first as the disturbance progresses and performance diminishes in Phase I. Then in Phase II in the post-disturbance degraded state the system no longer decreases performance and starts to recover. Operational resilience then occurs in Phase III during the restorative state. This measure comprises how fast (Φ) and low (A) resilience descends, how extensive the degraded state (E) is, and how quickly it recovers ($I I$). Φ and A are used to measure Phase I, E for Phase II, and $I I$ for Phase III. The mathematical expression for each of

these phases is simply the trapezoidal area during the timeframe of the respective phase. Panteli et al.'s (2015) model, however, fails to address how low the resilience can go.

Resilience measures of microgrids also include quantitative frameworks for weather-related disturbances Amiroun et al. (2019) and DC microgrids Liu, Lu and Wang (2019). Li et al. (2017) calculates resilience resulting from a disturbance and using the resilience function as

$$\text{Resilience} = \left(\frac{1}{\text{loss}} \right) \quad (2.9)$$

The performance loss of the system can be quantified as the largest deviation from a normal level where Q is the system performance

$$\text{loss} = \left(\frac{Q_o - Q_{\min}}{Q_{\min}} \right) \quad (2.10)$$

or the integration of the relative deviation for performance degradation as shown in Figure 4:

$$\text{loss} = \int_{t_1}^{t_4} \left(\frac{Q_o - Q(t)}{Q(t)} \right) dt \quad (2.11)$$

or to emphasize rapid recovery:

$$\text{loss} = \frac{1}{t_4 - t_1} \int_{t_1}^{t_4} \left(\frac{Q_o - Q(t)}{Q(t)} \right) dt \quad (2.12)$$

We believe the last measure emphasizing rapid recovery to be more comprehensive in fully capturing the resilience dimensions in that it includes both the dynamic and static resilience components that are not normally combined into one measure. However, the first term should be $t_4 - t_1$, not the reciprocal; otherwise as recovery time decreases, the loss would increase, and resilience would decrease.

Measures have also been proposed for pre-disturbance resilience to include average load loss ratio, probability of component failing, possibility of system islanding, generation and transmission margins. These measures have been applied to the microgrid being assessed while adjusting the hazard intensity (e.g., wind speed) Han et al. (2018). Again, for pre-disturbance, one is evaluating robustness, not resilience, as previously argued by Li et al. (2017).

The National Renewable Energy Laboratory (2019b) designates Value of Lost Load (*VoLL*) to be the most common measure to value resilience. National Renewable Energy Laboratory (2019b, 2) uses *VoLL* to approximate the “price that consumers are willing to pay for uninterrupted electricity.” *VoLL* ranges from \$1/kWh to \$300 kWh. *VoLL* will vary over time and by customer class and have a large range due to the range of attributes and context of outages; a grocery store will have much higher *VoLL* for the first few days of an outage but then will level off as there is less inventory that can spoil. Anderson et al. (2018) conclude that *VoLL* is difficult to calculate due to its being exogenous to the electricity consumer. Anderson et al. (2018, 10) assume *VoLL* at \$100 kWh and argue that *VoLL* should be calculated “as a function of the fraction of load met and number of hours that the critical load is sustained.” They also recommend that probabilities of RE damage, RE generation, and DG availability would provide more accuracy for *VoLL*.

Anderson et al. (2108) incorporate *VoLL* and L_c , the critical load served during the outage, to calculate a Value of Resiliency *VoR*:

$$VoR = VoLL \int_0^T L_c(t) dt \quad (2.13)$$

The utility industry assumes that the value of the lost load over time is determined at a fixed rate. Keogh and Cody (2013) argue that the value to the customers to have power restored is much greater one week after an outage than it is one hour after.

VoLL attempts to put a financial value on being able to avoid a power disruption. Military operations do not change in value based for similar reasons that we see for *VoLL*. In order for *VoLL* to be useful for a base commander at an INI, much further work must be done

to enable base commanders to state what they can pay for uninterrupted electricity for different categories of military missions. Budgeted allocations and mission priorities at the INI are evolving and competing constraints that complicate the ability to value uninterrupted electricity. This *VoLL* measure requires accurate forecasting of the critical load L_c , and it is expected that it would be very sensitive to the probabilities of damage.

To better place this research in context of the existing body of knowledge, this research in that it is focused on INIs, does not focus on on-grid utility centric strategies to assess resilience. Rather, this research will apply resilience and cost measures adapted for INIs to create a resilience and cost trade space. It is this trade space that will ensure that the resultant microgrid's performance behavior driven by different design choices and maintenance decisions is better understood in relation to the power capacity ratios and diversification of generation portfolio. And by applying this research's contributions to assess an INI's RE microgrid, the power capacity ratios, redundancy levels, and diversification of DER will be better understood than what is currently made possible by the literature.

This research will begin to explore the design space for microgrids knowing that more power capacity and diversification is better. What however is not understood is the relationship between power capacity, diversification, and resilience and costs. By being able to plot these relationships on a resilience and costs trade-off function for different microgrid architectures, it is expected that some ratios of power capacity and both amount and type of diversification will be more desirable to an INI's situation than others.

b. Probabilistic

Resilience measures that incorporate probability include one approach that measures resilience using two elements: loss of performance and length of recovery. Chang and Shinozuka (2004) evaluate the maximum acceptable loss of system performance r^* and maximum acceptable recovery time t^* :

$$R = P(r_0 < r^* \text{ and } t_1 < t^*) \quad (2.14)$$

This measure does introduce more realism than assuming the system has no uncertainty, by recognizing the uncertainty in quantifying resilience. Vugrin, Warren and

Ehlen (2010) also characterize resilience as a function of the uncertainty due to the probability and consequence of the disturbance to an attack.

We do have the ability to incorporate probability into resilience measures either using historical time series-data or to forecast future time-series data. Etienne et al. (2016) developed two agriculture industry resilience measures for droughts, based on probability of recovery from failure and the ratio of drought recovery time to drought time. Hashimoto, Stedinger and Loucks (1982) use the conditional probability of nonfailure at a future time given failure at an earlier time to suggest that there is a relationship between a system's reliability and its resilience. Although both offer a slightly different approach, they are both introduce probability over time and are useful.

Predictive modeling is used to forecast either system performance or factors influencing the system performance to measure resilience. Chanda and Mohankpurkar's (2018, 3680) code-based measure is developed for all time durations and includes both the outage duration and spatial impact. Their measure computed resilience several times for all outage durations and is a "temporal representation of resilience." Although forecasting the duration of the impact could be useful in an operations solution this research excludes forecasting in that design is the focus, not operations.

Several researchers introduce stochastic behavior into their models. Ouyang, Dueñas-Osorio and Min's (2012) resilience measure incorporates the stochastic behavior of the performance function as a time-dependent measure for measuring annual resilience of multi-hazards events. "Energy Infrastructure Resilience" (2015) similarly proposes that there are many probability density functions for the same system that reveal resilience for different threats and consequences.

The LT study modeled passenger counts for eleven passenger underground lines using a mean-reverting stochastic process that measured resilience as a function of both volatility and reversion rate by varying parameters for mean-reversion rate, mean-reversion level, and volatility. D'Lima and Medda (2015) grouped the results into behaviors representing different levels of volatility and resilience.

The disruptions in an underground line divert passengers and platform crowding to other lines. This disruption either increases or decreases the number of passengers depending upon the nature of the disruption. The passenger spikes will be gradual or steep depending upon the disruption's severity level.

The LT model calculates the resilience of the LT system to disturbances that include delays or disruptions in service. D'Lima and Medda (2015) simulate passenger counts on each underground tube-line using a mean-reverting process:

$$dX(t) = \lambda(\mu(t) - X(t))dt + \sigma dW(t) + dJ_t \quad (2.15)$$

$X(t)$ = Number of passengers on the line

λ = Mean-reversion rate (speed at which system can revert to normal following a disturbance which is proposed measure of resilience)

σ = Volatility of the process (controls randomness in the passenger numbers)

$\mu(t)$ = Mean-reversion level (time-dependent average level)

$W(t)$ = Brownian motion (randomness)

dJ_t = Jumps, severe disruptions

Using this approach, high volatility and mean reversion equate to an extremely resilient system. Although this research views recovery when subject to a more volatile disturbance as being very resilient, variability of a disturbance is well beyond the scope of this research. This measure of resilience is unique in that it places a higher value on a microgrid's ability to recover when facing a more volatile disturbance.

2. Nonquantitative Measures

There is robust literature available on nonquantitative measures that create conceptual frameworks tending to focus on capabilities (Kahan, Allen and George 2009; Labaka, Hernantes and Sarriegi 2015; Vlacheas et al. 2013; Bruyelle et al. 2014; Patterson et al. 2006; Vugrin, Warren and Ehlen 2011; Shirali et al. 2012a; Shirali et al. 2012b; Ainuddin and Routray 2012) and quantitative measures that assign a numerical value to different levels of

resilience (Cutter et al. 2008; Pettit, Fiskel and Croxton 2010; Shirali, Mohammadfam and Ebrahimpour 2013; Giachetti et al. 2003).

Shirali, Mohammadfam and Ebrahimpour (2013) use the one ordinal measurement to rank objects according to a criterion in that this measurement used the Likert scale which does not incorporate any mathematical operations. Pettit, Fiskel and Croxton’s (2010) measurement could be classified as interval, although defining the units does not define a zero element, in that they measured vulnerability and capability of supply chains using a weighted sum approach to 152 questions weighted by policymakers. Cutter et al. (2008) uses the ratio scale measurement to define the units and zero element using 36 resilience variables scored between 0 and 100 on a percentage scale to generate a total resilience index score. Each of these although having qualitative aspects, is a quantitative measure.

Li et al. (2017) differentiate resilience measures as measuring changes in system performance. In general, the differences in defining resilience, resiliency, reliability and robustness can be made by comparing the primary attributes and corresponding measures as shown in Table 4.

Table 4. Differences in measures for resilience, resiliency, reliability, and robustness.

	Resilience	Resiliency	Reliability	Robustness
Primary attributes	<ul style="list-style-type: none"> • Performance following HILP events • Static: ability to withstand a disturbance • Dynamic: ability to recover from a disturbance • Flexibility and survivability • Integrated in system's operational components 	<ul style="list-style-type: none"> • Typically implies dynamic resilience • Mostly synonymous with resilience 	<ul style="list-style-type: none"> • Performance following LIHP events 	<ul style="list-style-type: none"> • Resistance to change • Strength • Embedded in system design
Measures	<ul style="list-style-type: none"> • Increase in LCOE to continue to meet demand for t=14 days [%] • Generation capacity after disturbance/Generation capacity before disturbance [%] • Load loss ratio [%] • Reciprocal of microgrid performance [%] • Probability of failure [%] • Consequence of failure [\$] 	<ul style="list-style-type: none"> • Mean reversion rate [hours] • Ratio of recovery time to outage time [%] • Probability of recovery from outage [%] 	<ul style="list-style-type: none"> • SAIDI [hours] • SAIFI [interruptions/customer] 	<ul style="list-style-type: none"> • n,n+1,n+2

Lloret-Gallego et al. (2017) identify resilience characteristics of elasticity, plasticity, evolvability, adaptability in addition to the other attributes previously discussed that include vulnerability and recoverability. All of these characteristics should be pondered when asking if the microgrid will work when and how we expect it to despite catastrophic damage. And despite differentiating resilience, robustness, and reliability from each other, each characteristic is addressing this basic question from different perspectives.

C. ASSESSING RESILIENCE

Assessing resilience as used in this research is to take the multiple measures of resilience and contextualize them within a broader assessment to become actionable for decision makers to improve their microgrid's resilience. The term resilience when used to describe the model's results collectively includes all four of the resilience measures one of which is *resilience* the measure, one component of resilience. It is the assessment that is expected to be the actual informative and useful tool to permit decision makers to make their microgrid design choices. This research's models limit these microgrid design choices to the quantity, capacity and performance of the DER components: wind turbines, DG, Solar PV and battery, and the level of maintenance investment.

One can compare a resilience assessment to its resilience measurement used to make the assessment, as knowledge can be compared to the information used to generate the knowledge. The resilience measurement is used to assess the resilience. There are several examples of differing approaches to assessing resilience. Assessing resilience is more than measuring resilience; assessing evaluates the resilience measure to choose an preferred microgrid design.

Willis and Loa's (2015) observation that the resilience function's shape is a function of its design could also be used to assess resilience. By comparing the resilience function's shape to similar designs, one can decide to either accept the design as optimal or not. This relationship between design and resilience function shape could be useful in assessing resilience.

1. Energy Resilience Assessment (ERA) Tools

The Office of Secretary of Defense (OSD) has created an Energy Resilience Assessment Tool (ERAT). Figure 7 illustrates the eight steps to set up the simulation:

1. Make microgrid architectures (top left block);
2. Generate one year electrical and thermal load profiles (Critical Load Profile);
3. Generate one year of available solar energy for site latitude and weather (Resource Availability);
4. Generate failure rates for all technologies and systems based on models and input data (Reliability Model);
5. Simulate for one year (Monte Carlo Simulation);
6. Loop back to step 2, repeat several thousand times;
7. Average results for each architecture, calculate usage-based costs for grid power, solar PPA, and fuel consumption (Financial Model);
8. Plot all costs and unserved loads (Analyze Results).

The DOD has also created an Electric Resilience Assessment (ERA) Program-Distribution Tool using a notional Infrastructure Survey Tool (IST) Resilience Measurement Index dashboard for transportation facilities Ton and Wang (2015). Both tools primarily rely on critical load profiles.

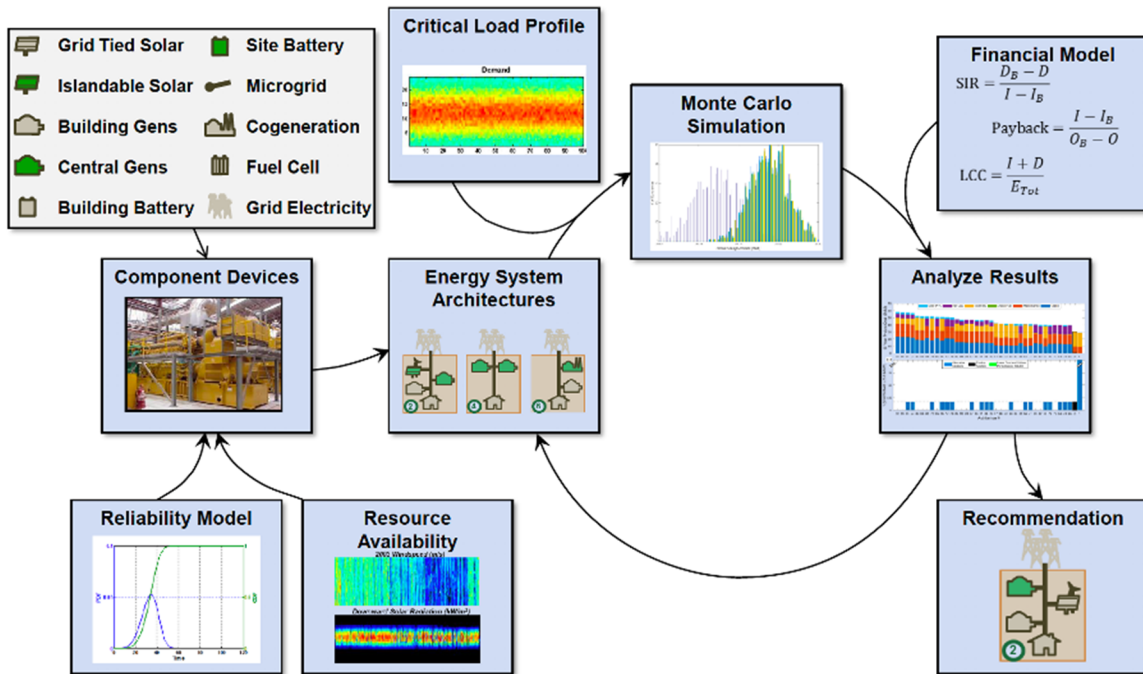


Figure 7. OSD’s Energy *Resilience* Assessment Tool emphasizing reliability. Adapted from Judson, Pina, and Whitehead (2018); Baxter (2018).

It should be noted that the OSD’s ERA tool actually provides decision makers with an assessed cost of reliability, not resilience. Although there are parallels here with the proposed research, there are also many differences. The ERA tool does not incorporate disturbances other than a utility outage; it does not use a measure that reflects both dynamic and static attributes of resilience; nor does it create tradeoff functions. Rather the ERA tool attempts to put a price on reliability without consideration for disturbances to microgrids inside the installation.

Judson et al. (2016) define resilience as occurring when losing the power from the grid. Other disturbances such as a cyberattack or extreme weather events are not studied. As a result, their assumption is that all operations continue on a military installation unless there is a loss of power from the grid. They have also assumed that the backup generation at the buildings will continue to be fueled and has been maintained.

Judson et al. (2016) conclude that centralizing diesel generation will improve resilience due to being able to interconnect the generation and operate in an islanded mode

from the local utility grid. They determine that PV and batteries will not provide resilience because the batteries would have to be extremely oversized to meet the load during utility outages. They did not consider the gensets' loading constraints which will influence the sizing of the gensets when coupled with RE. Finally, they define resilience for the longest potential outage with a binary assumption on continuing operations. Overall, despite generating trade-off functions for costs and resilience, their methodology will not be effective for INIs nor can it maximize resilience through design choices and maintenance levels. As a result, the ability to influence recovery time following the grid outage is not included in their framework.

Vugrin, Castillo and Silva-Monry (2017) developed a Resilience Analysis Process (RAP) for the DOE using measures of *outage magnitude* [customer days], *recovery costs* [\$], and *community impact* [# of assets] that could be adapted to generate Pareto frontiers of resiliency improvement costs vs. power outages. In that the outage magnitude is very much similar to SAIDI, this is more a measure of reliability than resilience.

2. Energy Security Assessment Tool (ESAT)

Of particular relevance to this research is the Navy's ESAT. Although the ESAT fails to define resilience, the Department of the Navy (2017, 5) does address it: "Resiliency depends to a great extent on the level of partnership with commercial utilities, distributed generation capacity, and grid and microgrid configurations." The Department of the Navy (2017b, 19) describes generation and microgrid planning that should "encompass a wide range of objectives ranging from serving the entire installation to optimizing secondary uses (such as steam or chilled water) and providing adequate "islanding capacity."

The need to clearly define resilience and incorporate measures that reflect the Navy's priorities in funding investments that strive to improve resilience could not be more clearly highlighted than by the ESAT tool. Between not having resilience adequately defined, using measures that do not provide any real indication of meeting the notional definition, incorporating subjective measures, and not being able to incorporate RE generation, it can easily be argued that this tool can be improved. This dissertation's research strives to improve upon the ESAT tool.

The ESAT needs input data for an installation's facilities required to have backup generation. This data includes the following requested input-fields in an Excel spreadsheet:

1. Facility Peak Load;
2. Quantity of Facility-Connected Generators;
3. Standby/Emergency Generator Capacity;
4. Maintenance;
5. Testing and condition of the generator(s);
6. Days of fuel the facility has on site at peak generator capacity;
7. If facility has equipment that requires a UPS;
8. If UPS is required;
9. Rate the maintenance;
10. Testing and condition of equipment;
11. Make;
12. Model;
13. Installation Year;
14. If has Automatic Transfer Switch;
15. Fuel Type;
16. Plant Replacement Value;
17. Annual Generator Maintenance Costs.

From this data three scores are calculated and weighted to generate an overall resilience score.

The Department of the Navy (2017) creates their own resilience score computation by summing and arbitrarily weighting three components:

R = Resilience score

1. B = Backup Generation (bg) capabilities score:
 - Percentage of facilities required to have on-site bg that do not have bg;
 - Maintenance, testing and condition score of the facility level generators;
 - Percentage of generator capacity to peak load;
 - Percentage of facilities with bg requirements that do not meet requirements for fuel sourcing
2. U = Uninterruptable Power Systems (UPS) capabilities score:
 - Percentage of facilities required to have UPS installed that do not have the requisite UPS and a maintenance;
 - Testing and condition score of the facility level UPS
3. S = Supported mission resiliency score: the number of facilities deemed to not have sufficient resilience.

$$R = .65B + .25U + .1S \quad (2.16)$$

Applying the ESAT tool to SNI's microgrid generates a resilience score of 72 as illustrated in Figure 8. The three components contributing to the resilience score: percentage of backup generation, percentage of UPS, and sufficiency of missions' energy resilience are weighted and summed to calculate the score.

2. RESILIENCY			
2.1	What percent of the installation's facilities that require energy resiliency have sufficient capabilities in place?	Score	
		65	
		Answer	Weight
2.1.1	How many facilities are required to have on-site backup generation according to their FAC Code, BFR, or other formal requirement?	10	0.4
2.1.2	How many facilities identified in response to 2.1.1 DO NOT have the requisite on-site backup generation?	0	
2.1.2.1	What is the installation's average score for meeting requirements of backup generation with sufficient capacity that is regularly maintained and tested?	FALSE	0.25
2.1.3	What is the total peak load for the facilities with requirements for on-site backup generation?	150	0.1
2.1.4	What is the total backup generation capacity installed at the facilities identified in	1211.8	
2.1.5	Percentage of facilities with backup generation requirements DO NOT meet requirements for fuel sourcing?	0	0.25
2.1.5.1	How Many facilities do not store more than 7 days of fuel?	0	
2.1.5.2	How many facilities do not have a fuel service plan?	0	
2.2	What percent of the installation's facilities that require UPS have sufficient capabilities in place?	Score	
		75	
2.2.1	How many facilities are required to have UPS installed?	1	0.75
2.2.2	How many with a UPS requirement do not have the requisite UPS?	0	
2.2.2.1	What is the installation's average score for meeting requirements for UPS with sufficient capacity that is regularly maintained and tested?	FALSE	0.25
2.3	Are there supported missions that do not have a sufficient level of energy Resiliency?	Score	
		100	
		Answer	Weight
2.3.1	Are there supported missions that do not have a sufficient level of energy Resiliency?	1	1
2. RESILIENCE			
Resiliency is focused primarily at the facility level ensuring that the most critical facilities will be able to continue normal under operation under conditions without grid power. Generation and microgrid planning can optimize the backup generation and distribution of power to critical facilities and providing adequate "islanding" capacity.			
		Score	
		72	
2.1	What percent of the installation's facilities that require backup generation have sufficient capabilities in place?	65	0.65
2.2	What percent of the installation's facilities that require UPS have sufficient capabilities in place?	75	0.2
2.3	Are there supported missions that do not have a sufficient level of energy resilience?	100	0.15

Figure 8. ESAT *resilience* score for SNI suggests SNI has poor *resilience*. Adapted from Department of the Navy (2017a).

These results for SNI confirm that the ESAT tool is not designed or intended for an isolated location. With six-fold generation capability over demand at SNI, resilience is still only just over 70%. There is no consideration for recovery or vulnerability. Additionally, this tool does not allow for any RE generation. Finally, the ESAT tool does not reflect the

remoteness of SNI and the corresponding impact on attempting to maintain and refuel backup generators at each facility. The ESAT generates a visual display tool to provide an overall sense of where investments could be made; see Figure 9.

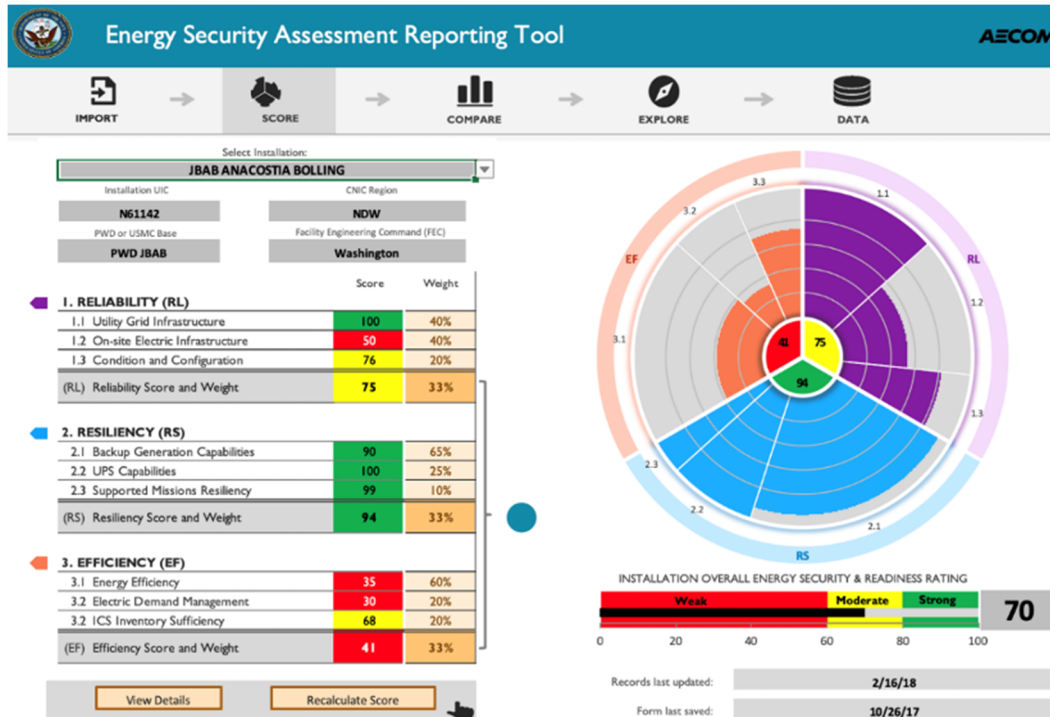


Figure 9. Energy Security Assessment Reporting tool highlights emphasis on backup generation. Source: Department of the Navy (2017a).

The ESAT tool does not apply to INIs because it assumes that there is no microgrid and the disturbance is limited to an outage from the utility grid. This tool primarily equates resilience to the installed capacity of backup and UPS to meet peak load. It does not create a meaningful definition that differentiates resilience from reliability through ability to both withstand and rapidly recover from unexpected disturbances. The ESAT does not address disturbances nor does it incorporate either actual or historical time series generation data. Adopting the ESAT approach will also not permit varying fuel consumption based upon generator loading nor factor in any costs such as *LCOE*. There is also no functional or meaningful power plant model. Perhaps the biggest shortcoming is the ESAT tool neither incorporates measures that reflect the definition and/or objective nor does it generate any

cost information to inform decision makers on the associated costs to increase the ESAT resilience score.

3. Incorporating Costs

Faraji et al. (2019) measured resilience and costs of two microgrids to highlight the relative effectiveness of the two microgrids. Their resilience measure is survivability, or unmet load in kWh/year. Faraji et al.’s (2019) research evaluated a grid-connected RE microgrid and an off-grid backup DG. They found no difference in resilience but the RE had lower costs. Although their assessment did consider costs and resilience, they did not consider a disturbance other than a blackout due to a power disruption from the utility provider. In that they did not assess an off-grid RE microgrid, nor incorporate a disturbance to the other off-grid microgrid, their study is useful for validation but still did not address these two gaps, off-grid RE microgrids and disturbances damaging islanded off-grid microgrids.

4. Other Tools to Assess Resilience

There are other microgrid resilience assessment tools, but none have been tailored to an INI or combine the costs with their assessment. The major approaches with the different tools are compiled in Table 5.

Table 5. Tools to assess microgrid resilience.

Approach	Tool	Measures	Findings	Citation
Energy security	OSD’s ERAT	Cost of reliability	Ability to influence recovery time following the grid outage is not included in their framework	Judson, Pina and Whitehead (2018); Baxter (2018)
	DOD’s ERA	Outage magnitude recovery costs, and community impact	Pareto frontiers of resiliency improvement costs vs. power outages	Ton and Wang (2015)
	Navy’s ESAT	Reliability, Efficiency and Resilience	Equates resilience to the installed capacity of backup and UPS	Department of the Navy (2017a)
Quantitative	Recovery Index	Load power restored/restoration time	Microgrids improve recovery rate and hence resilience	Mathew et al. (2016)

Approach	Tool	Measures	Findings	Citation
	Level of Resilience	Sag voltage percentage, reduction in load served, recovery time	Placement of microgrid resources affects resilience	Ibrahim and Alkhraibat (2020)
	Resiliency Vector	Degree connectivity	Resiliency is multi-objective optimization problem	Chanda and Srivastava (2015)
	Code based measure	Fraction of load unaffected by voltage or current distortion	Reliability factor is influenced by design	Chanda and Mohanpurkar (2018)
	General measure	Performance and time driven	Does not provide insights into points of failure, triggers, probabilities of failures or triggers, and asset conditions	Yodo and Wang (2016); Borisoglebsky and Varga (2019)
Probabilistic	Fragility functions	Failure probability as a function of weather	System resilience can be quantified to intensity of extreme weather	Hussain et al. (2019); Panteli et al. (2017b)
	Probabilistic analysis with uncertainty factors	Semi-quantitative uncertainty factors	Analytical output and implications for decision making are not necessarily consistent between approaches	Shortridge et al. (2017)
	Probability Bounds Analysis (PBA)	Aleatory uncertainty being represented using probability distributions, and epistemic uncertainty being represented using intervals		
Robust decision making	Uncertain input quantities			
Qualitative	Physical components and socio-economic dimensions	Resilience indicators for each dimension	Takes new elements, actors and roles into consideration	Lloret-Gallego et al. (2017)

D. MODELING RESILIENCE

Off-grid RE microgrids that have employed optimization models are presented to demonstrate how optimization has been used to reduce costs and maximize penetration of RE. Optimization, simulation and fuzzy-logic models are presented to demonstrate

circumstances in which different modeling approaches are most suitable for particular applications.

1. Optimized Off-Grid RE

There are many examples of off-grid RE microgrids that have been modeled and optimized, primarily for to minimize costs. Bates (2011) evaluated HOMER as a model of the power system at Lord Howe Island, Australia with inputs of demand and generation to conduct a financial analysis of six architecture options. Guevara-Stone (2015) studied Kodiak Island, Alaska where 99.7% of the power is provided by wind and pumped hydro. They conducted an extensive grid integration study to ensure the successful integration and maximum penetration of renewables could not only be attained but also be optimized.

The U.S. Department of Navy (2013) incorporated RE integration optimization models on DGAR, BIOT. A Sonic Detection and Ranging (SODAR) analysis demonstrated that wind turbine generation would support the microgrid solution more than PV generation and as much as 56% penetration of RE onto the microgrid solution can be obtained through 2 MW of PV, 2.2 MW of wind using no energy storage (demand response will be used), and a controls system.

Okinawa Electric Power Company (2012) confirmed that a 1 to 4 ratio of battery power to PV power is ideal to stabilize the PV power on Miyako Island, Japan made-up of 4 MW of solar PV, 4.8 MW of wind, 74 MW of oil and gas generation, and 4 MW battery storage. Kim (2015) found that on Gasa Island, Korea which is fully renewable, wind, PV, battery storage, and an energy management system were introduced to reduce the power generation costs by \$300K per year from previous diesel generation. Not one of these models or optimizations is done for resilience.

2. Optimization Models

One optimization in the literature maximized resilience and presented costs and repair times trade-off functions for airports. Faturechi, Levenberg and Miller-Hooks (2014) created an optimization model to maximize airport resilience. This model used a resilience measure as the ratio of take-off and landing capacities after vs. before the disruption. This

model incorporated both pre- and post-disturbance decision variables. This model presented resilience trade-off functions in budget vs. maximum repair times that can be adapted and applied to RE microgrids.

Vugrin, Turnquist and Brown (2014) proposed multi-objective optimization models for transportation networks. Their model seeks to maximize resilience while minimizing network flows, costs, and unmet demand. Although this resilience model could conduct multi-objective optimization this is outside the scope of this research.

Paasch (2016) at the University of Southern Denmark compared the optimization “potential advantage of applying string inverters with multiple Maximum-Power-Point-trackers (MPPT) in large PV plants compared to the use of one large central inverter with one MPPT.” Paasch (2016) conducted a comparative investigation of non-uniform irradiation events caused by moving clouds over a full year and sorting of the PV panels during construction and estimated an increase in the annual energy production by approximately 0.4%. This optimization incorporated irradiance forecasting with the objective function to maximize PV energy. Alzahrani et al. (2017) also used predictive modeling to forecast generation of solar PV to optimize a microgrid to reduce the grid consumption by maximizing the penetration of solar PV onto the grid. Alzahrani et al. (2017) despite showing that solar PV could be forecast using neural networks, did not either articulate or sufficiently demonstrate the benefit of forecasting.

There are several examples of modeling energy systems. One approach developed by NREL is an Integrated Energy Systems Model (IESM). The IESM used a System-of-Systems approach to modeling the complexities of an electrical grid with DER. Mittal et al.’s (2015) IESM incorporated a Home Energy Management System (HEMS) optimization engine with the objective to minimize the house’s cooling costs using constraints on comfort of the occupants by setting maximum and minimum acceptable temperatures for the home.

Xendee is a RE microgrid modeling tool for conducting multi-objective optimization. Xendee does not incorporate resilience into its objective functions. Rather, Xendee defines outage scenarios for the utility to determine the impact of decision making.

Outage costs in \$/kWh are allocated to the outage times and then Xendee can curtail the load at the specified costs, oversize the technologies or make new decisions. The outage costs change the *LCOE* costs depending on if Xendee decides to curtail or oversize certain technologies. This model provides greater benefits to INIs in that a base commander will understand how much resilience they can afford.

Those who have studied optimal design of RE microgrids for remote locations fail, however, to discuss resilience (Scioletti et al. 2017; Nejabatkhah et al. 2018; Kaur, Krishnasamy and Kandasamy 2018; Fathi, Beshr and Eteiba 2015; Goel and Sharma 2017; Sawle, Gupta and Bohre 2018; Garcia 2017; Mizani and Yazdani 2009; Katsigiannis, Georgilakis and Karapidakis 2012; Tucker and Negnevitsky 2011; Singh et al. 2015; Karimi and Kaserani 2017). Most all are optimizing to primarily minimize costs and some for carbon footprint. No one is optimizing to maximize resilience.

3. Simulation Models

Ross (2018) highlights the challenges of operating in islanded mode as shown by modeling a DC microgrid using SIMULINK. Simulations were run using a model for a microgrid employing a battery and implementing a super capacitor implementing a high energy storage system (HESS) in both grid connected and islanded modes. The conclusions indicated that the HESS reduces energy losses twice as much in grid-connected mode vs. islanded mode.

Alderson, Brown and Carlyle (2015) modeled operational resilience of a fuel delivery system. Using this model, they were able to assess operational resilience, identify critical vulnerabilities, and advise policymakers on investments to improve resilience. Yodo and Wang (2016) contend that while in the design phase, assessing a system's performance for operations is challenging. This is the primary reason they believe there is such little literature on the methodologies and tools for assessing resilience in the design phase. Although modeling is useful for operational resilience assessments, there is no evidence in the literature reviewed of how it has influenced microgrid design choices.

4. Fuzzy Logic Models

Muller (2012, 370) “estimates infrastructure architecture resilience using fuzzy logic.” Fuzzy logic is more powerful in accommodating the inherent ambiguity found in the interdependent functional relationships found between infrastructure systems. Further evaluation of the power of fuzzy logic to better handle these interdependent relationships is needed given the inherent proclivity of power systems to be more vulnerable to cascading failures. Although fuzzy logic is beyond the research scope, fuzzy logic optimization tools could be more useful than multi-objective optimization primarily due to the ambiguity created by the combined and unpredictable weather and demand profiles at INIs.

E. MEASURING COSTS

There are numerous cost measures in the literature. Most cost measures are life cycle costs and some cost measures also incorporate energy. The two most common are reviewed: Life Cycle Cost Analysis (*LCCA*) and Life cycle Cost of Energy (*LCOE*)

The International Renewable Energy Agency (2020) defines *LCOE* as the price of electricity required to ensure that revenues equal costs to include making a return on the investment at the WACC. Although a Naval installation receives revenues from utility payments paid by its building tenants, *LCOE* is still useful even though the revenues do not have to equal costs for the Navy. It is the utility provider’s need to ensure revenues cover costs that drove the creation of *LCOE*. *LCOE* conducts a net present value (NPV) calculation of both costs and electricity generation throughout the economic life of the DER. The NPV of the energy brings the future value of energy back to a present value using the same WACC to discount the future energy as used for costs.

Aldersey-Williams and Rubert (2019) state that *LCOE*’s promotion by NREL, the U.K. government, Lazard, and Ernst and Young helped create its widespread adoption and acceptance. However, there has been no previous theoretical review of *LCOE* in the literature. Aldersey-Williams and Rubert (2019) argue that *LCOE* must be cautiously applied and thoughtfully used given its sensitivity to WACC, inflation and future fuel prices.

LCOE when used by itself is inappropriate for a microgrid on an INI because the *LCOE* assumes that all energy generated, even beyond the energy consumed by the loads, can be sold otherwise the International Renewable Energy Agency's (2020) requirement that all revenues equal costs will not be met. Lotfi and Khodaei (2016), and the International Renewable Energy Agency (2019), calculate *LCOE* using the full capacity for electricity generation. However, a microgrid on an INI and most islands has no market to sell excess energy; consequently, including it in the discounting will underestimate the actual cost of the energy used.

The Department of Defense (2020a) has issued recent guidance to assess all energy resilience funding proposals to the Energy Resilience and Conservation Investment Program (ERCIP) using a *LCCA*. Although *LCOE* is different than *LCCA* due to discounting future energy, *LCOE* is still a useful measure of life cycle costs for microgrid INIs to allocate financial value to the excess energy capacity.

F. DISCUSSION AND CONCLUSION

The authors and papers most closely related to this research's resilience measures comprise Francis and Bekera (2014) for their invulnerability measure. We adapt their measure to the *invulnerability* measure in Chapter III. Their measure is similar to this research's *invulnerability* measure by also taking a ratio of the post disturbance performance level to the preperformance disturbance level. The primary difference is their measure also incorporates a speed recovery factor and a ratio of the post disturbance performance after recovery efforts to the preperformance disturbance level. This research did not separate the post disturbance performance level into two levels, rather just one. Although it is conceivable there could be different levels of performance following a disturbance and before full recovery, the benefit of introducing a speed recovery factor and another level of post disturbance performance is not considered worthwhile considering the added complexity to the model.

Renschler et al.'s (2010) approach to measuring resilience influenced the adaption of this research's *recovery* measure. This research also calculated the area beneath the post-disturbance performance curve. However, Renschler et al. (2010) used this area as their

resilience measure. Whereas this research adapted this measure further by taking a ratio of the area bounded between the post disturbance power generation curve and a constant level of pre-disturbance demand divided by this demand, and then subtracted from 1. Although Renschler et al.'s (2010) approach is related to this, it does not have a fixed range of values as this research's measure does, from 0–1, nor does it factor in the predisturbance level of performance. Both are considered essential when combining this adapted measure with the *invulnerability* measure as done in this research to create a measure of *resilience*, ξ .

Panteli et al.'s (2015) ΦAEP (pronounced FLEP) measure and how it segregates the resilience function into infrastructure resilience and operational resilience is also useful to this research. Panteli et al.'s (2015) research is similar in that it also calculates the speed of recovery and how extensive the post-disturbance degradation is. However, Panteli et al. (2015) is focused on grid-connected power systems and therefore uses number of lines tripped and number of lines restored in all but one of their four measures.

The authors and papers most closely related to this research's cost measures includes Anderson et al.'s (2018) Value of Resiliency *VoR* work. Anderson et al.'s (2018) research is much closer to this research's focus in terms of emphasizing RE power systems and attempting to monetize the impact of not being resilient, the *VoLL*. This work although very good to see another research effort to develop a measure for resilience that could be applied to RE microgrids, cannot be applied to INIs due to the base commander's inability to forecast or even place a value on lost loads presently.

Vugrin, Castillo and Silva-Monry's (2017) Pareto frontier of resiliency improvement costs vs. power outages is the closest to generating an equivalent trade space. Vugrin, Castillo and Silva-Monry's (2017) developed a resilience assessment process, for grid-connected systems. Their process also proposed creating pareto frontiers for mapping resilience costs to resilience measures. Their research did not actually accomplish this concept but created the idea to explore this further.

Willis and Loa's (2015) finding that the resilience function's shape is depending on its design helped shape the direction of the experiments. This concept pushed the direction of this research to better visualize the behavior of microgrid over time. Although Wills and

Loa (2015) did not present 3D graphs, nor do the analysis conducted in this research, their instinct that the shape of the curves is a byproduct of the design is very much at the essence of this research.

And finally, Trout's (2020) findings relating *MTTR* to different maintenance levels are extremely useful in providing the linkage between the maintenance level chosen in the cost model and its relationship to *MTTR* and time to recover in the resilience model. This research combined with Thompson et al.'s (2018) findings as they related maintenance to reliability resulting from equipment failures, is essential in forming the logic incorporated into the resilience and cost framework to link *MTTR* and time to recover.

This work differs from the literature first and foremost in its focus and application on INIs, a very narrow subset of remote island communities. Specifically, defining resilience and costs appropriately for an INI, subjected to HILP disturbances, is different than the literature. Additionally, this work differs from the literature by its adaptation of its cost model so as to not inaccurately value the generation serving the demand; the microgrid's power generation at an INI does not create revenues. Finally, the work done in this research links investments in maintenance to microgrid time to recover in a way that provides a more closely inter-connected resilience and cost trade space. This difference from the literature is pronounced as demonstrated by the contributions created providing the measures, decision-making tool, and trade-off functions that are otherwise not applicable to INIs in the literature.

This chapter presents the most relevant literature on resilience to demonstrate how researchers have shaped and informed a logical approach to assessing resilience. Resilience is defined by first portraying the behavior of a microgrid system subjected to a disturbance through the Microgrid Resilience Function before identifying the states and the associated dimensions for each of these states. State-driven dimensions are then used to define resilience. Then, the literature on measuring resilience shapes the proposed resilience measures so as to more realistically capture the behavior of the resilience function consistent with the adopted definition. The resilience measures developed and used in this research's models reflects this approach by calculating the behavior of the resilience

function that ultimately inform the assessment. Specifically, the literature influenced the state-driven dimensions, invulnerability equation, and recovery equation the most.

The literature reviewed and presented suggests two main themes. The first theme is that resilience is multi-dimensional, yet there has been no agreement on how to capture all the attributes of resilience in one score. The second theme is that resilience is influenced through design, operations, or both.

There are three obvious gaps in the research. The first is that cost and resilience measures are required for off-grid microgrids on islands having disturbances. The second gap is that resilience of off-grid microgrids on islands subjected to disturbances has not been studied, so it is not obvious how resilience is defined, which resilience and cost measures are meaningful, and which measures can be applied to INIs. The third gap is trade-offs in resilience and costs are needed to understand their relationships for different microgrid choices. National Renewable Energy Laboratory (2019b) did assess resilience vs. *VoLL*, but *VoLL* nor *LCOE* are neither ideal nor appropriate for INIs because there is no external utility provider. *VoLL* does not apply to military operations the same way it does to a grocery store or other grid-connected loads. Hamilton et al. (2016) did not generate a resilience measure for microgrids; rather, broadly considered analytics as to how they can influence resilience and *LCOE*. Hamilton et al. (2016)'s sensitivity analysis of *LCOE* to fuel prices, cost of lost mission, availability of RE credits, and availability of biofuels showed that *LCOE* is most sensitive to the fuel prices. While Hamilton et al. (2016) added to the literature in a useful way, their research left open work in defining resilience or incorporating data, and therefore did not answer how to measure resilience.

Recent studies have focused on microgrids and typically one or more performance capabilities. The overarching theme is that resilience is different from reliability due to the probability of the disturbance and its resultant impact. The trends and patterns in the literature suggest that the resilience function captures and contains any or mostly all dimensions of resilience, but not the linkage of these dimensions to the life cycle costs.

Although there is some debate about how important probability of the disturbance is, attempting to assess resilience using probabilities of disturbances is beyond the scope

of this research. Proponents of using the probability of disturbance argue that a more realistic determination of the disturbance happening is needed to prioritize which threats to design the microgrid's resilience. Those that place little value on this probability believe that differences in the probability of a threat striking has little benefit to designing a microgrid for resilience because without a disturbance there is no need for resilience. In this research, the probability of damage is calculated given that a disturbance occurs.

Munoz and Dunbar (2015) weighted measures to generate a resilience score coupled with Panteli et al.'s (2015) ΦAEP measure are most compelling to create a resilience measure for INI microgrids; they each created measures that are applicable to INIs and are complete in reflecting the full performance behavior for a resilience assessment. Their approach most clearly articulated an overall resilience score that fully captured the dimension of the respective state and will be used to influence the resilience measures used for INIs.

Despite significant work done to define resilience of power systems in recent years there is only a fraction of microgrid research into resilience. It is important to differentiate microgrids as a subset of power systems when defining resilience due to different capabilities and opportunities that effect their behavior following a disruption. The behavioral differences directly relate to the system's resilience. A microgrid's ability to recover from a disturbance is much more constrained than due to being off-grid and on a remote island such as an INI. As such, one must understand microgrids' behavioral differences from generic power systems before applying general power systems' resilience definitions to remote island locations.

Measuring and assessing resilience for islanded microgrids is different primarily due to the nature of the disturbance and the ability of an off-grid microgrid to recover. On-grid resilience measures and cost equations can be applied to off-grid islanded microgrids, but they will have different outcomes due to greater probabilities of damage to the DER from the disturbances and recoverability being impacted by multiple repair times for the different DER components. This research incorporates non-islanded resilience measures, adapts a cost equation to an off-grid island, and introduces the maintenance level into the resilience and cost models for disturbances other than loss of power from the utility.

Although there are numerous efforts to create resilience measures for power systems, there is a clear gap in both defining resilience and measuring it for off-grid islanded microgrids such as INIs. No researchers have proposed any known resilience measurements for INI RE microgrids. Similarly, this research failed to identify literature measuring resilience and generating trade-off functions for resilience and costs. All of this suggests that a resilience measure that captures the area under the resilience function will be deemed particularly practical and useful to decision makers when conveyed through resilience and costs trade-off functions for different microgrid design and maintenance options.

THIS PAGE INTENTIONALLY LEFT BLANK

III. INI RE MICROGRID RESILIENCE AND COST METHOD

This chapter presents a method for assessing the adequacy of a microgrid design to deliver resilience cost effectively. This method will ensure that an INI's base commander will know the price of resilience and can make more informed decisions before investing in a microgrid. The method's steps for implementing the models are presented in Section A. Cost and resilience models to measure an INI RE microgrid's performance are presented in Sections B and C, respectively, followed by a short discussion and conclusion in Section D.

A. METHOD

This method generates a trade-space of design alternatives to better enable a decision-maker to choose the microgrid architecture considering the acceptable combination of resilience and costs. This research generates tradeoff functions of the resilience and costs for the respective disturbance to help base commanders determine their appetite for resilience.

To implement this method, the model operator, henceforth modeler, must have previously selected an installation site for a microgrid based upon investor-driven criteria. The modeler compiles demand profile time series data as well as obtains a complete understanding of power generation capacity, type, maintenance costs and location of each DER. The modeler also establishes the conditional probability of damage to DER for a specific disturbance at the microgrid location. The modeler should implement this method in five basic steps: gather data, generate disturbance scenario, establish resilience and cost baseline, simulate microgrid system, and select preferred microgrid design.

1. Gather Data

The first step is to gather data to use as input variables. Historical demand profile data and DER design parameters are both required to make the model work.

Historical demand profile data includes the time series consumption over a certain time frame. The modeler must obtain time series interval data not to exceed one hour, for

at least one full day and ideally two weeks at the INI. The historical demand profile data does not have to be exactly hourly real data; if it is not available then the modeler must create and input a realistic time-series demand profile data to ensure the model is accurate for the INI's demand. The model will accept up to two weeks of historical demand profile data.

The modeler should gather the associated generation data for each DER to provide the exact values for each of the model's input variables, which include, the power rating, fuel consumption for diesel gensets, availability for wind turbines, and so on (see section B1, "Cost Model Nomenclature" and section C1, "Resilience Model Nomenclature"). DER data is crucial for the model to work; without this information the model's results will not be accurate for the INI's microgrid.

As might be expected, when gathering data, accuracy of some input variables is more important than for others—for example, weighted average cost of capital is more important than O&M costs for the cost model; for the resilience model, the wind turbine's time to repair is the more consequential variable. Expending effort to obtain exact information is more important for the input variables the measures are more sensitive to.

2. Select Disturbance Scenario

The modeler should select a disturbance scenario S_k that is the greatest concern for the INI. Only HILP scenarios will be used in that LIHP disturbances apply to reliability measures, not resilience. HILP disturbances include hurricane, earthquake, wildfire, tsunami and cyberattack. There are many others that could also be classified as HILP, known, and unknown; however, for the purpose of this research these disturbances are considered more likely than others. Once the disturbance is chosen, the probability of damage $P(d|S_k)$ for each DER must be chosen. The probabilities can be obtained from subject matter experts or if that not an option, then other performance information when subjected to this disturbance that is deemed realistic can be used.

3. Establish Resilience and Cost Baseline

In order to compare resilience and costs of alternative microgrid architectures to the installed microgrid at the INI, we must first assess the installed microgrid for resilience

and costs. The model uses the data and scenarios from the previous steps to calculate the resilience and cost measures. In this dissertation resilience includes each of the four resilience measures: *recovery*, *invulnerability*, *resilience*, and time to recover. Each of these resilience measures, and cost measures form the baseline for comparative analyses with alternative design and maintenance options.

Figure 10 outlines these sequential steps.

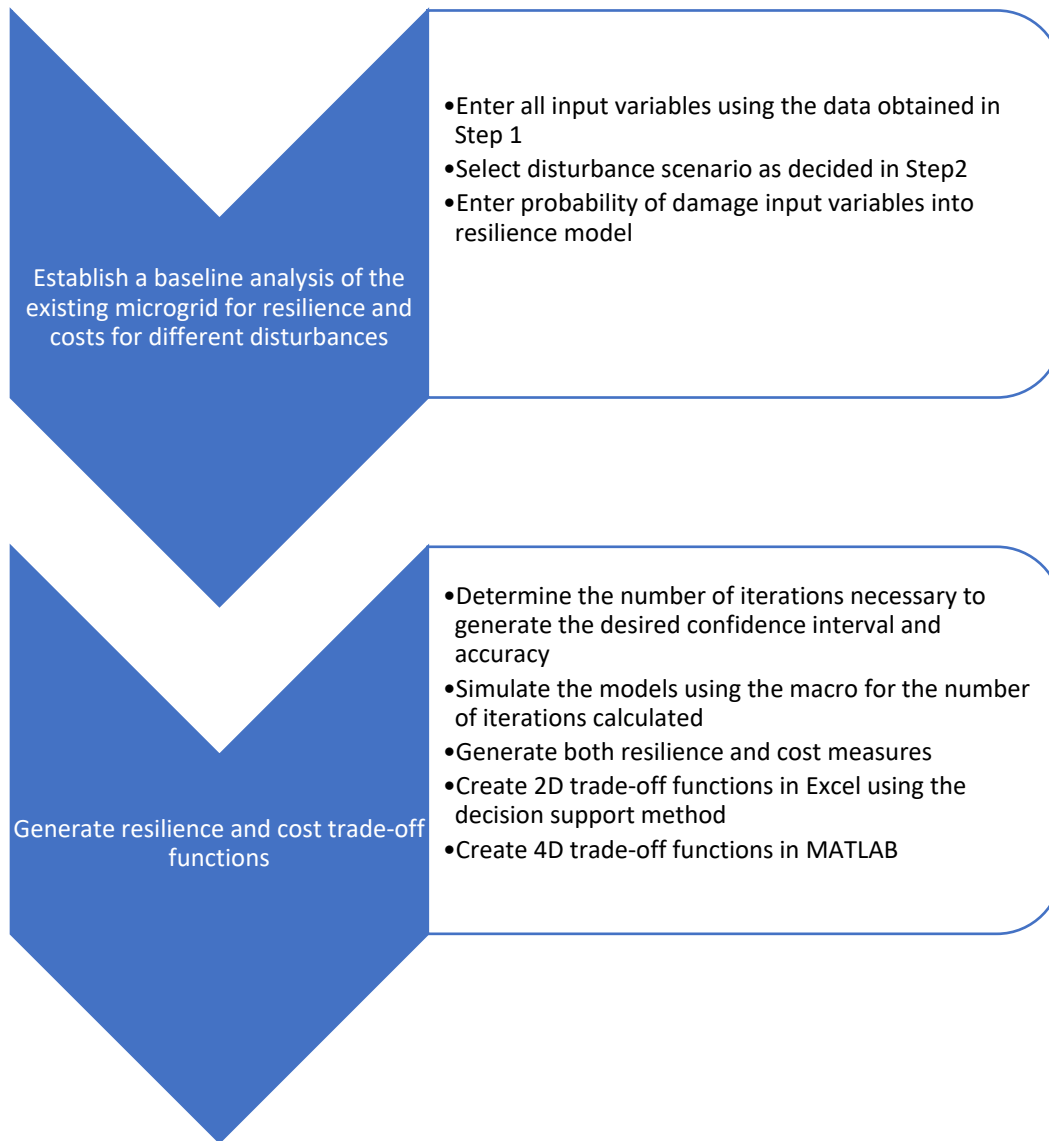


Figure 10. Steps to establish *resilience* and cost baseline.

4. Simulate Microgrid System

The modeler creates a model with the information from the previous steps. The modeler then simulates the model for different microgrid system architectures. The modeling approach is described in detail in Sections B and C. The model generates resilience and cost measures to measure the *resilience* of the respective microgrid for its associated costs. These measures generate trade-off functions for the design and maintenance choices.

The model is built in a spreadsheet using a macro. The macro automates the keystrokes to simulate the model for more than one iteration when conducting Monte Carlo simulations. A macro automatically populates each of the four resilience measures and cost measure for each simulation. Automating the simulations reduces the time and opportunity for error compared to manually simulating the model. The spreadsheet's Tool guidance worksheet offers further directions for running this macro, and Appendix B provided the macro's code.

Figure 11 provides the sequential simulation steps to run the model.

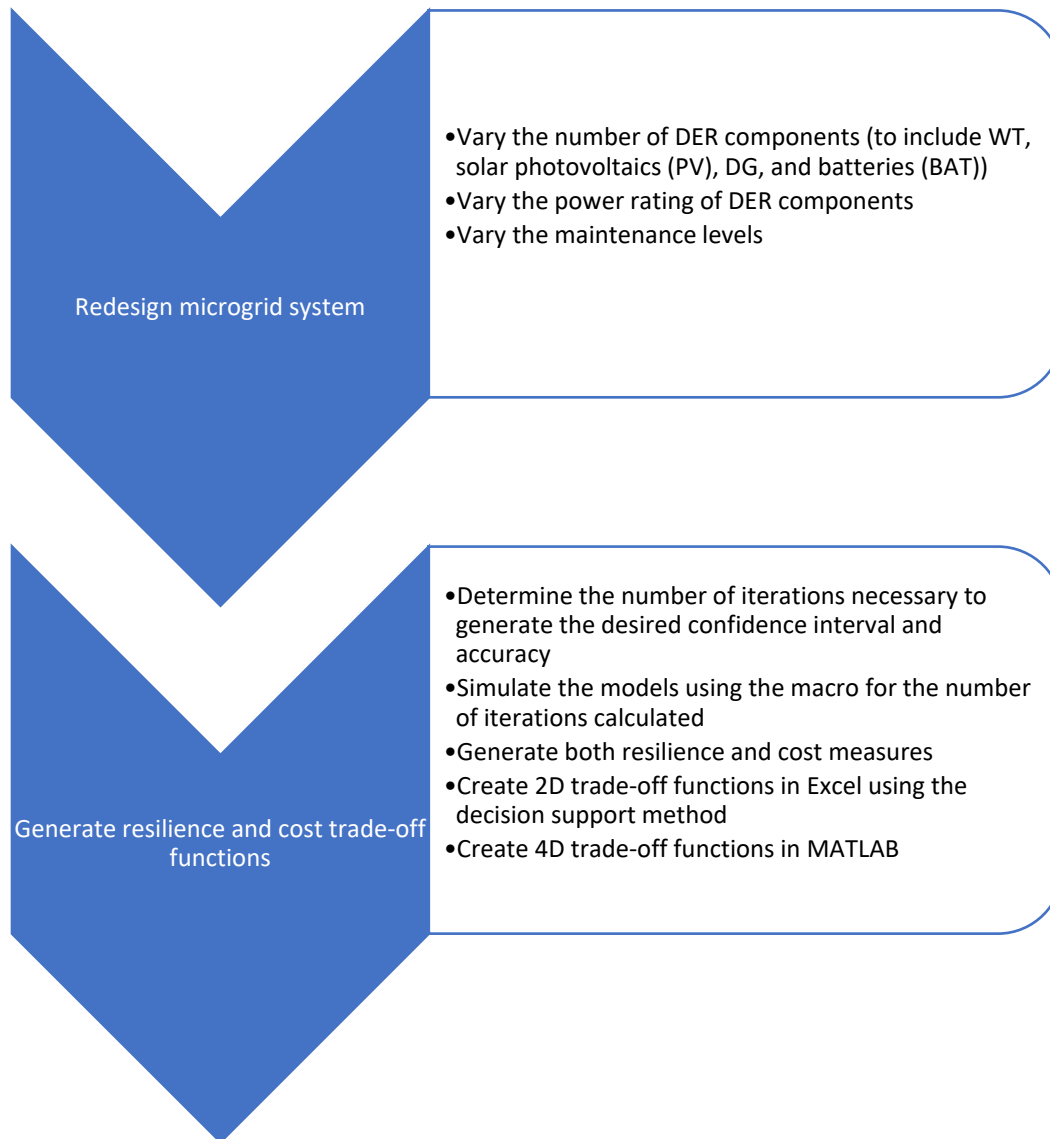


Figure 11. Steps to simulate the microgrid system

5. Select Design

Finally, the modeler analyzes the results to determine the main drivers of resilience and costs so as to introduce changes in either the microgrid design and/or the maintenance level. It is the trade space between resilience and costs that will enable a decision maker to narrow design options to only those that provide the desired resilience for the associated costs.

Figure 12 presents the complete method process flow.

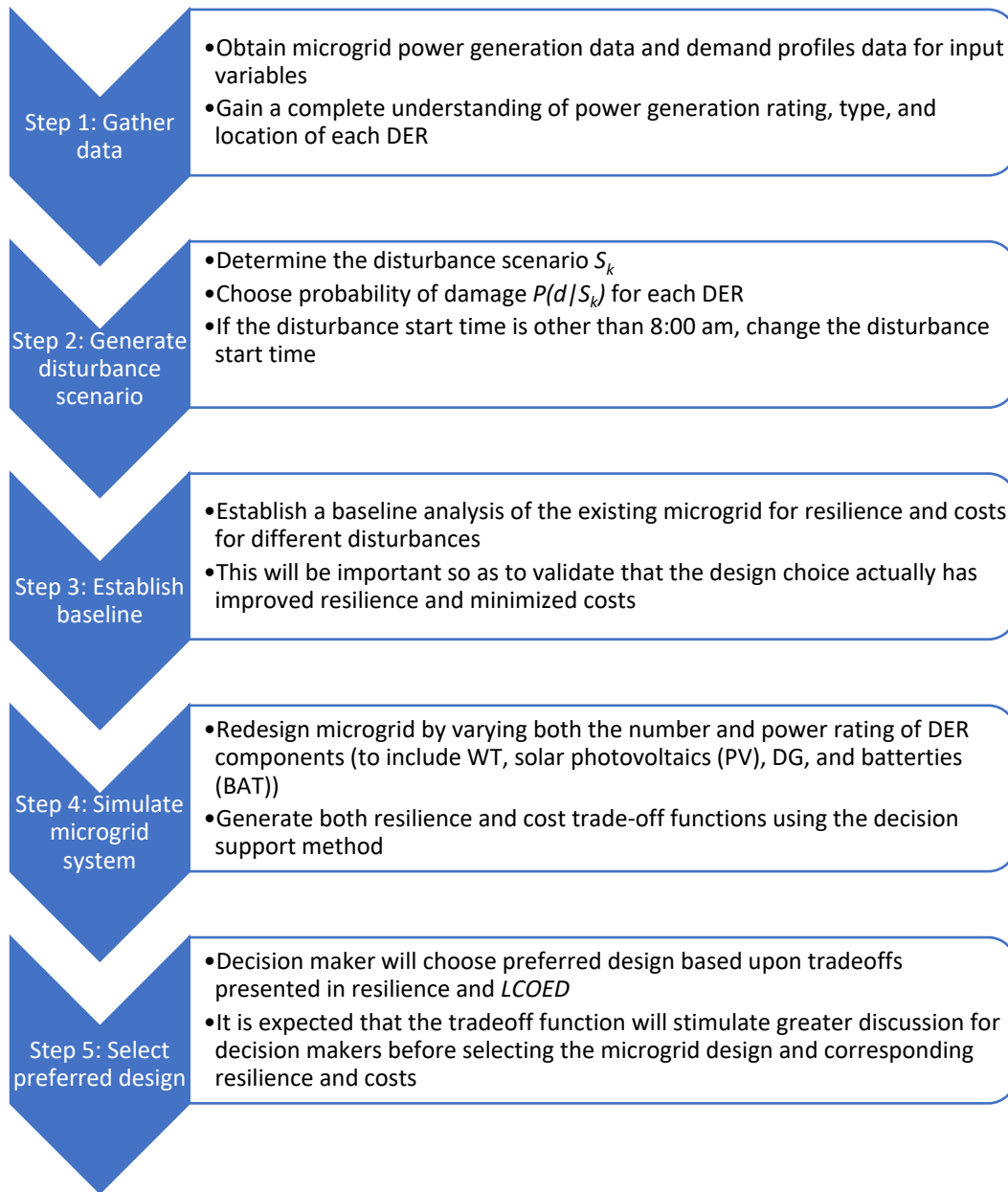


Figure 12. Microgrid method process to explore *resilience* and costs trade space to choose microgrid architecture design.

Figure 13 illustrates the relationship between the input and output variables. This figure illustrates not only the relationships between input, random, and output variables for calculating resilience and costs measures, but also the relationships that include decision variables when optimizing the model.

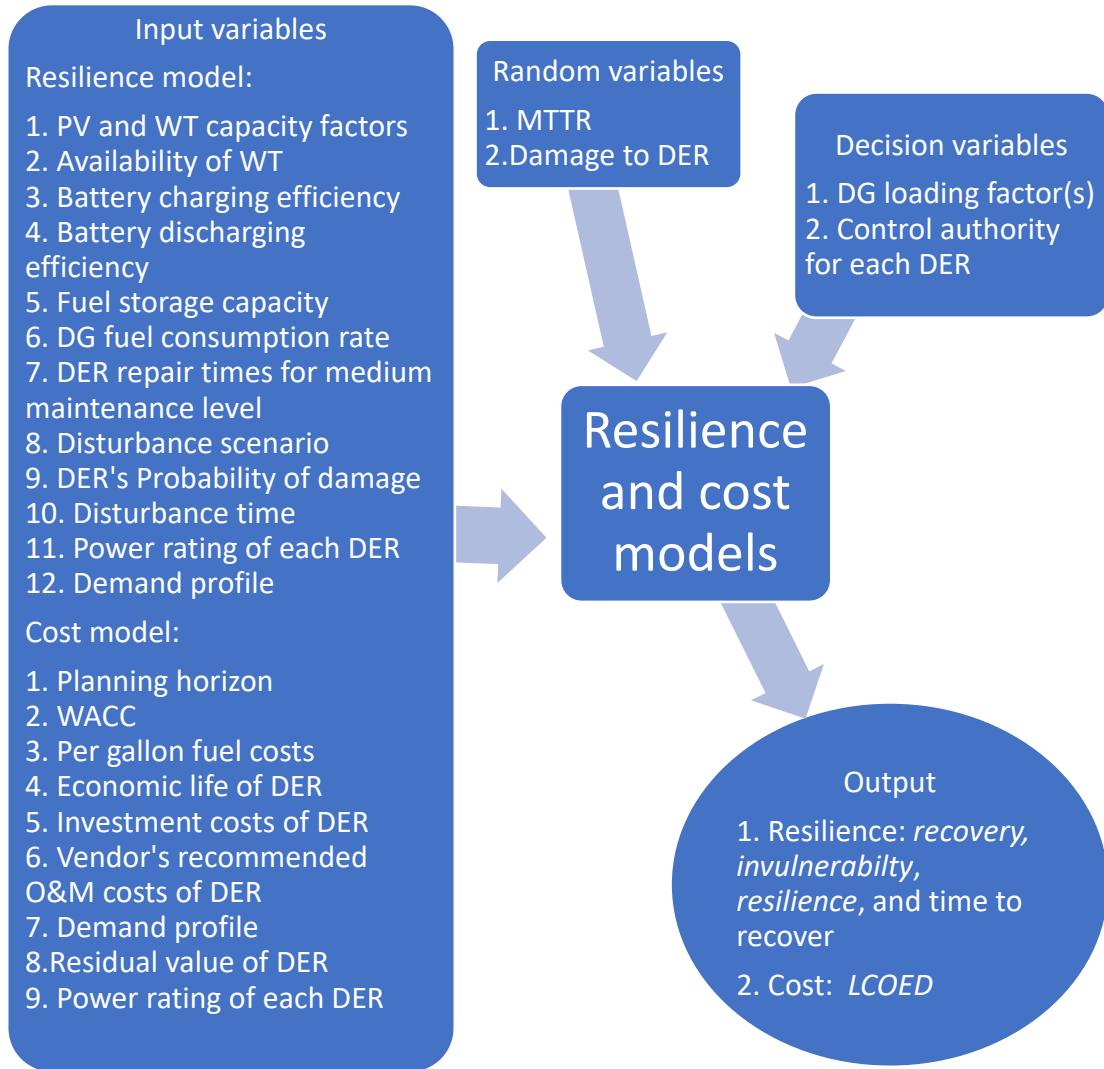


Figure 13. Data flow: Inputs and outputs for both models.

B. COST MODEL

The cost model quantifies the life cycle costs for a microgrid.

1. Nomenclature

The indices, superscripts, and different types of variables make up the nomenclature used in the cost model.

a. Indices

y Index for year

t Index for time period

i Index for DER unit

b. *Superscripts*

WT Wind turbine

PV Solar photovoltaic

DG Diesel genset

BAT Battery

y Year

c. *Input parameters*

n Economic life of DER type (e.g., WT, PV) [years]

p Planning horizon [years]

I_{yi} Investment costs of DER i in year y [\$]

J_{yi} Vendor's recommended O&M costs of DER
 i in year y [\$]

f Fuel cost per gallon [\$/gal]

g DG fuel consumption rate [gal/kWh]

r Weighted Average Cost of Capital (WACC)

D_t Critical infrastructure demand at time t [kW]

H_i Financial value of DER i at end of planning
horizon [\$]

P_{ti} Power rating of DER i at time t [kW]

d. *Variables*

$LCOE$ Life cycle Cost of Energy (LCOE) [\$/kWh]

$LCOED$	Life cycle Cost of Energy for Demand ($LCOED$)	[\$/kWh]
E_y	Microgrid's energy generated in year y	[kWh]
M_{yi}	O&M costs of DER i in year y	[\$]
m	Number of DER	
F_{yi}	Fuel costs for diesel genset i in year y	[\$]

e. Decision variables

L_{ti}	Loading factor of diesel genset i in time period t
μ_{ti}	A binary variable that equal 0 when DER i is off in time period t , and equals 1 otherwise

2. Problem Formulation

The planning horizon is set equal to the expected life of the DER component with the shortest expected economic life. Although the component with the shortest life does not represent the life of the microgrid system as a whole, we adopt this microgrid's timeframe for our planning horizon in order to simplify the economic analysis. INIs must comply with guidance from their leadership and the Department of the Navy (2013b) recommends the period of analysis (their term for planning horizon) as the lesser of either 40 years for energy projects or the life of the energy system for NAVFAC economic analyses. The microgrid's DER components economic lives range from 10–25 years and therefore the shortest life for batteries at ten years should be considered the life of the energy system and used for the planning horizon. Cost measures' calculations will undervalue if an unrealistically low economic life is used; at INIs, there are several instances of DGs operating more than twice their economic life.

a. LCOED

The Department of Energy (n.d.) defines $LCOE$ as the lifetime costs of the energy produced by a given source. The DoE uses the $LCOE$ to compare different power generation methods. This dissertation uses it to calculate the unit cost of energy for an

entire microgrid that may contain multiple, different power generative sources (e.g., solar, wind, diesel). For this reason, the DoE definition is adjusted to include a residual value because in this dissertation all costs will be done based on a planning horizon set to the shortest expected life of the generative sources. Hence any resource with a longer life will have residual value at the end of the planning horizon.

$$LCOE = \frac{\sum_{y=1}^p \sum_{i=1}^m \frac{I_y + M_y + F_y - H_i}{(1+r)^y}}{\sum_{y=1}^p \frac{E_y}{(1+r)^y}} \quad (3.1)$$

LCOE's numerator totals and discounts the costs and benefits in Equation 3.1. The denominator totals and also discounts the full power rating of the purchased microgrid to generate energy. The DOE assumes that demand will always exceed the generative power rating; and when the normal loads served by the utility have less demand than the generation, the utility will transmit and distribute to other loads on the grid to ensure there is no excess and unused generative power rating so as to control their costs. This obviously is not an option for an INI, and therefore this same assumption that the demand will always exceed the power generation rating cannot be made at an INI. The *LCOE* cost measure assumes that the microgrid generates energy its E_y using the full power rating of the microgrid. There is never any excess energy capacity when measuring costs with *LCOE*.

The investment costs I_{yi} represent the capital expenditure to purchase the DER. The O&M costs M_{yi} is dependent upon the maintenance level. The resilience model's *MTTR*, described in Section C.2.k is also dependent upon the maintenance level.

The base commander's operational decisions and the level of investment in O&M, training, spare parts, and spare DER influence the recovery of a damaged resource. The base commander can set the maintenance level for each DER at medium, low, or no maintenance. Three levels are chosen to simplify the model and reflect the full range of practical maintenance options. A medium maintenance level depends on the costs to meet the vendor's recommended annual maintenance J_{yi} for the DER. A low maintenance level reduces the manufacturer's recommended annual maintenance investments J_{yi} for the DER.

The model also has a maintenance level for when no maintenance is performed by the base. Although a fourth and high maintenance level could be used, Thompson et al. (2018) determined excessive maintenance to be unnecessary and therefore medium will be the highest maintenance level used in this model.

The pseudocode for determining M_{yi} follows:

```

IF maintenance level is medium
  THEN
     $M_{yi}^{medium} = J_{yi}$ 
  IF maintenance level is low
    THEN
       $M_{yi}^{low} = 0.22J_{yi}$ 
    ELSE
       $M_{yi}^{none} = 0$ 
    ENDIF
  ENDIF
ENDIF

```

The maintenance costs of each DER are assumed to be constant. We recognize that maintenance costs will increase when choosing to have more DER components due to increasing redundancy. However, the cost model does not increase each DER's maintenance costs to account for the added cost burden of maintaining more DER.

The energy generated in a year sums the power over time.

$$E_y = \sum_{t=1}^{8760} G_t \quad (3.2)$$

Equation 3.3 calculates the annual fuel costs. Recall the gensets are only employed when needed by the microgrid. When the demand is less than the microgrid power rating, some gensets can either be shut down or operated at a lower loading factor. Our fuel costs Equation 3.3 multiplies the DG's fuel consumption rate by the fuel costs to get the \$/hour cost before multiplying this by the DG's loading factor, nominal power rating and control authority to account for whether the DG is operating or not.

$$F_{yi} = \sum_{t=1}^{8760} g/L_t P_i^{DG} \mu_t^{DG} \quad (3.3)$$

The *LCOE* calculates a cost per kWh typically for a single source such as wind, solar or coal to compare generation costs between alternatives on a \$/kWh basis. *LCOE* assumes all the power generated has value, and all the energy is used. However, an off-grid island may be unable to use all the power that could be generated. Consequently, some power generation rating will be wasted and not used. At SNI they only need a fraction of their power rating to meet the demand, yet the Navy has already paid for the investment and maintenance costs for the microgrid. The *LCOE* would under-estimate the actual cost per kWh on islands with excess power rating such as SNI. The under-estimation will be considerable at the INIs' microgrid architectures with 1.5, 2, and 3 times as much generative power rating as demand.

To account for this aspect of islanded microgrids, we modify *LCOE* by only considering the demand vice the generative power rating. This modification is necessary because the *LCOE*, as mentioned previously, is primarily used for single energy sources. We are using it for microgrid architectures with multiple energy sources, which have different useful lives. We use the shortest life of all the energy sources as the planning horizon, and subtract the residual value of all the other sources with remaining useful lives. This equation addresses these modifications.

$$LCOED = \frac{\sum_{y=1}^p \sum_{i=1}^m \left(\frac{(I_{yi}^{WT} + M_{yi}^{WT}) + (I_{yi}^{PV} + M_{yi}^{PV}) + (I_{yi}^{DG} + M_{yi}^{DG} + F_{yi}) + (I_{yi}^{BAT} + M_{yi}^{BAT}) - (H_i^{WT} + H_i^{PV} + H_i^{DG})}{(1+r)^y} \right)}{\sum_{y=1}^p \sum_{t=1}^{8760} \frac{D_t}{(1+r)^y}} \quad (3.4)$$

The numerator in Equation 3.4 is the NPV of each DER by summing and discounting by *r* the investment, maintenance, and fuel costs for each year less the residual value at the end of the planning horizon. The first term in the numerator in Equation 3.4

sums each of the wind turbine's costs, the second term sums each of the solar PV panel's costs, the third term sums each of the diesel genset's costs, and the fourth term sums each of the battery's cost. Charging costs are excluded by this model due to those costs already being captured by the other DER components of the microgrid. Belderbos et al. (2016) uses charging costs instead of fuel costs for the battery, although suitable for an on-grid microgrid it is not suitable for an off-grid microgrid that is charging its batteries using power it has generated.

The per unit maintenance costs of each DER are assumed to not change based upon the number of DER. Despite recognizing that maintenance costs will increase when choosing to have more DER components when increasing redundancy, the cost model does not increase the per unit costs.

The denominator of Equation 3.4 is the NPV of the historical demand profile over the planning horizon. This model sums the hourly demand of the INI over a full year and then applies the WACC to bring this amount back to present value. The modeler then sums each of these yearly values over the planning horizon.

b. Cost measure differences

To understand the differences between *LCOED* and *LCOE* cost measures, the cost model is simulated for a microgrid with 7 MW generation power rating and a medium maintenance level as illustrated in Table 6. The demand profile is illustrated in Table 7 with the highest demand of 4MW but an average demand of 2.7MW. Consequently, the microgrid designs are all over-designed for the load with approximately 2.6 times more power generation rating than demand. Of significance and a reasonable expectation is that *LCOED* is approximately 2.6 times more than *LCOE* due to *LCOED* not valuing this same proportional difference in excess generation power rating because *LCOE* assumes all generative sources are producing at their power rating, but on an island with excess power rating and no place to sell the excess power rating, they will be usually operating at well below power rating, which can be seen in Table 6.

Table 6. Differences in cost measures for various microgrid architectures having a total power generation rating of 7 MW.

Power rating of each DER [KW]	# of WT	# of PV	# of DG	# of BAT	LCOE [\$/kWh]	LCOED [\$/kWh]
700	4	4	2	2	0.1096	0.2815
875	3	3	2	2	0.1140	0.2929
1,000	3	3	1	1	0.1117	0.2868

Table 7. Relationships between time step and time of day for critical infrastructure demand at time t .

Time step	Time step [hour]	D_t [kW]	Time step	Time step [hour]	D_t [kW]
0	0800	2,000	12	2000	2,800
1	0900	2,400	13	2100	2,800
2	1000	2,600	14	2200	2,800
3	1100	2,800	15	2300	2,600
4	1200	3,000	16	2400	2,000
5	1300	3,400	17	0100	2,000
6	1400	3,800	18	0200	2,000
7	1500	4,000	19	0300	2,000
8	1600	4,000	20	0400	2,000
9	1700	4,000	21	0500	2,000
10	1800	3,600	22	0600	2,000
11	1900	3,000	23	0700	2,000

C. RESILIENCE MODEL

The nomenclature, model outline, and problem formulation are essential to effectively formulate the problem. The background and application of each are essential to effectively implement the resilience model.

1. Nomenclature

The indices, superscripts, and different types of variables make up the nomenclature used in the resilience model. Each of the respective abbreviations is presented as used in the resilience model.

a. Indices

t	Index for time period
i	Index for DER unit
k	Index for disturbance scenario
d	Index for disturbance start time

b. Superscripts

WT	Wind turbine
PV	Solar photovoltaic
DG	Diesel genset
BAT	Battery
C	Charge

c. Input parameters

P_i	Nominal power rating of DER i at time $t = 0$	[kW]
S_k	Disturbance for scenario k	
C	Capacity factor of DER	
A	Availability factor of WT	
D_t	Critical infrastructure demand at time t	[kW]
S	Fuel storage capacity	[gallons]
B_i	Initial energy capacity of battery i at time $t = 0$	[kWh]
η_c	Efficiency of battery charging	
η_d	Efficiency of battery discharging	
λ	Time To Repair a damaged DER	[hours]
q	Quantity of DER units	
$P(d S_k)$	Probability of DER being damaged given disturbance S_k	

occurs

W DG's maximum fuel consumption rate [gallons/hour]

d. Decision variables

L_{ti} Loading factor of diesel genset i in time period t

μ_{ti} A binary variable that equal 0 when DER i is off in time period t , and equals 1 otherwise

e. Variables

P_t Power rating of microgrid at time t [kW]

P_{ti} Power rating at time t of DER number i [kW]

G_t Power generated by microgrid at time t [kW]

ξ Resilience

U_i A binary variable that equal 0 when DER i is damaged, and equals 1 otherwise

z_{ti} Fuel consumption for DG i in time period t [gallons]

B_{ti} Energy level for battery i in time period t [kWh]

T_t Unmet demand at time t [kW]

P_{ti}^C Excess microgrid power available to charge battery i in time period t [kW]

V_{ti} A binary variable that equals 1 when a damaged DER i is restored in time period t , and equals 0 otherwise

O_{ti} A binary variable that equals 1 when a damaged DER i is available in time period t , and equals 0 otherwise

$MTTR_i$ Mean Time To Repair ($MTTR$) the damaged DER [hours]

number i . $MTTR$ is exponentially distributed with mean λ
 m Number of DER

2. Model Outline and Problem Formulation

The purpose of the model is to inform decision-makers of how microgrid designs influence resilience and costs. The Department of Defense (2020c) stipulates that DOD components must plan and program for energy resilience and energy security and assess energy resilience at all installations in support of mission assurance objectives. Base commanders at INIs therefore are expected to ensure their critical infrastructure is resilient to ensure mission assurance when a disturbance hits the INI. Base commanders do not have either tools or the ability to determine type and which combination of microgrid DER components and investment maintenance level will provide the greatest resilience for a specific disturbance.

We model the behavior of a RE microgrid over time while subjecting it to a disturbance. Resilience is calculated by adjusting the microgrid's power rating at each time step dependent upon whether the damaged DER has been restored or not. The time to repair a damaged DER improves as maintenance increases. The financier of the microgrid can then determine their appetite for capital and maintenance investments by being equipped with an understanding of the relationship between costs and resilience.

We are interested in how the microgrid behaves in response to disruptive events, the model assumes the disruptive event occurs at time t_d , and then determines how the system behaves. The model makes two simplifying assumptions. First, the model assumes the disruptive event occurs at a point in time. Many events such as hurricanes can last for hours and even days. HILP disturbances also include earthquakes, wildfires, tsunamis and cyberattacks all of which can vary from seconds and hours to days, and all of which have high impact. Second, we assume, that if damage occurs, it occurs immediately following the disruptive event. In this model the nature of the disruptive events are all of a high impact over a short time period, and immediate damage is a reasonable assumption. Another implicit assumption we make is we know the disruptive event occurs. For cyberattacks, it is possible the operator of the microgrid does not know it is attacked or is under attack

which does not change the analysis but does place greater emphasis on the design vice operational decisions. Not knowing a disturbance has occurred, precludes any operational decisions or actions.

a. Resilience measure

The resilience measure ξ incorporates measures for vulnerability and recovery. *Invulnerability* is defined as the microgrid system's ability to withstand damage from a specific disturbance. *Recovery* is the microgrid system's ability to rapidly and completely return to the pre-disturbance performance level. Factors that affect recovery include the chosen design, maintenance level of investment, and post-disturbance operations. The microgrid's behavior can be described in five states: pre-disturbance, degradation, stabilization, recovery, and post-disturbance. The microgrid system's behavior is portrayed using the microgrid resilience function in Figure 14. *Recovery* (green), the resilience measure, is distinguished from recovery (magenta), one of the five states. Robustness, adaptability, tolerance, and anticipation are not specifically measured because they are considered measured because they are considered either outside the timeframe of t_d-t_{fr} or already incorporated in the two resilience measures of *invulnerability* or *recovery*.

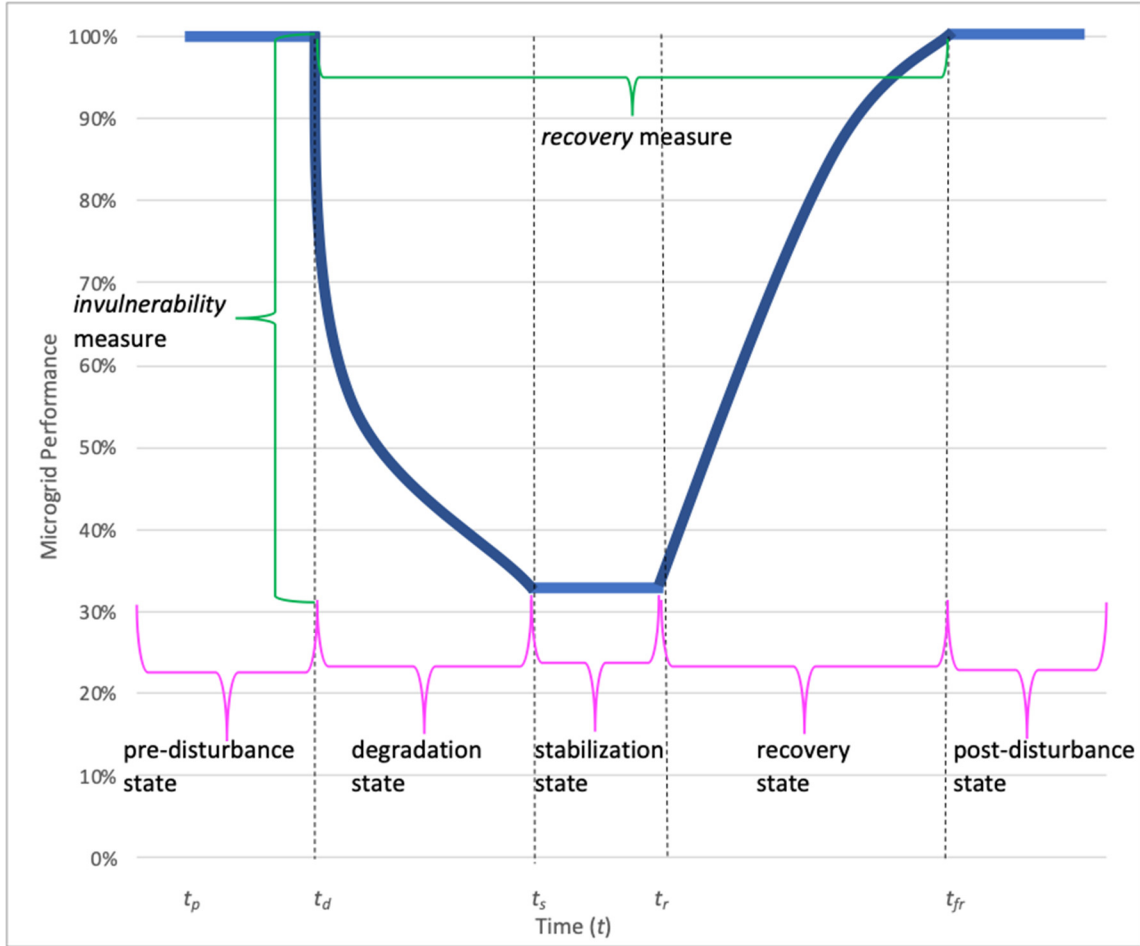


Figure 14. Microgrid *resilience* function relates performance and time to *resilience* measures.

The microgrid resilience function shows how the two measures relate to performance and time in relation to the five states of interest when the microgrid is subjected to a disturbance.

The resilience equation calculates an aggregate resilience score weighting *invulnerability* and *recovery* equally as shown in Equation 3.5.

$$\xi = 0.5(\textit{invulnerability} + \textit{recovery}) \quad (3.5)$$

b. *Invulnerability measure*

We adopt Francis and Bekera’s (2014) *invulnerability* measure. This measure calculates the extent of post-disturbance performance loss by taking the fully diminished

power rating of a damaged microgrid and dividing this by the microgrid’s power rating before the disturbance. This measure can be influenced by both the maintenance investment level as well as design decisions that include the number, power rating, efficiency, and location of the DER.

Disturbance type, damage and restoration are all distinct and separate factors that impact the *invulnerability* measure and should be evaluated independently so as to distinguish and evaluate the probabilistic nature of damage, from the probability of damage and probability of restoration. This research assumes all damaged DER will be restored and therefore does not incorporate probability of restoration. The probability that a disturbance occurs is exclusive of the probability of damage; a hurricane can strike an INI and cause no damage. The microgrid design choices are all evaluated by assessing their resilience to a disturbance. The probability of a disturbance does not change how a microgrid behaves or demonstrates its resilience. Rather, this research incorporates the probability of damage to a DER for a specific disturbance and excludes the probability of a disturbance from the model, by assuming the disturbance has occurred.

We assume that the demand does not drop below P_{t_s} . This is a reasonable assumption due to the disturbance’s damage being limited to immediately following the disturbance start time and focused on the microgrid.

The *invulnerability* equation calculates the ratio of the microgrid’s power rating when it has been stabilized following the disturbance divided by the microgrid’s power rating when the disturbance first occurs as seen in Equation 3.6:

$$invulnerability = \frac{P_{t_s}}{P_{t_d}} \quad (3.6)$$

c. Recovery measure

We adapt Renschler et al.’s (2010, 6) recovery measure (their equation 3), which is “the normalized shaded area underneath the function describing the functionality of the system under the system response.” This measure calculates the ratio of the energy the

microgrid generates without performance loss to the disrupted microgrid's energy generated. Design decisions that include both the number and power rating of the DER as well as the choice to increase the level of maintenance investment influence this measure.

The *recovery* equation calculates the ratio of the area bounded between the demand and post-disturbance generation function over the demand profile function as seen in Equation 3.7:

$$recovery = 1 - \frac{\sum_{t=t_d}^{t_{fr}} D_t - G_t}{\sum_{t=t_d}^{t_{fr}} D_t} \quad (3.7)$$

The demand profile D_t is assumed to always be greater than zero and follows a historical projection. Whereas the generation is calculated for the disrupted microgrid's diminished power rating to generate power. The diminished power rating is due to damaged DER until all damaged DER have been restored. Recovery of the DER will occur based upon the maintenance level and is discussed further in the next section. Finally, the ratio is subtracted from 1 so as to be consistent with the *invulnerability* measure wherein the maximum recovery is 1 and minimum 0.

The recovery measure accurately captures the nonlinear behavior in performance due to the disturbance inflicting an immediate decline in performance followed by a gradual restoration. By calculating the ratio of unmet demand to demand at each time step following a disturbance, the area, a more accurate indication of the ability of the microgrid to rapidly recover is calculated than a simpler calculation using the area bounded by a resilience triangle.

d. Maintenance level

The time to repair a damaged DER will impact *recovery* by influencing the time to recover. A shorter Mean Time to Repair, $MTTR_i$, will result in a shorter time to recover time and better *recovery*. We assume that greater investments in maintenance will reduce $MTTR_i$.

There are several assumptions made in calculating $MTTR_i$. Trout (2020) identifies the failure's severity level and assumes that the technician is competent and available to make the repair. This second assumption is reasonable for an average severity level of damage. It would be unrealistic at an INI to expect the technician to have the competency to effect an extensive repair. Anderson et al. (2017) found that SNI had at least three power plant operators that are technicians on site at all times. Keeping at least three operators onsite ensures that there are enough operators to man the power plant with at least one operator at all times, and usually rotating every eight hours on average. Other assumptions that are made for INIs are that most spare parts are onsite, on-island. This latter assumption is rather unlikely in many cases.

There are limitations in applying $MTTR$. The first is that $MTTR$ does not include the lead time for spare parts or the ability of a contracted service level agreement (SLA) to effect the repair. Trout (2020) describes lead time and SLAs as components of Mean Time to Recovery and not $MTTR$. Lead time for spare parts and contracted SLA are driven by operational decisions and therefore not included in this research's focus on design solutions. The lead time for spare parts is an assumption that the spare parts are on-island for INIs.

Thompson et al. (2018) found that, despite preventative maintenance usually reducing failure rates, excessive maintenance may be both wasteful and harmful. They analyzed a U.S. Army Corps of Engineers facility and maintenance information database of more than 100,000 power, mechanical and electronic components that included 13,000 unit-years of information just on heating, ventilation and air conditioning equipment. Their results demonstrated that when reducing the maintenance hours for shell-and-tube condensers to a lower tercile having maintenance hours that are 22% of a middle tercile's maintenance hours, the mean annual failures increased by a factor of 1.33. Similarly when reducing the maintenance hours again from the lower tercile to no maintenance, the mean annual failures increased by a factor of 2.42.

$MTTR_i$ varies with the maintenance level; as the level of maintenance increases, $MTTR_i$ decreases. When the time step equals the $MTTR_i$, the damaged DER will be restored and V_i set to 1.

The pseudocode for determining $MTTR_i$ follows:

```

 $\lambda^{none} = 2.5(\lambda^{medium})$ 
 $\lambda^{low} = 1.5(\lambda^{medium})$ 

DO  $i = 1$  TO  $q$ 
  IF maintenance level is low
    THEN
       $MTTR_i \sim Exp(\lambda^{low})$ 
    ELSE
      IF maintenance level is medium
        THEN
           $MTTR_i \sim Exp(\lambda^{medium})$ 
        ELSE
           $MTTR_i \sim Exp(\lambda^{none})$ 
      ENDIF
    ENDIF
  ENDDO

```

The Organization of American States (2001) reviewed hurricane damage to buildings and concluded that building and equipment maintenance is a very cost effective disaster mitigation measure. Without maintenance, all other disaster mitigation methods could prove to be insufficient. Their findings, mostly focused on hotels indicated that roofs, walls and equipment are more vulnerable to failure at near breakdown or any technically deficient level. Specifically, they indicate that maintenance should ensure a facility can resist the effects of extreme natural disasters with minimal repair following the disturbance.

The assumption that greater investments in maintenance will reduce $MTTR_i$ is supported by Trout (2020) as he argues that although $MTTR$ is reactive maintenance, it provides an indication of the effectiveness of preventative maintenance. Trout (2020) goes on to state that $MTTR$ provides insights into how equipment is purchased, maintenance is scheduled, and maintenance is performed.

Applying Thompson et al.'s (2018) findings to this research, the annual maintenance costs M_{yi} should procure a corresponding amount of a technician's maintenance labor hours; more investment in maintenance should deliver more

maintenance hours. Trout (2020) and the Organization of American States' (2001) showed that MTTR is influenced by maintenance, and Thompson et al. (2018) showed the relationship between the mean number of failures and each level of maintenance. Although $MTTR_i$ following damage is not the same as mean failures resulting from different maintenance levels, it is expected that there will be a similar relative improvement in $MTTR_i$ for greater maintenance investments as Thompson et al. (2018) found for an improvement in the mean number of failures resulting from maintenance levels.

We assume that greater investments in maintenance will result in greater availability of spare parts to use when repairing a damaged DER component. And similar to what Thompson et al. (2018) found, in general more but not excessive maintenance improves reliability. A better-maintained DER should be better able to withstand a disturbance by virtue of being more lubricated and having newer parts that overall should perform better in the face of a disturbance. Although failure due to disturbance induced damage to well-maintained DER is different than what Thompson et al. (2018) found as they related maintenance to reliability resulting from equipment failures, it is a starting point supported by Trout (2020) and the Organization of American States' (2001) findings for relating the $MTTR$ to different maintenance levels. This relationship between *invulnerability* and $MTTR$ will be evaluated further through sensitivity analysis of *invulnerability* to time to repair a damaged DER K .

The model calculates the availability O_{ti} of a specific DER component by considering both whether the component has been damaged as well as whether it has been restored. This is done so a previously damaged DER will be restored and contribute power generation to the overall microgrid power rating.

The pseudocode for determining a DER's availability follows:

```

DO  $i = 1$  TO  $q$ 
  DO  $t = t_d$  TO  $t_{fr}$ 
    IF  $U_i = 1$  (DER is undamaged) or  $V_t = 1$  (restored
      at  $t = MTTR_i$ 
    THEN
       $O_{ti} = 1$  (DER is available)

```



```

ELSE
    Oti = 0 (DER is unavailable)
ENDIF
ENDDO
ENDDO

```

e. Conditional probabilities of damage

The conditional probabilities of damage $P(d|S_k)$ is an input variable for each DER. The assumption is the disturbance S_k has occurred. The $P(d|S_k)$ represents that the DER will be damaged. The disturbance will either completely damage the DER, or not at all, which is reflective of most damage scenarios of the resource either being damaged and not operating at all or escaping damage and being fully operational. This assumption is made to simplify the model.

A DER will be damaged by a disturbance if it meets the conditional probability of damage given that a disturbance has occurred. Let U_i denote whether resource i is damaged after event S_k occurs. The designers of the microgrid influence the probability of damage by hardening the components and infrastructure. For instance, base commanders can bury power lines underground, which greatly reduces the probability of hurricane damage. The literature reviewed indicates that WTs will have a different probability of damage for a weather-related disturbance than solar photovoltaic panels and therefore the modeler must use realistic probabilities of damage for the respective DER as input variables.

The pseudocode for determining if a DER has been damaged follows:

```

DO i = 1 TO q
    Generate a uniform random number
    IF random number < P(d|Sk)
        THEN
            Ui = 0 (DER damaged)
        ELSE
            Ui = 1 (DER undamaged)
        ENDIF
    ENDDO

```

Common-cause failures could also contribute to identical DER types becoming unable to generate power as a result of the other DER being damaged by the disturbance. Common-cause failures can arise from various situations that include a uniformly and incorrect action by a technician when performing preventative maintenance on all wind turbines for instance. All PV panels despite being separate could suffer common cause failure due to being anchored to the same tracking array. Similarly, all the inverters in a PV system may fail at the same time and together due to the same cyberattack. Common-cause failures although having been deemed to be very low-probability have not been included in this method.

f. Formulation

The objective function Equation 3.8 maximizes resilience in order to both reduce time to recover and the unmet demand.

$$\text{maximize } \xi = 0.5(\text{invulnerability} + \text{recovery}) \quad (3.8)$$

Recovery or *invulnerability* can be maximized instead of resilience if that is desired.

The model’s decision variables include each genset’s loading factor to be varied hourly so as to operate the diesel gensets as efficiently as possible in that Wheeler (2017) found that only high load conditions maximized efficiency.

When optimizing, the model varies the control authority hourly to turn various DER generation off and on to maximize resilience. We permit the batteries to play a somewhat complex role in that the battery can be either charging or discharging and as such the decision to have them charge or discharge will alter the resilience measures.

(1) Microgrid power rating

The resilience measure incorporates calculations that use the power rating P_t of the microgrid by summing the power rating of each DER component as indicated in Equation 3.9. This model calculates the total loss of power rating of the respective DER components following a disturbance by including the conditional probability of damage to the DER given a disturbance scenario. The microgrid power is calculated by summing each of the

DER's power rating from the time the disturbance starts until the microgrid is fully recovered. Each DER's power rating is adjusted for efficiency terms as well as whether or not it is damaged.

$$\begin{aligned}
P_t = & \sum_{t=t_d}^{t_{fr}} \sum_{i=1}^q P_{ii}^{WT} C^{WT} A O_{ii}^{WT} \mu_{ii}^{WT} + \sum_{t=t_d}^{t_{fr}} \sum_{i=1}^q P_{ii}^{PV} C^{PV} O_{ii}^{PV} \mu_{ii}^{PV} + \\
& \sum_{t=t_d}^{t_{fr}} \sum_{i=1}^q L_{ii} P_{ii}^{DG} O_{ii}^{DG} \mu_{ii}^{DG} + \sum_{t=t_d}^{t_{fr}} \sum_{i=1}^q P_{ii}^{BAT} O_{ii}^{BAT} \eta_d \mu_{ii}^{BAT}
\end{aligned} \tag{3.9}$$

The first term in Equation 3.9 represents the power rating of the wind turbines by summing each wind turbine's power. We multiply the power rating of the wind turbine P_{ii}^{WT} by the wind turbine's power rating and availability factors C^{WT} and A^{WT} . The capacity factor is a ratio of the actual energy produced in a time period to the maximum possible. The availability factor is the percentage of time that the wind turbine operates, that is it is not inoperable due to maintenance being needed and/or performed. This model multiplies the power generation rating by O_{ii}^{WT} in order to reduce the DER's power rating to zero if it is not available due to being damaged and not restored. Finally, we multiply by the control authority μ_{ii}^{WT} to the WT on or off.

The Renewable Energy Research Laboratory, University of Massachusetts (n.d.) articulates that a capacity factor is not the same as, nor an indicator of efficiency. Capacity factors are used to calculate a RE's generation. Capacity factors indicate how much power a particular RE generates for a specific location, and is the ratio of the actual energy produced in a given time period to the maximum possible. Availability factors are used to reduce the generation by the percentage of time the wind turbine is projected to be down for maintenance.

Fitch et al. (2013) found the diurnal variations during the night increase the WT's generation by a factor of three compared to the daytime. To account for this increase at night P_{ii}^{WT} is multiplied by 3 for twelve hours from 8:00 pm until 8:00 am daily. In that the capacity factor C^{WT} already incorporates this increase due to diurnal behaviors, the WT's capacity factor is reduced in-half in order to not overestimate the WT generation.

The second term in Equation 3.9 sums the power rating each PV panel. The power rating of the PV panel P_i^{PV} is multiplied by the PV panel's capacity factor C^{PV} . This model does not incorporate a solar PV availability factor due to PV systems generally having availability over 98% and therefore it is assumed to be 1 for this model. This model multiplies the power generation rating by O_i^{PV} in order to reduce the DER's power rating to zero if it is not available due to being damaged and not restored. Finally, we multiply by the control authority μ_i^{PV} to the PV on or off.

To account for diurnal variations at night due to no irradiance the PV generation P_i^{PV} is 0 kW from 8:00 pm until 8:00 am daily. In that the capacity factor C^{PV} already incorporates this diurnal behavior, the PV's capacity factor is doubled in order to not underestimate the PV generation.

The third term in Equation 3.9 represents the power rating of the diesel gensets by summing each diesel genset's power rating. This model uses a loading factor L_{ti} for each respective genset to account for variable loading. This model multiplies the power generation rating by the availability variable O_i^{DG} . Finally, we multiply by the control authority μ_i^{DG} to the DG on or off.

The fourth term after the equality sign in Equation 3.9 represents the dischargeable power rating of the battery. This model multiplies the power rating of the battery P_i^{BAT} by the availability variable O_i^{DG} . We apply the battery's discharging efficiency η_d to this term to account for losses due to discharging. Finally, we multiply by the control authority μ_i^{BAT} to the BAT on or off.

(2) Unmet demand

The unmet demand due to insufficient power rating is:

$$T_t = D_t - P_t \quad \forall t \quad (3.10)$$

The pseudocode for determining the microgrid's generation is:

```

IF  $D_t > \sum_{i=1}^m P_{ti}$ 
  THEN
     $G_t = \sum_{i=1}^m P_{ti}$ 
  ELSE
     $G_t = D_t$ 
  ENDF
ENDIF

```

This amount of demand response, T_t , is a result of the power balance equation's constraint that generation can never exceed demand:

$$D_t \geq G_t \quad \forall t \quad (3.11)$$

coupled with the requirement that

$$G_t \leq P_t \quad \forall t \quad (3.12)$$

G_t is the power generated by the microgrid. In that power can never be generated without demand D_t , it must always be less than or equal to the demand. Additionally, the microgrid can not generate more power than its power rating. It should be noted that the demand includes the power used to charge the batteries.

(3) DG fuel consumption

Equation 3.13 calculates each diesel genset's fuel consumption at each time step using a fixed rate of fuel consumption, W , for the gensets. Each DG's fuel consumption varies based with the loading factor and and control authority variables. When the genset is both on, $\mu_i^{DG} = 1$ and available, $O_i = 1$, the consumption equals the loading factor L_{ti} times the genset's maximum consumption rate W . The DG is available when it is not damaged. Otherwise, the consumption is zero gallons/hour.

$$z_{ii} = WO_i L_{ti} \mu_i^{DG} \quad \forall t, i \quad (3.13)$$

(4) Sizing the battery

The battery serves a useful role in a microgrid by storing excess energy capacity and having it available for the future when there is unmet demand. The size of the battery should be determined after the microgrid power rating is first selected in order to meet the demand. Later, in Chapter IV, useful ratios on the battery's power rating to the microgrid power rating, and the microgrid's power generation rating will be presented. Although these recommended, ratios can be used as a starting point, they do not have to be rather instead an iterative process can be used starting with a smaller battery first.

The nominal power rating P_i^{BAT} and nominal energy capacity B_i are both input variables. The default choice for the nominal power rating should be such that it is equal to the nominal power rating of the diesel gensets P_i^{DG} in order to have sufficient power rating to deliver power in lieu of a damaged DG. The default choice for energy capacity is to provide sufficient power rating in order to have sufficient energy capacity to deliver power long enough to be able to repair a damaged DG. If DGs are not employed, then the energy capacity should be sufficient enough to repair the DERs. However, the value should be input to provide resilience and costs for the ratio of BAT power to the microgrid's nominal power rating $\frac{P^{BAT}}{P}$.

(5) Battery's energy level

We assume the battery's initial energy level to be fully charged as provided by the input variable B_{oi} . Having the battery fully charged at the point in time just prior to the disturbance impacting the microgrid is a simplification for the model. This best case assumption reflects that the microgrid should only discharge its batteries when the demand exceeds the generation rating of the microgrid. Under predisturbance conditions, it is expected that the microgrid's power rating always exceeds demand. These conditions preclude the need to discharge the battery prior to the disturbance.

The energy management strategy only uses the batteries for transition when there is unmet demand from DER generation. Batteries are expensive and used for short-term storage. Fuel is used for long-term storage.

The model assumes the INI will first dispatch generation to the load and only charge an uncharged and undamaged battery when there is excess microgrid power rating P_{ii}^C . As such, the battery should only need to be charged after it has discharged to help meet the demand, when the microgrid has been damaged by a disturbance and/or to use any excess power rating when operating a DG at its lower loading factor. This situation can occur when the demand profile requires the use of the smallest power rating DG's generation at an amount that is less than its lower loading factor.

We determine the battery's energy level by first checking for excess microgrid power P_{ii}^C available to charge the batteries. If the first battery's energy level B_{t-li} is less than its initial nominal level B_i and there is excess microgrid power rating $-T_t$ then the power available to charge the batteries is governed by equation 3.14:

$$P_{ii}^C = \frac{-T_t + P_i^{BAT}}{\eta_c} \quad (3.14)$$

Equation 3.14 subtracts the excess power rating T_t from the battery's power rating P_i^{BAT} and divides this amount by the battery's charging efficiency. This calculates the excess microgrid power P_{ii}^C .

For all other batteries if the numbered battery sequenced before the battery has any power available to charge it $P_{ii-1}^C > 0$ then $P_{ii}^C = P_{ii-1}^C - P_{i-1}^{BAT}$ so as to reduce the amount of P_{ii}^C for that battery by the amount used to charge the battery before it. Otherwise, there is no power available to charge the battery.

The pseudocode for determining the microgrid's excess power to charge a battery follows:

```

DO  $i = 1$  TO  $q$ 
  DO  $t = t_d$  TO  $t_{fr}$ 
    IF  $B_{t-1i} < B_i$  AND  $T_t < 0$  (excess power rating)
      THEN
        Set excess microgrid power
        available to charge the battery
        
$$P_{ti}^C = \frac{-T_t + P_i^{BAT}}{\eta_c}$$

      ELSE
        IF  $P_{ti}^C = 0$ 
          THEN
            Set excess microgrid power to
            charge the battery  $P_{ti}^C = P_{ti-1}^C - P_{i-1}^{BAT}$ 
          ELSE
            Set excess microgrid power to
            charge the battery  $P_{ti}^C = 0$ 
          ENDIF
        ENDIF
      ENDIF
    ENDDO
  ENDDO

```

Let B_{ti} denote the energy in the battery at time t . The new energy level of the battery is calculated by reducing the energy level by being discharged or increasing it by being charged. The battery will either charge using the excess microgrid power P_{ti}^C or discharge using the rated power of the battery to discharge, P_i^{BAT} as governed by the control authority if the new energy level is less than or equal to the original nominal energy capacity B_{0i} and is greater than or equal to 0, and the rated power of the battery to discharge, P_i^{BAT} is less than the demand D_t . We limit the battery's energy level by discharging down to 0 kWh and charging up to its original nominal energy capacity B_{0i} . Finally, if the rated power of the battery to discharge P_i^{BAT} exceeds the demand D_t , then the battery is discharged using the level of the demand D_t instead of P_i^{BAT} .

The pseudocode for determining the battery's energy level follows:


```

DO i = 1 TO q
  DO t = td TO tfr
    IF Bt-1i - PiBAT(t) ≥ 0 OR Bt-1i + PtiC(t) ≥ 0 AND PiBAT < Dt
      THEN
        IF μtiBAT = 1 (discharging)
          Bti = Bt-1i - PiBAT(t)
        ELSE (charging)
          Bti = Bt-1i + PtiC(t)
        ENDIF
      ELSE
        IF Bt-1i - PiBAT(t) < 0 (overdischarged)
          THEN
            Bti = Bt-1i
          ELSE
            IF Bt-1i + PtiC(t) > Bi (overcharged)
              THEN
                Bti = Bi
              ELSE
                IF Dt < PiBAT
                  THEN
                    IF μtiBAT = 1 (discharging)
                      THEN
                        Bti = Bt-1i - PiBAT(t)
                      ELSE (charging)
                        Bti = Bt-1i + PtiC(t)
                      ENDIF
                    ENDIF
                ENDIF
              ENDIF
            ENDIF
          ENDIF
        ENDIF
      ENDIF
    ENDDO
  ENDDO

```

(6) Constraints

Equations 3.15–3.17 define the constraints for optimization. Equation 3.15 ensures that the total fuel consumed by the gensets from t_d to t_{fr} is less than the fuel capacity S . The DGs' operating loading limits (Equation 3.16) ensures no wet stacking by being

underloaded, nor being unable to take on more load due to overloading. Finally, all control authority decision variables must be binary as indicated in Equation 3.17.

$$\sum_{t=t_d}^{t_{fr}} \sum_{i=1}^q z_{ti} \leq S \quad (3.15)$$

$$0.3 \leq L_{ti} \leq 0.8 \quad \forall t, \forall i \quad (3.16)$$

$$\mu_{ti} = \text{binary} \quad \forall t, \forall i \quad (3.17)$$

D. DISCUSSION AND CONCLUSION

This chapter presents cost and resilience models to measure an INI RE microgrid's performance. The two models ensure that an INI's base commander will know the cost of resilience so as to make a more informed decision before investing in a microgrid.

Using the proposed definition of resilience, *the microgrid's invulnerability and rapid and full recoverability from an improbable and severe disturbance*, the resilience measure ensures that the most invulnerable and rapidly recovering microgrid can score the highest. This measure highlights the endogenous factors of the system such as the number and power rating of the DER that most improve resilience.

For exposition, the model in its entirety is presented here again:

$$LCOE = \frac{\sum_{y=1}^p \sum_{i=1}^m \frac{I_y + M_y + F_y - H_i}{(1+r)^y}}{\sum_{y=1}^p \frac{E_y}{(1+r)^y}}$$

$$LCOED = \frac{\sum_{y=1}^p \sum_{i=1}^m \left(\frac{(I_{yi}^{WT} + M_{yi}^{WT}) + (I_{yi}^{PV} + M_{yi}^{PV}) + (I_{yi}^{DG} + M_{yi}^{DG} + F_{yi}) + (I_{yi}^{BAT} + M_{yi}^{BAT}) - (H_i^{WT} + H_i^{PV} + H_i^{DG})}{(1+r)^y} \right)}{\sum_{y=1}^p \frac{\sum_{t=1}^{8760} D_t}{(1+r)^y}}$$

$$E_y = \sum_{t=1}^{8760} G_t$$

$$F_{yi} = \sum_{t=1}^{8760} g f L_{ii} P_i^{DG} \mu_{ii}^{DG}$$

maximize $\xi = 0.5(\text{invulnerability} + \text{recovery})$

$$\text{invulnerability} = \frac{P_{t_s}}{P_{t_d}}$$

$$\text{recovery} = 1 - \frac{\sum_{t=t_d}^{t_{fr}} D_t - G_t}{\sum_{t=t_d}^{t_{fr}} D_t}$$

$$P_t = \sum_{t=t_d}^{t_{fr}} \sum_{i=1}^q P_{ii}^{WT} C^{WT} A O_{ii}^{WT} \mu_{ii}^{WT} + \sum_{t=t_d}^{t_{fr}} \sum_{i=1}^q P_{ii}^{PV} C^{PV} O_{ii}^{PV} \mu_{ii}^{PV} +$$

$$\sum_{t=t_d}^{t_{fr}} \sum_{i=1}^q L_{ii} P_{ii}^{DG} O_{ii}^{DG} \mu_{ii}^{DG} + \sum_{t=t_d}^{t_{fr}} \sum_{i=1}^q P_{ii}^{BAT} O_{ii}^{BAT} \eta_d \mu_{ii}^{BAT}$$

$$T_t = D_t - P_t \quad \forall t$$

$$D_t \geq G_t \quad \forall t$$

$$G_t \leq P_t \quad \forall t$$

$$z_{ii} = W O_{ii} L_{ii} \mu_{ii}^{DG} \quad \forall t, i$$

$$P_{ii}^C = \frac{-T_t + P_i^{BAT}}{\eta_c}$$

$$\sum_{t=t_d}^{t_{fr}} \sum_{i=1}^q z_{ii} \leq S$$

$$0.3 \leq L_{ii} \leq 0.8 \quad \forall t, \forall i$$

$$\mu_{ii} = \text{binary} \quad \forall t, \forall i$$

THIS PAGE INTENTIONALLY LEFT BLANK

IV. EXPERIMENTS

The method presented in Chapter III is implemented to conduct experiments that will generate meaningful and useful findings that can be generalized for future microgrid design resilience and costs trade space exploration. The model is built using Microsoft Excel in order to generate the resilience and cost measures within a tool that is expected to be implemented by all of the Navy's utilities and energy community without any software limitations. Section A provides the model's parameters so others may replicate this work using the models presented in Chapter III. Section B shows the sensitivity of the model to the variables. Section C validates the cost model by duplicating results with another *LCOE* model's findings. Then, in Sections D through G, experiments are conducted to answer design questions we want to explore using the models. Section H presents a discussion and conclusion of the findings.

A. PARAMETERS

The parameters used as input variables for the model are presented by first providing the reference used as a basis for the parameter's value, and the rationale for their values. The actual values used for each of the resilience and costs input variables is presented in Tables 10 and 11 to simplify replicating these results.

For each power generation type—wind turbines, solar PV, gensets, and batteries—four scenarios are chosen: hurricane, wildfire, earthquake, and cyberattack. Only one scenario is chosen for the simulation.

We start with the literature to establish point estimates to adapt to our model. Although the exact values are not important for our model, they do give us the ability to establish relatively reasonable parameters. For wind turbines, Rose et al. (2012) determined the probability of hurricane damage as 46% for a Category 3 hurricane with wind speeds of 50 m/s or higher, Smith (2014) found that 90% of the wildfires led to substantial downtime or total loss, and Avossa et al. (2017) saw a 50% probability of failure for seismic loads from earthquakes in the fore and aft direction. For solar PV, Sepanski et al. (2018) analyzed 210 wildfire-damage incidents to buildings with PV and determined that 75 fires,

or 36%, resulted in damage to the PV system. Nicolas et al. (2019) determined the probability of earthquake damage to be lower and hurricane damage higher for solar PV than for wind turbines.

The literature reviewed did not provide any probabilities of damage for diesel gensets or batteries. So, the diesel gensets' probabilities of damage are assumed as just under the smaller of PV or WT. The batteries' probabilities of damage are set at less than diesel gensets except for the wildfire scenario because of batteries chemical composition being more vulnerable to fire. The basis and rationale applied to generate the probabilities of damage to gensets is based upon the protection provided to the DGs by operating inside buildings. And these scenarios seemed more likely than other HILP scenarios. For example, a meteor strike would represent a high-impact event but is unlikely to occur.

We also recognize that INIs by virtue of being a military installation are targets for hostile warfare attacks. An intentional act of aggression against the INI is a HILP disturbance. A missile attack on CLDJ is possible. For a missile attack on an INI, we will assume that all DER will have an equal probability of damage and that it should be the highest of the other probabilities, 0.9.

Patel and Zaveri (2010) determined the mean probability of SCADA equipment damage resulting from a cyberattack as 25%. The DER probabilities of damage for the disturbances shown are presented in Table 8.

Table 8. Probability of damage given disturbance S_k occurs for scenario k .

DER	$P(d S_k)$			
	Hurricane	Wildfire	Earthquake	Cyberattack
WT	0.50	0.90	0.50	0.25
PV	0.70	0.40	0.25	0.25
DG	0.30	0.20	0.15	0.25
BAT	0.20	0.50	0.10	0.25

The time to repair a damaged DER varies for different maintenance levels and type of DER. Pfaffel et al. (2017) provided mean down time per failure for each of seven onshore WTs that averaged 96.38 hours. Baschel et al. (2018) provided a five-day *MTTR*

for inverters in a PV system based upon field experience. Inverters are the most likely to fail of all solar PV components. Junior et al. (2017) calculated a *MTTR* for a diesel genset at 4.77 days. And Rimatrix5 (2020) uses a *MTTR* of just six hours for batteries. Applying the relationship from Thompson et al. (2018) discussed in Chapter III, the medium maintenance time to repair values are multiplied by 1.5 to obtain the low maintenance time to repair values, and 2.5 to obtain the time to repair for no maintenance. Values used for λ , time to repair, are provided in Table 9 and only the medium maintenance level values are input variables.

Table 9. Mean values of time to repair for each DER. Input variable values are designated with yellow cells.

	λ [hours]			
maintenance level	<i>WT</i>	<i>PV</i>	<i>DG</i>	<i>BAT</i>
none	240	300	285	15
low	144	180	171	9
medium	96	120	114	6

One-hundred thousand (100,000) gallons is determined as sufficient storage to operate five 1 MW DGs continuously for two weeks. This is estimated assuming all five DGs operate continuously.

Li and Tseng (2015) determined the charge and discharge efficiencies for a lithium-ion battery. The energy capacity of a battery is established to provide two hours at their full power rating. The assumption is that two hours will be sufficient time to bring any DGs up online to meet the demand.

Appalachian State University (2007) provided an average WT availability factor of 0.98. C^{WT} uses the capacity factor provided by IRENA (2020) and halves it so as to compensate for tripling the nighttime power generation of the wind turbines, as discussed in Chapter III C.2.f.(1).

C^{PV} is the capacity factor provided by IRENA (2020) and doubles it. As previously discussed in Chapter III C.2.f.(1), this is to compensate for the model not generating PV power at night.

The residual value is determined as directly relating to the proportional remaining economic life. The proportion is determined using the planning horizon and economic life and provided in Table 10 which shows all the parameters used to simulate the resilience model unless otherwise stated.

Table 10. Resilience model input parameters used in simulations.

Variable	Parameter	Value
S	Fuel storage capacity	100,000 gallons
η_c	Efficiency of battery charging	0.97
η_d	Efficiency of battery discharging	0.98
B_i	Nominal energy capacity of battery number i	$2P_i^{BAT}$
C^{WT}	Capacity factor of WT	0.22
C^{PV}	Capacity factor of PV	0.36
A	Availability factor of WT	0.98
H_i	Residual value of DER number i at end of planning horizon (p = years of planning horizon; n = DER's economic life)	$\$ \frac{I_i(n-p)}{n}$

Each DER has input variables for the cost model. Diesel Service & Supply (n.d.) provided the diesel fuel consumptions that are extrapolated for an 80% loaded DG to generate the fuel consumption rate. Clavier et al. (2013) provided DG and Li-ion batteries investment and O&M costs. Oviroh and Jen (2018) estimated the lifetime of a diesel genset. Mongird et al. (2019) established the economic life and O&M costs based upon energy capacity vice power rating for a lithium-ion battery. Smith et al. (2017) concluded that a ten-year lifetime is possible for lithium-ion batteries using a life prediction model. IRENA (2020) calculated the investment, O&M costs, capacity and economic life for onshore wind and solar PV. Hill et al. (2008) state that the industry accepted lifetime for a WT is 20 years. The Department of Defense (2020b) provided the DG fuel costs and the costs for Alaska are believed most fitting to apply to INIs given the remoteness. The International Renewable Energy Agency (IRENA) (2020) calculated the WACC r for Organization for Economic Co-operation and Development (OECD) countries. Table 11 provides the economic life, investment and maintenance costs, capacity factors used in the cost model.

Table 11. Cost model parameters used in simulations. All values are input parameters.

DER	Economic life n [years]	Planning horizon p [years]	Investment costs I [\$/kW]	O&M costs J [\$/kW]	Fuel costs f [\$/gal]	Fuel consumption rate g [gal/kWh]	WACC r [%]
WT	20	10	1,636	38.00	—	—	7.5
PV	25		3,081	18.30	—	—	
DG	30		620	15.50	2.60	0.06	
BAT	10		4,200; \$271/kWh	\$1,500.00/year	—	—	

B. SENSITIVITY ANALYSIS

The number of simulations are calculated to achieve a 90% confidence interval and a level of precision at ten minutes per hour, or 0.0333. Using the standard deviation for 500 simulations we solved for 7,500 required simulations and present the solution in Appendix C, Liu (2020,2). The demand profile portrayed in Figure 15 is used for all sensitivity analyses, and we see a rather typical daily demand profile increasing in the morning, peaking midday, and then returning to a base level by the evening. Unless otherwise stated, the maintenance level in every case is set at medium. The disturbance is a hurricane in that INIs are all subject to a hurricane. And unless otherwise stated the variance is calculated by increasing and decreasing the base value by 50%.

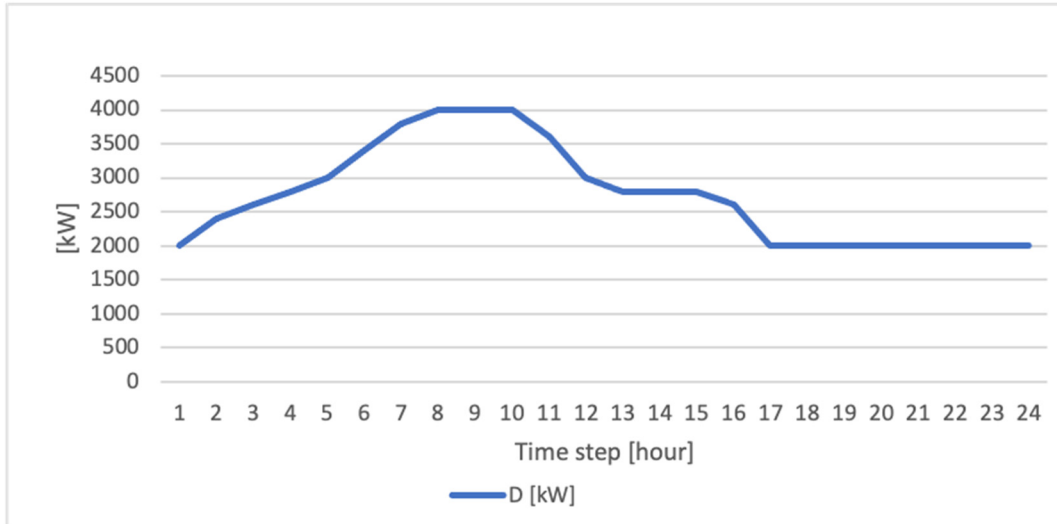


Figure 15. Daily demand profile portraying typical increase and decrease in consumption throughout the day.

Figure 16 illustrates the sensitivity of time to recover to the probabilities of damage to a WT for the hurricane scenario in Table 8 versus the maintenance levels. Only a hurricane scenario and the WT are considered in order to assess the value of conducting sensitivity analyses on more than one maintenance level. The generation power rating is 4.5 MW employing three of each DER at 500 kW. The sensitivity to each variation in $P(d|S_k)$ is calculated by varying the values in Table 8 for a WT and then running 7,500 simulations of the resilience model. Monte Carlo simulations are averaged for 7,500 simulations so as to obtain a 90% confidence interval. The blue represents an increase in $P(d|S_k)$ by 50%, orange the base value chosen for $P(d|S_k)$, and gray a decrease in $P(d|S_k)$ by 50%.

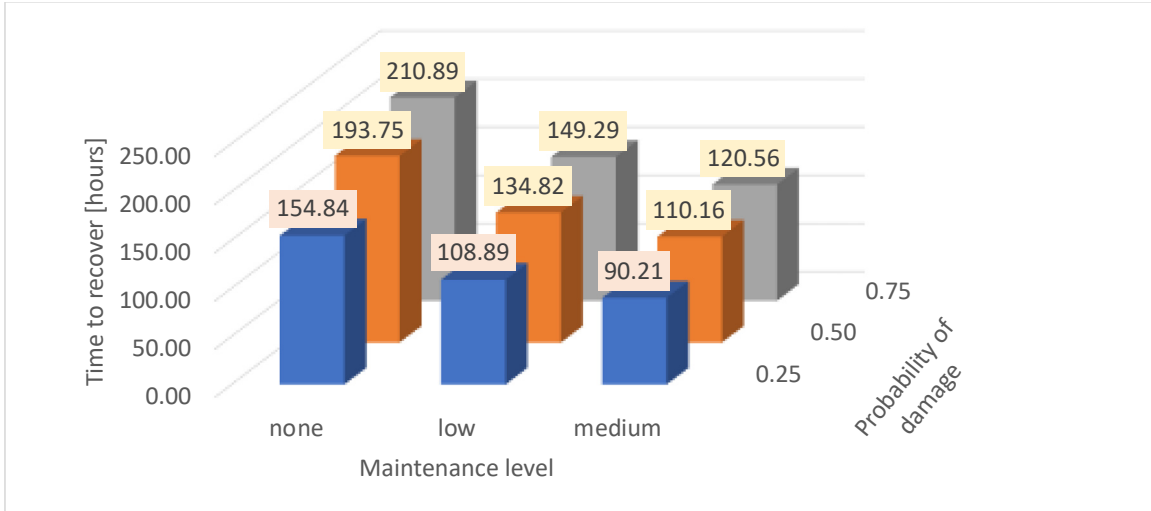


Figure 16. The sensitivity of time to recover to varying the WT's probability of damage 50% and maintenance level.

1. Sensitivity of Resilience Measures to Resilience Input Variables.

Figures 17–19 illustrate the sensitivity of *recovery*, *invulnerability* and time to recover to the resilience input variables for the hurricane scenario. Time to recover is the time that it takes the microgrid to fully recover, different than *recovery*. The sensitivity to each variation in the resilience model's parameters is calculated by varying the values in Tables 10 one at a time. The generation power rating is 3 MW employing two of each DER at 500 kW. The variance is calculated by increasing and decreasing the parameter's value by 50% except when increasing would exceed the maximum value as in battery charging efficiency, DG fuel consumption rate and WT's availability factor.

All three resilience measures are least sensitive to the battery's charging efficiency and fuel consumption rate. *Recovery* and time to recover are most sensitive to the time to repair K . *Invulnerability* is the most sensitive to $P(d^{DG}|S_k)$.

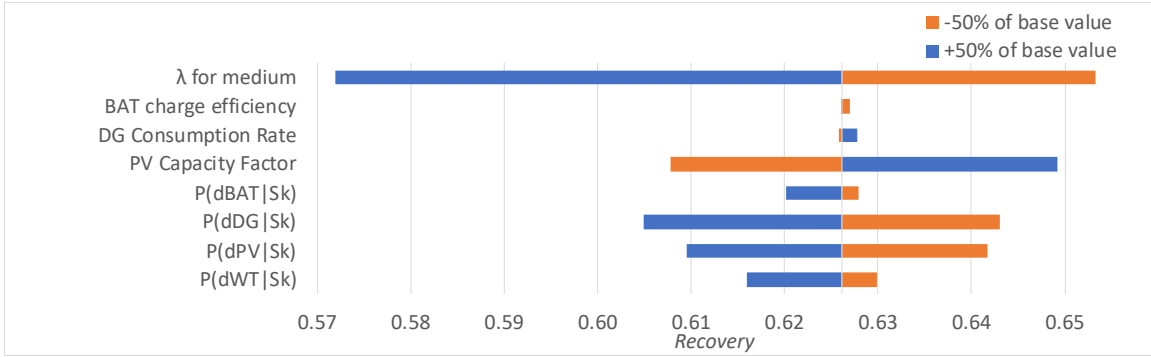


Figure 17. The sensitivity of *recovery* to *resilience* input variables.

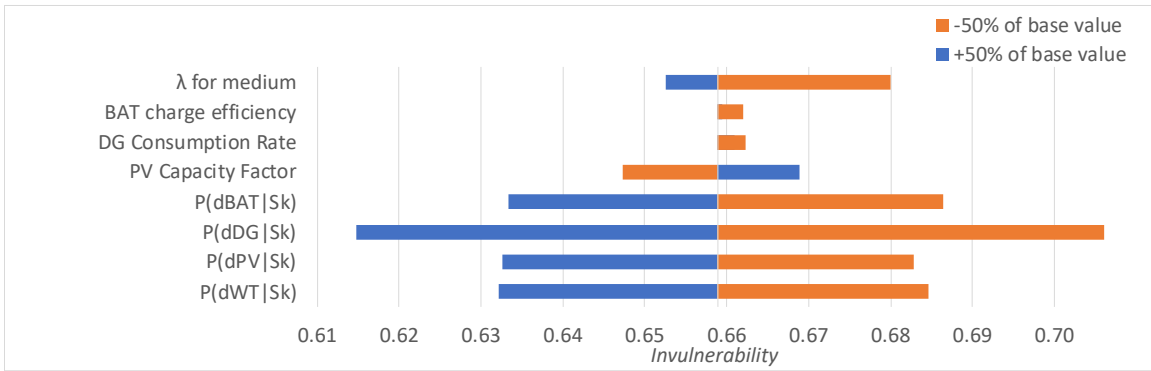


Figure 18. The sensitivity of *invulnerability* to *resilience* input variables.

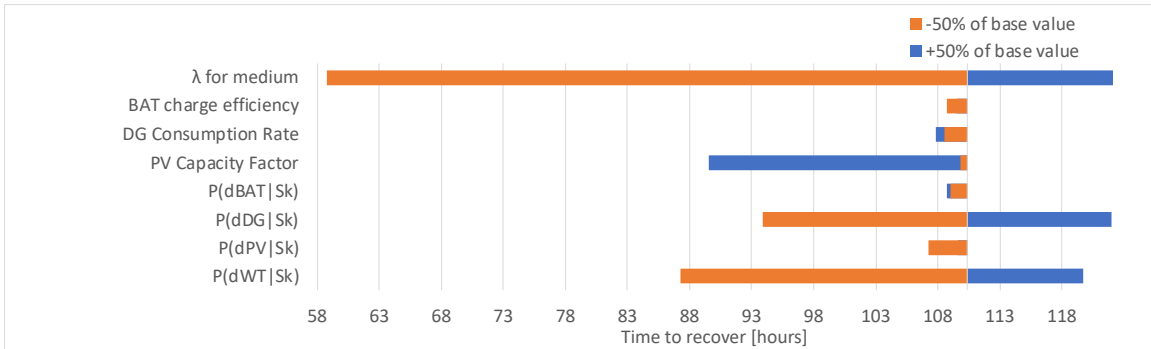


Figure 19. The sensitivity of *time to recover* to *resilience* input variables.

2. Sensitivity of Resilience Measures to Time to Repair λ .

Figure 20 illustrates the sensitivity to time to recover to repair λ . The sensitivity to each variation in λ is calculated by varying the base values in Table 9 for each DER one at a time. The generation power rating is 3 MW employing two of each DER at 500 kW. Time to recover is not excessively sensitive to the PV, DG, or BAT time to repair λ but is especially sensitive to the WTs' time to repair λ . If the base commander can invest more to reduce WT time to repair, this would provide far more benefit in improving the time to recover than the other DERs.

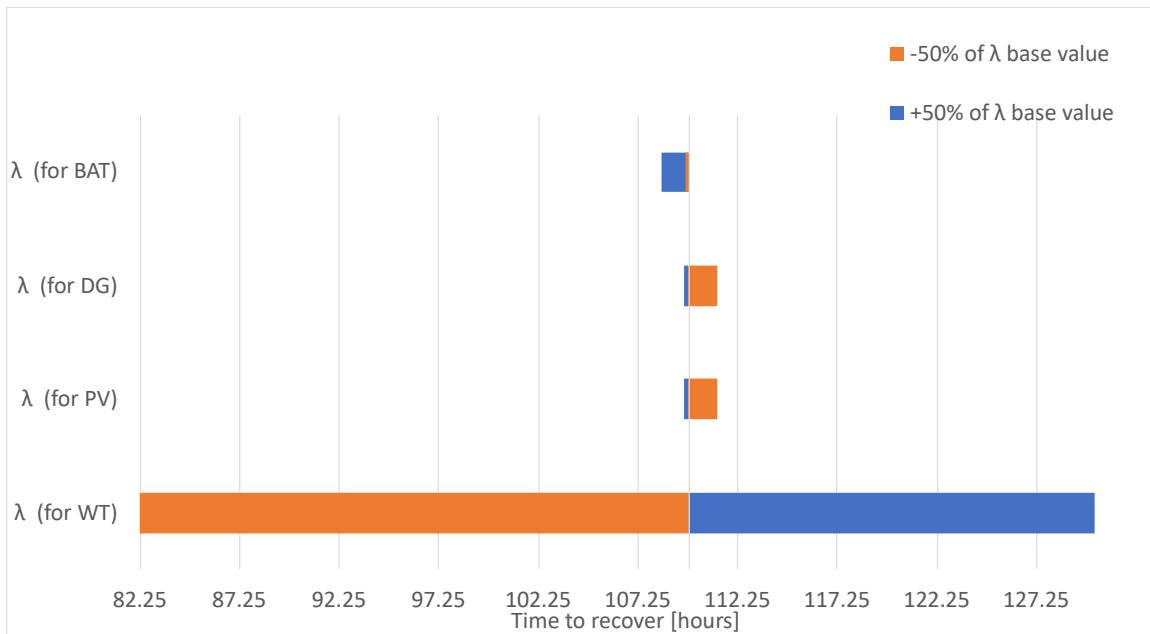


Figure 20. The sensitivity of time to recover to each DER's time to repair λ input variables.

The sensitivity of *recovery*, *invulnerability* and time to recover to repair time λ for both a low and no maintenance is measured. The generation power rating is 4.5 MW employing three of each DER at 500 kW. *Recovery* and *invulnerability* had approximately the same sensitivity of 30% change to the 50% variance in λ . However, the *invulnerability* had little sensitivity to λ as illustrated in Figures 21 and 22. Therefore, if *invulnerability* is more important than *recovery*, there should not be any emphasis on investing in λ .

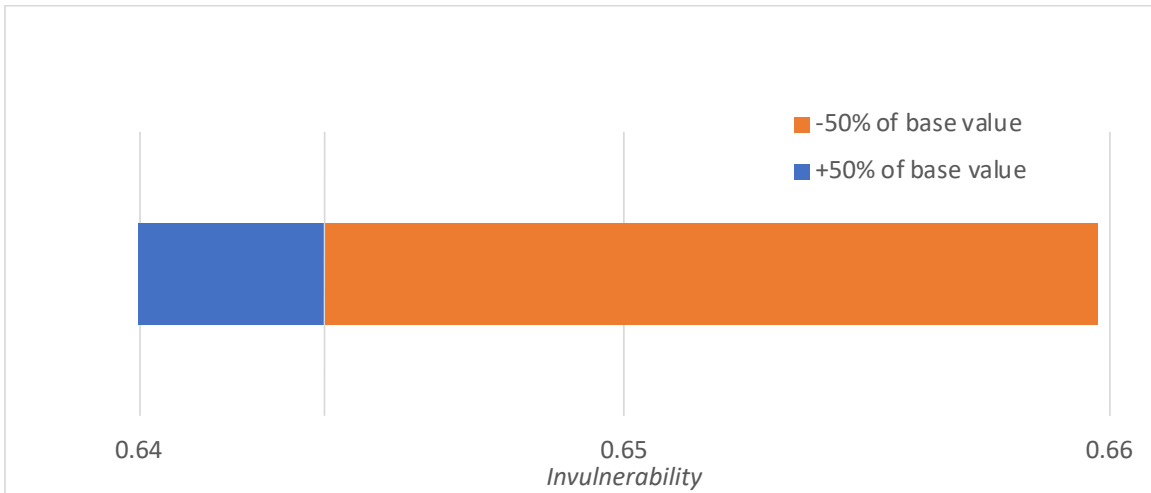


Figure 21. The sensitivity of *invulnerability* to λ for no maintenance.

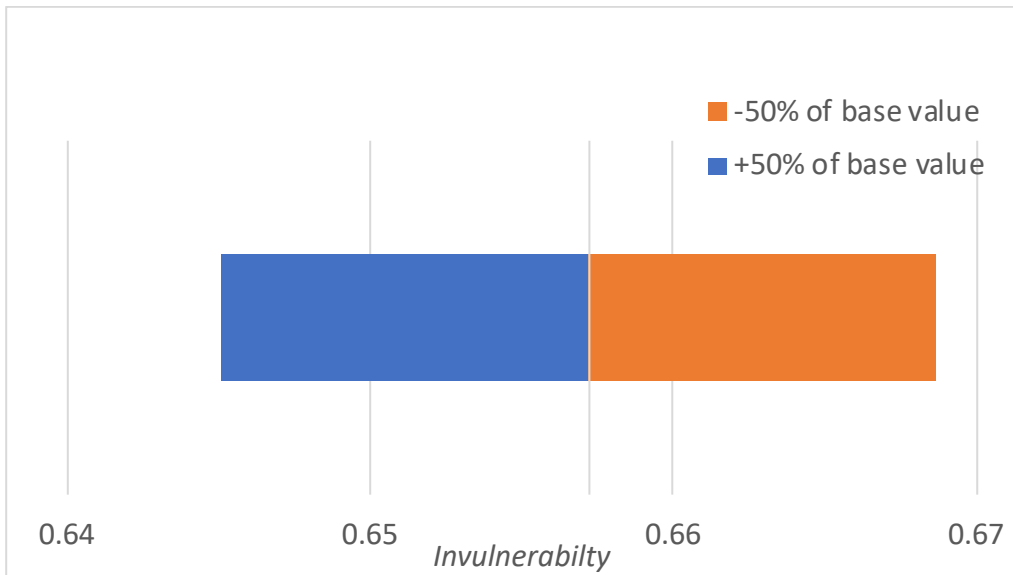


Figure 22. The sensitivity of *invulnerability* to λ for reduced maintenance.

3. Sensitivity of Resilience Measures to Battery Discharge Efficiency.

The sensitivity of *recovery*, *invulnerability* and time to recover to battery discharge efficiency is measured to better understand the sensitivities of the resilience measures to the battery discharge efficiency. The generation power rating is 4.5 MW employing three of each DER at 500 kW. *Recovery* and *invulnerability* had approximately a 30% decrease

for a 50% decrease in battery discharge efficiency. However, time to recover increased by over seven times from the base value as illustrated in Figure 23. Therefore, it is important to use batteries that have good, ideally 0.98 or better, battery discharge efficiencies.

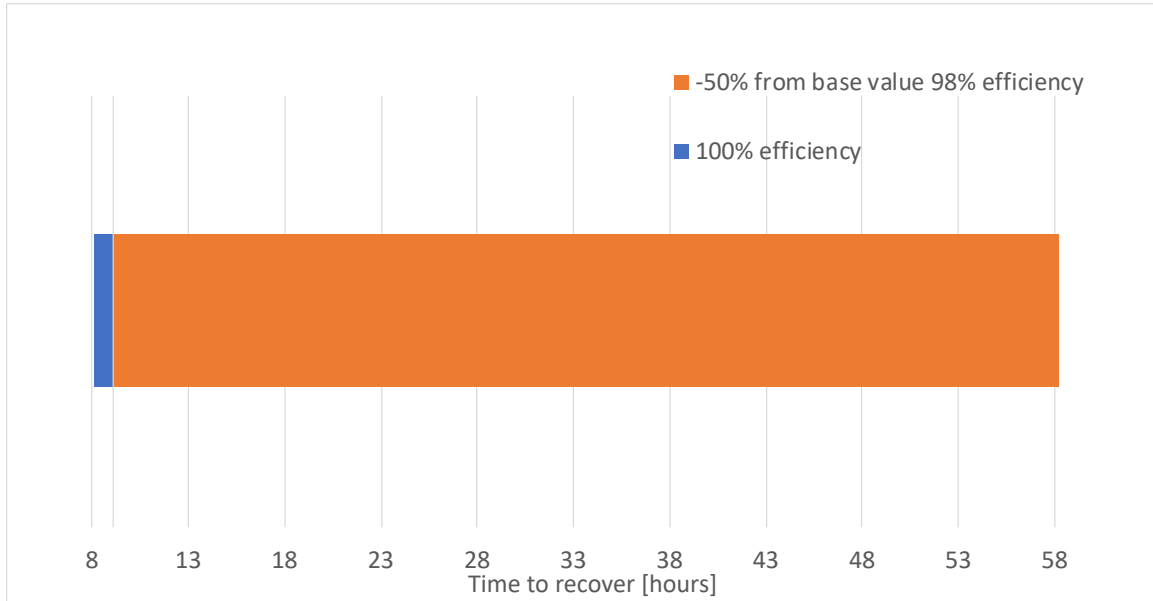


Figure 23. The sensitivity of time to recover to battery discharge efficiency.

4. Sensitivity of Resilience Measures to WT’s Capacity and Availability Factors.

The sensitivity of *recovery*, *invulnerability* and time to recover to C^{WT} and A^{WT} is measured. The generation power rating is 4.5 MW employing three of each DER at 500 kW. Although time to recover almost doubles for a 50% decrease, *recovery* does not vary more than 5% as illustrated in Figures 24 and 25.

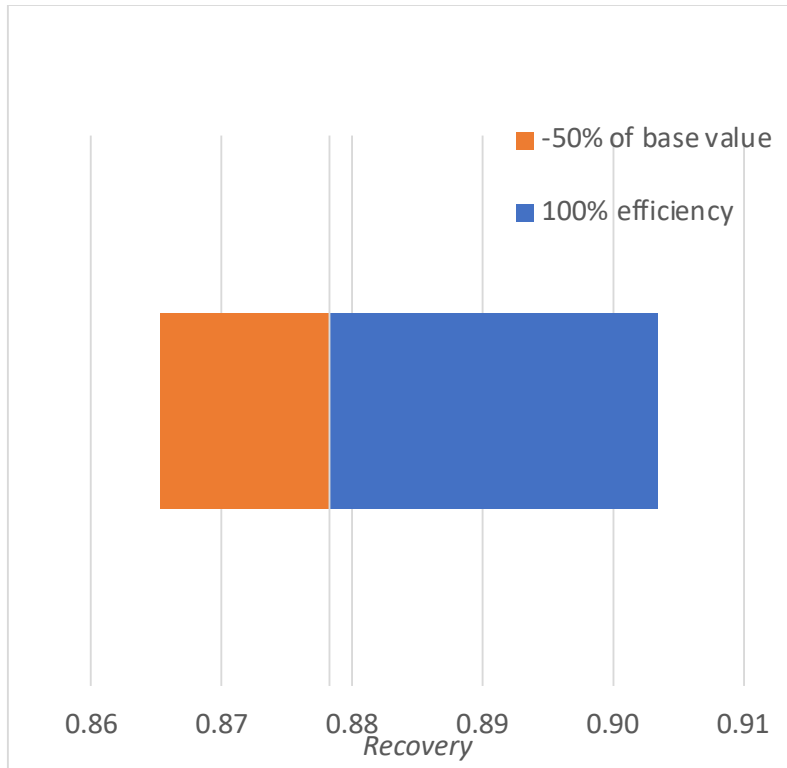


Figure 24. The sensitivity of *recovery* to C^{WT} .

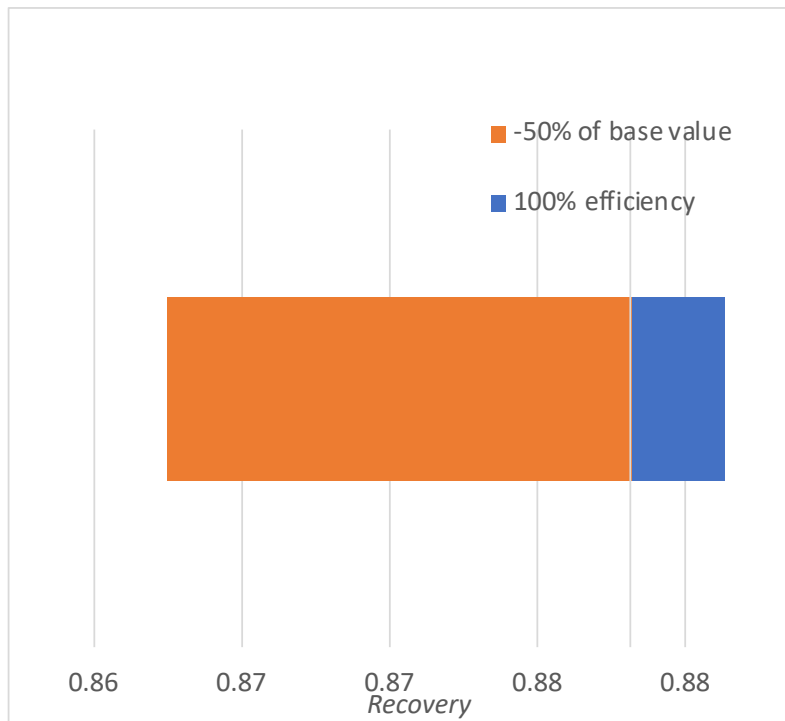


Figure 25. The sensitivity of *recovery* to A^{WT} .

5. Sensitivity of Time to Recover to Time of Disturbance

Figure 26 illustrates the sensitivity of time to recover to the time of the disturbance. The sensitivity of time to recover to the time of disturbance is calculated by varying the disturbance time for each hour of the day. The generation power rating is 3 MW employing two of each DER at 500 kW. Despite the diurnal variations in power generation, there is no sensitivity in time to recover to the disturbance start time. Therefore, choosing a DER that has better generation during the day versus nighttime, or vice versa, should not be considered important.

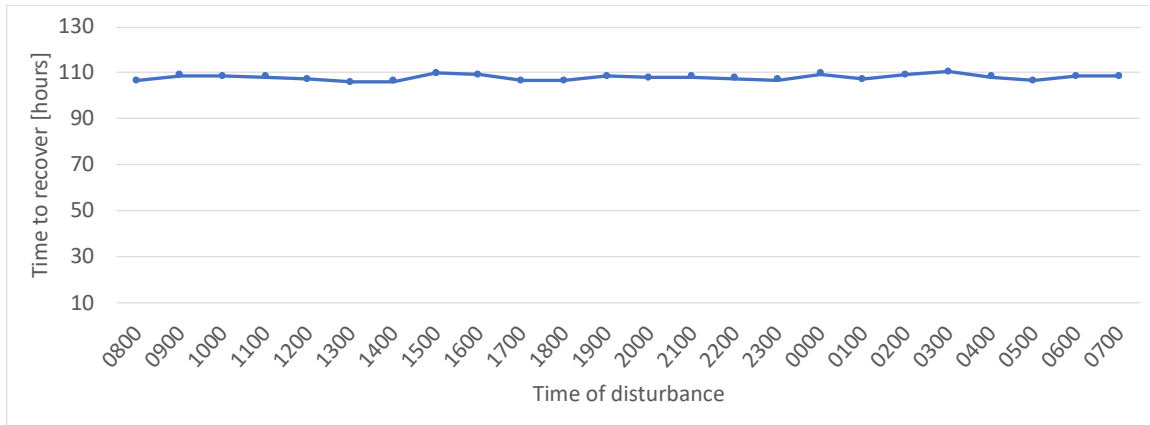


Figure 26. The sensitivity of time to recover to the time of disturbance.

Figure 27 illustrates the sensitivity of time to recover to the time of the disturbance and different ratios of RE power and type of RE to the overall power rating. The sensitivity to a morning and evening disturbance is calculated by varying the disturbance time for the respective ratio of power capacities. There is a slight improvement in the time to recover

only when the ratio of $\frac{\sum_{i=1}^m P_i^{WT}}{P_i} > 0.83$ and the disturbance starts in the evening.

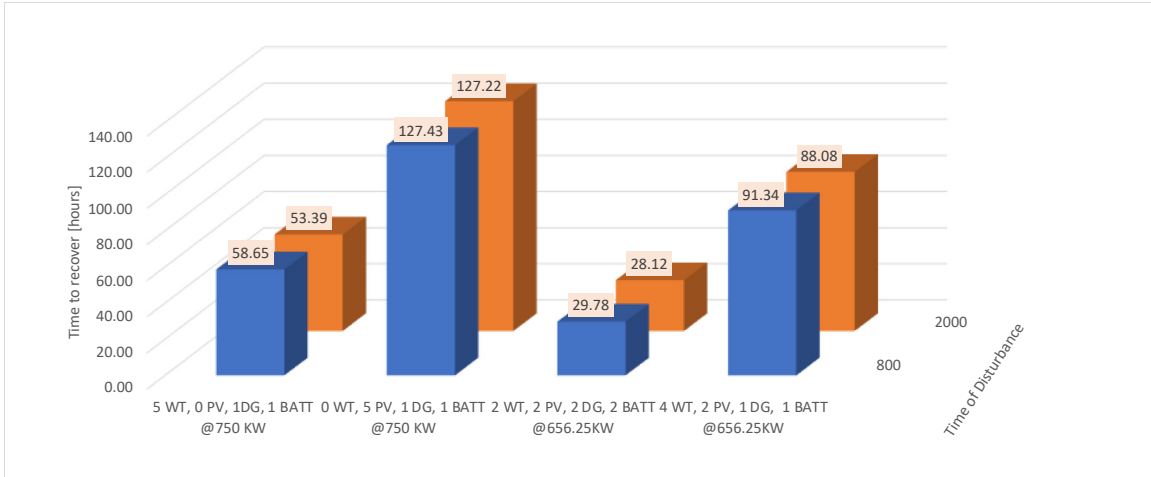


Figure 27. The sensitivity of time to recover to the time of disturbance and ratio of P^{WT}/P and P^{PV}/P .

6. Sensitivity of *LCOED* Cost Measure to Cost Input Variables

Figure 28 illustrates the sensitivity of *LCOED* to the cost model's input variables. The sensitivity to each variation is calculated by varying the base values in Tables 12 and 13 for each DER one at a time. The generation power rating is 3 MW employing two of each DER at 500 kW. *LCOED* is most sensitive to the fuel consumption rate and fuel costs and least sensitive to O&M costs.

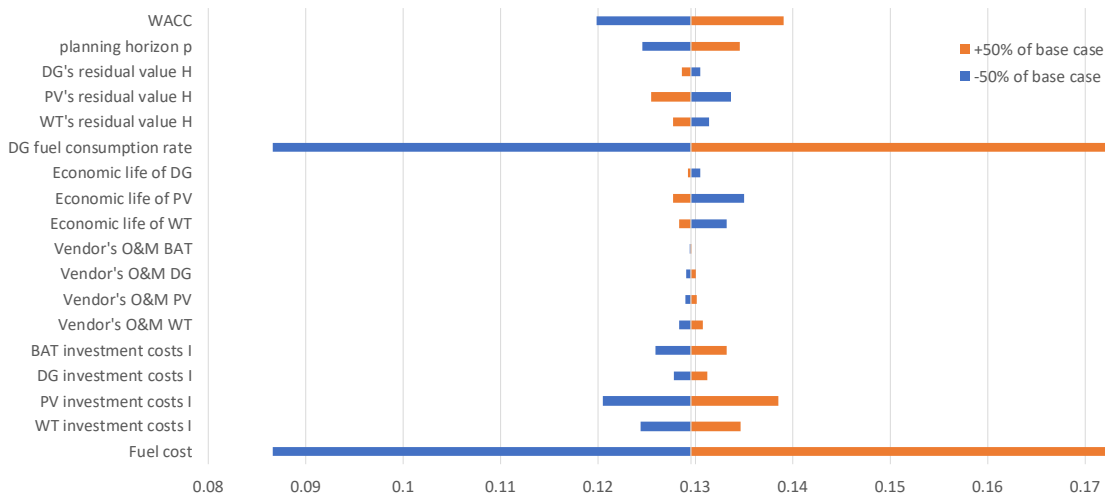


Figure 28. The sensitivity of *LCOED* to cost input variables.

Resilience is least sensitive to the battery's charging efficiency and fuel consumption rate, and most sensitive to the WT's time to repair λ . *LCOED* is most sensitive to the fuel consumption rate and fuel costs and least sensitive to O&M costs. Varying the charging efficiency has the smallest impact on resilience because the batteries play a smaller, albeit important, role in the recovery. For the parameters simulated, this is unlikely. The O&M costs have the least influence on the cost measure due to being proportionally much smaller than the investment costs over the planning horizon.

However, improving the WT's time to repair will increase resilience much more than improving the time to repair the other DERs. This is due to the diurnal behaviors resulting in the WT having a higher daily contribution factor. And, it is expected that the WACC will have impact on the costs due to its exponential application in the NPV calculations for the cost measures.

C. VALIDATION

1. Framework

To validate the models to ensure the assumptions create theoretical model behavior, demonstrate reproducibility and generalizability, and ultimately duplicate past performance using retrospective experiments, Thomsen et al.'s (1999) framework is used.

Thomsen et al. (1999) present their trajectory of validation efforts and argue there are three essential reasons to conduct validation. First, the assumptions must be validated to ensure the model behaves as predicted by theories and observations. Second, the representation must be validated, that is, the model's authenticity, reproducibility and generalizability must be demonstrated. And finally, the advice and usefulness the model can provide must be validated through either using retrospective experiments to duplicate past performance, what-if scenarios, comparison of the model's predictions with actual performance, or attempting to change the future based upon the model's simulations. Thomsen et al.'s (1999) main point worth considering is that no single case validates a model.

2. Assumptions

The model's assumptions are first built from either information obtained from other researchers or using reasonable assumptions that are evaluated for each measure's sensitivity to these parameters. We assume that the microgrid's demand following a disturbance will mimic its historical demand. Similarly, we assume that the microgrid's demand will not drop below the microgrid's post-disturbance power rating.

We place greater value on energy used today than in the future in our cost model. When we evaluate storage of our microgrid's excess power rating, our cost measure discounts future energy. This is a logical but not necessarily appropriate approach for a utility that sells their energy, but even less so for an INI.

We also assume that there is no per unit increase in maintenance as redundancy increases. There will be an increased maintenance burden associated with having more DER with the same nominal power rating. However, this is not incorporated into the cost model.

3. Reproducibility

a. *Cost model reproducibility*

The ability to reproduce the same findings as other researchers in literature have produced using their models provides useful validation. Lotfi and Khodaei (2016) calculated *LCOE* for a microgrid with 50% gas-fired generation (DG), 30% WT, and 20% PV. They incorporated energy storage with a contribution factor that is 44% of the gas-fired generation's contribution factor. The contribution factor represents what percentage of microgrid power is generated by the DER. According to Hossein Lotfi (email to author, June 22, 2020), the planning horizon is 20 years and WACC 10%. There is no information provided for the DER's economic life, fuel costs, investment costs, maintenance costs, or capacities used to generate their findings.

Lotfi and Khodaei's (2016) *LCOE* published data is used to validate the model for the microgrid architecture shown in Table 12. The *LCOE* calculated by the cost model is the same as Lotfi and Khodaei's *LCOE*.

Table 12. Microgrid architecture validated for *LCOE*.

DER	DER's nominal power rating P_i [kW]	Resilience model's contribution factors [%]	Cost model's <i>LCOE</i> [\$/kWh]	Lotfi and Khodaei's (2016) <i>LCOE</i> [\$/kWh]	Cost model's <i>LCOE</i> [\$/kWh]
WT ₁	500	19.7	0.0766	0.0882	0.0889
WT ₂	500				
WT ₃	500				
PV ₁	500	4.6	0.2938		
PV ₂	500				
DG ₁	500	55.5	0.2358		
DG ₂	500				
DG ₃	500				
DG ₄	500				
DG ₅	500				
BAT ₁	350	20.3	0.0163		
BAT ₂	350				

Lotfi and Khodaei (2016) first conclude that decreasing the share of DG's power and increasing that of RE DERs would cause all contribution factors except for the DG's to increase. To validate their finding, we calculate the contribution factors for the microgrid architecture, using the resilience model, with decreased share of DG power shown in Table 13.

Table 13. Contribution factors for microgrid architecture with decreased DG power.

DER	DER's nominal power rating P_i [kW]	Resilience model's contribution factors [%]
WT ₁	1,000	42.5
WT ₂	1,000	
WT ₃	1,000	
PV ₁	1,000	10.0
PV ₂	1,000	
DG ₁	500	25.6
DG ₂	500	
BAT ₁	350	21.9
BAT ₂	350	

The new contribution factors are consistent with Lotfi and Khodaei's (2016) findings in that all contribution factors increased except for the DG's contribution factor.

Lotfi and Khodaei's (2016, 5) second conclusion is that increasing the share of RE DER's power "with high *LCOE* would not be economical since the total *LCOE* becomes larger than the utility price." To validate Lotfi and Khodaei's (2016) second finding we increase the share of PVs, by doubling the number and power, to calculate the *LCOE* for the microgrid shown in Table 14. This new *LCOE* is consistent with Lotfi and Khodaei's (2016) findings in that it is more costly than the original microgrid's *LCOE* of \$0.0889/kWh.

Table 14. DER's *LCOE* after increasing share of PV.

DER	DER's nominal power rating P_i [kW]	Cost model's <i>LCOE</i> [\$/kWh]
WT ₁	500	0.0947
WT ₂	500	
PV ₁	500	
PV ₂	500	
PV ₃	500	
PV ₄	500	
DG ₁	500	

DER	DER's nominal power rating P_i [kW]	Cost model's <i>LCOE</i> [\$/kWh]
DG ₂	500	
DG ₃	500	
DG ₄	500	
DG ₅	500	
BAT ₁	350	
BAT ₂	350	

Lotfi and Khodaei's (2016, 5) third conclusion is a "change in the *LCOE* of the DER with the highest (lowest) contribution factor would have the most (least) effect on the total *LCOE*." To validate Lotfi and Khodaei's (2016) third finding we calculate the microgrid's *LCOE* by increasing each DER's *LCOE* 10% one by one for the original microgrid architecture shown in Table 15.

Table 15. Microgrid *LCOE* after increasing each DER's *LCOE* by 10%.

DER	DER's original <i>LCOE</i> [\$/kWh]	DER's new <i>LCOE</i> [\$/kWh]	Cost model's microgrid <i>LCOE</i> [\$/kWh]
WT	0.0766	0.0843	0.0995
PV	0.2938	0.3232	0.0997
DG	0.2358	0.2594	0.1067
BAT	0.0163	0.0179	0.0997

Lotfi and Khodaei's (2016, 5) "DER with the highest contribution factor" in this model is DG, and the lowest is PV as indicated in Table 12. And this model's DER having Lotfi and Khodaei's (2016, 5) "change in the *LCOE* of the DER with the highest contribution factor," is DG, which did have the most impact on the total *LCOE*, although the change in the DER with lowest contribution factor, PV, did not have the least effect; rather, the BATs have the least effect but the differences between WT, PV, and BAT are negligible and well within the errors of this model. This is partially consistent with Lotfi and Khodaei's (2016) findings.

Lotfi and Khodaei's (2016, 5) final conclusion is "a decrease in a DER capacity factor, while other parameters are unchanged, would cause its own contribution factor to

decrease, whereas other DERs contribution factors would increase. In this situation, the total *LCOE* would decrease (increase) if that DER's *LCOE* is greater (smaller) than the total *LCOE*." To validate Lotfi and Khodaei's (2016) final finding, we decrease the capacity factor of PV by 50%. The contribution factors are now WT 20.1%, PV 2.4%, DG 56.8%, and BAT 20.7%. These changes in the contribution factors are consistent with Lotfi and Khodaei's (2016) findings in that the PV's contribution factor did decrease from 4.6% to 2.4% and all other contribution factors increased from their original amounts. The PV's *LCOE* is greater than the total *LCOE* and after decreasing the capacity factor the total *LCOE* increased to \$0.0977 which is inconsistent with Lotfi and Khodaei's (2016) findings.

We then restore the PV to the original capacity factor and decreased the capacity factor of the WT by 50%. The contribution factors are now WT 10.9%, PV 5.1%, DG 61.5%, and BAT 22.5 %. This is consistent with Lotfi and Khodaei's (2016) findings in that the WT's contribution factor did decrease from 19.7% to 10.9% and all other contribution factors increased from their original. The WT's *LCOE* is less than the total *LCOE* and after decreasing the capacity factor the total *LCOE* increased to \$0.0977 which is consistent with Lotfi and Khodaei's (2016) findings.

b. Resilience, and cost model reproducibility

Faraji et al. (2019) assessed resilience and costs of two energy systems to a power outage. The first microgrid is a DG, and the second a RE microgrid with PV and BAT. The load modeled is a small clinic that had a peak load of 2.5 kW and average load of 1 kW. The parameters used in their analysis are presented in Table 16.

Table 16. Parameters for Faraji et al.'s (2019) DG, and PV microgrids.

Parameter	DG microgrid	PV microgrid	
	DG	PV	BAT
Total power rating [kW]	2.8	10.0	20.0
DER component power rating [kW]	2.8	1.0	1.0
Number of components	1	10	20
Efficiency [%]	95.00	16.25	95.00
Economic life	15,000 hours	25 years	10 years

Parameter	DG microgrid	PV microgrid	
	DG	PV	BAT
Planning horizon [years]	25		
WACC [%]	18		
Investment costs [\$]	1,400	3,500	2,480
Maintenance costs [\$/year]	166.03	100.00	-725.00
Fuel costs [\$/gallon]	1.10	0.00	0.00
<i>MTTR</i> [hours]	48		

The results of Faraji et al.'s (2019) analysis indicate that the PV microgrid is less expensive than the DG microgrid but has almost the same resilience as the DC microgrid using their resilience measure, survivability of load. These same parameters are used to simulate the resilience and cost models 500 iterations, and generated the findings presented in Table 17. The findings on the cost measures are consistent between Faraji et al.'s model and this dissertation's cost model in that the PV system is cheaper than the DG, and the *LCOE* calculations are the same for the PV microgrid, and are within \$0.05/kWh of the DG's *LCOE*. The findings on the resilience measures are similar but not exactly the same as Faraji et al. The resilience measures using the resilience model demonstrate that the PV microgrid has greater resilience than the DG microgrid. This most likely is due to the resilience model incorporating probability of damage, an exponential probability distribution on the *MTTR*, and a resilience measure that more accurately measures the microgrid performance over the time to recover.

Table 17. Simulation results for Faraji et al.’s (2019) DG, and PV microgrid.

Cost and resilience measure	DG microgrid			PV microgrid		
	Faraji et al. (2019)	Cost model	Resilience model	Faraji et al. (2019)	Cost model	Resilience model
<i>LCOE</i> [\$/kWh]	0.0396	0.0949		-0.0032	0.0081	
<i>Survivability of load</i> (unmet load) [kWh/year]	0.0			2.7×10^{-15}		
<i>resilience</i>			0.61			0.83
<i>invulnerability</i>			0.48			0.67
<i>recovery</i>			0.73			1.00
<i>time to recover</i> [hours]			16.70			1.00

This model’s *LCOE* is the same as Lotfi and Khodaei’s (2016), their first three findings are consistent with this model, and their last finding is mostly consistent. This model’s *LCOE* is within \$0.05/kWh of Faraji et al.’s (2019) two microgrids, consistent in showing that PV is less expensive, and mostly consistent in the resilience findings. In deference to Thomsen et al.’s (1999) position that no single case validates a model, two cases are used to validate the resilience and cost models. Both of these cases validate that the assumptions made generate reproduceable results using the resilience and cost models. The third and final reason for validation will be explored in Sections C through N to convey the model’s usefulness and corresponding advice for decision makers.

D. EXCESS POWER GENERATION RATING

A microgrid with a power generation rating much greater than the power demand it serves, and especially when the microgrid uses a diverse and redundant set of power generative sources, will have greater resilience than a microgrid in which its power rating is more or less equal to demand. The reason is twofold: (1) in the face of a disturbance, extra power is an obvious buffer to partial losses of power generation; and (2) multiple, different power generative sources are less likely to all be damaged in a disruption compared to a single, monolithic power source. Of course, having excess power will lead

to higher costs. The decision is to determine the best tradeoff between increased resilience for increased costs. Each of these experiments varies the microgrid architectures, and maintenance levels so as to understand the relationship between power rating, diversification, and resilience and costs. These relationships are plotted as resilience versus costs and confirm that some design architectures may be more desirable to an INI's situation.

This section presents experiments showing how the microgrid's power rating impacts resilience and costs for each of the microgrid's different maintenance levels. Each microgrid architecture chosen has a different power rating ratio. Some of the results generated by the experiments are presented in a 4D visualization with different colors for each microgrid architecture's experiment. Each microgrid's function is a shape created through interpolation of the data points generated for each experiment. Each microgrid architecture generates three data points corresponding to each of the three maintenance levels. The lighter shading of the data points is used for more maintenance; light shading is for medium maintenance, medium shading for low maintenance, and dark shading for no maintenance. The 2D graphs for *LCOED* vs. *resilience*, *recovery*, and *invulnerability* are provided in Appendix A.

The findings shown for each experiment, help us understand that maintenance matters most when the power to demand ratio is less than 1.5. We also will see how resilience grows exponentially while costs increase linearly. Finally, we explore the trade space to show when increasing beyond some power rating ratios provides no further benefits to either resilience, costs, or both.

- 1. Ratio of Microgrid Nominal Power Generation Rating to Demand, and Maintenance Level with Constant DER Nominal Power Rating Impacts on Resilience and Costs**

This section conducts simulations to evaluate the impact of varying the ratio of power generation rating to demand and the annual maintenance investment level on resilience and costs for a hurricane scenario. The number of simulations are calculated to achieve a 90% confidence interval and a level of precision at ten minutes per hour, or

0.0333. Using the standard deviation for 500 simulations we solve for 7,500 required simulations and present the solution in Appendix C, Liu (2020,2).

We test how varying the maintenance level will impact resilience for a microgrid with the same proportion of DER components but different overall power rating. Although this is not a redundancy experiment, it does provide useful information when comparing these results to the next experiment that maintains a constant number of microgrid DER components. Three different microgrid architectures with different ratios of generation to demand are evaluated as shown in Table 18, all with the same power rating for each DER. The starting time for the disturbance is 8:00 am.

Table 18. Microgrid architectures with same power rating for each DER.

Architecture	Ratio of microgrid nominal power generation rating to average demand $\frac{P^{WT} + P^{PV} + P^{DG}}{\overline{D}_i}$	Microgrid nominal power generation rating $P^{WT} + P^{PV} + P^{DG}$ [MW]	DER nominal power rating P_i [kW]	# of WT m^{WT}	# of PV m^{PV}	# of DG m^{DG}	# of BAT m^{BAT}
3 of each DER	1.2	3.15	350	3	3	3	3
4 of each DER	1.5	4.20	350	4	4	4	4
5 of each DER	1.9	5.25	350	5	5	5	5

The first microgrid architecture with $\frac{P^{WT} + P^{PV} + P^{DG}}{\overline{D}_i} = 1.2$ is displayed in Figure 29.

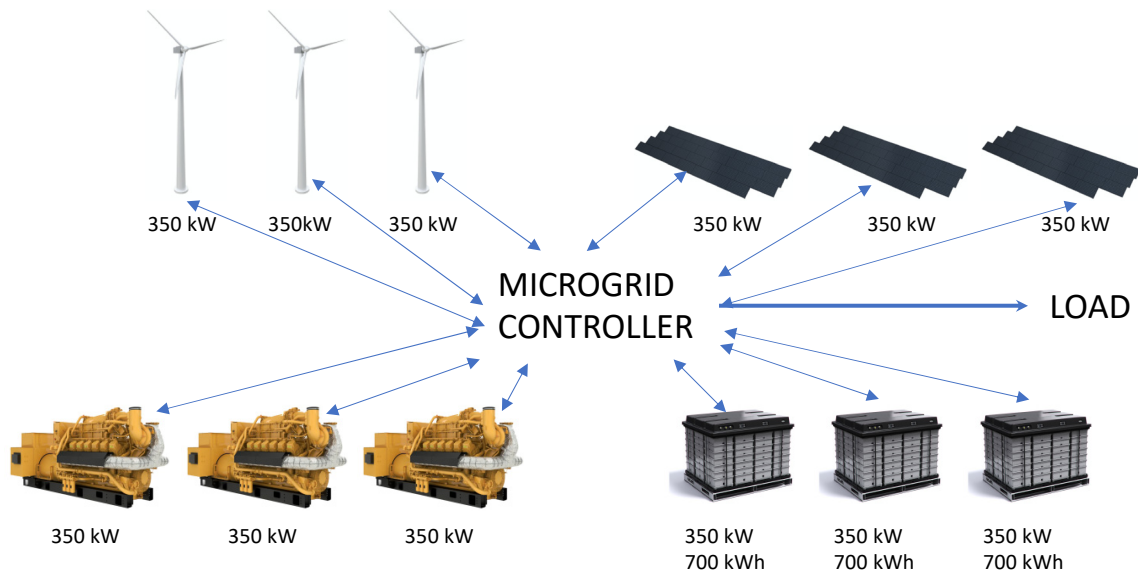


Figure 29. Microgrid architecture with three of each DER at 350 kW and 3.15 MW overall power generation rating.

It should be noted that the microgrid’s nominal power rating must be sufficient to meet the demand. If it is undersized, the microgrid despite recovering, will still be unable to meet the demand. Therefore, the demand profile must be considered so as to size the microgrid with sufficient power to meet the demand.

Increasing either the maintenance investment, power rating, or both should provide greater resilience, but as the power rating grows beyond demand, resilience will approach a point of diminishing returns. The assumptions are made and articulated in Sections A and B that include assuming the disturbance scenario is a hurricane; nothing else is varied for each architecture other than the number of DER components in order to create the different overall microgrid power ratings.

Time to recover is the time it takes the microgrid to fully recover. When the ratio of microgrid power generation rating to demand is greater than 1.5 the importance of maintenance is much less due to the small differences in resilience between having no maintenance and a medium level of maintenance, as seen in Figures 86–88. Maintenance is only significant when the microgrid’s power rating is closer to the demand. This is due

to gaining more benefits from faster recovery when the microgrid has less excess power rating.

Figure 30 shows that excess power rating by having more power generation leads to large improvements in the time to recover the microgrid. However, the cost per kWh also increases significantly. Also, we note maintenance policies become inconsequential when the microgrid has a lot of excess power over demand.

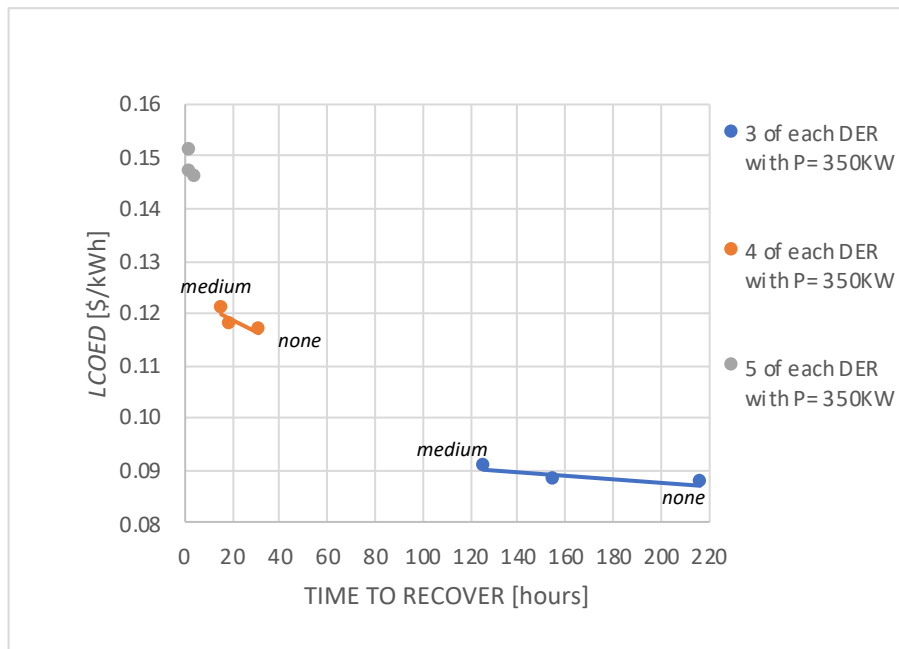


Figure 30. The effects of maintenance level on *LCOED* and time to recover.

Figure 31 shows a decreasing return in improvements of resilience as the microgrid’s power generation rating is increased beyond a ratio of 1.5. Increasing the power rating from 1.2 to 1.5 increases resilience from 0.65 to 0.82. A further increase of power rating ratio to 2 yields a 0.89. Meanwhile the cost increases linearly with increases in the power rating ratio.

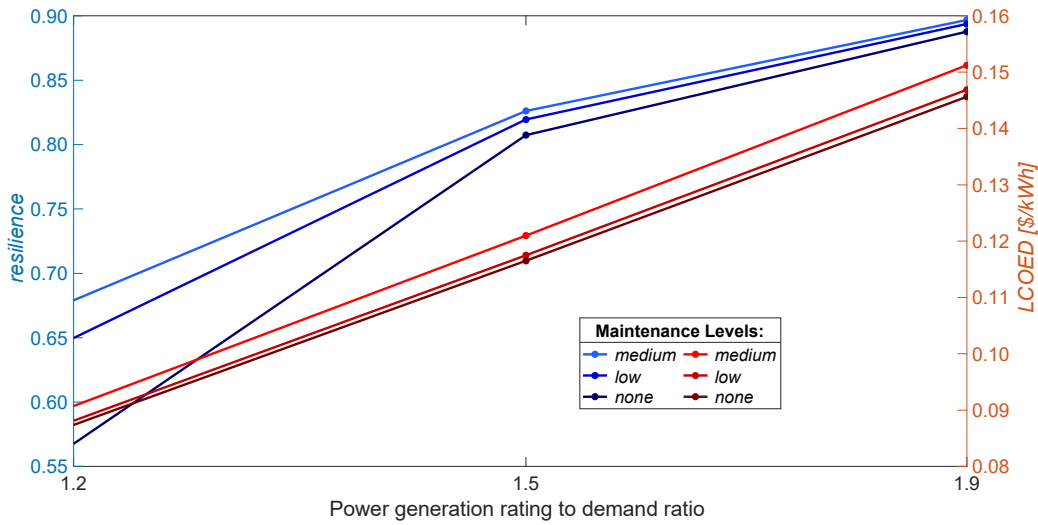


Figure 31. Linear increase in costs and nonlinear increase in *resilience* as power rating ratio increases.

As shown in this experiments' figures in Appendix A.1, increasing the microgrid's power rating improves *recovery*, *invulnerability*, *resilience* and time to recover but there is a greater improvement in *recovery* than there is in *invulnerability* for the same cost. Therefore, a decision maker who values *invulnerability* more than *recovery* will need to invest significantly more both in maintenance and investment costs to realize greater benefits in *invulnerability*. Also, seen in these figures in Appendix A is that increasing maintenance improves *recovery*, *invulnerability* and time to recover in all architectures but has less impact when exceeding a ratio of the generation to average demand greater than 1.5. Therefore, decision makers should invest less in maintenance as the power rating increasingly exceeds demand.

Resilience costs more to improve when $\frac{P^{WT} + P^{PV} + P^{DG}}{D_t} = 1.5$. At a medium maintenance level and $\frac{P^{WT} + P^{PV} + P^{DG}}{D_t} = 1.5$, $LCOED = \$0.12/\text{kWh}$ and $resilience = 0.83$.

$LCOED$ increases in a linear manner, and resilience increases in a nonlinear manner as the power rating ratio increases. There is little improvement due to maintenance levels for the 1.9 ratio of microgrid power generation rating to demand.

The cost of resilience can now be better understood by decision makers. Doubling the ratio of power generation rating to demand can greatly reduce time to recover but at significant costs compared to the same ratio of one. The base commander can now decide whether restoring power four days earlier is worth an additional \$0.03/kWh as seen in Figure 30.

When pondering why a power rating ratio of 1.5 is a point of decreasing gains in resilience and steadily increasing costs, we recognize that this ratio approximates an amount that when the power rating is reduced for efficiencies, and damage due to the disturbance, the microgrid's generation will more closely meet the demand. By having the microgrid sized so there is no excess power rating upon being degraded, there are no wasted costs. This ratio is also dependent upon the probabilities of damage. Overall, this provides a useful insight on maintenance, maintenance matters when excess power is approximately 50% or greater than the demand.

2. Ratio of Microgrid Nominal Power Generation Rating to Demand, and Maintenance Level with Constant Number of DER Impact on Resilience and Costs

Figure 32 illustrates the sensitivity of time to recover to the redundancy level and the microgrid's nominal power rating over the average demand, $\frac{P}{D_t}$. In general, there is much greater improvement in time to recover when redundancy is increased for greater ratios of $\frac{P}{D_t}$ but there are diminishing improvements when $\frac{P}{D_t} > 1.5$. When $\frac{P}{D_t} = 0.5$ the microgrid never recovers within the two week timeframe simulated; hence all time to recover hours are 337 hours, one hour beyond the two weeks evaluated.



Figure 32. The sensitivity of time to recover to each microgrid ratio of power rating to demand and redundancy level.

To understand how the ratios of power generation rating to demand influence resilience and costs we model microgrids with different capacities for each DER and overall microgrid power rating. The number of DER is maintained as shown in Table 19.

Table 19. Microgrid architectures for different ratios of $\frac{P^{WT} + P^{PV} + P^{DG}}{D_t}$.

Ratio of microgrid nominal power generation rating to average demand $\frac{P^{WT} + P^{PV} + P^{DG}}{D_t}$	Microgrid nominal power generation rating $P^{WT} + P^{PV} + P^{DG}$ [kW]	DER nominal power rating P_i [kW]	# of WTs m^{WT}	# of PVs m^{PV}	# of DGs m^{DG}	# of BATs m^{BAT}
1.25	3,413	1,138	1	1	1	1
1.50	4,095	1,365	1	1	1	1
2.00	5,462	1,820	1	1	1	1
3.00	8,193	2,730	1	1	1	1
4.00	10,924	3,640	1	1	1	1

Figure 33 shows that resilience grows exponentially with respect to increases in the power rating to demand ratio, while the total life cycle costs grow linearly. We also see how maintenance matters less as the power rating ratio increases. Finally, it costs more to

realize similar gains in *resilience* as we increase the power rating ratio. *LCOED* increases in a linear manner, and *resilience* increases in an exponential manner as the power rating ratio increases.

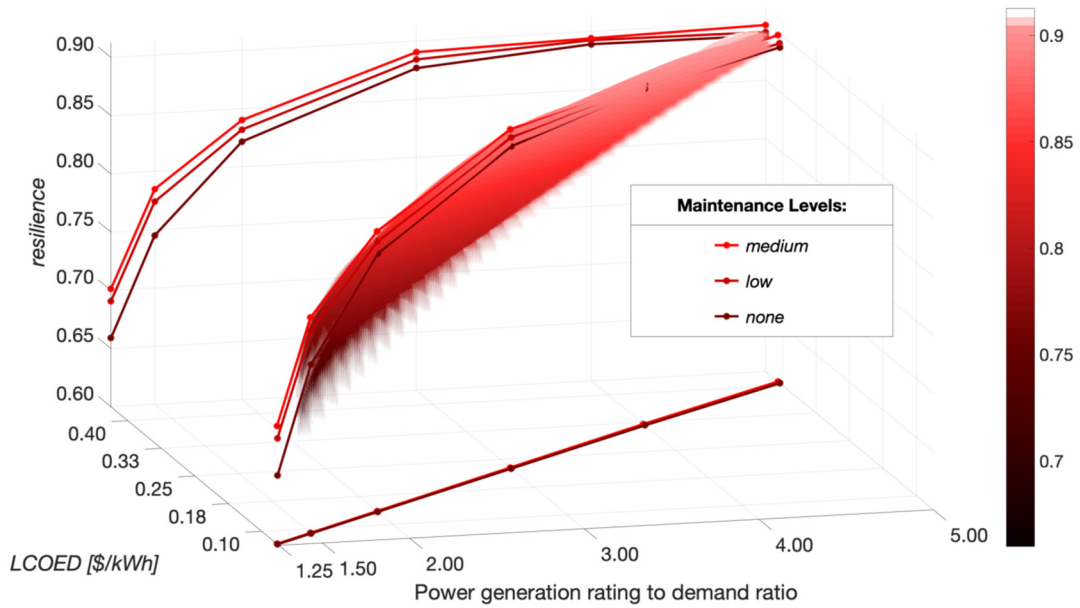


Figure 33. Power generation rating to demand ratio as viewed from a power rating perspective.

Figure 34 shows how the maintenance level is a factor a decision maker should consider only when $\frac{P^{WT} + P^{PV} + P^{DG}}{D_t} < 1.5$. This finding is consistent with the previous experiment's results.

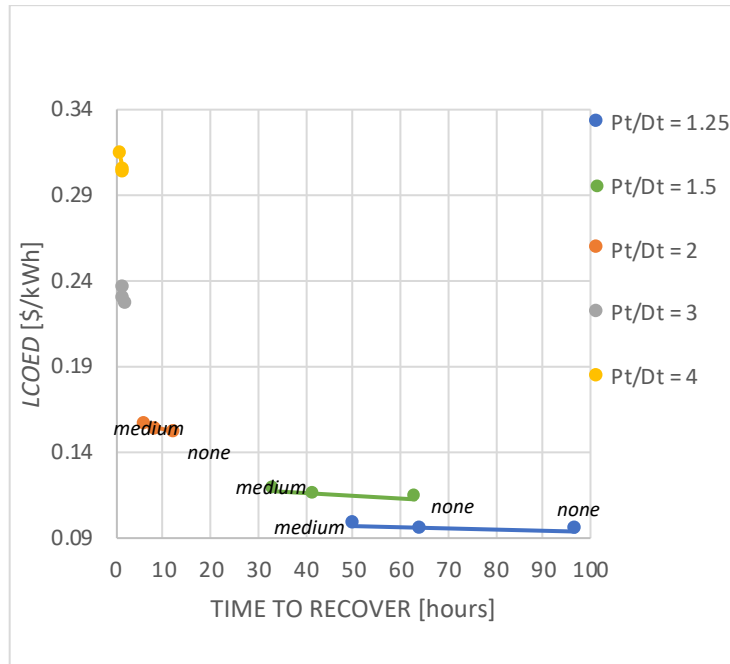


Figure 34. The effects of microgrid power rating to demand ratio on *LCOED* and time to recover.

This experiment compared to the previous experiment highlights the benefit of redundancy for the same power rating ratio. In the previous experiment, the power rating ratio of 1.5 has an overall power rating of 4.2 MW with 4 WTs, 4 PV, 4 DG, and 4 BAT with *resilience* = 0.83 and *LCOED* = \$0.12/kWh. In this experiment, for an approximate power rating ratio of 1.5, the overall power rating is 4.1 MW with 1 WT, 1 PV, 1 DG, and 1 BAT with *resilience* = 0.77 and *LCOED* = \$0.12/kWh. The first experiment has an 8% higher resilience, for equivalent costs. This improvement is attributed to redundancy and shows how the architecture’s power rating ratio can improve resilience, and costs by incorporating redundancy.

Figure 35 highlights the exponentially decreasing returns on resilience while costs increase linearly. We can also more clearly see how there is effectively no improvement in resilience beyond a power rating ratio of four. Increasing the power rating ratio from 2 to 3 increases *resilience* from 0.83 to 0.88. A further increase of power rating ratio to 4 yields a 0.89. Meanwhile the cost increases linearly with smaller increases in power rating ratio.

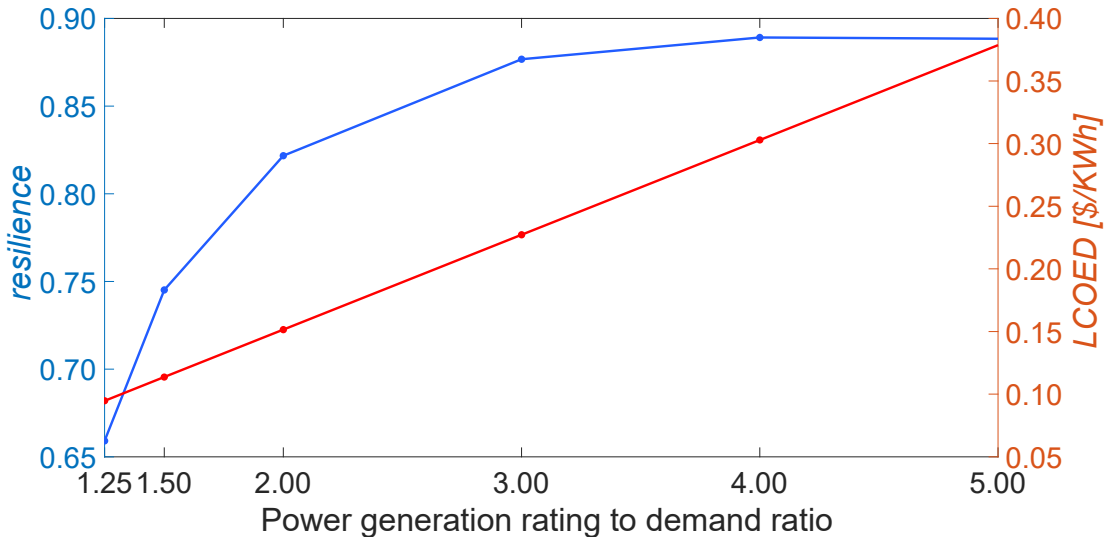


Figure 35. Exponential increase in *resilience* as costs linearly increase.

Figure 36 shows how *invulnerability* and *recovery* follow an exponential function of power rating. We observe how *invulnerability* contributes more to *resilience* than recovery after a ratio of 1.5.

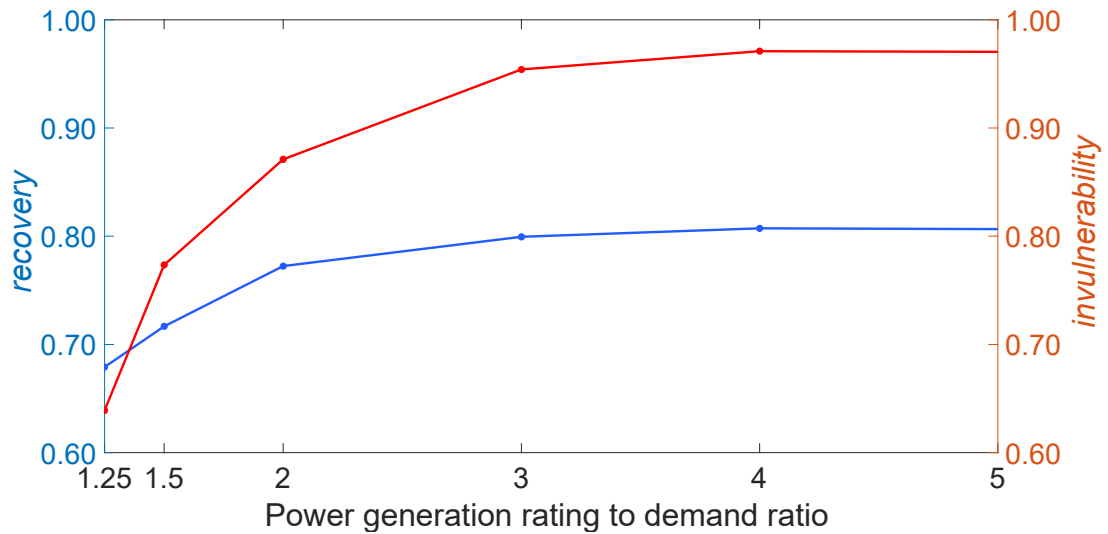


Figure 36. Exponential increase in *recovery* and *invulnerability* as the power rating ratio increases.

Exceeding a power rating ratio of four costs more without any further gains in *resilience*. The previous experiment provided better results for the same power rating ratio

due to its microgrid incorporating redundancy. This provides us an additional and more useful insight when sizing a microgrid so that we incorporate redundancy and do not exceed a ratio of four for the power to demand ratio.

3. Ratio of RE Nominal Power to DG Nominal Power with Constant DER Nominal Power Rating Impact on Resilience and Costs

To incorporate RE it will be useful to understand how varying the nominal power rating ratio of the RE DER to the DG DER will impact a microgrid’s resilience. RE will behave differently than DG in this model due to diurnal factors, and the different probabilities of damage. These differences in the model do not fully reflect all the differences such as the greater and inherent uncertainty in RE power generation. Each microgrid modeled has the same nominal power rating for each DER but a different overall microgrid nominal power generation rating. Five different microgrid architectures employing DER components with a nominal power rating of 1,500 kW are evaluated as shown in Table 20.

Table 20. Microgrid architectures for proportion of DER with constant DER power rating.

Ratio of RE nominal power rating to DG nominal power rating $\frac{P^{WT} + P^{PV}}{P^{DG}}$	Ratio of RE nominal power rating to nominal microgrid power generation rating $\frac{P^{WT} + P^{PV}}{P}$	Microgrid nominal power rating P [MW]	DER nominal power rating P_i [kW]	# of WT m^{WT}	# of PV m^{PV}	# of DG m^{DG}	# of BAT m^{BAT}
2	0.50	18	1,500	3	3	3	3
3	0.60	15	1,500	3	3	2	2
4	0.67	9	1,500	2	2	1	1
5	0.71	21	1,500	5	5	2	2
6	0.75	12	1,500	3	3	1	1

The nominal BAT power rating is maintained the same as the nominal DG power rating,

$P^{BAT} = P^{DG}$. The microgrid architecture with $\frac{P^{WT} + P^{PV}}{P^{DG}} = 2$ is portrayed in Figure 37.

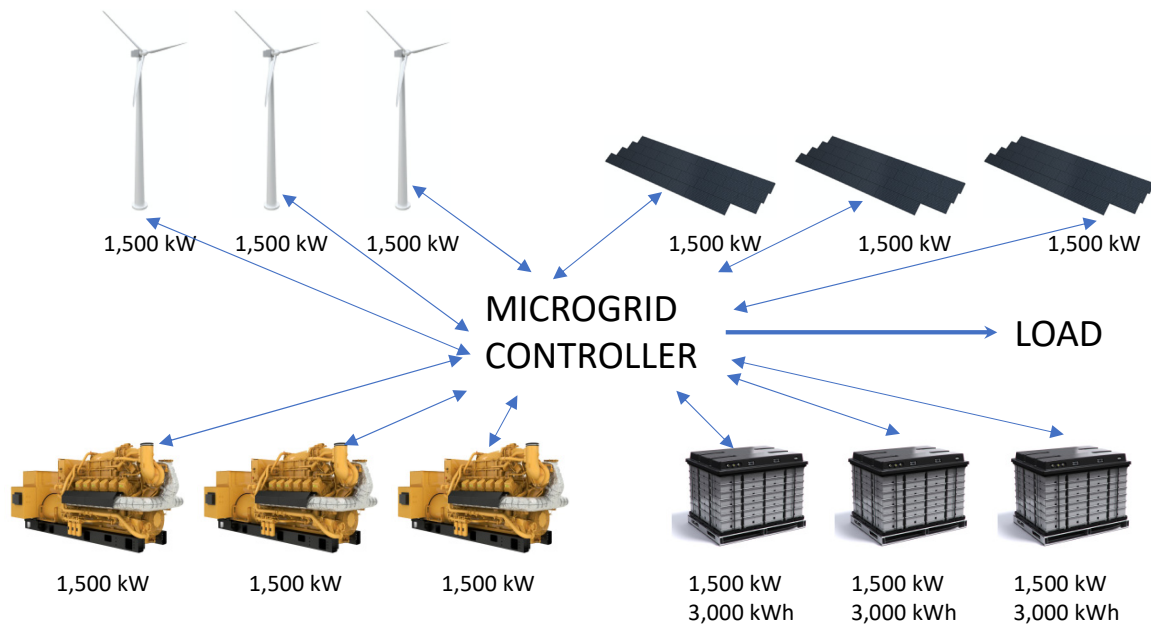


Figure 37. Microgrid architecture with RE/DG = 2 employing three of each DER at 1,500 kW and 13.5MW overall power generation rating.

The expectation is that increasing the microgrid's proportion of RE/DG will provide greater resilience, but that resilience as before will approach a point of diminishing returns considering the costs. The assumptions are made and articulated in Sections A and C for a hurricane scenario; nothing else is changed for each architecture other than the number of DER components in order to create the different overall proportions of microgrid power ratings.

Figure 38 shows again how maintenance matters more for smaller microgrid power ratings. We also see how the largest power ratings are the proportions of two or five with maintenance having less benefits due to the small differences in time to recover between low and high.

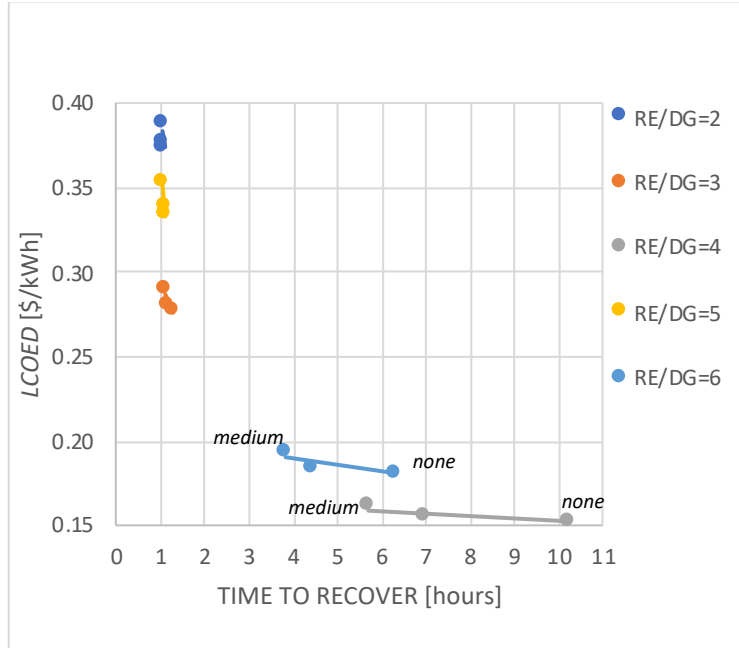


Figure 38. The effects of RE proportion to DG on *LCOED* and time to recover. RE/DG = 4 is at bottom because it has the least power rating.

Recall from Table 21 that as we increase the power rating ratio from 2 to 6, our microgrid’s power rating varies from 18 kW to 15 kW when increasing our ratio from 2 to 3, 15 kW to 9 kW when increasing our ratio from 3 to 4, 9 kW to 21 kW when increasing our ratio from 4 to 5, and 21 kW to 12 kW when increasing our ratio from 5 to 6. We also see that the smallest power ratings are the proportions of $\frac{P^{WT} + P^{PV}}{P^{DG}} = 4$ and $\frac{P^{WT} + P^{PV}}{P^{DG}} = 6$ with the fewest costs and the most improvement in resilience due to maintenance. The ratios of 2, 3, or 5 demonstrating the greatest resilience improvements are a byproduct of the greater microgrid power rating, and not due to any proportional relationships between RE and DG.

Also, increasing the microgrid’s power rating improves *recovery*, *invulnerability* and time to recover but there is a much greater improvement in *recovery* than there is in *invulnerability* for the same cost. Therefore, a decision maker who values *invulnerability*

more than *recovery* will need to invest significantly more both in maintenance and capital investments to realize greater benefits in *invulnerability*.

The cost of resilience can now be better understood by decision makers. $\frac{P^{WT} + P^{PV}}{P^{DG}} = 3$ reduces time to recover by almost four hours for an additional \$.10/kWh. The base commander can now decide if restoring power four hours earlier is worth these additional costs.

Why we ask when we exceed RE power rating that is triple the DG power rating do both resilience and costs plummet? In this experiment, it is mostly due to the most significant decrease in power rating from 15 MW to 9 MW, the lowest power rating of any of the architectures. This experiment does not generate anything overly meaningful other than confirming that maintenance expenditures improve resilience increasingly less as excess power rating increases.

4. Ratio of RE Nominal Power to DG Nominal Power with Constant Microgrid Nominal Power Generation Rating Impact on Resilience and Costs

To better understand how varying the proportion and power capacities of RE DER to DG DER will impact resilience we will maintain the same nominal microgrid power generation rating. Each microgrid modeled has different power ratings for each DER but the same overall microgrid power rating of 7 MW. The BAT power rating is maintained the same as the DG power rating, $P^{BAT} = P^{DG}$. Five different microgrid architectures employing DER components with varying power ratings are evaluated as indicated in Table 21.

Table 21. Ratio of RE nominal power rating to DG nominal power rating

Ratio of RE nominal power rating to DG nominal power rating $\frac{P^{WT} + P^{PV}}{P^{DG}}$	Ratio of RE nominal power rating to microgrid nominal power rating $\frac{P^{WT} + P^{PV}}{P}$	Micro-grid nominal power rating P [MW]	Micro-grid nominal power generation rating $P^{WT} + P^{PV} + P^{DG}$ [MW]	DER nominal rating P_i [kW]	# of WT m^{WT}	# of PV m^{PV}	# of DG m^{DG}	# of BAT m^{BAT}
2	0.50	9.33	7	778	3	3	3	3
3	0.60	8.75	7	875	3	3	2	2
4	0.67	8.40	7	700	4	4	2	2
5	0.71	8.17	7	583	5	5	2	2
6	0.75	8.00	7	1,000	3	3	1	1

Figure 39 illustrates the microgrid architecture having a ratio of $\frac{P^{WT} + P^{PV}}{P^{DG}} = 2$.

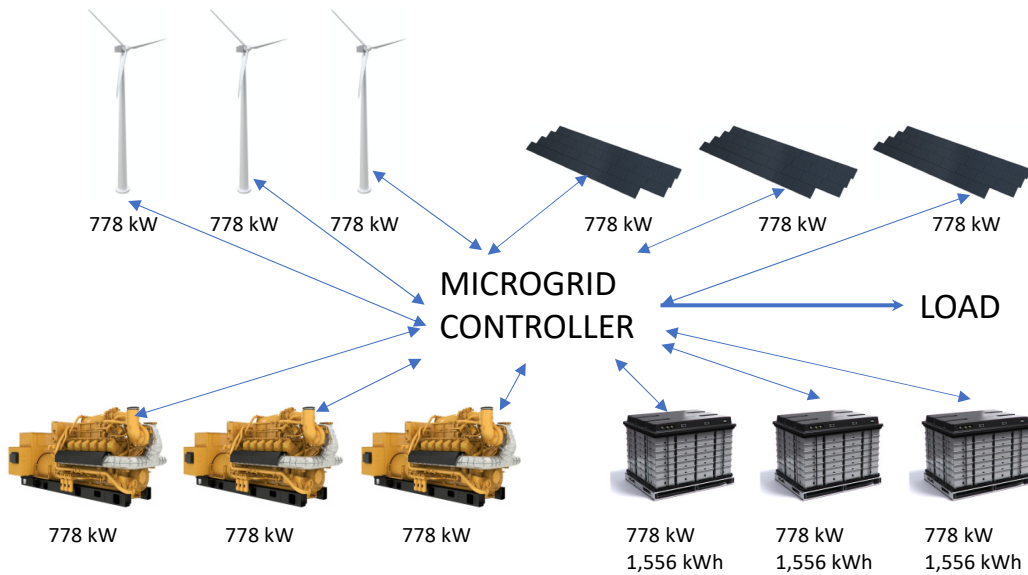


Figure 39. Microgrid architecture with RE/DG = 2 employing three of each DER at 778 kW and 7 MW overall nominal power generation rating.

Monte Carlo simulations are averaged for 7,500 simulations as before. The expectation is that increasing the proportion of RE/DG power of the microgrid will provide greater resilience, but that resilience will approach a point of diminishing returns considering the costs. The assumptions are made and articulated in Sections A and C for a hurricane scenario; nothing else is changed for each architecture other than the number of DER components in order to create the different overall proportions of microgrid power capacities.

Figure 40 shows when $\frac{P^{WT} + P^{PV}}{P^{DG}} = 2$ there are significantly less improvements in time to recover for greater maintenance investments.

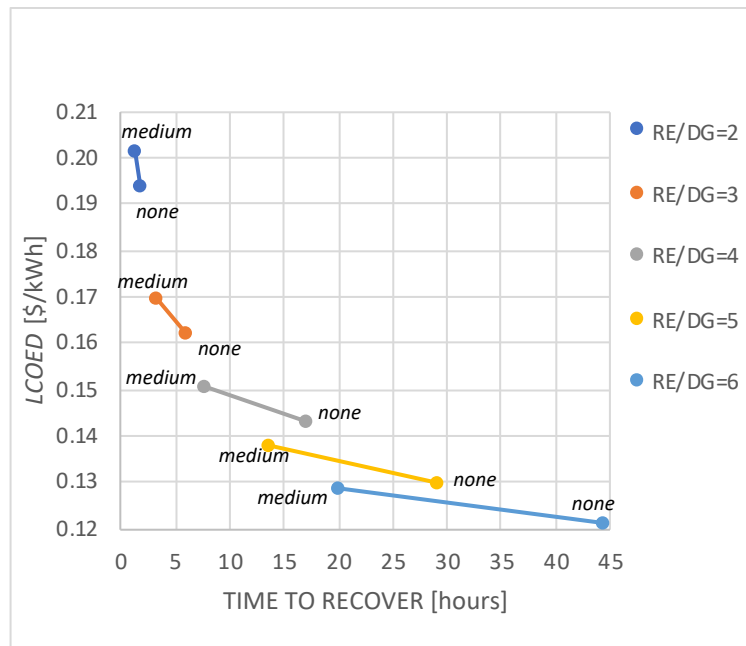


Figure 40. The effects of RE proportion on *LCOED* and time to recover.

Figure 41 shows decreasing *resilience* and exponentially decreasing costs as the power rating ratio increases.

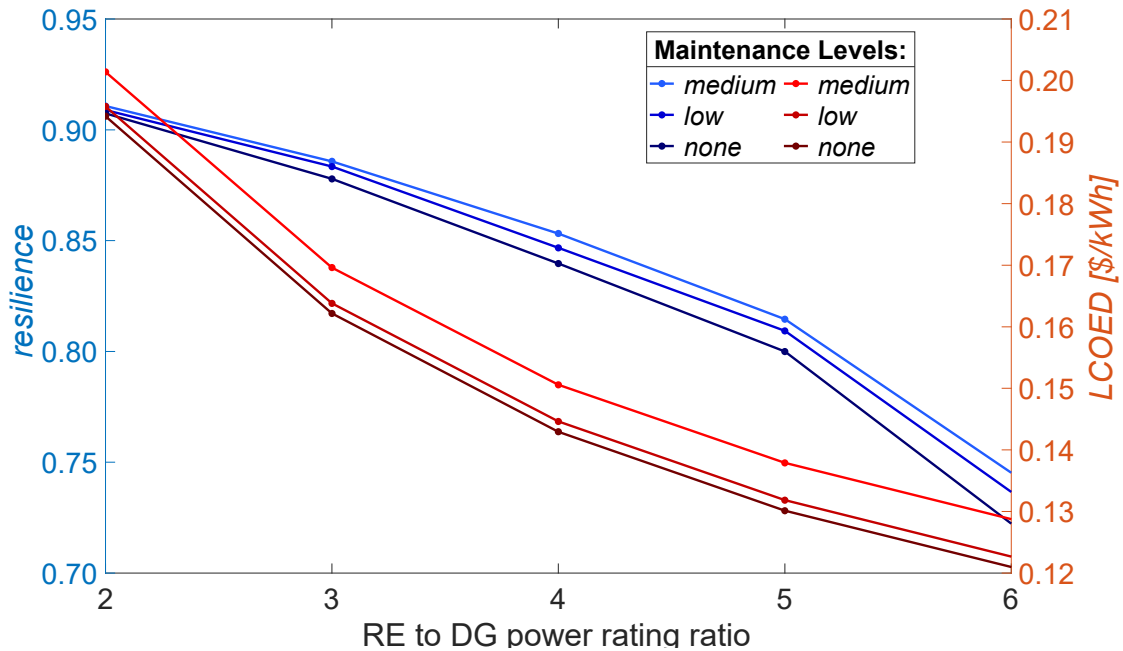


Figure 41. Resilience and costs decrease as RE to DG power rating ratio increases.

This experiment confirms that a lower proportion of $\frac{P^{WT} + P^{PV}}{P^{DG}}$ improves time to recover but costs more. Additionally, smaller power rating ratios of RE (WT and PV) to DG provide more resilience but at a higher cost.

Why we ask when does more proportional RE reduce resilience? This is due to the efficiencies and diurnal impacts on RE being greater than DG. More RE and less DG does not improve the excess power rating.

5. Ratio of WT Nominal Power to DG Nominal Power with Constant Microgrid Nominal Power Generation Rating Impact on Resilience and Costs

WTs are employed at three of the six INIs and we want to understand how varying the proportion and power ratings of a single WT DER to DG DER will impact resilience while maintaining the microgrid power rating as constant. This experiment further explores the relationship for the WT and DG in that the redundancy experiments confirm that WT

and DG provide the best resilience for the least costs in a quintuple redundancy level architecture.

We model each microgrid using different power ratings for each DER but with the same overall microgrid power rating of 4 MW. And we maintain the nominal BAT power rating the same as the nominal DG power rating, $P^{BAT} = P^{DG}$. Table 22 provides the five different microgrid architectures employing DER components with varying power ratings.

Table 22. Microgrid architectures for proportion of DER with constant microgrid power generation rating.

Ratio of WT nominal power rating to DG nominal power rating $\frac{P^{WT}}{P^{DG}}$	Ratio of WT nominal power rating to microgrid nominal power rating $\frac{P^{WT}}{P}$	Microgrid nominal power rating P [MW]	Microgrid nominal power generation rating $P^{WT} + P^{DG}$ [MW]	DER nominal power rating P_i [kW]	# of WT m^{WT}	# of PV m^{PV}	# of DG m^{DG}	# of BAT m^{BAT}
2	0.50	5.33	4	1,333	2	0	1	1
3	0.60	5.00	4	1,000	3	0	1	1
4	0.67	4.80	4	800	4	0	1	1
5	0.71	4.66	4	667	5	0	1	1

Monte Carlo simulations are averaged for 7,500 simulations as before. The expectation is that increasing either or both the maintenance investment and proportion of WT/DG of the microgrid will provide greater resilience, but that resilience will approach a point of diminishing returns considering the costs. The assumptions are made and articulated in Sections A and C for a hurricane scenario; nothing else is changed for each architecture other than the number of DER components in order to create the different overall proportions of microgrid power ratings.

Figure 42 shows us how a smaller ratio of WT to DG power provides better time to recover. The smaller ratios cost more, and maintenance improves time to recover in all instances.

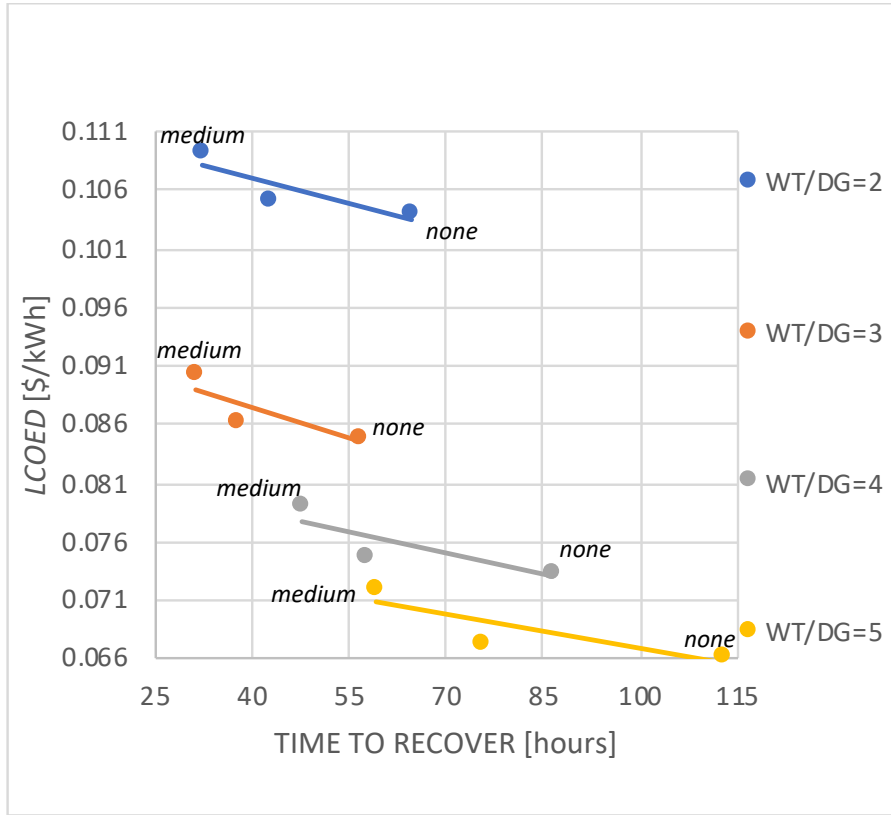


Figure 42. The effects of maintenance level and WT proportion on *LCOED* and time to recover.

Figure 43 highlights how both resilience and costs decrease with increasing power rating ratios.

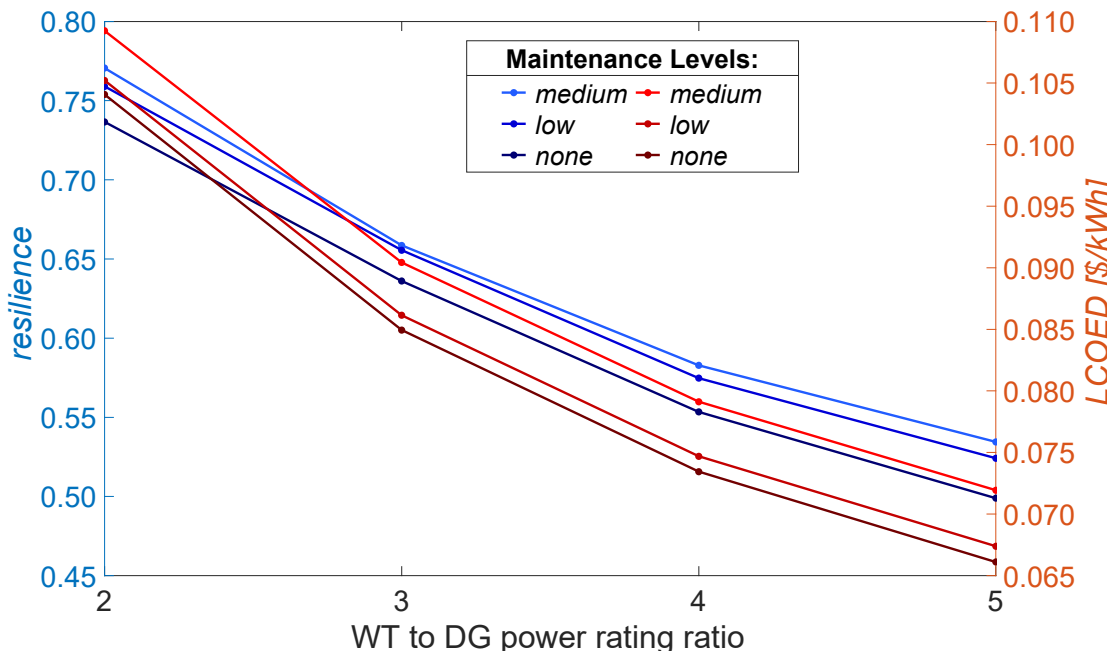


Figure 43. *Resilience* and *LCOED* decrease as WT to DG power rating ratio increases.

This experiment, like the one before confirms this same behavior in resilience and costs for increasing RE to DG. We can generalize that a greater proportional amount of RE, combined with DG, decreases *resilience* and costs.

6. Ratio of BAT Nominal Power Rating to Microgrid Nominal Power Rating with Constant Microgrid Nominal Power Generation Rating Impact on Resilience and Costs

RE generation is stochastic and can benefit from energy storage. Through arbitrage, we can preserve something that has greater financial value to us at a future date, and increase the cost-effectiveness of our microgrid. Energy storage can store excess capacity for the future, store intermittent and variable power over time, and supply steady, not generated with stochastic variability, power to a load. Batteries can do this extremely efficiently, but the question remains on how much storage is appropriate. The battery's capacity should ensure the demand can still be met while the microgrid transitions unmet demand from damaged generative DER to undamaged DER. We venture to understand how much storage is needed before seeing the costs of resilience rapidly increase for the

system. Each microgrid modeled has the same power ratings for each DER and the same overall microgrid generation power rating of 6 MW and medium maintenance as shown in Table 23. Only one of each DER component is employed, and the power rating of each of the generation DER is maintained at 2 MW.

Table 23. Microgrid architectures for storage relationships. $P^{WT} + P^{PV} + P^{DG} = 6$ MW in all instances.

Ratio of BAT nominal power rating to microgrid nominal power generation rating $\frac{P^{BAT}}{P^{WT} + P^{PV} + P^{DG}}$	BAT nominal power rating P^{BAT} [MW]	DER nominal power rating P_i [MW]	# of WT m^{WT}	# of PV m^{PV}	# of DG m^{DG}	# of BAT m^{BAT}
0.17	1.0	2.0	1	1	1	1
0.25	1.5	2.0	1	1	1	1
0.33	2.0	2.0	1	1	1	1
1.00	6.0	2.0	1	1	1	1
2.00	12.0	2.0	1	1	1	1
4.00	24.0	2.0	1	1	1	1
8.00	48.0	2.0	1	1	1	1
16.00	96.0	2.0	1	1	1	1

Figure 44 highlights how maintenance only matters when the ratio is less than 0.25. We also see no improvement in resilience, by increasing this ratio, beyond this ratio of 0.33.

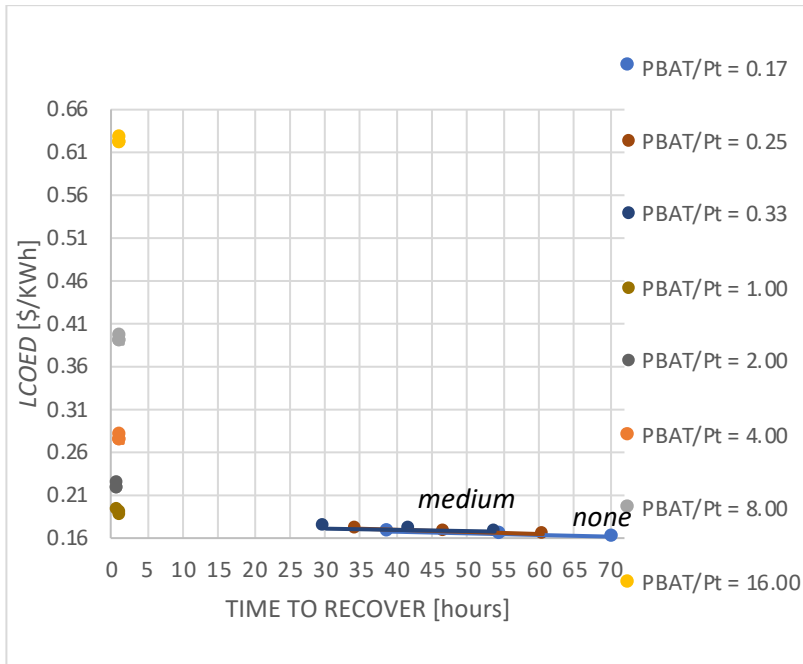


Figure 44. The effects of storage on *LCOED* and time to recover.

Figure 45 shows that after increasing the ratio beyond 2 MWh nominal battery capacity to 1 MW microgrid nominal power rating (a power rating ratio of 1) there is virtually no improvement in *resilience*, but costs continue to increase. This is consistent with the energy management strategy only employing the batteries to transition from one DER to another. Figure 46 shows the battery's contribution to *recovery* but not *invulnerability*.

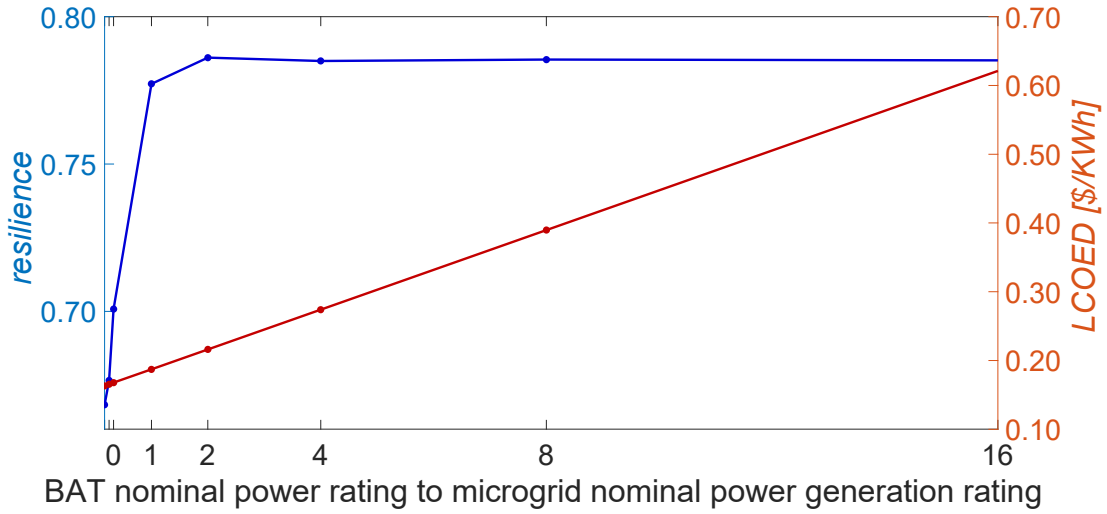


Figure 45. Costs and *resilience* increase as power rating ratio increases.

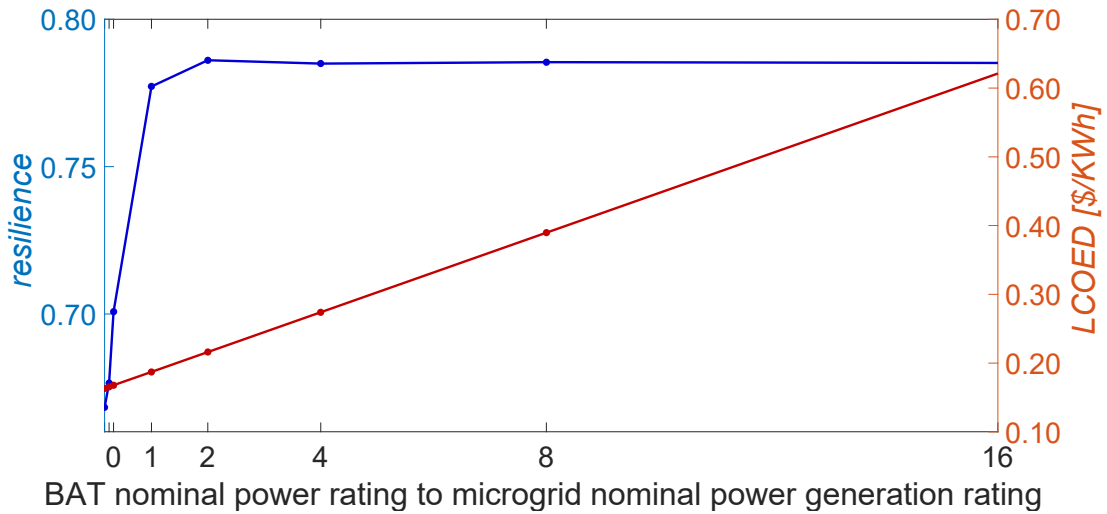


Figure 46. *Recovery* increases but *invulnerability* stays constant.

Why should the battery power rating not exceed the microgrid's power generation rating? The answer lies in the employment of the battery. Assuming the microgrid is designed with sufficient generation to meet the demand, the worst-case scenario would damage all generation, and this would require the same amount of power from another source, a battery, any more capacity would be unused. Hence, a battery with power rating the same as the microgrid's power generation rating should be used as an initial starting

point for sizing the battery. This could be very useful to an INI's microgrid project planning and estimating team.

E. ALTERING REDUNDANCY LEVELS

Experiments are conducted to understand how redundancy, and diversification of DER components, with constant microgrid power generation rating impacts resilience and costs for different maintenance levels. Redundancy as applied in this research means having multiple DER components instead of just one, with the total power rating of the redundant architecture being the same as the either without redundancy or at a different level of redundancy. This is different than having excess power rating. This is an important distinction that must be understood when comparing the results of the model's simulations.

The results generated by each of the experiments are presented in a 4D visualization with different colors for each microgrid architecture's experiment as shown in Table 24. Each function is a surface mesh interpolation of the 15 data points for each experiment. No redundancy is often designated, n , and n represents just one component. One level of redundancy, $n+1$, will be referred to as double, $n+2$ triple, $n+3$ quadruple, and $n+4$ quintuplet. The lighter shading of the data points is used for more maintenance; light shading is for medium maintenance, low shading for low maintenance, and dark shading for no maintenance. 2D graphs for *LCOED* vs. *resilience*, *recovery*, and *invulnerability* are provided in Appendix A.

Figure 47 highlights how maintenance is only significant when there is no redundancy and particularly so for the WT+PV+DG architecture (gray shape). Each function represents a different architecture and will be evaluated further in the individual experiments that follow. The brighter the color shading highlights more maintenance, and the darkest color shading is for no maintenance. These functions also show how *resilience* increases and costs remain constant as the redundancy level increases. The best architecture, least costs and equivalent resilience, is the WT and DG generation. The only architecture with significantly less resilience than the others is the combined WT, PV, and DG generation.

Table 24. Legend for Figure 47. Colors designate the microgrid architecture for each experiment.

- III.E.1 WT+PV+DG+BAT
- III.E.2 WT+DG+BAT
- III.E.2 PV+DG+BAT
- III.E.2 WT+PV+DG+BAT
- III.E.3 WT
- III.E.3 PV
- III.E.3 WT+PV

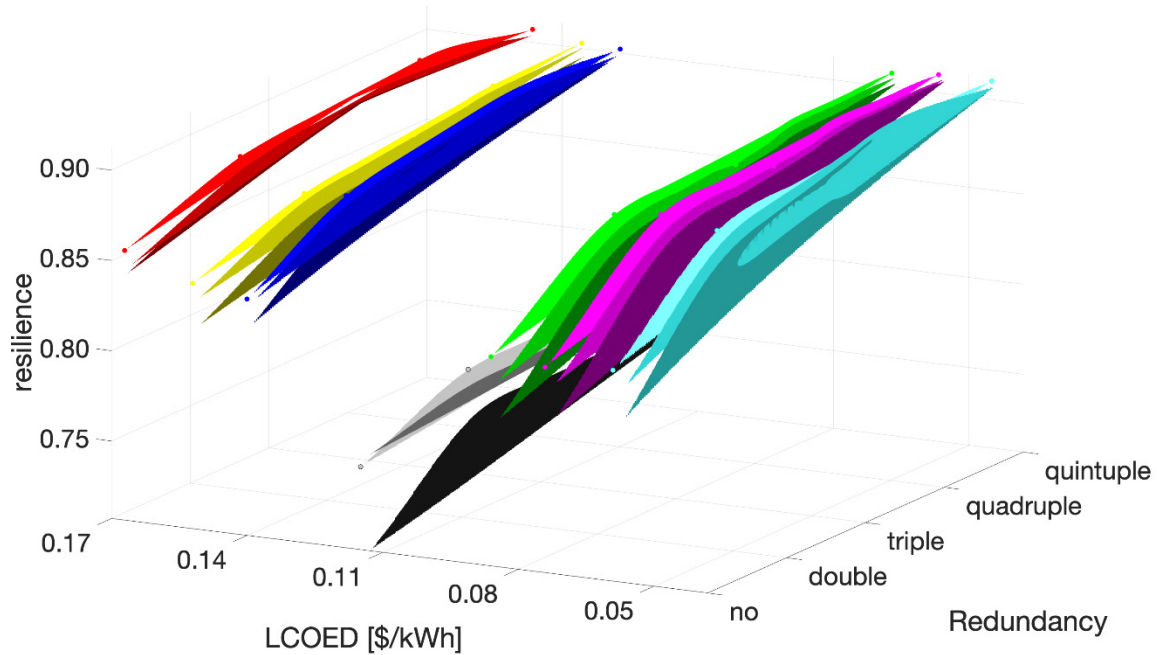


Figure 47. Wind turbines provide least costs for similar *resilience*; darker datapoints are with no maintenance, brighter are medium maintenance.

Why would WT+PV+DG significantly underperform compared to the other architectures? The answer might lie in individual DER power capacities being the smallest in this architecture, at 267kW for a quintuple redundancy level. This will be explored further in the following experiments.

1. Redundancy and Maintenance Levels Impact on Resilience and Costs

It should be useful to understand how varying the redundancy of each DER will impact resilience while maintaining the microgrid power rating as constant. Each microgrid modeled has different power ratings for each DER but the same overall microgrid power rating of 6 MW. The BAT power rating is maintained the same as the DG power rating. Five different microgrid architectures employing DER components with varying power ratings are evaluated as shown in Table 25.

Table 25. Microgrid architectures for redundancy.

Redundancy	Total microgrid nominal power generation rating P [MW]	DER's nominal power rating P_i [kW]	# of WT m^{WT}	# of PV m^{PV}	# of DG m^{DG}	# of BAT m^{BAT}
no	6	2,000	1	1	1	1
double	6	1,000	2	2	2	2
triple	6	667	3	3	3	3
quadruple	6	500	4	4	4	4
quintuple	6	400	5	5	5	5

A microgrid architecture with no redundancy is portrayed in Figure 48.

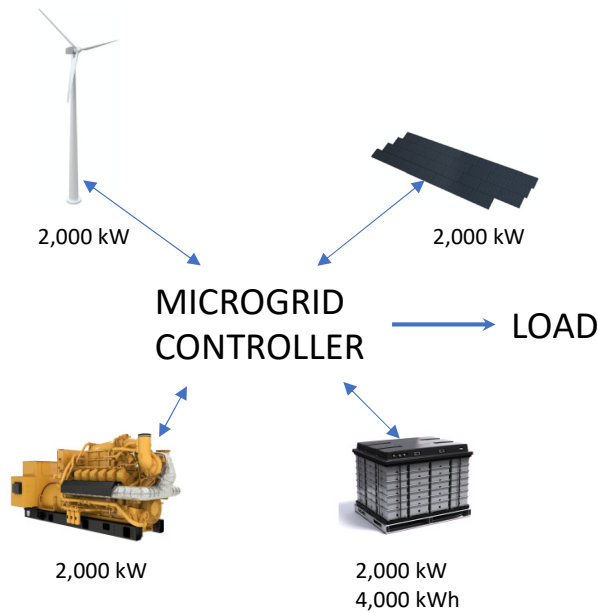


Figure 48. Microgrid architecture with no redundancy employing one of each DER at 2,000 kW and 6 MW overall power generation rating.

Monte Carlo simulations are averaged for 7,500 simulations as before. The expectation is that increasing either or both the maintenance investment and proportion of redundancy of the microgrid will provide greater resilience, but it will approach a point of diminishing returns considering the costs. The assumptions are made and articulated in Sections A and B for a hurricane scenario; nothing else is changed for each architecture other than the number of DER components in order to create the different overall proportions of microgrid power capacities. The unlabeled data points correspond to a medium maintenance threshold.

Redundancy should improve resilience because we assume probability of damage to each DER is independent. Even if all the PVs for example are located in the same area, this would be true. However, we would recommend a base commander purposely distribute the DERs locations to minimize common failure modes affecting all of them. The probability of all the redundant DERs being simultaneously damaged is less than the probability of a single DER with the same power rating being damaged. This conclusion would be invalid if there is a common cause failure. The question here is how much redundancy is good, and also at what point is additional redundancy not worthwhile.

Figure 49 shows, in general, that greater redundancy provides greater resilience for the same costs. The best redundancy is quintuple. Maintenance has the most significance for no redundancy.

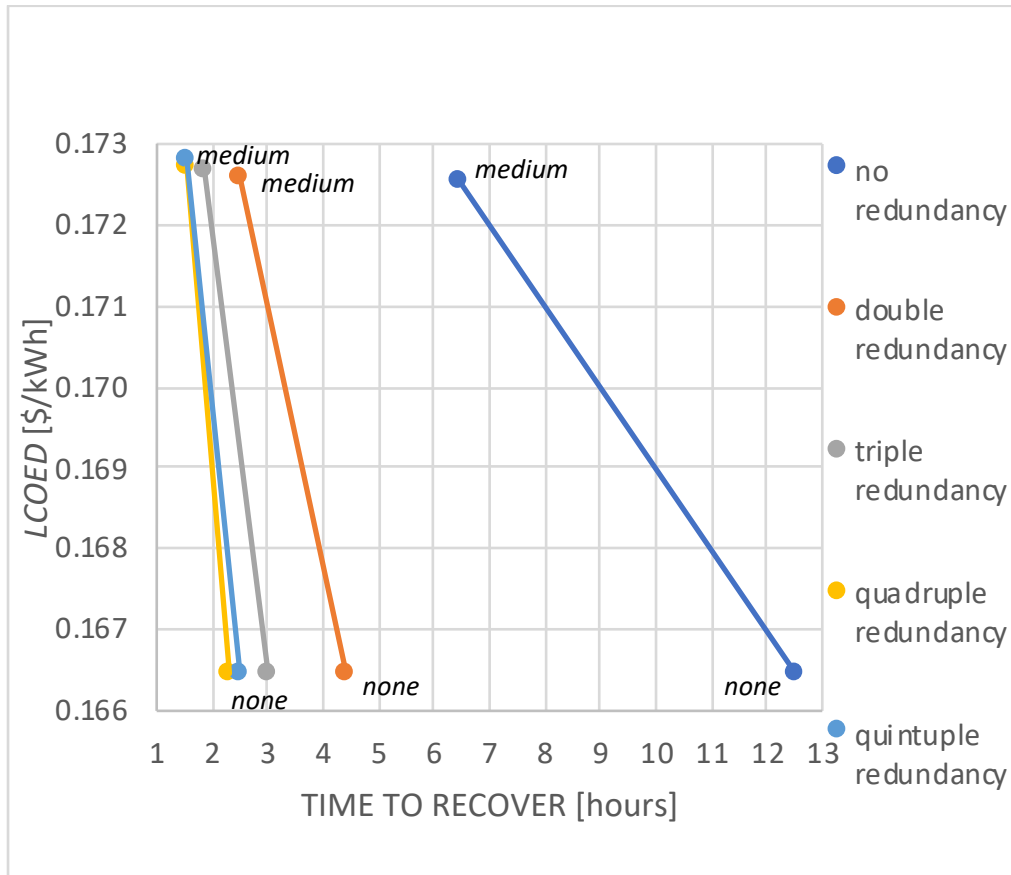


Figure 49. The effects of redundancy levels on *LCOED* and time to recover.

Figure 50 shows the exponential improvement in resilience as redundancy increases, and how maintenance improves resilience but costs more. We note that there is no improvement in *resilience* for more than quadruple redundancy. Again, we see no change in costs for the different levels of redundancy.

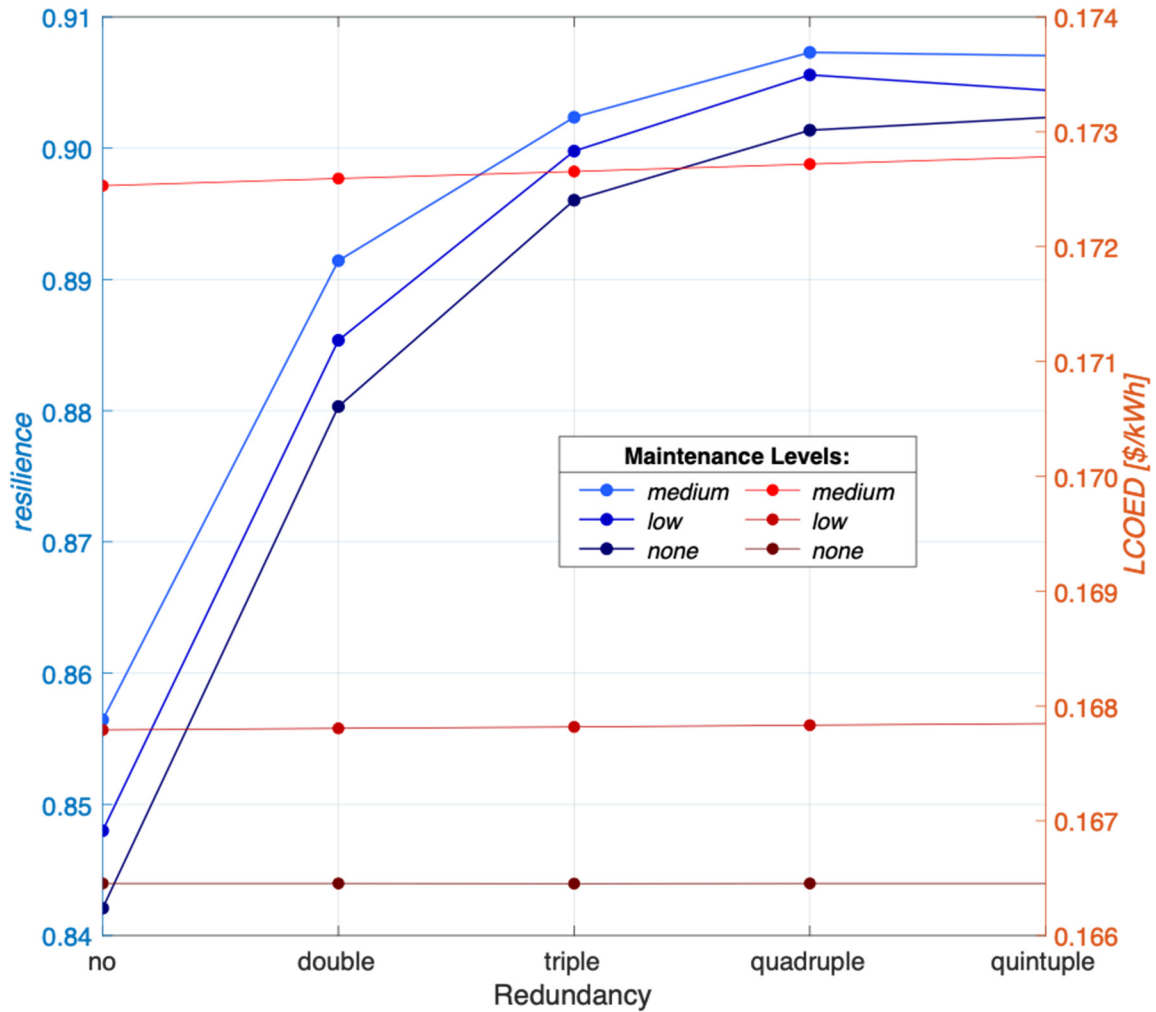


Figure 50. Resilience and LCOED vs. redundancy.

We consider why redundancy improves resilience. This is a result of decreasing the impact of damage. Two components will be less likely to both be damaged when subjected to the same disturbance. Therefore, as redundancy is increased, less damage to the overall power rating is inflicted.

2. Functional Redundancy and Maintenance Levels Impact on Resilience and Costs

Which combination of RE is better and if just one RE type is best? To answer this question, each microgrid modeled has different capacities for each DER, but the same overall microgrid power rating of 4 MW. The BAT power rating is maintained the same as

the DG power rating. Three different microgrid architectures employing DER components with varying capacities are evaluated as shown in Table 26.

Table 26. Microgrid architectures for functional redundancy. Architecture color corresponds to that shown in architectures illustrated in Figure 47.

Architecture	Functional redundancy level	Total microgrid nominal power generation rating P [MW]	DER's nominal power rating P_i [kW]	# of WT m^{WT}	# of PV m^{PV}	# of DG m^{DG}	# of BAT m^{BAT}
WT+DG	no	4	2,000	1	0	1	1
	double	4	1,000	2	0	2	2
	triple	4	667	3	0	3	3
	quadruple	4	500	4	0	4	4
	quintuple	4	400	5	0	5	5
PV+DG	no	4	2,000	0	1	1	1
	double	4	1,000	0	2	2	2
	triple	4	667	0	3	3	3
	quadruple	4	500	0	4	4	4
	quintuple	4	400	0	5	5	5
PV+WT+DG	no	4	1,333	1	1	1	1
	double	4	667	2	2	2	2
	triple	4	444	3	3	3	3
	quadruple	4	333	4	4	4	4
	quintuple	4	267	5	5	5	5

The best redundancy level is quintuple in all instances. For the best WT+DG architecture, *resilience* = 0.90 and *LCOED* = \$0.1424/kWh. For the best PV+DG architecture *resilience* = 0.90 and *LCOED* = \$0.1527/kWh. And for the best combined WT+PV+DG architecture *resilience* = 0.80 and *LCOED* = \$0.1111/kWh. PV+DG architecture has the highest costs, WT+PV+DG the least.

Figure 51 shows how the improvements in *resilience* are very little beyond a quintuple redundancy level. We also see how WT, PV and DG has very minor *resilience* improvements after a double redundancy level, whereas the WT and DG and PV and DG still see steady improvements at least until a triple redundancy level.

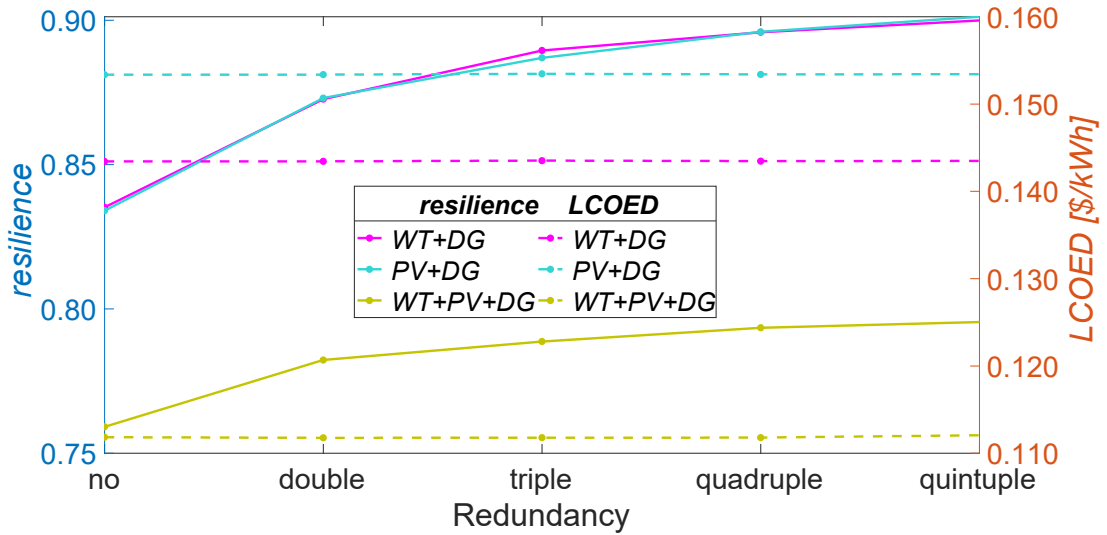


Figure 51. Resilience and LCOED vs. functional redundancy.

Figure 52 shows how *recovery* increases exponentially but *invulnerability* is almost constant. There is no difference in the behavior of the respective functions.

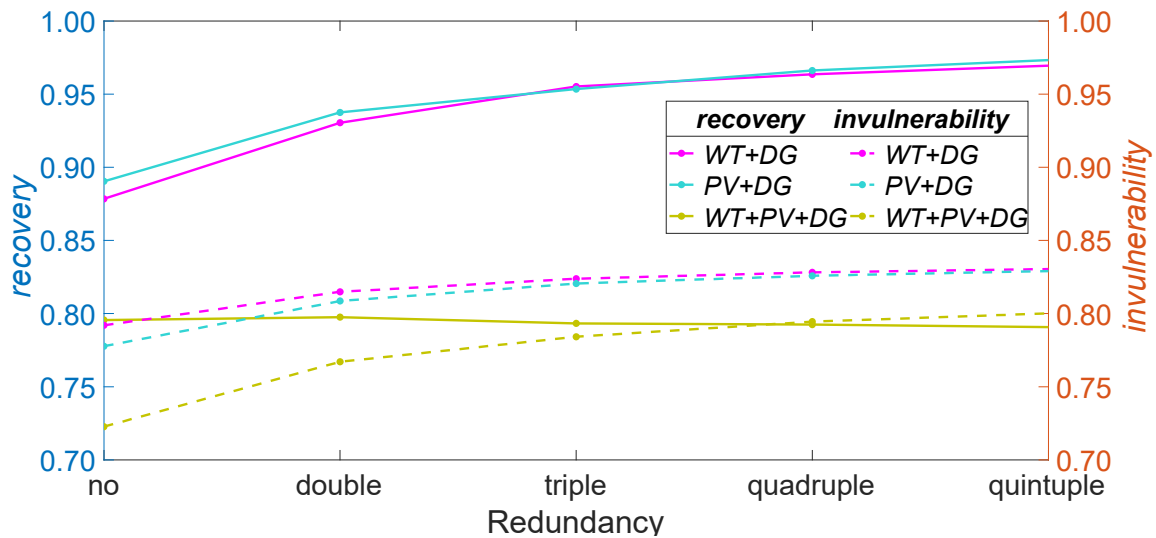


Figure 52. Recovery and invulnerability vs. functional redundancy.

Figure 53 shows how maintenance matters most for the combined architecture with WT, PV and DG, and with no or little redundancy. Also, we see how more redundancy

improves time to recover. For WT+PV+DG we see time to recover improve from 110 hours without maintenance or redundancy to 40 hours with quintuple redundancy and no maintenance.

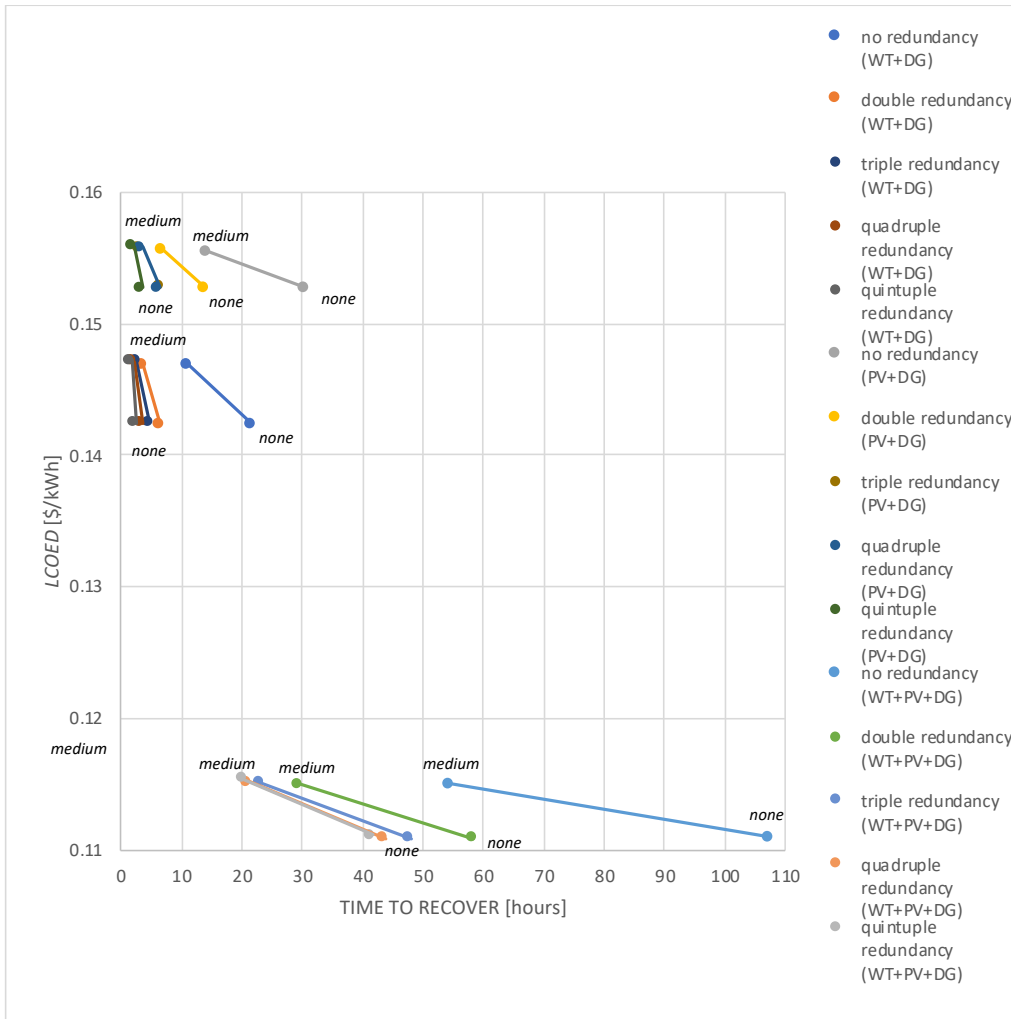


Figure 53. The effects of functional redundancy on *LCOED* and time to recover.

Why then does WT+PV+DG perform the least? This architecture has the smallest power rating for each redundancy level, two-thirds the other architecture's power rating. This should be investigated further to determine if the characteristics of the ratio of individual DER's power rating to the overall power rating. The WT+PV+DG only sees an improvement in resilience by adding one level of redundancy. The individual DER power

rating goes from 667 kW to 444 kW when increasing from double to triple, which is likely a minimum threshold for the DER to still be effective in enhancing resilience.

3. RE Redundancy and Maintenance Levels Impact on Resilience and Costs

We undertake to learn which RE combination, without DG, provides greater value: more WTs, more PV, or both WT and PV? Each microgrid modeled has different capacities for each DER, but with the same overall microgrid power rating of 4 MW. The BAT nominal power rating is maintained at the same as the total nominal power generation rating, $P_i^{BAT} = P_i^{WT} + P_i^{PV}$. Three different microgrid architectures employing DER components with varying capacities are evaluated as shown in Table 27.

Table 27. Microgrid architectures for PV and WT combinations. Architecture color corresponds to the architecture illustrated in Figure 47.

Architecture	RE redundancy	Total microgrid nominal power generation rating P [MW]	Nominal power generation rating of WT, PV and DG P_i [MW]	Nominal power rating of BAT P_i^{BAT} [MW]	# of WT m^{WT}	# of PV m^{PV}	# of DG m^{DG}	# of BAT m^{BAT}
WT	no	4	4.00	4.00	1	0	0	1
	double	4	2.00	2.00	2	0	0	2
	triple	4	1.33	1.33	3	0	0	3
	quadruple	4	1.00	1.00	4	0	0	4
	quintuple	4	0.80	0.80	5	0	0	5
PV	no	4	4	4.00	0	1	0	1
	double	4	4	2.00	0	2	0	2
	triple	4	1.33	1.33	0	3	0	3
	quadruple	4	1.00	1.00	0	4	0	4
	quintuple	4	0.80	0.80	0	5	0	5
PV+WT	no	4	2.00	4.00	1	1	0	1
	double	4	1.00	2.00	2	2	0	2
	triple	4	0.67	1.33	3	3	0	3
	quadruple	4	0.50	1.00	4	4	0	4
	quintuple	4	0.40	0.80	5	5	0	5

The least costly redundancy level is quintuple and no maintenance in all instances. For the best WT architecture, $resilience = 0.91$ and $LCOED = \$0.0468/kWh$. For the best PV architecture $resilience = 0.90$ and $LCOED = \$0.0674/kWh$. And for the best combined PV+WT architecture $resilience=0.91$ and $LCOED = \$0.0571/kWh$.

For decision makers, maintenance has much greater benefit when there is no redundancy incorporated in the microgrid. Wind turbines with more redundancy and no maintenance offers the most resilience for the least costs.

Figure 54 shows how maintenance matters much more for these RE architectures, especially those with no or little redundancy. Also, we see how more redundancy improves time to recover. However, the improvements are relatively minor compared to the architectures that combined RE and DG. We only see a few hours at most decrease in time to recover as we increase redundancy from no redundancy to quintuple.

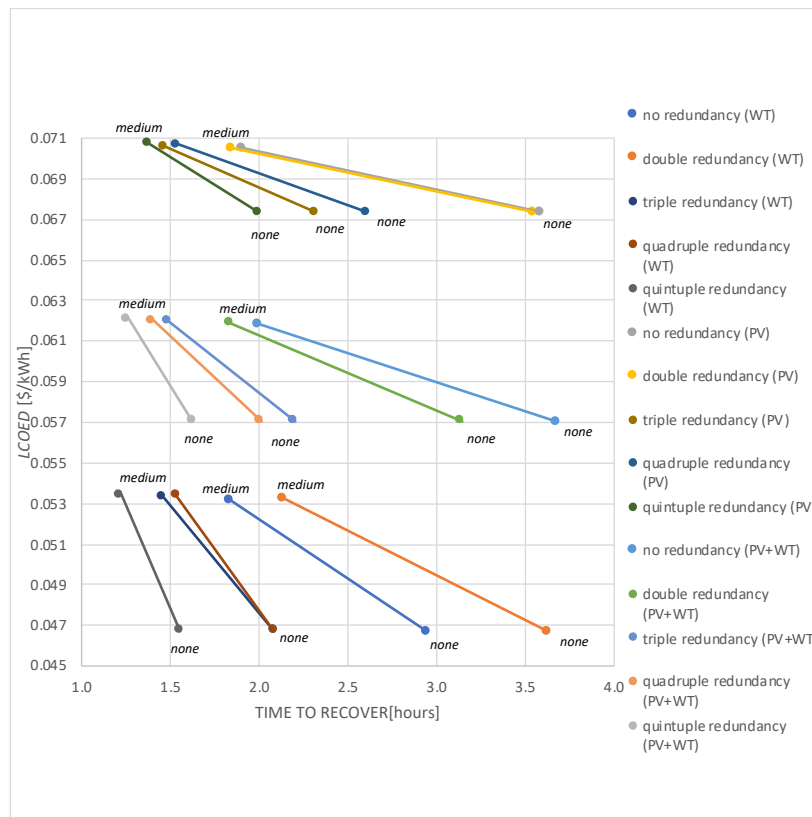


Figure 54. The effects of RE redundancy on $LCOED$ and time to recover.

Figure 55 shows all three architectures increasing resilience exponentially while costs remain unchanged. WT has the least costs and same resilience.

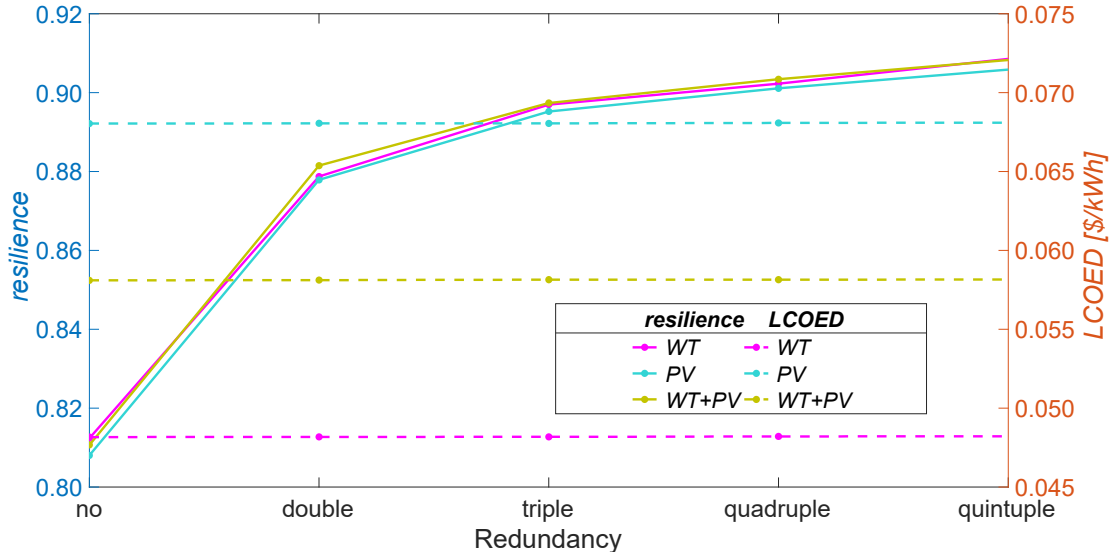


Figure 55. Resilience and LCOED vs. RE redundancy.

Why would WT by themselves offer significant cost savings for the same resilience? The answer is in the diurnal benefits of the WT over the PV. The WTs operate day and night and increase their production at night due to diurnal behavior. The PV does not generate power at night. This a useful insight in that if PV is incorporated in the microgrid it should be at a greater amount than the WT in order to generate the same amount as the WT.

F. VALUE OF INVESTING FOR INVULNERABILITY VS. RECOVERY

A base commander has a finite and limited budget and often must decide how best to invest funds to improve overall resilience. One option is increasing power rating. Another option is to invest in maintenance, spare parts, and an overall power rating to recover faster. This section analyzes the tradeoff between these two options.

We attempt to understand how investing in an increased power rating P affects *invulnerability* and *recovery* compared to an alternative of increased maintenance M.

Comparisons are made in architectures that invest the same amount to increasing the nominal microgrid power rating as would have been invested for medium maintenance. Each microgrid modeled has the different capacities for each DER and overall microgrid power rating. The power rating of each DER is illustrated in Table 28.

Table 28. Microgrid architectures for power rating or maintenance investments.

Investment		Microgrid nominal power generation rating $P^{WT}+P^{PV}+P^{DG}$ [kW]	WT power	PV power	DG power	BAT power
Power rating [K]	Maintenance [K]		P_i^{WT} [kW]	P_i^{PV} [kW]	P_i^{DG} [kW]	P_i^{BAT} [kW]
0	0	4,500	1,500	1,500	1,500	1,500
720	0	5,500	1,500	1,500	2,500	1,500
0	720	4,500	1,500	1,500	1,500	1,500

The *LCOED* for a microgrid with three of each DER at 500 kW with a medium level of maintenance is \$0.1443/kWh. The equivalent *LCOED* for this same microgrid with no maintenance is \$0.1399/kWh. The difference is an increase in *LCOED* by \$0.0044/kWh. If we apply this increase to the energy generated in a year to meet the demand of 23,878,400 kWh, this will cost \$105,064 annually more and represents the opportunity to invest this amount instead of maintenance into power rating. We apply this savings annually calculating a present value using a 7.5% discount rate due to not performing maintenance over the ten years planning horizon to determine the amount we can invest instead in power rating approximates \$720K.

LCOED vs. *recovery*, *invulnerability*, *resilience* and time to recover is plotted in Figures 56–59, medium and no maintenance levels as annotated. To gain insights into investing in increased power rating, the DG power rating is increased from 1,500 kW to 2,500 kW. And to understand how investing in maintenance influences recovery and invulnerability, we invest additional annual amount in maintenance to maintain the DER at a medium level compared to no maintenance at all.

We observe in Figures 56–59 that in all instances an investment in maintenance provides much greater resilience for appreciably less costs than investing the equivalent amount into increased power rating. We observe that there is less improvement in *invulnerability* than there is in *recovery*. Additionally, an investment in maintenance reduces the time to recover by half the time to recover for an investment in power rating. A base commander can now understand how any additional funding that he has to spend will enhance resilience based upon the commander’s decision to invest in more power rating or maintenance. This should be useful information at the end of the fiscal year when funding opportunities require quicker decisions on how to invest the money.

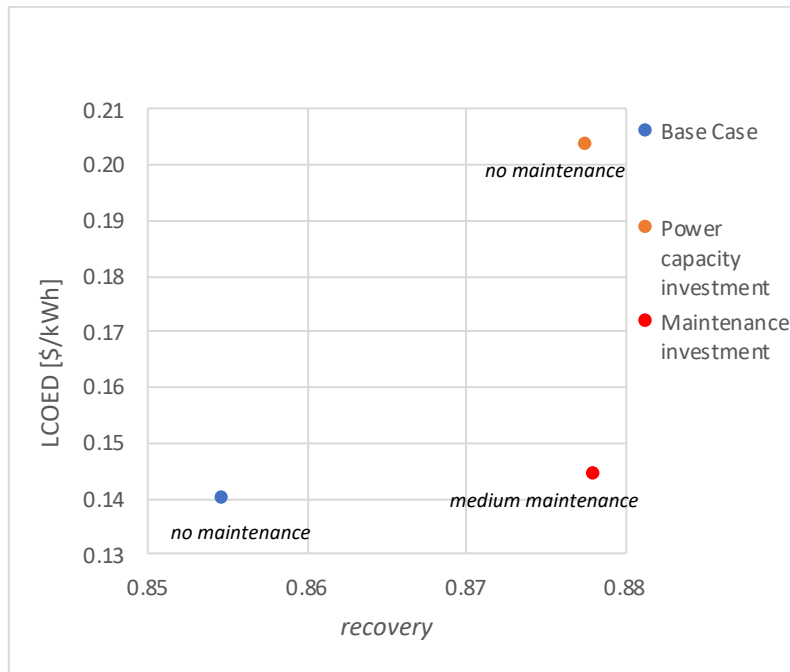


Figure 56. The effects of investing in power rating or maintenance on *LCOED* and *recovery*.

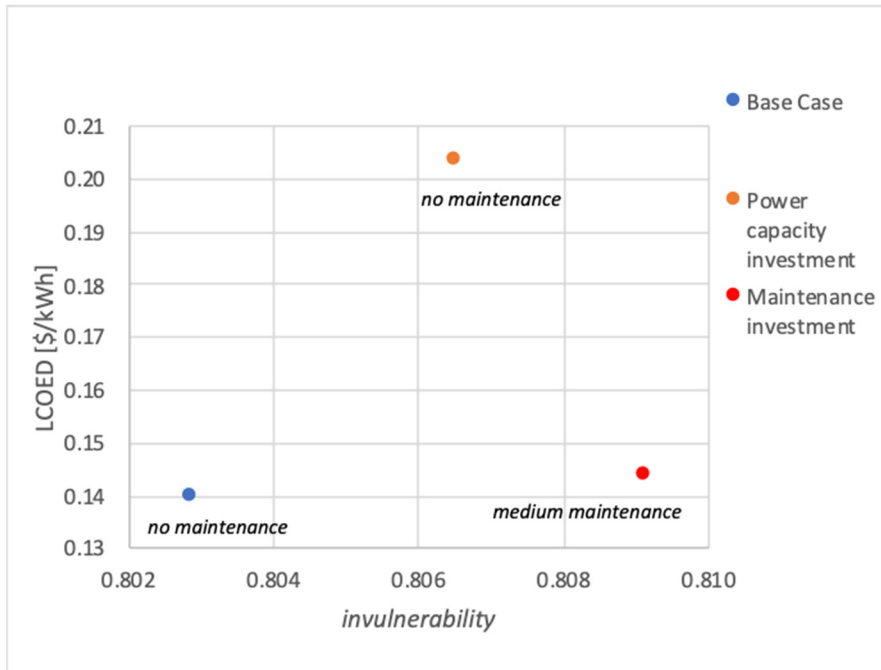


Figure 57. The effects of investing in power rating or maintenance on *LCOED* and *invulnerability*.

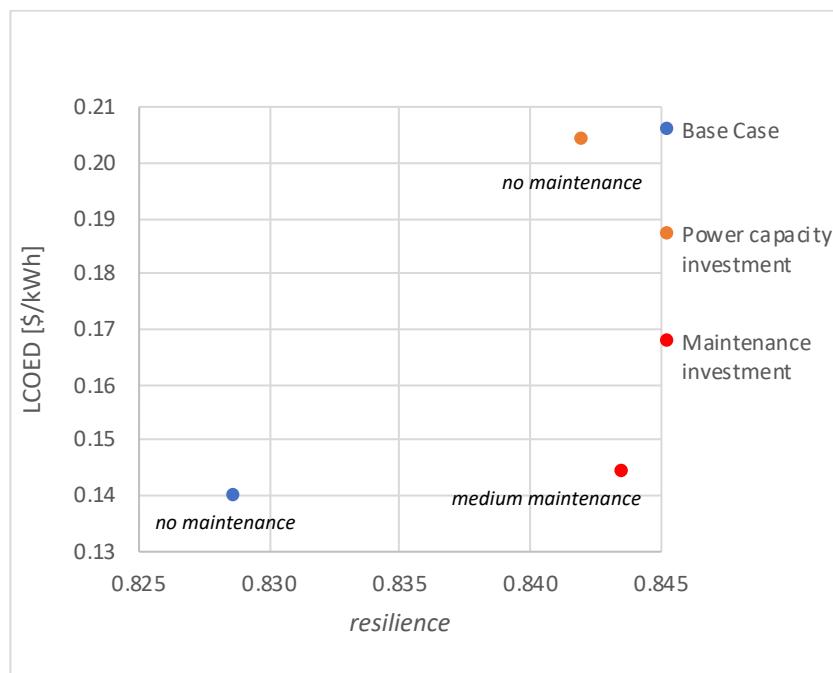


Figure 58. The effects of investing in power rating or maintenance on *LCOED* and *resilience*.

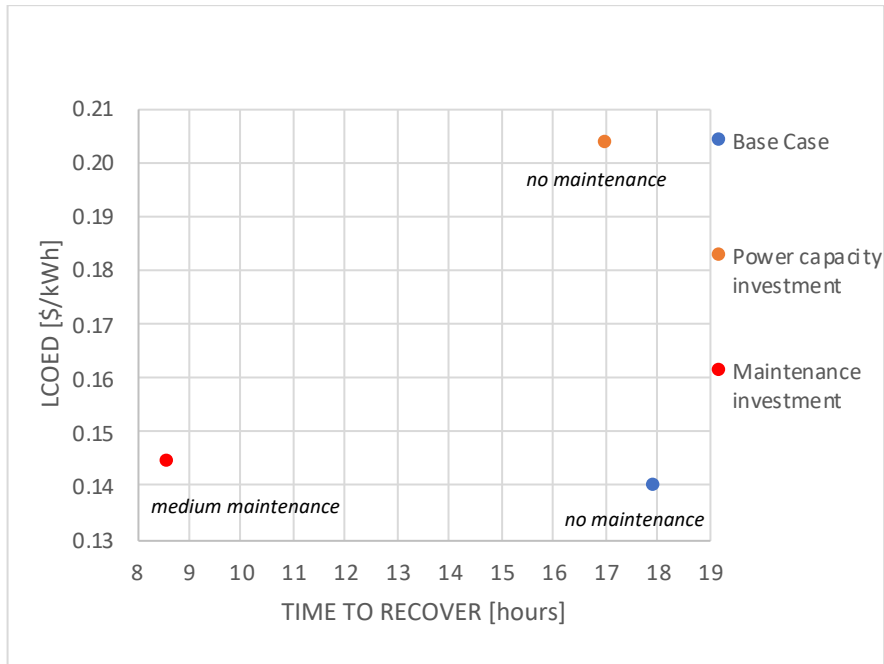


Figure 59. The effects of investing in power rating or maintenance on *LCOED* and time to recover.

G. FUEL COSTS IMPACT ON DG-PARITY FOR PV

The cost of fuel for RE sources such as solar to be more cost competitive than DG is useful when deciding whether to invest in PV as a RE DER. It is no surprise that researchers have arrived at different conclusions in that their findings can widely depending upon whether or not the RE transmission, distribution, storage costs and subsidies are included in their analysis. Another factor that absolutely must be included in the analysis is fuel price. This section investigates the fuel price that would make DG cost competitive with PV.

The cost model is used to determine at what point increasing fuel costs make PV cost competitive. The *LCOE* for five 500 kW PV is \$0.0904/kWh using a twenty-year planning horizon. This *LCOE* is within the range Branker et al. (2011) determined for solar PV from 0.062-0.860 \$/kWh. The *LCOE* for five 500 kW DGs is determined for fuel prices from \$1/gal to \$5/gal. The results indicate that fuel costs will have to drop to \$1.00/gal for PV to be more cost competitive than DG. These results are displayed in Figure 60.

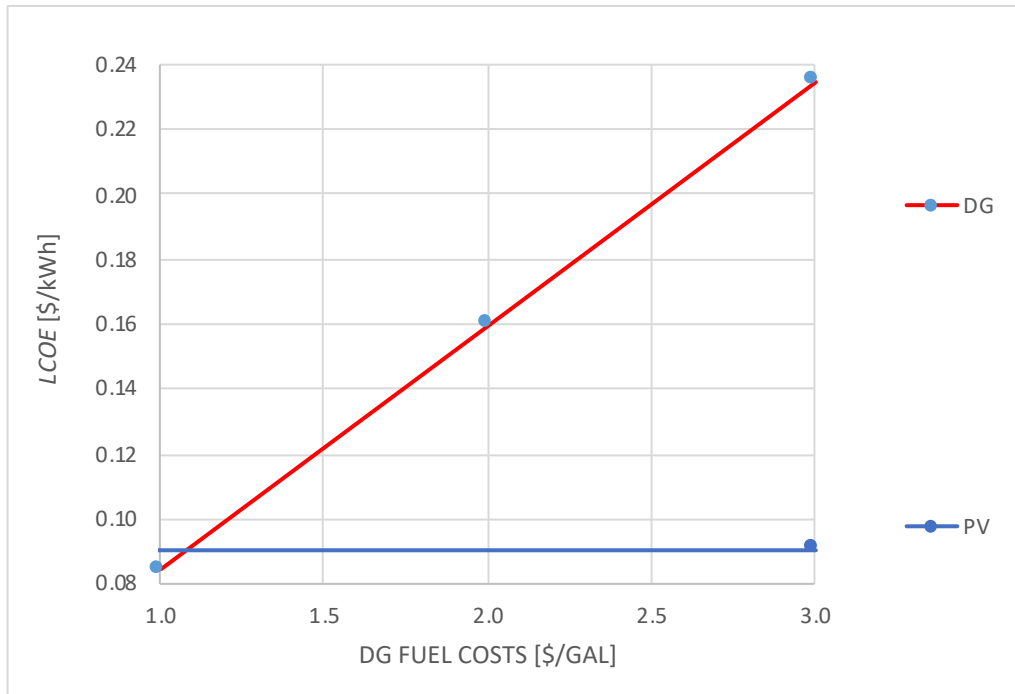


Figure 60. The effects of fuel costs on DG-parity for PV.

The comparison is strictly on the generation, not the actual delivery costs of power. Although this analysis is thought-provoking, a more meaningful experiment could be run that would incorporate the total fuel costs for an INI. That is, the INI's fuel costs should also include the shipping costs for the fuel. Despite being of value, this work to more completely incorporate all costs can be done as future work.

Lazard (2017) calculates a *LCOE* of \$0.197-0.281/kWh for DGs assuming a price for diesel at \$2.50/gallon, a 20-year planning horizon, 8% WACC, and replacement costs of 65% of the investment costs every 25,000 hours of operation, and a PV *LCOE* to be \$0.076-0.1500/kWh. Our model calculates a DG *LCOE* of \$0.2247/kWh and PV of \$0.0937/kWh using these same assumptions.

Lazard (2017) measures the sensitivity of a DG's *LCOE* to fuel prices and finds that *LCOE* can be reduced by as much as 22% when the fuel price is decreased to 25% and will be increased by as much as 16% when the fuel price is increased by 25%. Our model calculates the *LCOE* as \$0.1782/kWh when reducing the fuel price 25% to \$1.88/gallon. This new *LCOE* is 21% less than *LCOE* at \$2.50/gallon. Our model calculates the *LCOE*

as \$0.2720/kWh when increasing the fuel price 25% to \$3.13/gallon. This new *LCOE* is 21% more than the *LCOE* at \$2.50/gallon. Both the decrease and increase in fuel prices impact *LCOE* are most consistent with Lazard’s findings.

We still may give thought to why fuel costs, even when including shipping costs, would have to drop by more than half for PV to be financially worthwhile. The answer lies in the *LCOE* calculation. In that it does not consider the costs of the environmental impacts, *LCOE* does not provide a complete accounting of the total costs of each. The financial impact upon the environment and of course INI includes the air and water quality impact upon those working at the INI, as well as the impact of the noise on the wildlife and habitat. The Navy expends other funds to address these at greater levels due to incorporating DG in lieu of RE. As such if the financial costs associated with the environmental impacts of each are incorporated into *LCOE*, then arguably the break-even point will be much higher than \$1.00/gallon.

H. COMPARISON OF REDUNDANCY ARCHITECTURES

A compilation of the architectures for each experiment is made in Table 29 to better highlight which architectures provided less costs for the resilience. The WT quintuple microgrid is the best choice providing the most resilience for the least costs.

Table 29. Best architectures compared for experiments, all quintuple and no maintenance, except IV.E.1 which is quadruple. Colors correspond to functions shown in Figure 47.

Experiment	<i>resilience</i>	<i>LCOED</i> [\$/kWh]	Microgrid nominal power generation rating $P^{WT}+P^{PV}+P^{DG}$ [MW]
IV.E.1	0.90	0.1665	6
IV.E.2 WT+DG	0.90	0.1424	4
IV.E.2 PV+DG	0.90	0.1527	4
IV.E.2 WT+PV+ DG	0.78	0.1111	4
IV.E.3 WT	0.91	0.0468	4
IV.E.3 PV	0.90	0.0674	4
IV.E.3 PV+WT	0.91	0.0571	4

I. DISCUSSION AND CONCLUSION

Sensitivity analyses highlight that resilience is not very sensitive to the disturbance start time but is very sensitive to the WT's time to repair a damaged DER. *LCOED* is most sensitive to the fuel consumption rate and fuel costs and least sensitive to O&M costs.

The models are simulated to analyze questions on the impact of redundancy, power rating ratios, maintenance, value of investing in *invulnerability* vs. *recovery*, and fuel costs for DG to be competitive with PV by conducting ten experiments. The experiments generate meaningful results by providing constant ratios to attain better resilience and less costs as well as the trade-off functions and 4D graphs that highlight the relationships between design choices and maintenance investments and resilience and costs.

Increasing maintenance improved resilience in all architectures but has significantly less impact for a ratio with 1.5 times or more the generation as average demand. Therefore, decision makers should invest less maintenance dollars as the power rating increasingly exceeds demand. Maintenance is only significant when the microgrid's power rating is closer to the demand and for smaller costs as measured by *LCOED*, and when the architecture's generation is only RE.

The ratio of microgrid power to demand should not exceed four because there are no further improvements in resilience, only increasing costs. This is a result of the exponential growth in resilience and linear costs increase as the power to demand ratio is increased. Doubling the ratio of power to demand can greatly reduce time to recover but at significant costs compared to a ratio of one.

We confirm that given the option to invest more in more maintenance or more power rating, that maintenance improves *resilience* more. This can be useful to help a base commander determine where to invest any incremental, smaller amounts of funding to reflect their emphasis on one of these two resilience measures.

We confirm that the battery should be sized to equal the microgrid's generative power rating. Finally, fuel costs will have to decrease below \$1.00/gal for PV to be more cost competitive than DG.

A generalization about the behavior of our two measures to increasing the power to demand ratio or redundancy is that *resilience* exponentially increases, and *LCOED* linearly increase for the power to demand ratio but remains constant for redundancy. We observe that the resilience function no longer increases after the quintuple redundancy level.

The architecture combining RE and DG with the least costs is WT+DG. The only architecture with significantly less resilience than the others is the WT+PV+DG functional redundancy. WTs, without DG, has the highest resilience and the least costs; but of course, does not have the diversification that WT and DG does.

THIS PAGE INTENTIONALLY LEFT BLANK

V. DEMONSTRATION

Installed microgrid architectures should prove useful to assessing resilience and costs using actual historical demand profile data. This chapter applies the model to an existing microgrid at Naval Station Rota, Spain. This model is applied to the existing microgrid at Rota to assess whether redundancy can enhance the base case microgrid and an optimized microgrid architecture. The findings are provided in Section A. In Section B the RE microgrids at SCI, SNI and GTMO are assessed and the findings are presented. Section C compares the resilience and cost models with other models. Finally, the Discussion and Conclusion are presented in Section D.

A. ROTA'S ENERGY SYSTEM

Naval Station Rota is a 6,100 acre Spanish Base Naval de Rota with 5,200 acres maintained by the U.S. Navy (Globalsecurity.org (n.d.)). The U.S. Navy has been operating at Rota since 1953 and today there are more than 6,000 Americans in Rota. Rota is significant strategically due to being halfway between the United States and Southwest Asia, and for the close proximity of its airfield and port facilities within the same installation. Sullivan (2018) notes that Naval Station Rota is Europe's only installation with a contiguous port, airfield, fuels and munitions.

Naval Station Rota has 12.5 MW of backup DG generation composed of five 2.5 MW DGs. In addition to the DG generation, a recent project is now underway to install approximately 6 MW of solar PV.

Naval Station Rota converts the power provided by the local utility provider Endesa from 50 Hertz to 60 Hertz. This frequency conversion is necessary in order to power the 60 Hertz electrical loads for the U.S. operations on the base. Without the conversion, these loads could not be powered. As such, Naval Station Rota is comparable to an INI in that it is responsible for making the power usable for the load, independent of the grid-connected utility provider.

Given its close similarity to an INI, Naval Station Rota is a useful location to assess resilience using this model. The naval station wants to increase resilience and better

understand its costs before investing in a solution. Therefore, the cost of both design, and maintenance recommendations that increase resilience should be especially useful to the base commander.

An analysis of the air terminal within Naval Station Rota is conducted. A 1.25 MW DG provides backup power to an average load of 200 kW. This DG is oversized and runs significantly below its design rating which in turn contributes to extreme inefficiencies due to wet stacking – i.e., the inability to burn all the fuel supplied to the engine. To increase resilience, an optimized microgrid including a smaller DG, PV, and a BAT is evaluated and compared to the existing 1.25 MW DG. The 2D graphs for *LCOED* vs. *resilience*, *recovery*, and *invulnerability* are provided in Appendix A.

1. Parameters

Because Rota is located just eight miles from Cadiz in the Atlantic Ocean, the following parameters are pertinent for the scenarios modeled in this demonstration as they are considered the most likely disturbances to strike this location. Patel and Zaveri (2010) determined the mean probability of SCADA equipment damage resulting from a cyberattack as 25%. Birkman et al. (2010) determined that although the chance of a tsunami is low for Cadiz, it would have severe negative consequences. Nicolas et al. (2019) found DG and WT to have the same vulnerability to damage to a tsunami as their respective vulnerability to a hurricane, and BAT and PV to have the same vulnerability level as a WT. The probabilities of damage for the cyberattack, and for the tsunami scenarios are presented in Table 30.

Table 30. Probability of damage given disturbance S_k occurs for a cyberattack, and a tsunami.

	$P(d/S_k)$	
	Cyberattack	Tsunami
DER		
WT	0.25	0.5
PV	0.25	0.5
DG	0.25	0.5
BAT	0.25	0.5

As the table suggests, a tsunami is more likely to inflict damage than a cyberattack, which means that resilience to a tsunami should provide even greater resilience to a cyberattack.

The mean values of time to repair each DER, K , are kept as presented in Table 9. The parameters used in simulations remained the same as presented in Tables 10 and 11 except for those provided by Naval Station Rota’s utilities energy manager as indicated in Table 31. All DER investment costs are unchanged from the previous experiments except PV which is reduced to \$2,000/kW as provided by IRENA (2020) for Spain. DER maintenance costs are kept the same for WT.

Table 31. Parameters used in simulations.

Variable	Parameter	Value
f	DG fuel costs	\$2.99/gal
W	DG fuel consumption rate	22.94 gal/hr
J^{PV}	PV O&M costs	\$24.00/kW
J^{DG}	DG O&M costs	\$6.32/kW
J^{BAT}	BAT O&M costs	\$2,252/year

Table 32 is the hourly demand profile over two weeks we use in the model.

Table 32. Air terminal demand at time t .

Day	Time [hour]	D [KW]	Day	Time [hour]	D [KW]	Day	Time [hour]	D [KW]	Day	Time [hour]	D [KW]	Day	Time [hour]	D [KW]
1	0	185.2	4	72	185	7	144	195	10	216	185	13	288	195
	1	180.9		73	181		145	194		217	181		289	194
	2	169.3		74	169		146	179		218	169		290	179
	3	167		75	167		147	174		219	167		291	174
	4	164		76	164		148	174		220	164		292	174
	5	171.4		77	171		149	178		221	171		293	178
	6	185.1		78	185		150	189		222	185		294	189
	7	219		79	219		151	195		223	219		295	195
	8	246.7		80	247		152	194		224	247		296	194
	9	206.8		81	207		153	175		225	207		297	175
	10	199.8		82	200		154	169		226	200		298	169
	11	195.2		83	195		155	159		227	195		299	159
	12	182.2		84	182		156	154		228	182		300	154
	13	184.9		85	185		157	155		229	185		301	155
	14	180.2		86	180		158	156		230	180		302	156
	15	180.9		87	181		159	158		231	181		303	158
	16	179		88	179		160	158		232	179		304	158
	17	165.6		89	166		161	151		233	166		305	151
	18	176.4		90	176		162	176		234	176		306	176
	19	185.7		91	186		163	182		235	186		307	182
	20	182.9		92	183		164	186		236	183		308	186
	21	187.8		93	188		165	188		237	188		309	188
	22	184.6		94	185		166	183		238	185		310	183
	23	182		95	182		167	188		239	182		311	188
2	24	185	5	96	212	8	168	185	11	240	185	14	312	195
	25	181		97	217		169	181		241	181		313	194
	26	169		98	196		170	169		242	169		314	179
	27	167		99	186		171	167		243	167		315	174
	28	164		100	197		172	164		244	164		316	174
	29	171		101	191		173	171		245	171		317	178
	30	185		102	213		174	185		246	185		318	189
	31	219		103	259		175	219		247	219		319	195
	32	247		104	268		176	247		248	247		320	194
	33	207		105	259		177	207		249	207		321	175
	34	200		106	249		178	200		250	200		322	169
	35	195		107	249		179	195		251	195		323	159
	36	182		108	238		180	182		252	182		324	154
	37	185		109	254		181	185		253	185		325	155
	38	180		110	238		182	180		254	180		326	156
	39	181		111	240		183	181		255	181		327	158
	40	179		112	247		184	179		256	179		328	158
	41	166		113	226		185	166		257	166		329	151
	42	176		114	219		186	176		258	176		330	176
	43	186		115	222		187	186		259	186		331	182
	44	183		116	220		188	183		260	183		332	186
	45	188		117	221		189	188		261	188		333	188
	46	185		118	219		190	185		262	185		334	183
	47	182		119	216		191	182		263	182		335	188
3	48	185	6	120	195	9	192	185	12	264	212		336	195
	49	181		121	194		193	181		265	217			
	50	169		122	179		194	169		266	196			
	51	167		123	174		195	167		267	186			
	52	164		124	174		196	164		268	197			
	53	171		125	178		197	171		269	191			
	54	185		126	189		198	185		270	213			
	55	219		127	195		199	219		271	259			
	56	247		128	194		200	247		272	268			
	57	207		129	175		201	207		273	259			
	58	200		130	169		202	200		274	249			
	59	195		131	159		203	195		275	249			
	60	182		132	154		204	182		276	238			
	61	185		133	155		205	185		277	254			
	62	180		134	156		206	180		278	238			
	63	181		135	158		207	181		279	240			
	64	179		136	158		208	179		280	247			
	65	166		137	151		209	166		281	226			
	66	176		138	176		210	176		282	219			
	67	186		139	182		211	186		283	222			
	68	183		140	186		212	183		284	220			
	69	188		141	188		213	188		285	221			
	70	185		142	183		214	185		286	219			
	71	182		143	188		215	182		287	216			

This profile is based on historical demand data provided by the utilities energy manager at Naval Station Rota. Time step 0 corresponds to 8:00 am, with daytime indicated in orange and nighttime in gray.

2. Base Case Impact of Redundancy, and Maintenance on Resilience and Costs

Simulations are conducted to evaluate the impact of the annual maintenance investment level on resilience and costs for cyberattack and tsunami disturbance scenarios. The convention used to differentiate redundancy levels is double for two components, triple for three, and so on. The existing base case microgrid architecture with redundancy is evaluated as indicated in Table 33. The disturbance start time of 8:00 a.m. on the first day is chosen so as to evaluate the impact upon a complete workday.

Table 33. Microgrid architectures for impact of redundancy and maintenance.

Redundancy	Microgrid nominal power rating P [kW]	DG nominal power rating P_i^{DG} [kW]	# of DGs m^{DG}
no	1,250	1,250	1
double	1,250	625	2
triple	1,250	417	3
quadruple	1,250	313	4
quintuple	1,250	250	5

The first microgrid architecture (base case) with no redundancy is displayed in Figure 61.

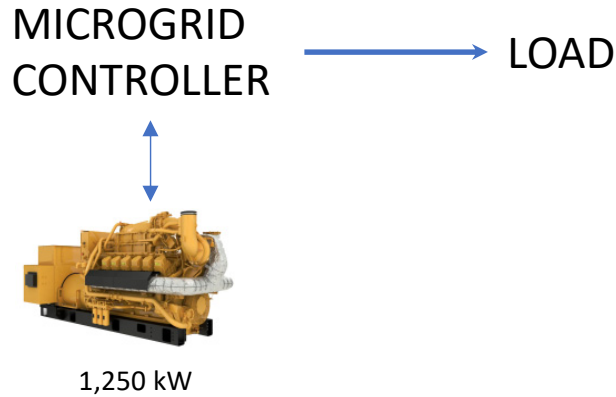


Figure 61. Microgrid architecture with one 1,250 kW DG.

Monte Carlo simulations are averaged for 7,500 simulations as before. As seen in Figure 62 and the figures in Appendix A, generally, redundancy improves resilience for equivalent costs, approximately 30% improvement in time to recover, than the base case without redundancy. Also, more maintenance is worthwhile. A *resilience* of 1 is the maximum and cannot be improved upon. A resilience of 0.69 for instance can be improved through redundancy.

The best architecture for both the tsunami and cyberattack is quintuple. The best architecture for a tsunami has a *resilience* = 0.91, and for a cyberattack has a *resilience* = 0.92. Both have a *LCOED* = \$1.2324/kWh at a medium maintenance level.

Figure 62 shows how redundancy quickly improves resilience. We also see again how maintenance is more worthwhile when there is no redundancy. The costs are all the same, so there is no reason not to incorporate redundancy. We also observe how maintenance only improves the time to recover when there is no redundancy.

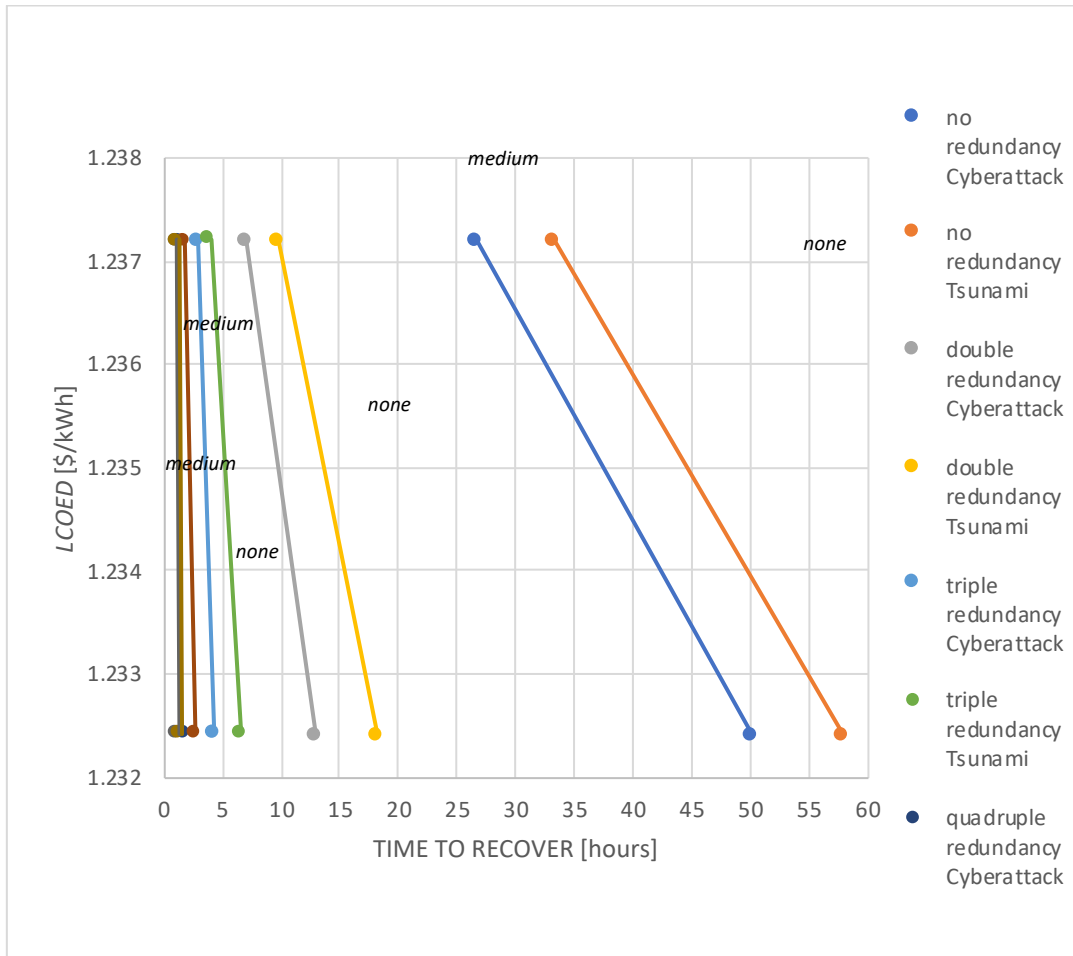


Figure 62. Redundancy’s impact on time to recover and *LCOED* for base case.

Why does increased redundancy so quickly decrease the rate of improving resilience? The answer is related to the demand profile. For this demand profile, when the redundancy level gets to triple, each DER’s size is more closely matched to the demand and therefore we see much less improvements in redundancy after this point. Additionally, the combined probability of damage considering the independent probabilities mathematically multiplies the probabilities by each other and as we add more the net decrease in probability is rapid and significant.

3. Optimized Microgrid's Impact of Redundancy, and Maintenance on Resilience and Costs for a Morning Tsunami

We should understand how varying the redundancy of each DER will impact resilience at Rota in order to make recommendations that will provide the most resilience for the least costs. Each microgrid modeled employs different capacities for each DER but the same overall microgrid power rating of 516 kW. 516 kW is determined using the Xendee optimization model. Five different microgrid architectures employing DER components with varying capacities are evaluated as shown in Table 34.

Table 34. Microgrid architectures for redundancy.

Redundancy	Microgrid nominal power generation rating $P^{PV} + P^{DG}$ [kW]	PV nominal power rating P_i^{PV} [kW]	DG nominal power rating P_i^{DG} [kW]	BAT nominal power rating P_i^{BAT} [kW]	# of PV m^{PV}	# of DG m^{DG}	# of BAT m^{BAT}
no	516	196.0	320.0	383.0	1	1	1
double	516	98.0	160.0	191.5	2	2	2
triple	516	65.3	107.0	127.7	3	3	3
quadruple	516	49.0	80.0	95.8	4	4	4
quintuple	516	39.2	64.0	76.6	5	5	5

A RE microgrid for Rota optimized to minimize costs and created by Xendee is used as shown with no redundancy in Figure 63. We subject this microgrid to the tsunami because it is the only natural disaster that seems likely to strike based upon the literature reviewed and Birkman et al.'s (2010) findings. The tsunami commences at 8:00 am on the first day. The same demand profile as provided in Table 32 is used as before, and the ratio of the demand to power generation rating is constant.

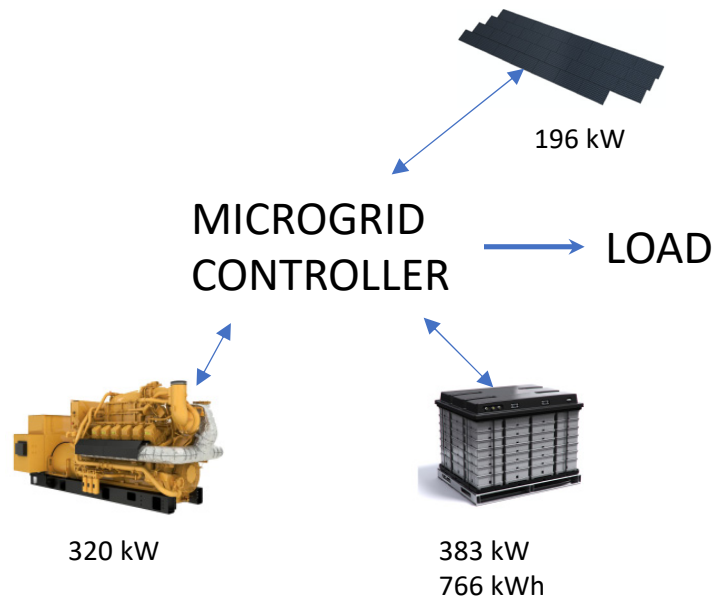


Figure 63. Microgrid architecture with no redundancy employing 516 kW overall microgrid power generation rating.

Figure 64 illustrates the behavior of the architecture without redundancy during one simulation. In this iteration, the DGs and BATs are immediately damaged by the tsunami. The mean time to repair the DG is 60 hours, and the mean time to repair the BAT is 10 hours. For a low maintenance level, the microgrid is able to satisfy the demand once the battery recovers after 10 hours. This case illustrates the benefit of redundancy because the DG remains unoperational for another 50 hours more.

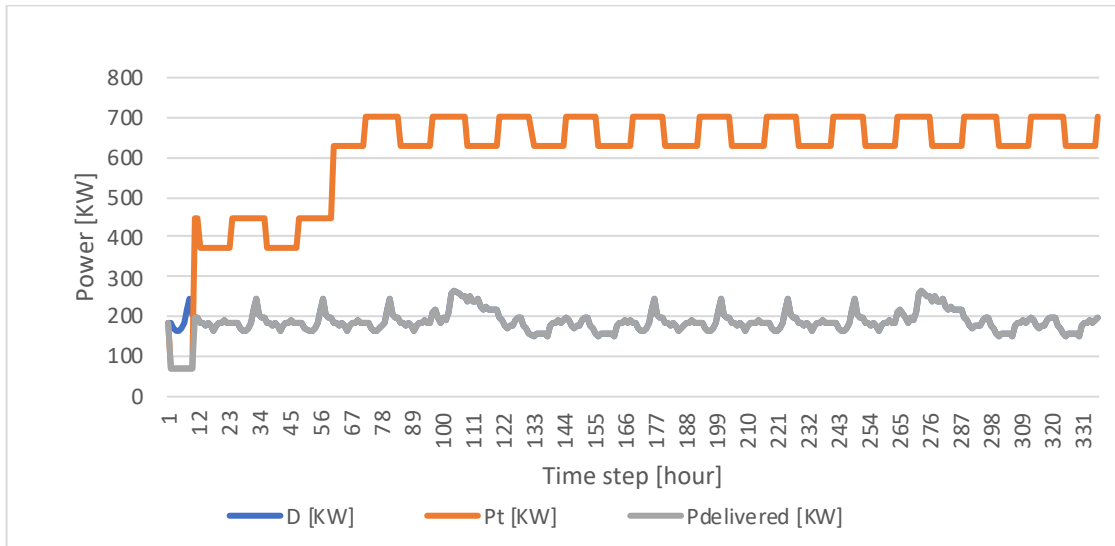


Figure 64. Demand, power rating and delivered power.

Figure 65 shows the battery's behavior; the blue line represents the single battery. At ten hours, the damaged battery is restored to operation and immediately discharges. However, there is insufficient excess power rating to charge the battery until the DG is repaired at 60 hours.

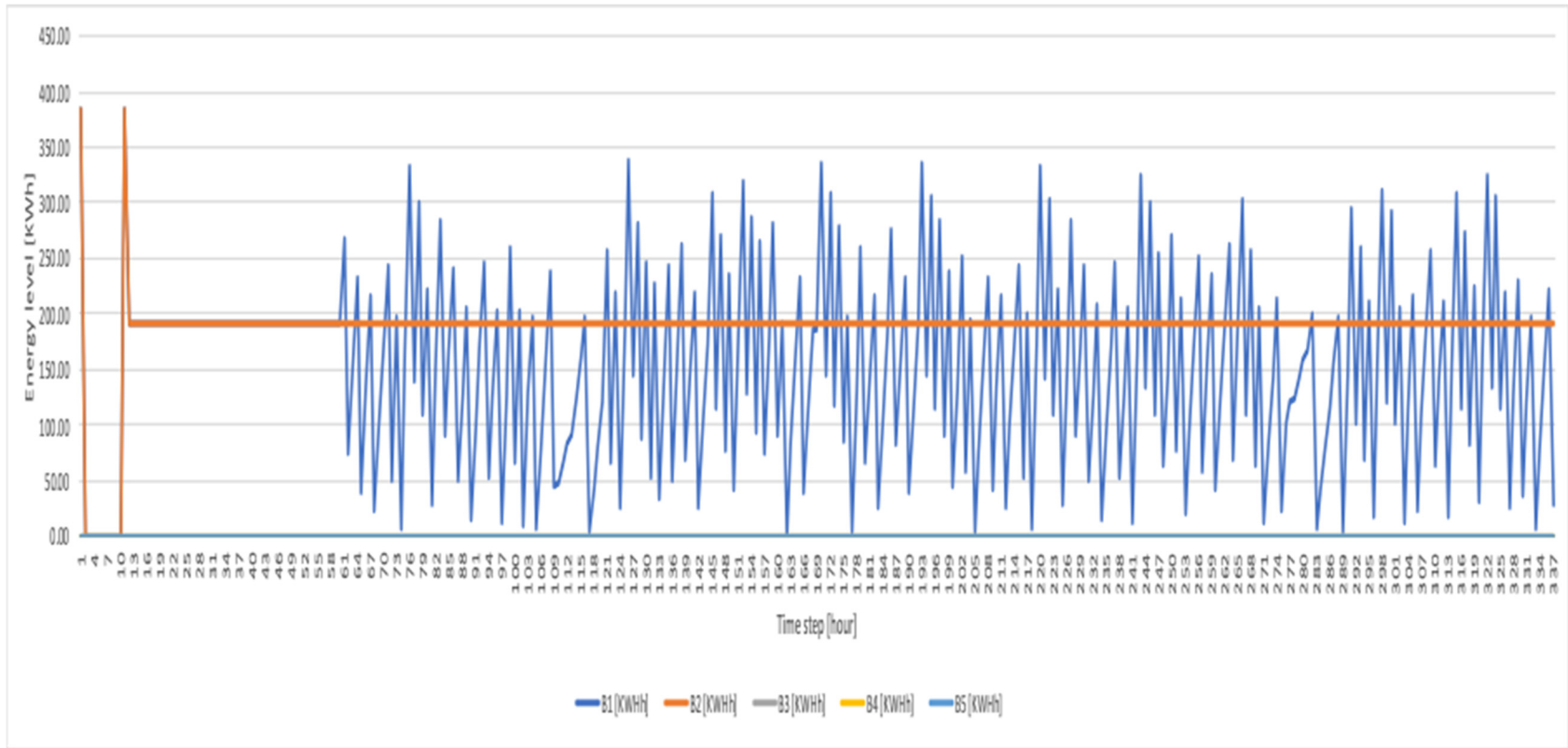


Figure 65. Battery energy level.

Figure 66 illustrates the diesel genset's behavior. There is no fuel consumption while it is damaged. Once it is restored at 60 hours, the diesel genset operates at 18.35 gallons/hour.

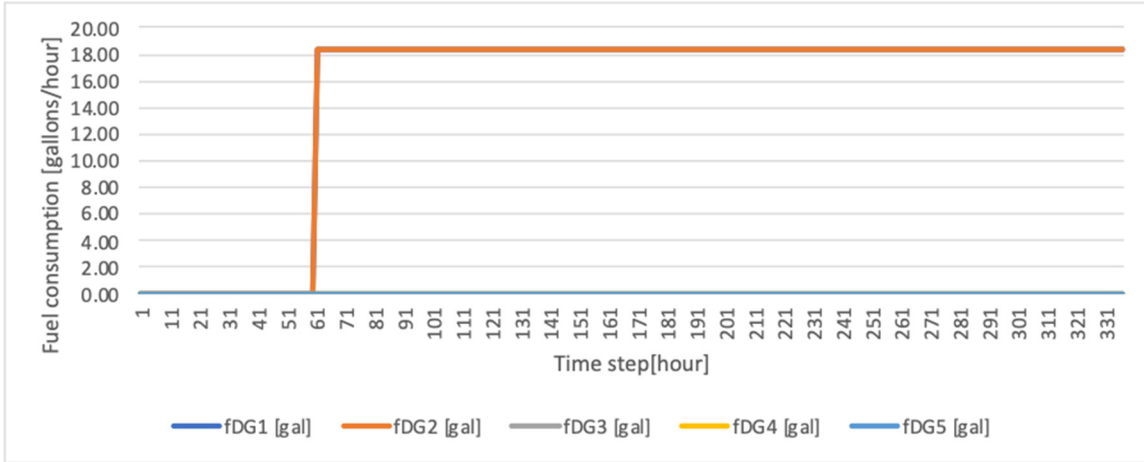


Figure 66. Diesel genset fuel consumption.

The best architecture is quintuple and provides a *resilience* = 0.91, with no maintenance and a *LCOED* = \$0.3644/kWh. This is a significant improvement in *resilience* especially considering it costs appreciably less than the base case microgrid.

In general, the optimized microgrid is a much better option than the base case. This RE microgrid is optimized to minimize costs and we see that it performs much more cost effectively than the base case. Greater redundancy provides greater *recovery*, *invulnerability*, *resilience* and better time to recover at less costs. Maintenance is somewhat significant but should not exceed a low maintenance level.

Figure 67 shows how maintenance improves time to recover relatively more than the base case and the time to recover is less than three hours. Again, we see benefits of redundancy and diversification, as well as we now see maintenance benefits throughout all redundancy levels.

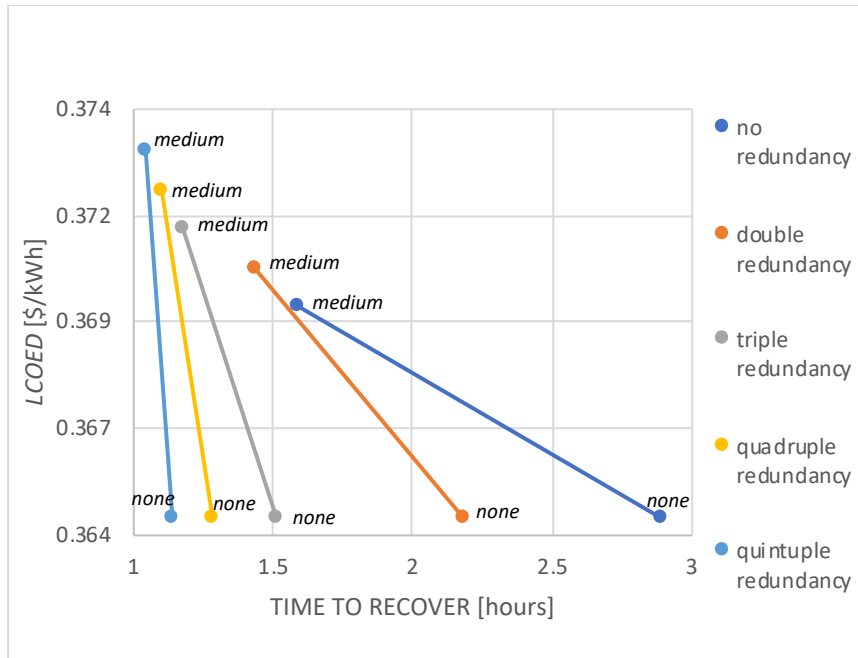


Figure 67. The effects of redundancy on *LCOED* and time to recover.

Why does the optimized microgrid have much better resilience for significantly less costs compared to the base case? Not only this microgrid sized more closely to the demand, with generation more than half the base case, there is the added diversification benefit of PV and BAT. This microgrid architecture is clearly the best choice for Rota due to its fractional costs compared to the base case, with much better resilience.

Figure 68 illustrates how the base case has greater opportunity for improvements in resilience but costs almost four times the optimized microgrid. We observe how the optimized microgrid has better resilience and both maintain a constant costs for changes in redundancy. Finally, these 4D functions show how both maintenance and redundancy impact resilience and costs less for the optimized microgrid due to the volume of the shape being appreciably less, have a *LCOED* that is less than a third of the base case's *LCOED*.

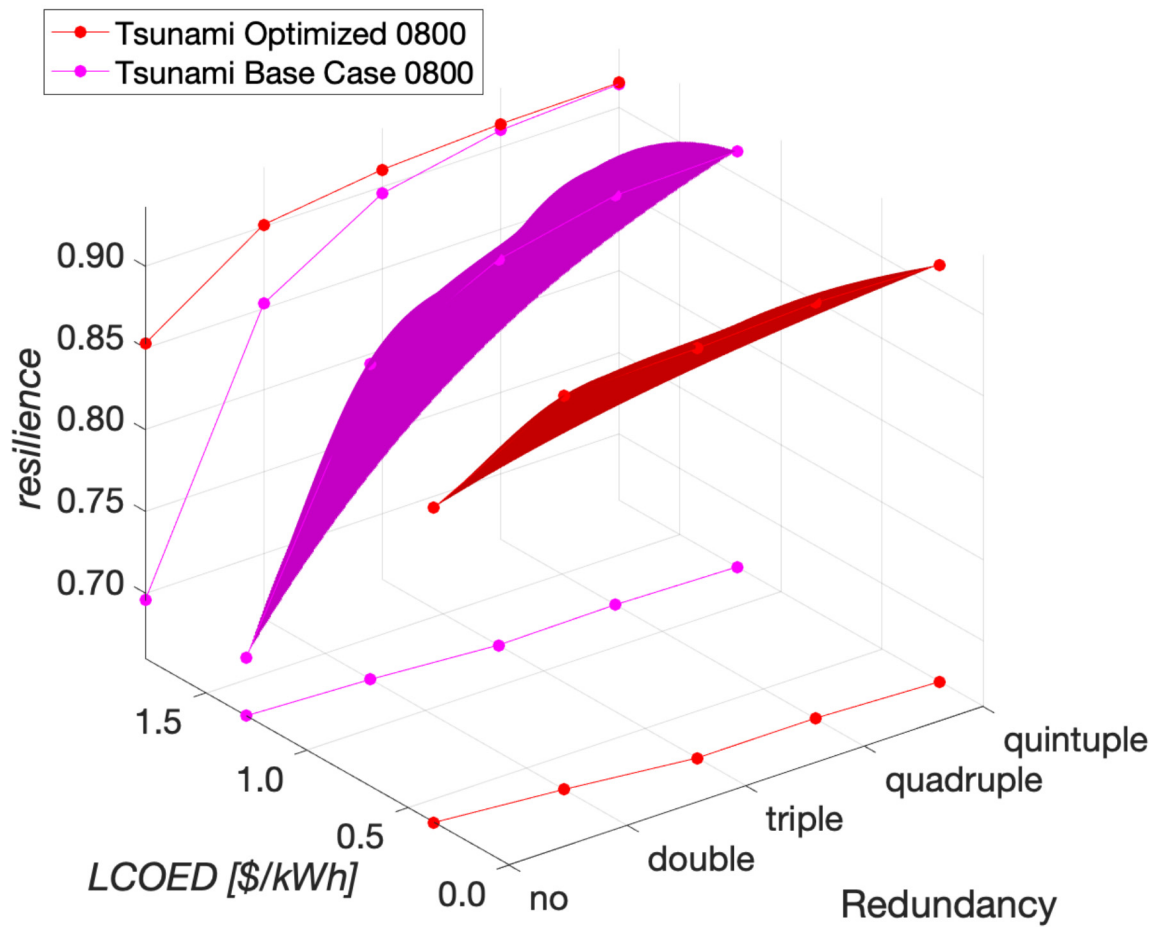


Figure 68. Optimized and base case microgrid's resilience, and costs as a function of redundancy during a morning tsunami.

Figure 69 shows how the optimized microgrid has appreciably greater *resilience*, and lower costs. Both microgrids have an exponential increase in *resilience*.

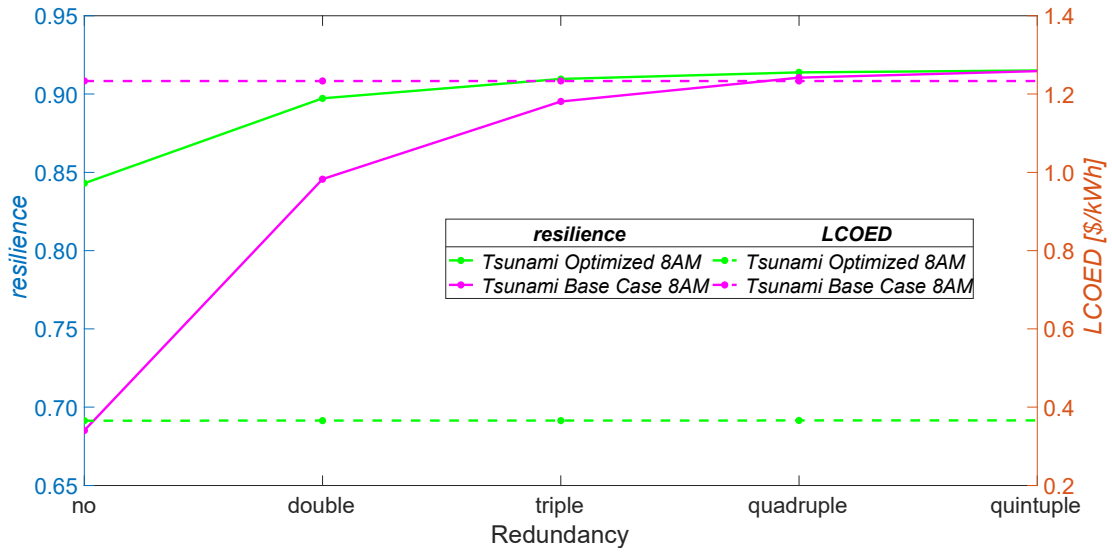


Figure 69. Optimized and base case microgrids' *resilience*, and costs as a function of redundancy.

In Figure 70 we see how *recovery* and *invulnerability* both exponentially increase with more redundancy. We also observe how the base case sees no improvement in *invulnerability* until triple redundancy.

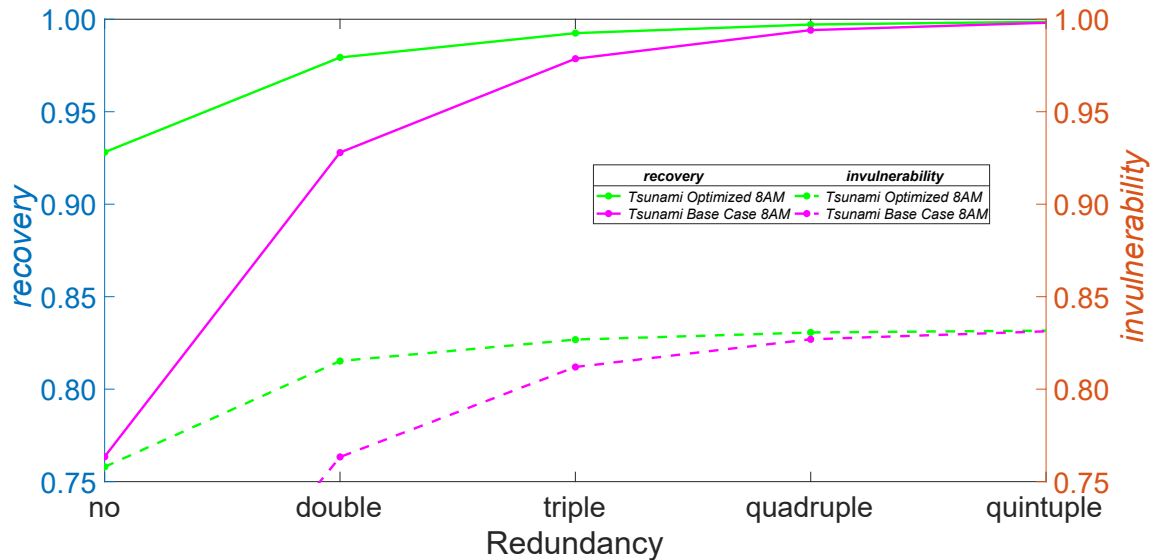


Figure 70. Optimized and base case microgrids' *recovery*, and *invulnerability* as a function of redundancy.

4. Optimized Microgrid's Impact of Redundancy, and Maintenance on Resilience and Costs for a Midnight Tsunami

Will the individual diurnal differences in the PV have any significant impact collectively on resilience when the tsunami strikes at midnight compared to the morning? To determine how a tsunami that strikes at midnight will change the findings, the redundancy experiment for a tsunami with a disturbance start time of midnight is conducted and compared to the experiment's results for a tsunami that strikes in the morning. The previous parameters and architectures remain the same.

Medium and no maintenance levels are as annotated. The best architecture is again quintuple and provides a resilience = 0.92, and for no maintenance has a $LCOED = \$0.3644/\text{kWh}$.

Figure 71 shows a slight degradation in time to recover for the same costs, and otherwise the findings are almost identical to the morning tsunami. Maintenance plays the same role as in the morning tsunami. There is no change in resilience or costs due to diurnal factors.

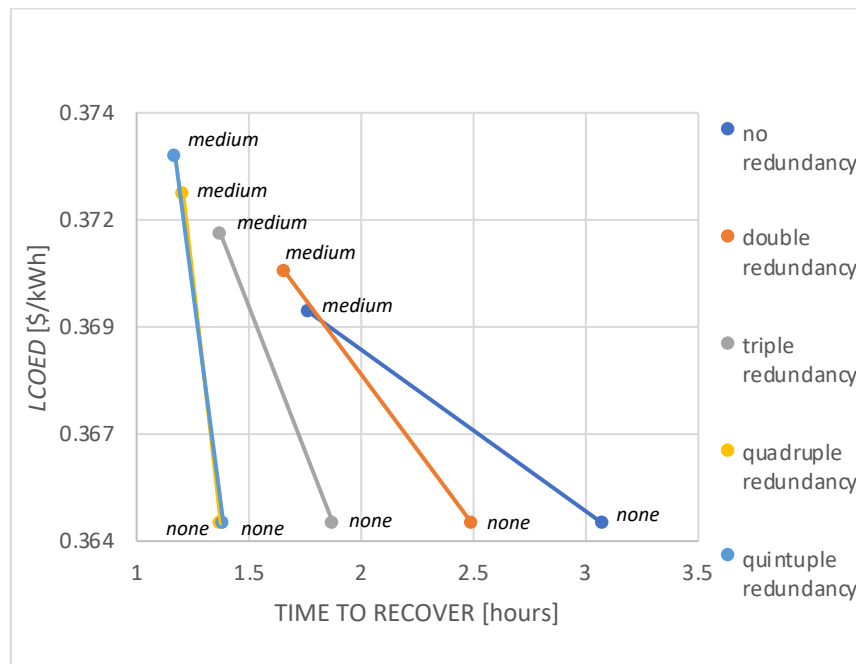


Figure 71. The effects of redundancy and maintenance level on $LCOED$ and time to recover.

Again, redundancy improves time to recover for less costs. Yet, we may reflect upon why we have any degradation in resilience when the disturbance strikes at night versus the morning. The only DER subject to diurnal behavior is the PV. The answer lies in the time to recover. The time to recover in all instances is less than four hours, before sunrise. As such, the PV is unable to generate any power between the midnight and full recovery hence the slight degradation in *resilience*.

5. Design Options

When we compare the base case without redundancy to adding redundancy and compare this again to the optimized microgrid with redundancy we can see the following for a morning tsunami as shown in Table 35.

Table 35. Design options for Rota compared; optimized architecture provides 30% higher resilience for only 30% of the base case’s costs.

Architecture	Maintenance	LCOED [\$/kWh]	resilience
Base case, only one DG	medium	1.2372	0.70
Quintuple DG	none	1.2324	0.91
Optimized, quintuple	none	0.3644	0.91

Clearly the optimized quintuple microgrid is the best choice.

B. SCI, SNI, AND GTMO MICROGRIDS

Of the six INIs—DGAR, CLDJ, GTMO, AUTECH, SNI, and SCI—have RE installed, and therefore SCI, SNI, and GTMO are assessed using the resilience and cost models. The microgrid architectures illustrated in Figures 72–74 are modeled as before for a hurricane disturbance using historical demand profile time-series data as illustrated in Figure 75. SCI’s exact same microgrid architecture is modeled. However, SNI has 7, 100 kW, wind turbines but to adapt this to the model, the microgrid is reduced to five 140 kW WT. GTMO has 13 DGs with various capacities totaling 33 MW. To adapt GTMO’s microgrid to this model, its microgrid is reduced to five 6.6 MW DGs.

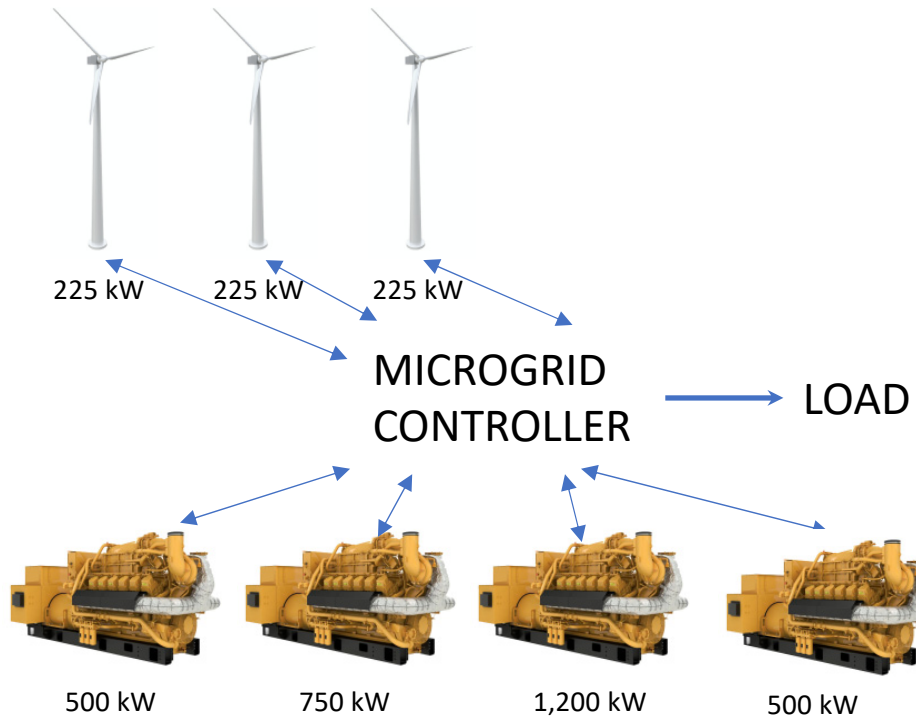


Figure 72. SCI's RE microgrid.

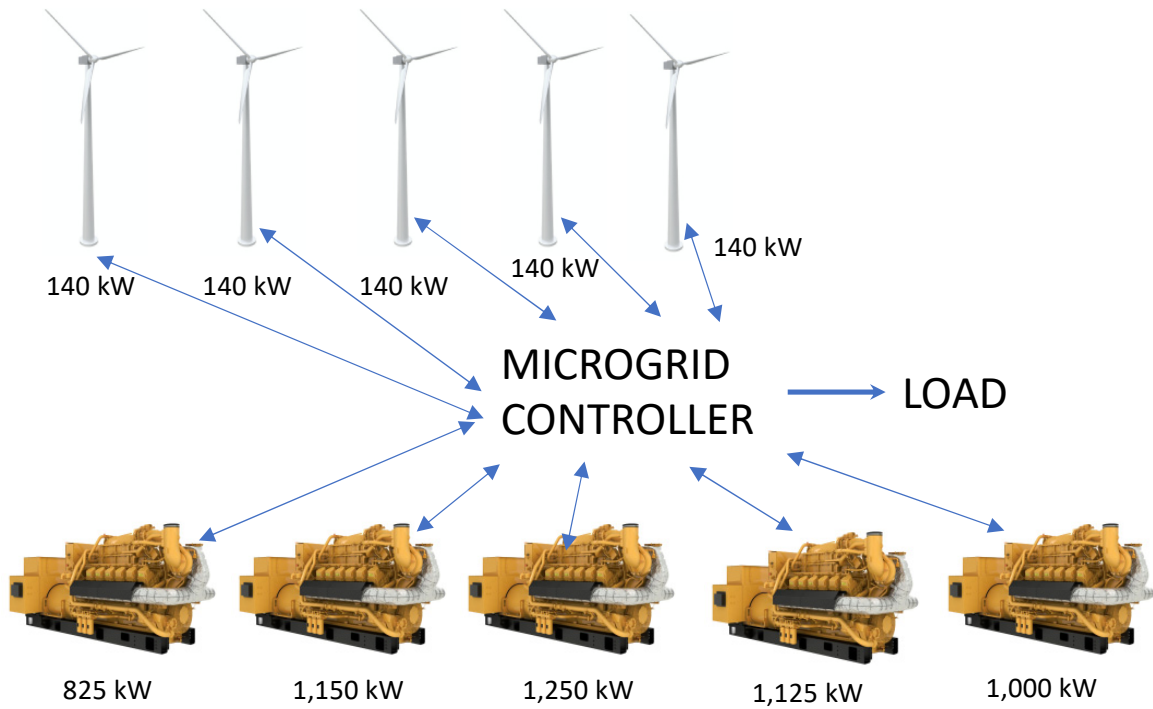


Figure 73. SNI's adapted RE microgrid.

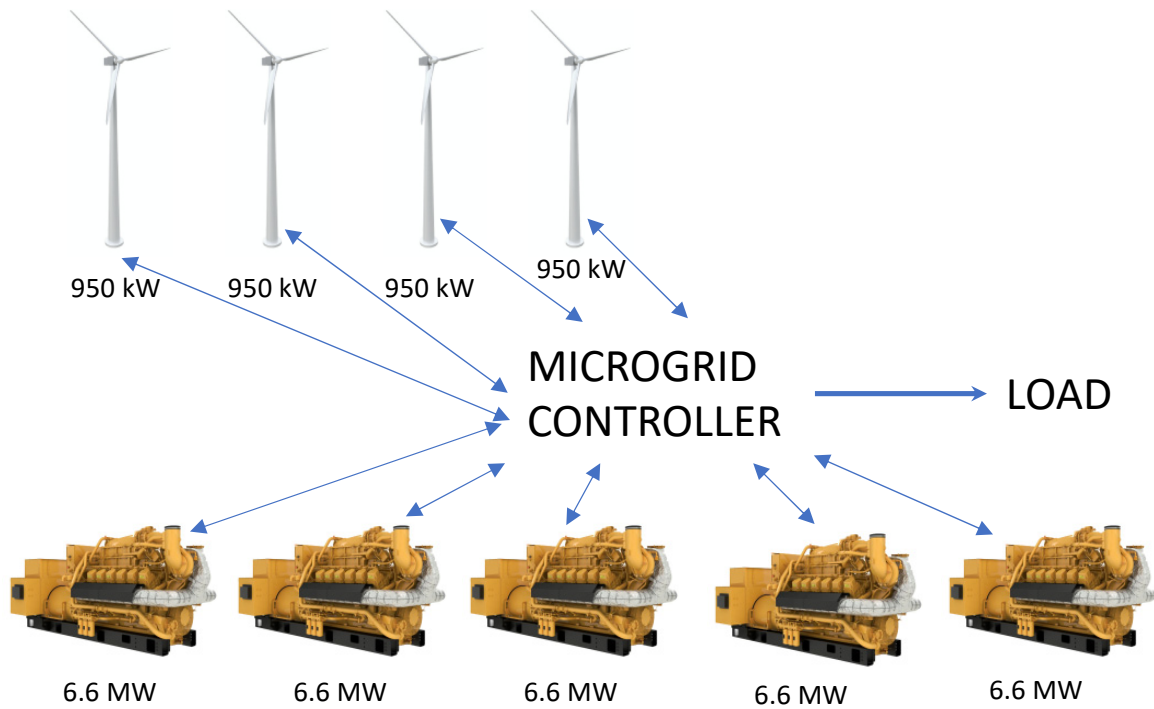


Figure 74. GTMO's adapted RE microgrid.

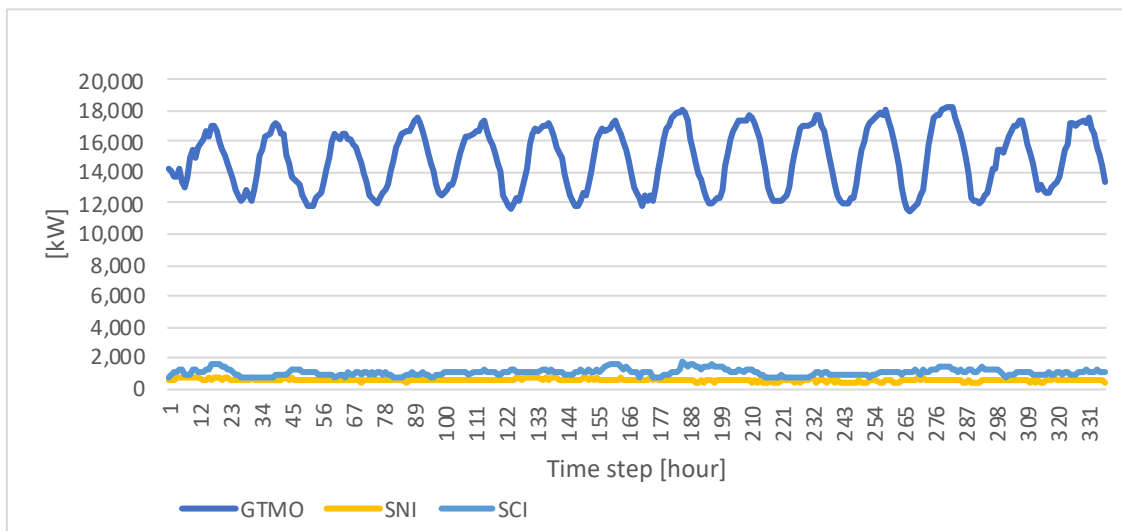


Figure 75. GTMO, SNI, and SCI demand profiles.

SNI time to recover is fastest because of the excess power rating present in the system at eight times more power rating than the demand compared to SCI and GTMO, which both have approximately twice the power rating as the demand. GTMO has almost

three times the time to recover as SCI and 15 times the time to recover as SNI, and approximately ten times the cost of either SCI or SNI. GTMO also benefits the most by maintenance.

The level of maintenance only increases resilience at SCI; SNI and GTMO sees no increase in resilience due to maintenance. Medium maintenance reduces the time to recover by almost 50% at GTMO, 40% at SCI and 15% at SNI. Medium maintenance reduces costs by \$9M at GTMO, \$800k at SCI and \$1.5M at SNI.

At SCI and SNI, the level of maintenance does not affect invulnerability and has little impact, ~0.1% increase, at GTMO. For a higher ratio power rating/demand as seen at SNI, the maintenance level will reduce costs by ~ 12%.

Figure 76 shows how maintenance only improves recovery at GTMO. We also observe that SNI's *LCOED* is almost four times SCI's or GTMO's *LCOED*.

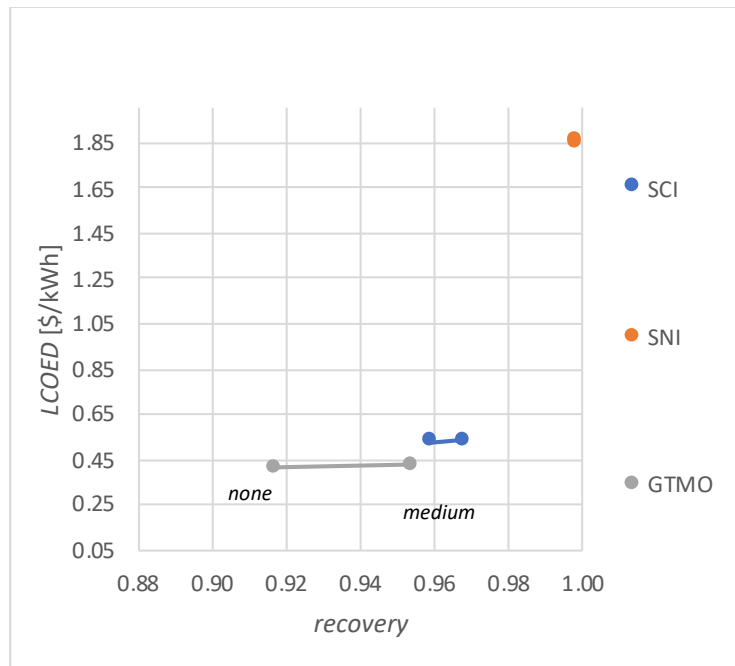


Figure 76. *LCOED* vs. *recovery* for SNI, SCI, and GTMO.

Figure 77 illustrates that SNI has the least invulnerability. SCI and GTMO have almost the same *invulnerability*.

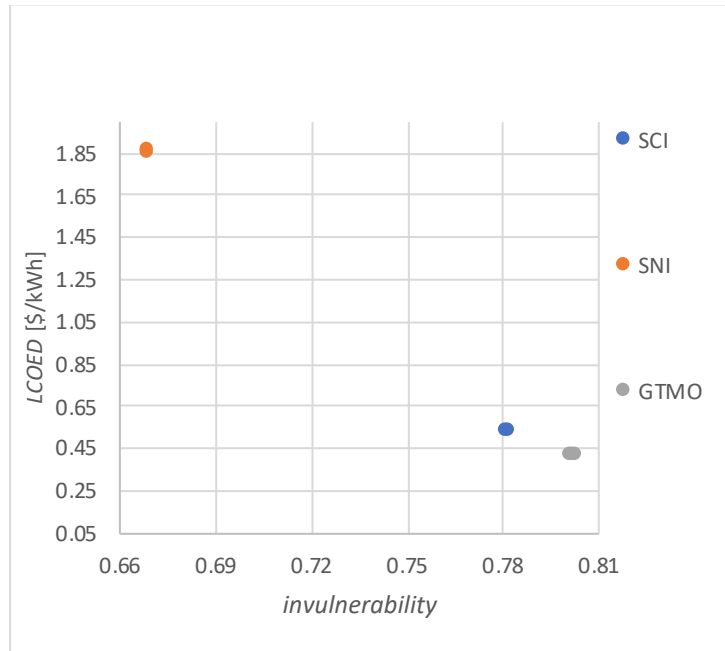


Figure 77. *LCOED vs. invulnerability* for SNI, SCI, and GTMO.

Figure 78 shows us that SNI has the least resilience and highest *LCOED*.

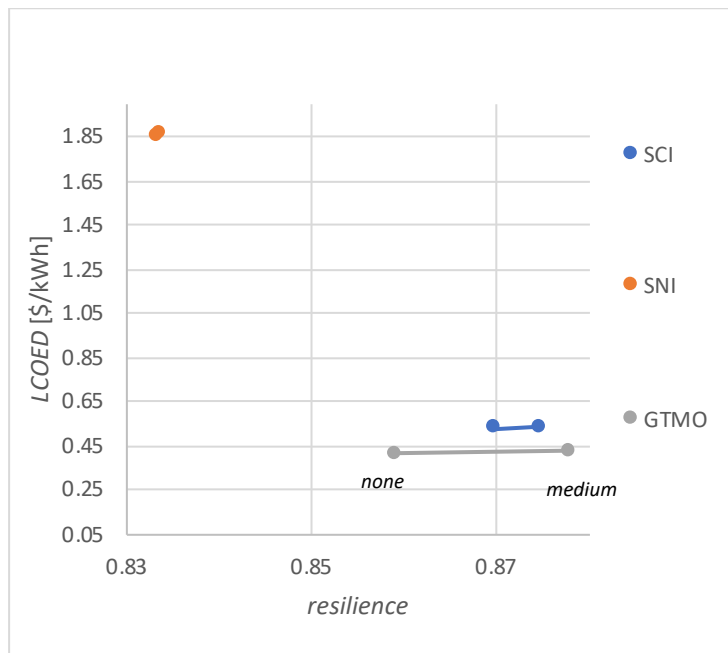


Figure 78. *LCOED vs. resilience* for SNI, SCI, and GTMO.

Figure 79 shows that SNI has the best time to recover, and GTMO the least. GTMO's time to recover is as much as more than a day longer than SNI's time to recover.

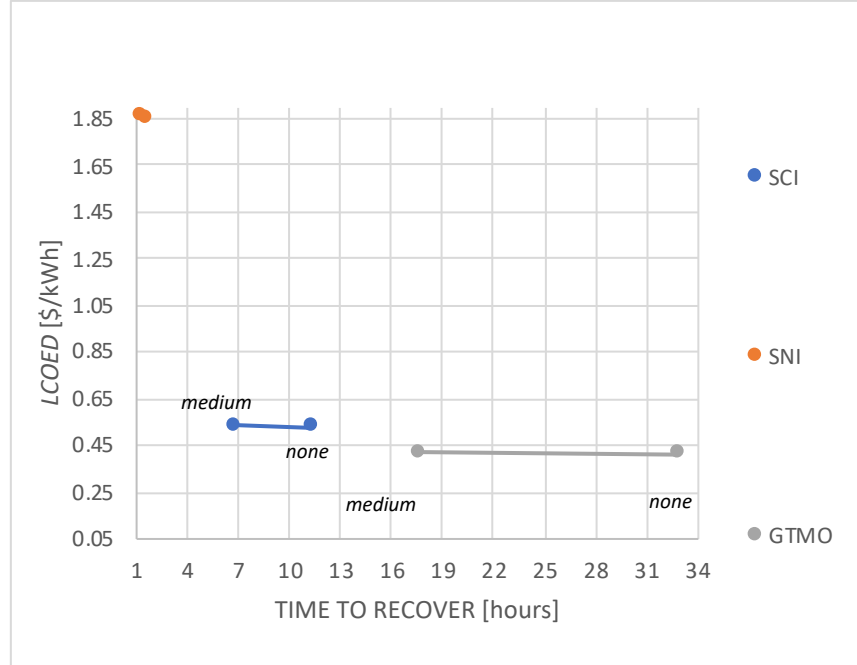


Figure 79. *LCOED* vs. time to recover for SNI, SCI, and GTMO.

1. Comparison of Resilience and Costs

The models are simulated as before using the respective demand profiles. All DGs at SCI and SNI are sized at 1MW, and the WTs at SCI are sized at 225 kW and SNI at 100 kW. For GTMO, the DGs are sized at 6 MW and the WTs 0.95 MW. 3D graphs are created for SCI, SNI and GTMO to illustrate how *LCOED* and *resilience* vary with different combinations of WTs and DGs.

We conduct simulations and demonstrate how resilience changes with each combination of WTs and DGs. As shown, there are three distinct findings. First there is more improvement in *resilience* at SCI by adding more WTs. Also, SNI sees little improvement in more than three DGs which is due to the demand profile being approximately half the demand profile as SCI.

Second, GTMO’s *resilience* is approximately half that of SCI and SNI’s *resilience* for one and two DGs but approaches the same level of *resilience* with three DGs. SCI and SNI have comparable *resilience* for the design combinations of WT and DG.

And the third finding is that there is significant improvement in *resilience* when increasing from one to two DGs but this improvement as DGs increase rapidly diminishes when increasing from two to five DGs. Only at GTMO is there significant improvement from two to three DGs.

Why would the time to recover be so much better at SNI than SNI and GTMO? This likely has to do with the limitation of the model not being able to handle more than 5 of any DER. As such, GTMO’s adapted microgrid has WT and DG capacities that are excessive for the demand.

Figure 80 illustrates SNI’s much higher *LCOED*. We see that in all three INIs adding DGs increases costs significantly more than WTs.

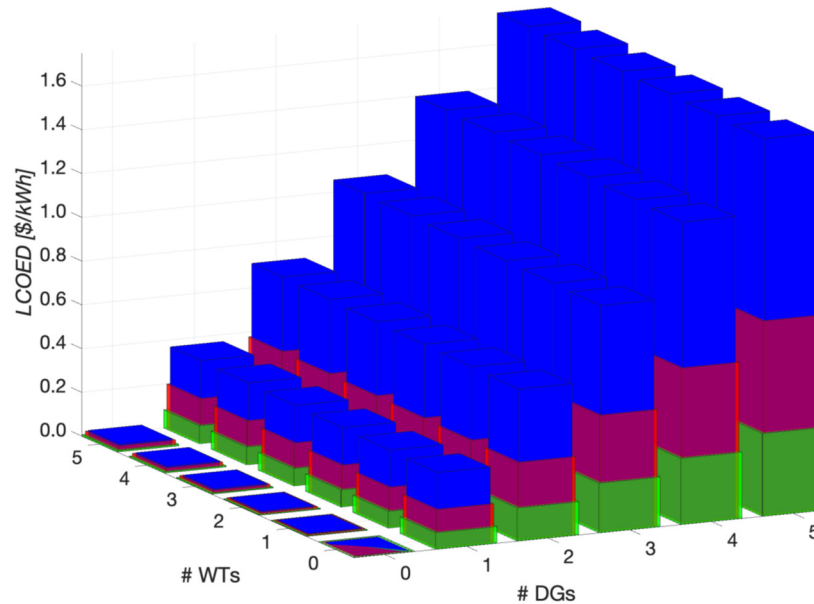


Figure 80. *LCOED* vs. # of WTs and DGs for SCI, SNI, and GTMO.

Figures 81–83 highlight higher *resilience* with yellow, and the darker and blue areas have lower resilience. We use a color map that degrades from blue to yellow with the resilience values for the data points. The values of *resilience* are indicated in the color bar on the right. We observe that it takes 3 DGs at GTMO to improve *resilience*, and this approximates \$0.3/kWh. At SCI and SNI we see similar improvements in *resilience* with 2 DGs and at SNI this approximates \$0.8/kWh and at SCI \$0.4/kWh.

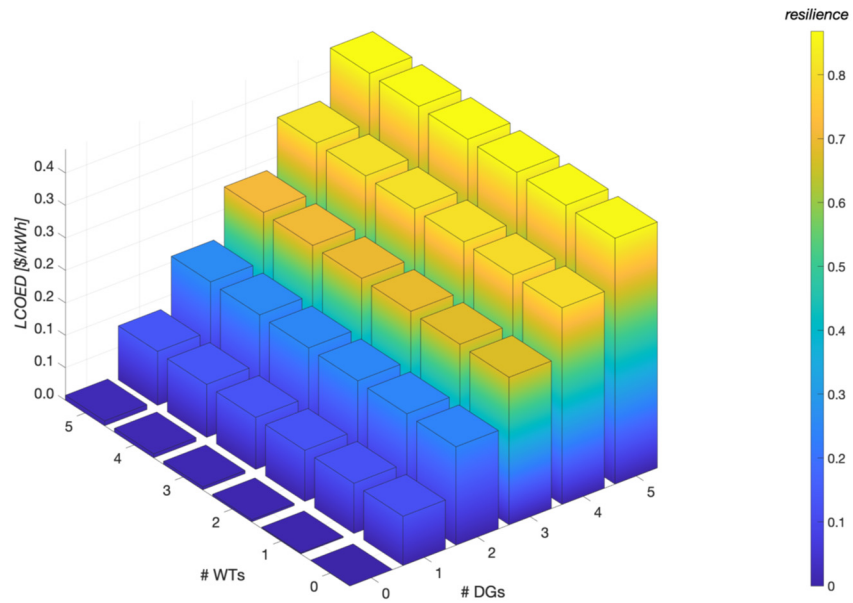


Figure 81. *LCOED* vs. # of WTs and DGs for GTMO.

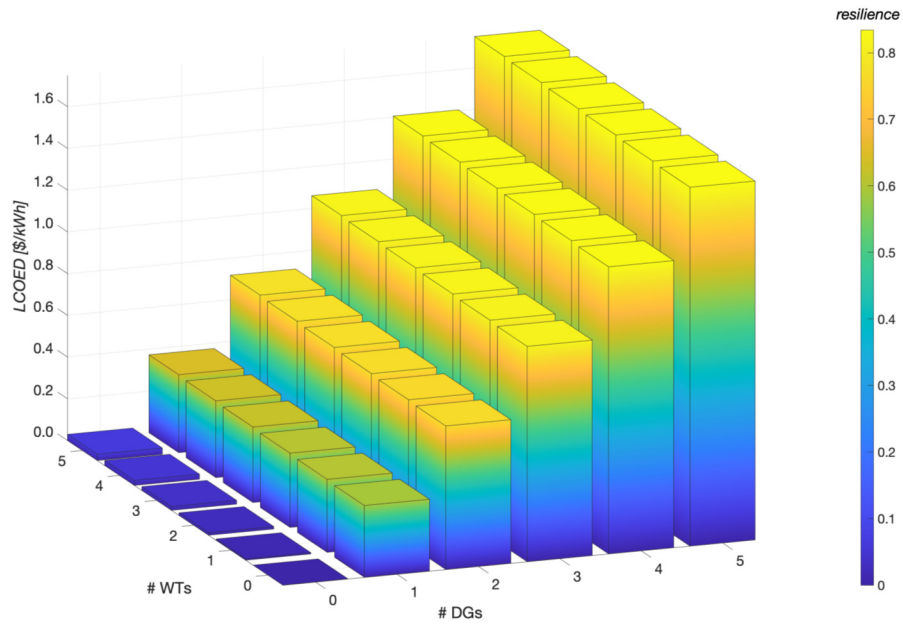


Figure 82. *LCOED* vs. # of WTs and DGs for SNI.

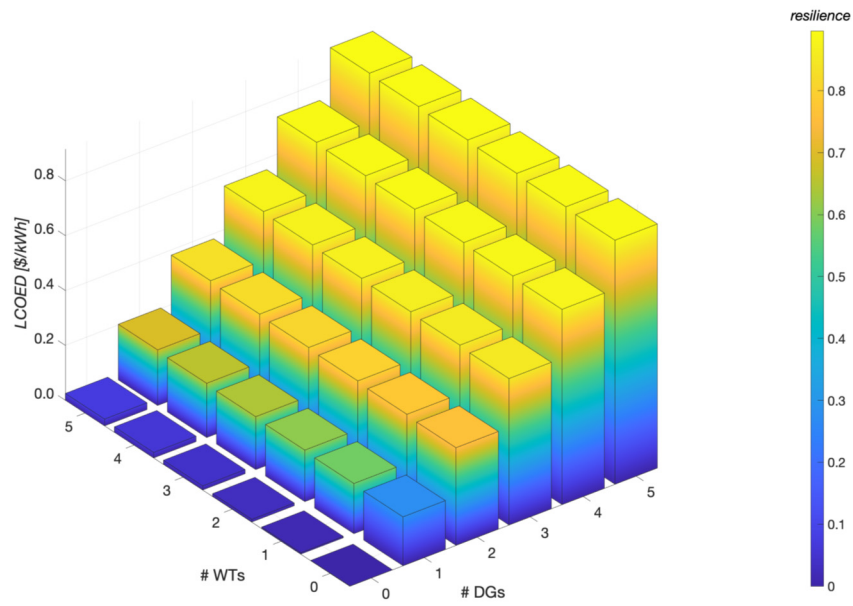


Figure 83. *LCOED* vs. # of WTs and DGs for SCI.

Figure 84 shows us that GTMO has the most increase in resilience while increasing from 2 to 3 DG. However, SNI and SCI see the biggest gain in resilience while increasing from one to two DGs.

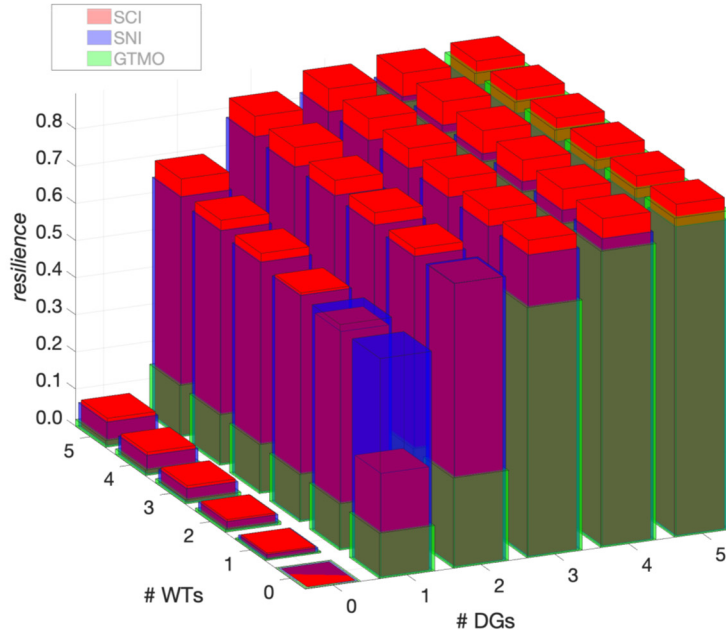


Figure 84. Resilience vs. # of WTGs and DGs for SCI, SNI, and GTMO.

Figures 85–87 highlight higher *LCOED* with yellow, and the darker and blue areas have lower *LCOED*. At SCI, 3 DG + 2 WT has a *resilience* at 96.4% of the maximum reached with 5DG + 5WT with the benefit of saving a 40% of the *LCOED* compared to the 5DG + 5WT architecture. At SNI, 3DG + 1WT exhibits a lower *LCOED* at \$1.0378/kWh (compared to \$1.7495/kWh for the 5DG+5WT architecture) while maintaining a relatively high *resilience* = 0.81 which is 97.6% of the highest *resilience* of 0.83 associated with the 5DG+5WT architecture. And at GTMO, 4DG + 1 WT has a *resilience* at 91.7% of the 5DG+5WT architecture’s *resilience* of 0.87, and at a savings of 20% of the *LCOED*.

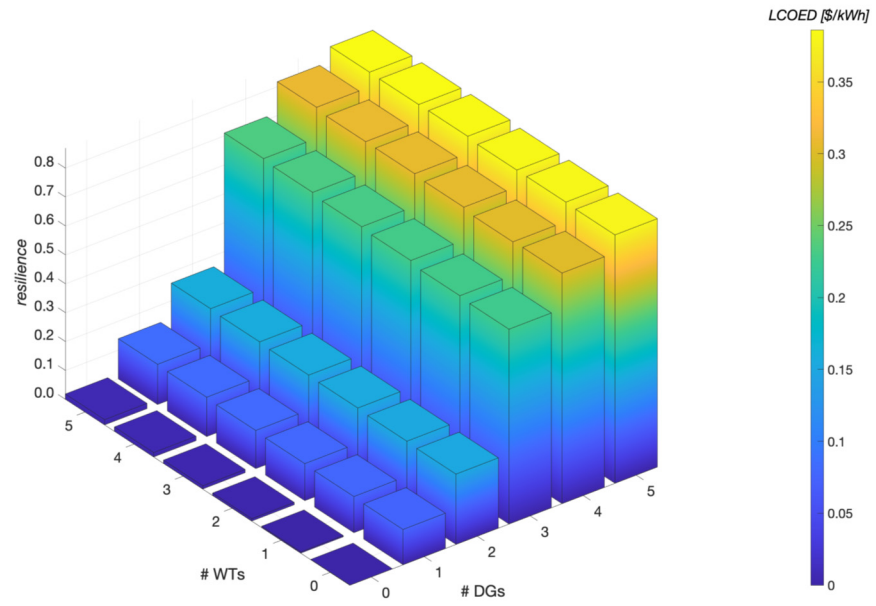


Figure 85. *Resilience vs. # of WTs and DGs for GTMO.*

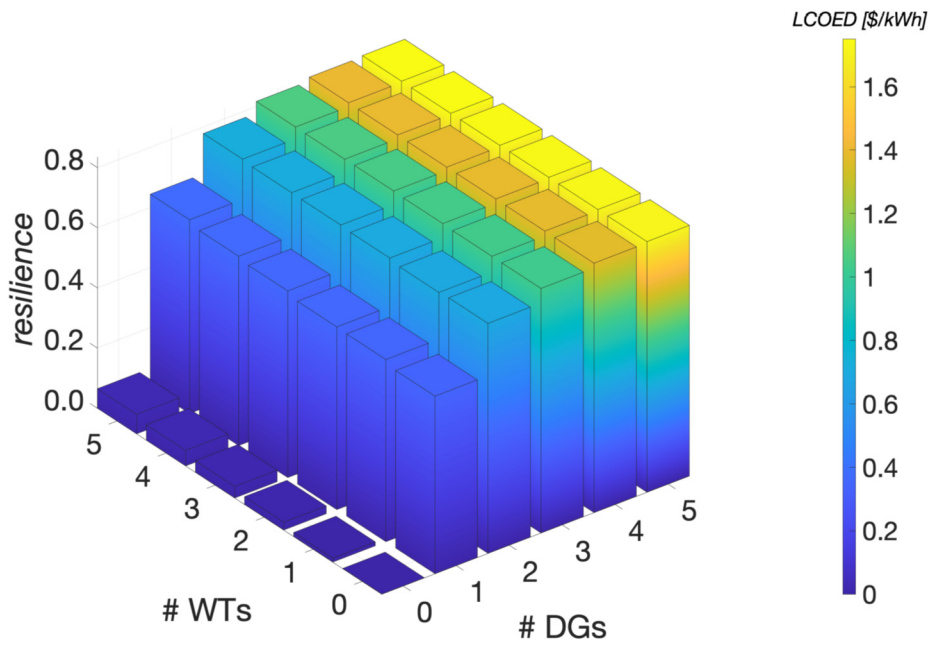


Figure 86. *Resilience vs. # of WTs and DGs for SNI.*

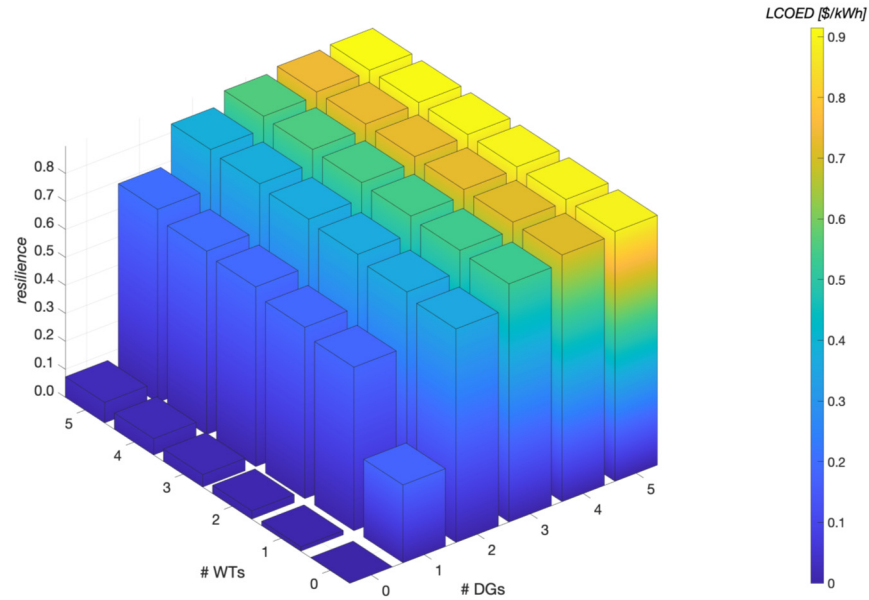


Figure 87. *Resilience vs. # of WTs and DGs for SCI.*

DG redundancy of triple (3 DGs) is best for all three INIs, without regard for the number of wind turbines. Redundancy of WT beyond double (2 WTs) is not beneficial due to very little improvement in resilience with constant increase in costs.

We may ask why all SCI and SNI see almost no benefit in employing more than 4 DGs. This can be explained by the ratio of the power rating to demand. If we calculate the microgrid’s generation at four times the demand, and then divide this by the average power rating of the one DG, at each INI, we see that SNI should have 2 DGs, and SCI 3 DGs and 2 WTs, which is mostly consistent with this finding.

C. COMPARATIVE ANALYSIS OF MODELS

This method presented is more useful to INIs than the resilience assessments reviewed in Table 5. Specifically, the cost measure *LCOED* is a unique adaptation of *LCOE* that ensures the costs measurement is pertinent to an off-grid microgrid such as an INI. None of the other resilience assessments have a suitable cost measure for an off-grid INI. This method also gives a decision maker a tool to visualize the trade-offs in resilience and costs for the combined impact of both design and maintenance choices while other models

do not create these same trade-offs. Finally, this method generates an aggregate *resilience* measure weighting *invulnerability* and *recovery* equally for the INI.

D. DISCUSSION AND CONCLUSION

The optimized microgrid at Rota, the comparative resilience and costs of the existing RE INIs, and the resilience for the RE INIs' WT and DG design options generate useful and general findings. The highlights of each these will be reviewed and discussed.

The optimized quintuple microgrid at Rota provides 30% higher resilience for 30% of the quintuple base case's costs. For the same architecture, greater redundancy provides greater resilience for the same costs. Maintenance is mostly insignificant, except for the no redundancy when a medium maintenance level is best.

SNI's time to recover is fastest because of the excess power rating present in the system at eight times more power rating than the demand compared to SCI and GTMO which both have approximately twice the power rating as the demand. GTMO has almost three times the time to recover. GTMO also benefits the most from maintenance.

Medium maintenance reduces the time to recover by almost 50% at GTMO, 40% at SCI and 20% at SNI. Medium maintenance increases costs by at 1% at GTMO, SCI and SNI.

First there is more improvement in *resilience* at SCI by adding more WTs. Second, GTMO's *resilience* is approximately half that of SCI and SNI's *resilience* for one and two DGs but approaches the same level of *resilience* with three DGs. And finally, there is significant improvement in *resilience* when increasing from one to two DGs but this improvement as DGs increase rapidly diminishes when increasing from two to five DGs.

None of the three RE INIs will benefit in more than 4 DGs and 2 WTs.

VI. CONCLUSION

The experiments and demonstration generated findings that have ensured the contribution on trade space of resilience and costs is meaningful and based upon a more systematic approach than this research found in the literature. General takeaways on the tradeoffs in resilience and costs confirm that redundancy imparts more resilience for no additional costs. When exceeding a ratio of microgrid power rating 50% greater than the demand, investments in maintenance have diminishing improvements on resilience gains. Storage should not exceed the microgrid generation power rating. Finally, maintenance is mostly insignificant, and fuel costs will have to decrease below \$1.00/gal for PV to be more cost competitive than DG.

Each of the graphs presented in this dissertation enhance the visualization of this design trade space. Armed with a 4D graph and moving through the different perspectives through a dynamic display should provide the INI's base commander with a faster, better, and more intuitive ability to target a preferred RE microgrid design for their INI.

One area this research did not consider is the corresponding increase in maintenance complexity by introducing redundancy. Although having more than one single DG improves resilience, it creates a detrimental aftereffect by adding more costs to maintain more DGs. A base commander should acknowledge this and understand that the maintenance plan will need to accommodate the compounded maintenance complexity.

Another consideration this research neglects that an INI base commander should consider before implementing a microgrid decision, is the heightened vulnerability of the microgrid to a cyberattack by virtue of implementing a networked power system. Although we consider cyberattack disturbance scenarios as it relates to the probability of damage to a DER, there are unknown cyberattack risks that are not able to be incorporated into the method and model. The expectation is that future applications of this model should reevaluate these risks and revise the model to factor the full impact of a cyberattack's damage potential.

This research also did not explore if the base commander should implement different maintenance levels for different DER. The experiments conducted in this research all maintained the maintenance level the same for each of the four DERs. The base commander should consider, for example, if there is value in reducing the maintenance level of the PV to no maintenance while maintaining the DG at a medium maintenance level.

Finally, this research did not explore other combinations of the disturbance's impact and probability. Although most unlikely, work should be done to assess the designs for high-impact high-probability disturbances.

This research has made a primary contribution to the body of knowledge by developing a useful and tailored cost (*LCOED*) and resilience (ξ) measure for renewable energy microgrids on islands. Additionally, our decision-making tool generated these two measures by subjecting RE microgrids to HILP disturbances. Finally, the resilience and costs trade analysis convey meaningful findings that shows how decisions on excess power rating, redundancy, diversification and maintenance relate to resilience and costs. It is through the analysis of this third contribution that more informed decisions can be made that will be more likely to deliver the desired combination of resilience and costs.

A. FINDINGS

Knowing and understanding which parameters have the most and least influence on the resilience measures is useful to exploring the design space. The levels of excess power rating, redundancy, amount and type of DER diversification confirm not just that more power and diversification is better, rather, there are power rating ratios with a threshold for further improvements, redundancy levels, and diversification portfolios that provide more resilience for the costs.

We learned from the sensitivity analyses that the models are much more sensitive to some input variables than most. Resilience is not very sensitive to the disturbance start time but is overly sensitive to the wind turbine's time to repair a damaged DER, due to the wind turbines having a much greater relative power contribution than the same sized solar photovoltaic panel or diesel genset. *LCOED* is most sensitive to the fuel consumption rate

and fuel costs and least sensitive to O&M costs. Finally, fuel costs will have to decrease below \$1.00/gal for PV to be more cost competitive than DG.

Although the maintenance level impacts future operations on the microgrid differently than a design decision, it is a decision made at the same time as design decisions and usually by the same decision maker. Greater maintenance levels do not provide more resilience when the generation approaches and exceeds 1.5 times the demand. Maintenance only matters as it influences resilience or costs when the power generation more closely meets the demand, the generation is all RE, and when there is no redundancy. At Rota more maintenance is worthwhile only for microgrids without redundancy. And a greater level of maintenance increases resilience only at SCI and GTMO, not at SNI.

We also observe that given a choice in investing extra funding dollars in maintenance or power rating, that maintenance provides more benefits. Specifically, a maintenance investment will improve resilience more than an increased power rating investment.

Resilience increases exponentially and costs remain unchanged as the redundancy level increases. The WT quintuple architecture costs the least to provide the highest resilience compared to the other architectures modeled.

The ratio of power to demand should not exceed four because there are no further improvements in resilience, only costs increases. Doubling the ratio of power to demand can greatly reduce time to recover but at significant costs compared to a ratio of one. Additionally, we learned that when combining PV and WT, that the PV power rating should be more than the WT to account for diurnal behavior differences in power generation.

A generalization we can make about the behavior of our two measures to increasing the power to demand ratio or redundancy is that resilience exponentially increases, and *LCOED* linearly increase for the power to demand ratio but remains the same for redundancy.

This research explored the relationships between energy storage and generation. There are no further improvements to be gained in resilience or costs by exceeding a battery power rating equal to the microgrid generation.

The optimized quintuple microgrid at Rota provides 30% higher resilience for 30% of the quintuple base case's costs and is the clear choice. The midnight tsunami findings are similar as the morning tsunami although there is a slight degradation in resilience with little change in costs. Rota can attain greater resilience for the same costs by incorporating redundancy.

Finally, this research assessed resilience at three of the RE INIs to identify meaningful findings. Resilience increases at SCI by adding more WTs. Also, SNI sees little improvement with more than three DGs. SCI and SNI has significant improvement in resilience when increasing from one to two DGs but this improvement as DGs increase rapidly diminishes when increasing from two to five DGs. Only at GTMO is there significant improvement from two to three DGs. The RE INIs should not install more than 4 DGs and 2 WTs. However, applying this method at CLDJ, DGAR and AUTEK should generate more accurate and specific recommendations for the all INIs and islanded location.

B. RECOMMENDATIONS

Base commanders at INIs should sagaciously invest in design and maintenance of microgrids to maximize resilience and minimize costs. This research's contributions and findings improve a base commander's ability to decide how best to invest in resilience.

1. Designing a Microgrid

Systems engineers should design microgrids with as much redundancy as practical while recognizing the diminishing returns on resilience for the same investment. The microgrid's power rating to demand ratio should not exceed four. Microgrids should diversify DG generation, giving preference to WT over PV. Energy storage should not exceed the microgrid's power generation rating. Rota should install the optimized

quintuple microgrid. Any of the three RE INIs should install no more than 4 DGs and 2 WTs.

2. Maintaining a Microgrid

Investments in maintenance should not exceed a low level, and it is best to reduce maintenance as excess power generation increases beyond 50% of the demand. If the generation is all RE, then maintenance matters more than microgrids that incorporate DG power.

SNI should not increase their current maintenance level, and SCI and GTMO should implement a higher, or medium maintenance level. Rota should only implement maintenance at a medium maintenance level for the existing base case microgrid.

3. Limitations

The cost and resilience model's method is useful in establishing a resilience and costs baseline for installed microgrids. We evaluate and compare the alternative design and maintenance choices to the baseline installed microgrid using the resilience and cost measures of each. However, there are still practical limitations.

There is no hourly time-series data for all INIs. This limited the analysis to only SCI, SNI, and GTMO. Additionally, there is not an exhaustive list of costs for an INI.

All resilience dimensions were not considered. Specifically, adaptability.

We also did not have sufficient data to portray the expected erratic behavior of the demand. INIs' due to their operational military missions have unique and erratic requirements for meeting the demand due to supporting the mission.

Additionally, the model is limited by not considering common cause failures. Although low probability, these common cause failures can be high impact. If every solar PV has a technical fault that is exposed during lightning storms, that is high impact and should be considered further.

Another limitation is the model calculates the *MTTR* for each DER type but not individual DER components. All the wind turbines will have the same *MTTR*. This prevents

us from generating a different *MTTR* for each of the wind turbines, each of the PV, DG, or BAT.

There is no consideration for the availability of spare parts and repair equipment needed to repair a damaged DER. It is quite possible that a damaged wind turbine will require a crane that will have to be shipped to the INI.

These limitations can each affect the conclusions drawn by reducing the accuracy of the results when running either an insufficient number of simulations to verify the performance trends or an exiguous number of iterations for each simulation. Although distinctions could be drawn between architectures, the experiments were not sufficient to make strong claims of findings specific to one technology, DER. We also exclude the minute-to-minute variations in RE generation that could be more accurately modeled using more granular time-steps. In general, the conclusions are still valid regardless of these limitations when making resilience and cost comparisons between redundancy levels created from the same architecture.

4. Future Work

There is both opportunity and a need to continue this research in greater depth and for more remote off-grid island microgrids. Further improvements in the method, models, and analytics should benefit decision makers.

We can improve our assumptions. Assuming that the microgrid's demand following a disturbance will mimic its historical demand oversimplifies reality. In fact, we would expect a reduced demand that we should be using to assess resilience. Additionally, we should incorporate the erratic behavior of an INI's demand.

Similarly, we seek full recovery to the pre-disturbance performance level assuming that is a desired end state. Rather, recovery is not needed at this level and should be attained when the microgrid's performance has reached a level to meet the reduced demand. Finally, we should not assume that the microgrid's demand will not drop below the microgrid's post-disturbance power rating.

We also make an assumption in our cost model that should be improved. In valuing energy storage, we are placing greater value on a kilowatt-hour used today than in the future. This is an unreasonable and inappropriate assumption for an INI.

Disturbances and their damage can be made more realistic. The expected damage could incorporate the independent probability of the disturbance with the independent probability of damage. Additionally, we can introduce stochastic behavior to better handle the complexity of common cause failures. Damage can be reassessed at each time step as opposed to an instantaneous point-in-time by extending the disturbance over time. And finally, we can introduce variability in the intensity of the disturbance at each time step.

The total costs for an INI can be more comprehensive. When evaluating the price of DG fuel for PV to be competitive with DG, the fuel costs should also include the shipping costs to the INI. Also, we should more carefully research the added costs to maintain the DGs by virtue of being on an INI to more accurately be accounted within the cost measure. We should also not assume that the DER cost of maintenance increases linearly as we increase redundancy. Rather, we should increase the maintenance costs as we increase redundancy. Finally, it will be beneficial to include all environmental costs, from manufacturing to disposal, that are a byproduct of the DER.

Further work can be done to more clearly articulate how threat dependent resilience is. The design differences that provide the most resilience for the most threats should be highlighted by greater analysis of resilience assessments for different threats.

Practical applications could investigate how protection relays may impact the degradation portion of the problem. The remaining INIs that include DGAR, CLDJ and AUTEK should conduct resilience assessments to compare to the RE INIs at SNI, SCI and GTMO. Finally, McMurdo, Antarctica should use these models to assess their resilience and costs.

We can research improvements that would make DERs less vulnerable. The cost and resilience improvement in increasing a DER's *invulnerability* should generate meaningful and useful findings when varying the $P(d|S_k)$.

Obvious extensions of this research involve data analytics to generate more meaningful findings. Recommendations for a design option will be possible simply by matching an architecture's resilience function shape to a shape from previously assessed architectures. We can determine through mathematical analysis of the shapes if there is a common relationship at the shared points of intersection that contributes to the particular combination of resilience and costs. There is much more we can be done to identify relationships between the experimental results through more complex graphing tools.

More granular time series data will improve the accuracy of the results. Increasing the number of 4D surface plots' datapoints as well as increasing the number of architectures will enable more extensive comparisons between the measures and the design and maintenance choices.

Common cause failures is an obvious avenue for research. Much further can be done to study how decisions on microgrid architectures relate to common cause failures and the resultant impact on resilience and costs.

The models can incorporate multi-objective optimization to more accurately identify the optimal solutions by maximizing resilience and minimizing costs. The optimization model's architecture can be directly input into the resilience model.

Finally, we can more completely investigate the financial aspects of resilience. Specifically, researchers can do more extensive and comparative analysis of the findings in the comparison of optimal points. Financial tools that more completely value the future energy that has been stored, as well as the unintended complexity costs that are introduced with redundancy, should provide more accurate recommendations.

THIS PAGE INTENTIONALLY LEFT BLANK

APPENDIX A. RESILIENCE MEASURES VS. COSTS FIGURES

These 2D figures provide more granular detail to the previous figures. The *LCOED* vs. *recovery*, *LCOED* vs. *invulnerability*, and *LCOED* vs. *invulnerability* each contribute to the resilience figures. These 2D figures also contribute to the corresponding 4D graphs that compare and contrast the behavior of the different microgrid architectures. In all figures, the maintenance levels are annotated next to datapoints that are not grouped together for the same architecture.

A. EXCESS POWER GENERATION RATING

The 2D Figures 88–105 augment the power rating experiments previously presented.

1. Ratio of Microgrid Nominal Power Generation Rating to Demand, and Maintenance Level with Constant DER Nominal Power Rating Impact on Resilience and Costs

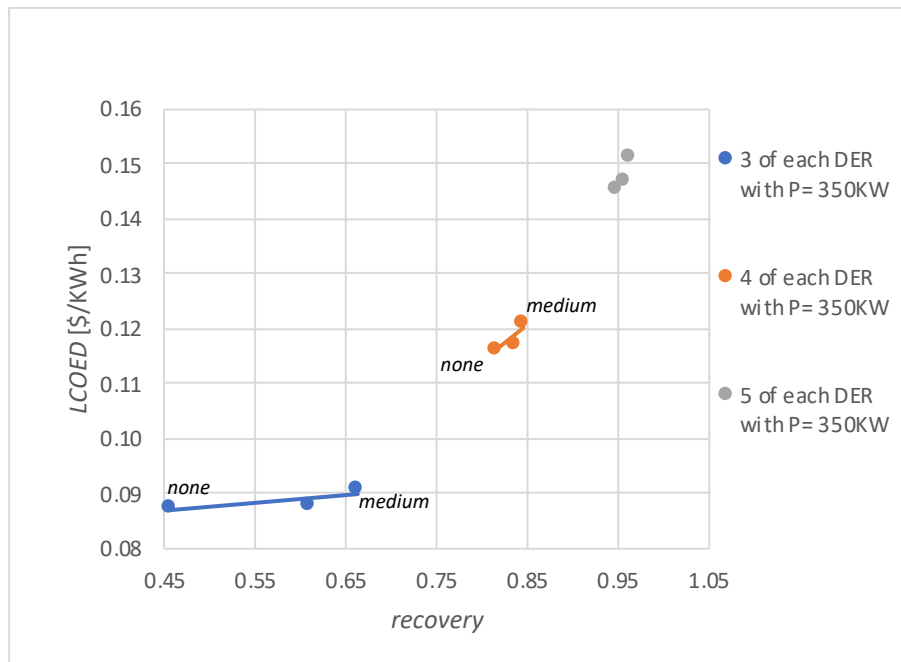


Figure 88. The effects of maintenance level on *LCOED* and *recovery*.

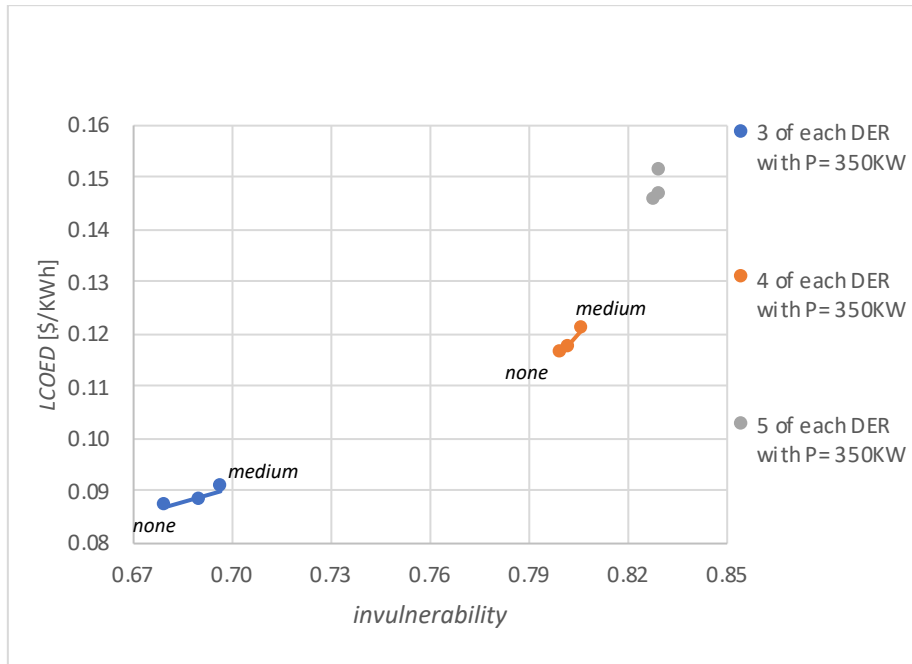


Figure 89. The effects of maintenance level on *LCOED* and *invulnerability*.

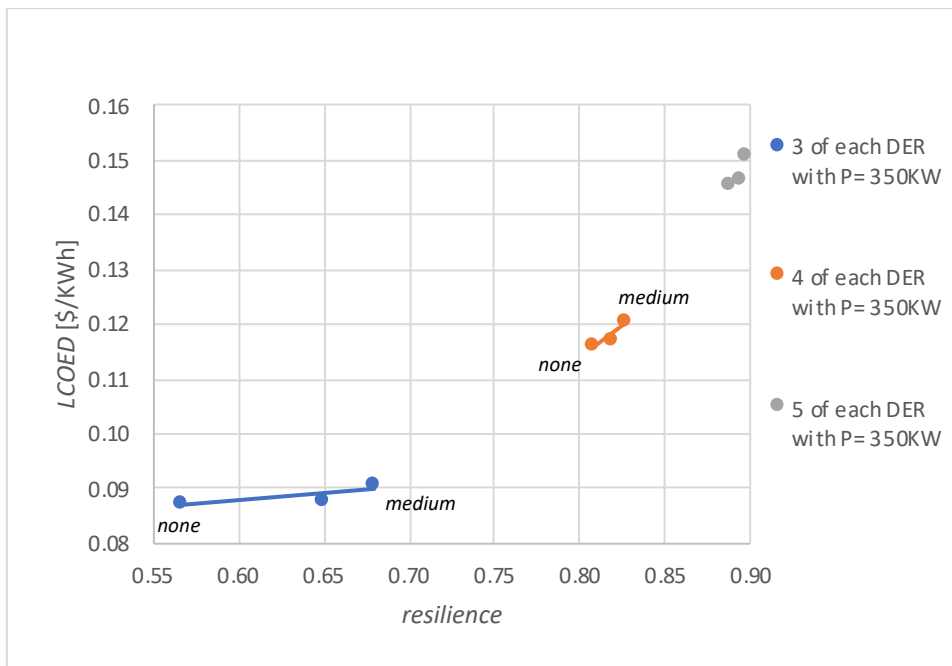


Figure 90. The effects of maintenance level on *LCOED* and *resilience*.

2. **Ratio of Microgrid Nominal Power Generation Rating to Demand with Constant Number of DER, and Maintenance Level Impact on Resilience and Costs**

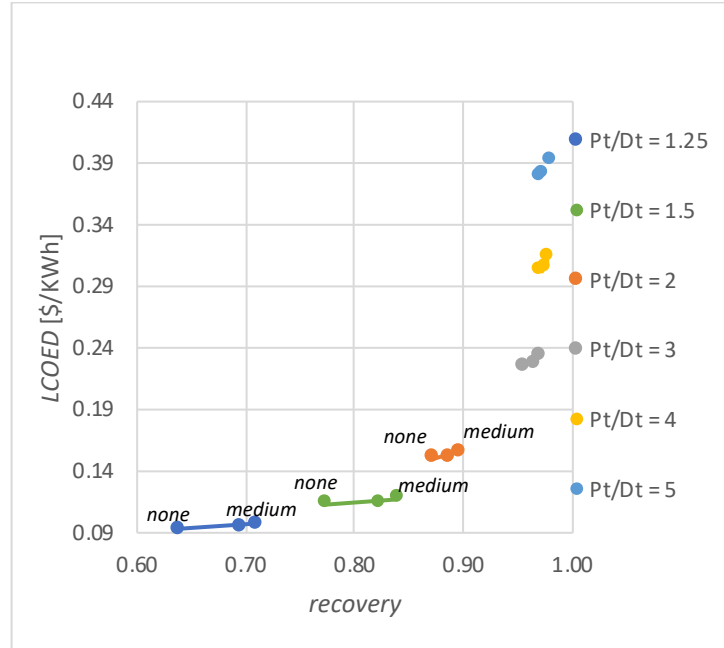


Figure 91. The effects of microgrid power rating to demand ratio on *LCOED* and *recovery*.

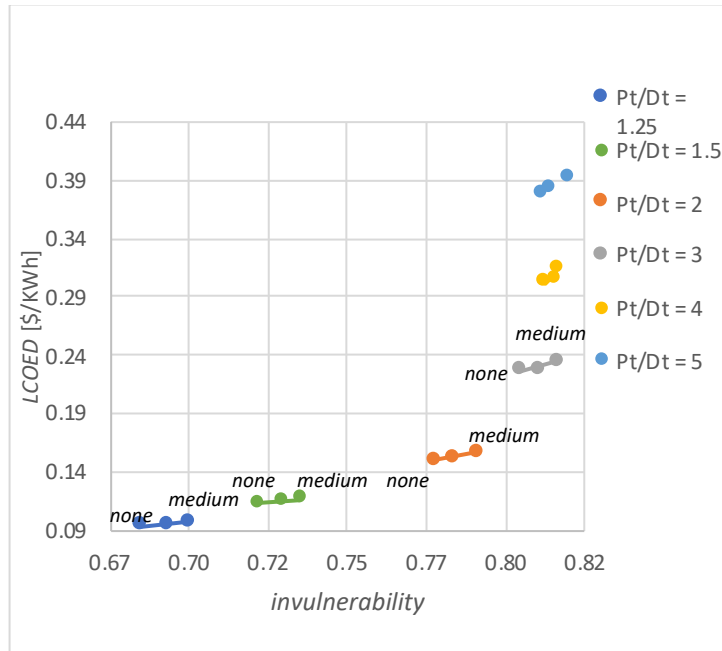


Figure 92. The effects of microgrid power rating to demand ratio on *LCOED* and *invulnerability*.

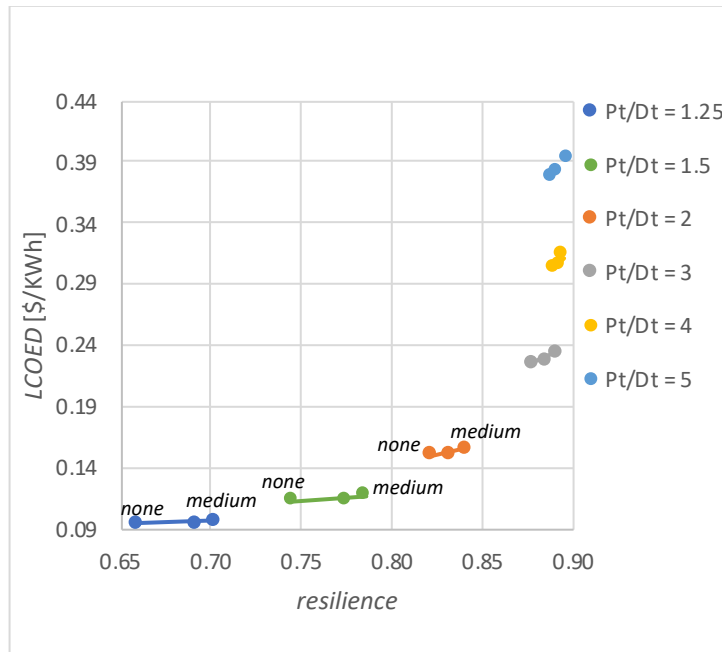


Figure 93. The effects of microgrid power rating to demand ratio on *LCOED* and *resilience*.

3. **Ratio of Nominal RE Power to Nominal DG Power and Maintenance Level with Constant DER Nominal Power Rating Impact on Resilience and Costs**

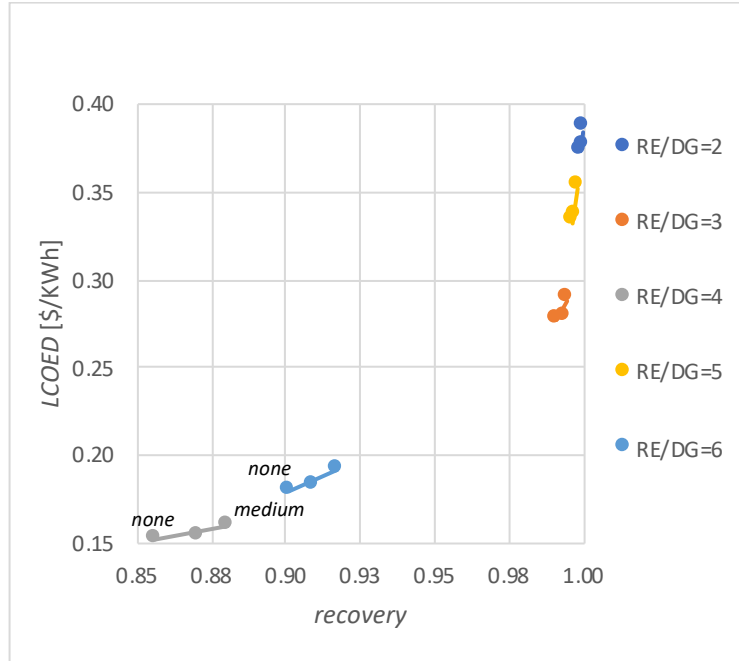


Figure 94. The effects of maintenance level and RE proportion on *LCOED* and *recovery*.

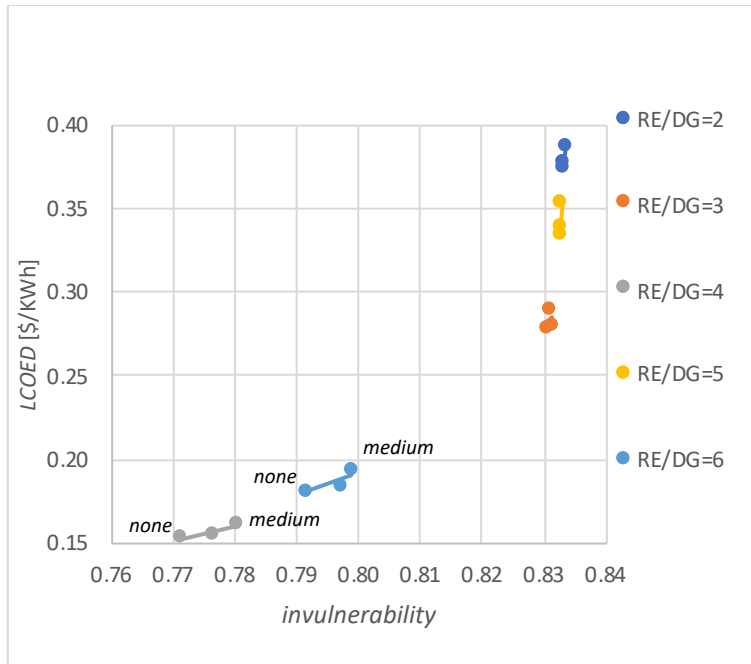


Figure 95. The effects of maintenance level and RE proportion on *LCOED* and *invulnerability*.

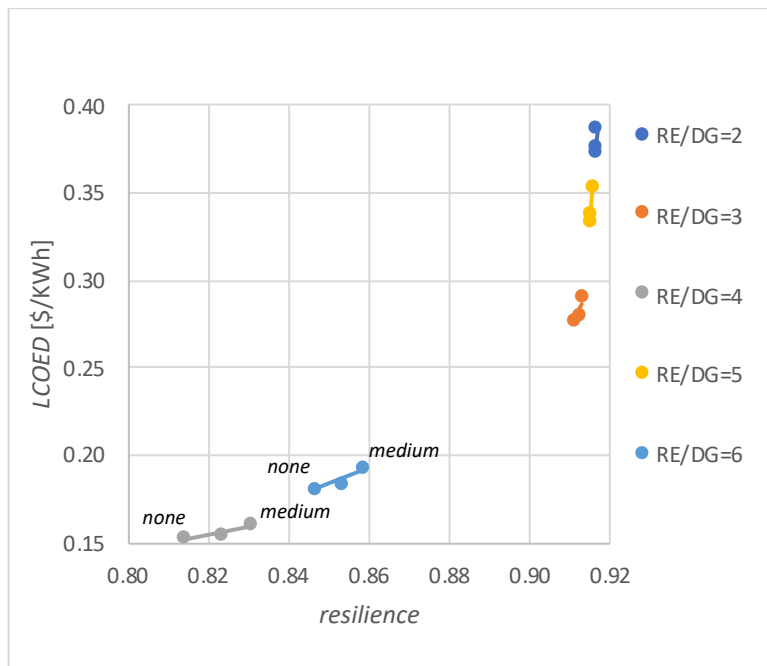


Figure 96. The effects of maintenance level and RE proportion on *LCOED* and *resilience*.

4. **Ratio of Nominal RE Power to Nominal DG Power and Maintenance Level with Constant Microgrid Nominal Power Generation Impact on Resilience and Costs**

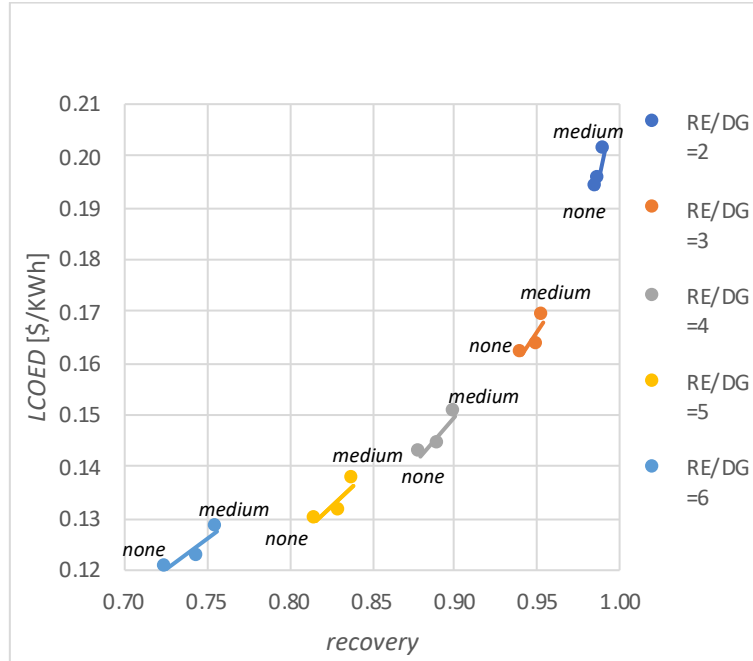


Figure 97. The effects of maintenance level and RE proportion on *LCOED* and *recovery*.

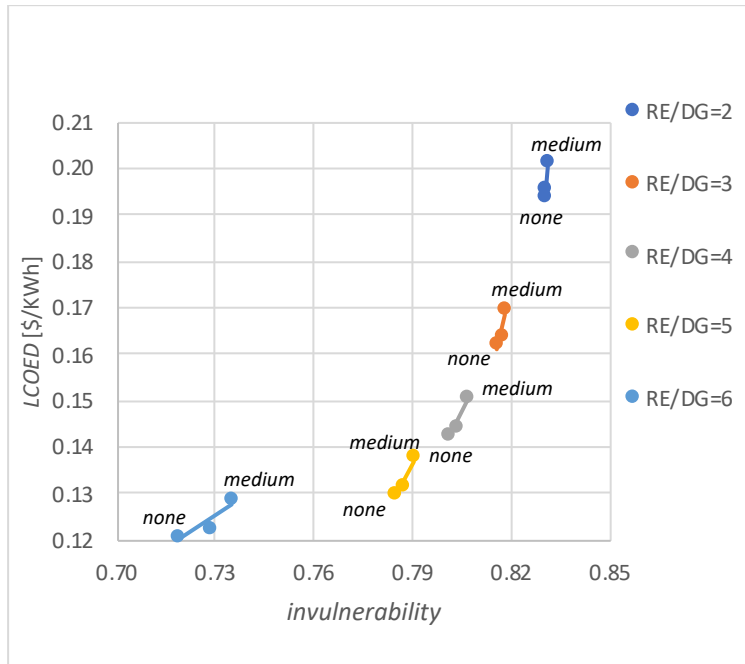


Figure 98. The effects of maintenance level and RE proportion on *LCOED* and *invulnerability*.

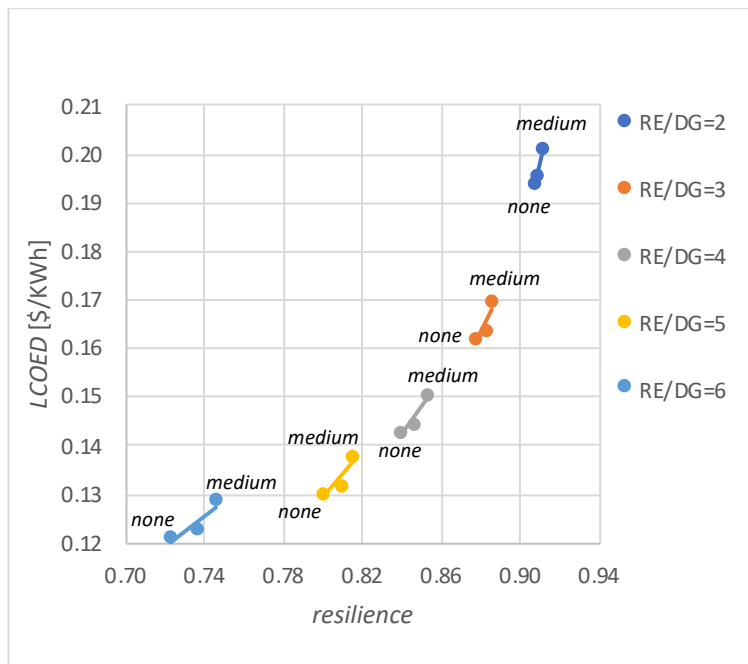


Figure 99. The effects of maintenance level and RE proportion on *LCOED* and *resilience*.

5. **Ratio of WT Power to DG Power, and Maintenance Level with Constant Microgrid Power Generation Rating Impact on Resilience and Costs**

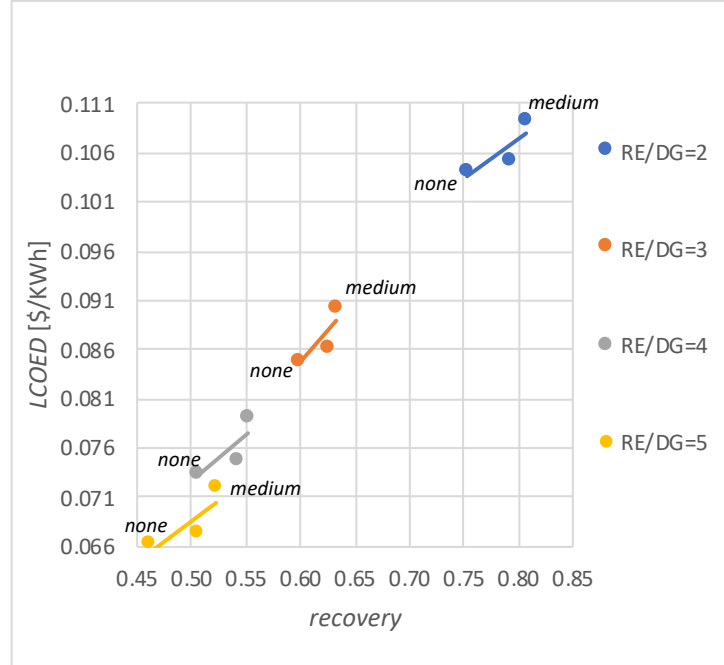


Figure 100. The effects of maintenance level and WT proportion on *LCOED* and *recovery*.

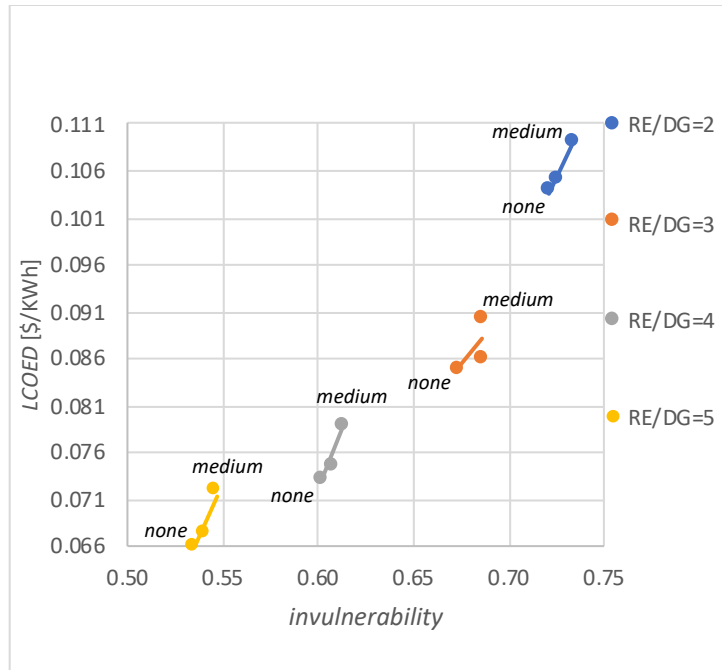


Figure 101. The effects of maintenance level and WT proportion on *LCOED* and *invulnerability*.

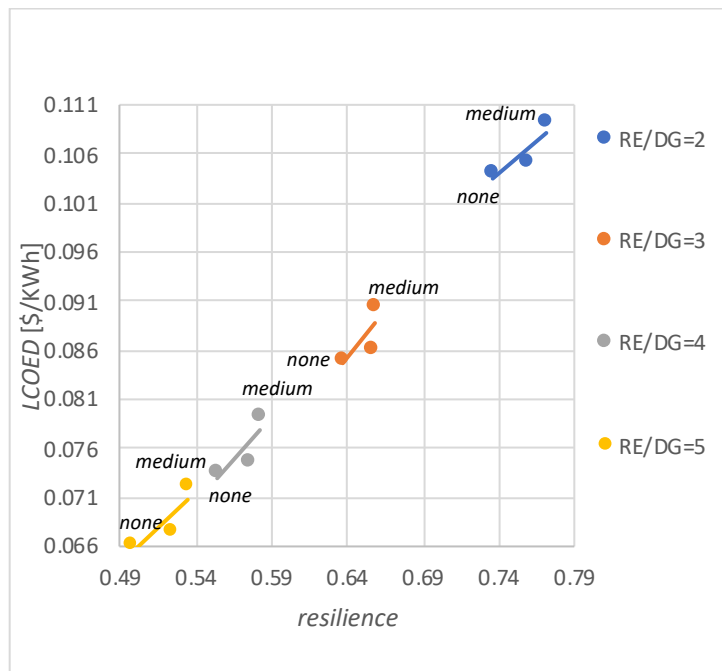


Figure 102. The effects of maintenance level and WT proportion on *LCOED* and *resilience*

6. Ratio of BAT Power Rating to Microgrid Power Rating, and Maintenance Level Impact on Resilience and Costs

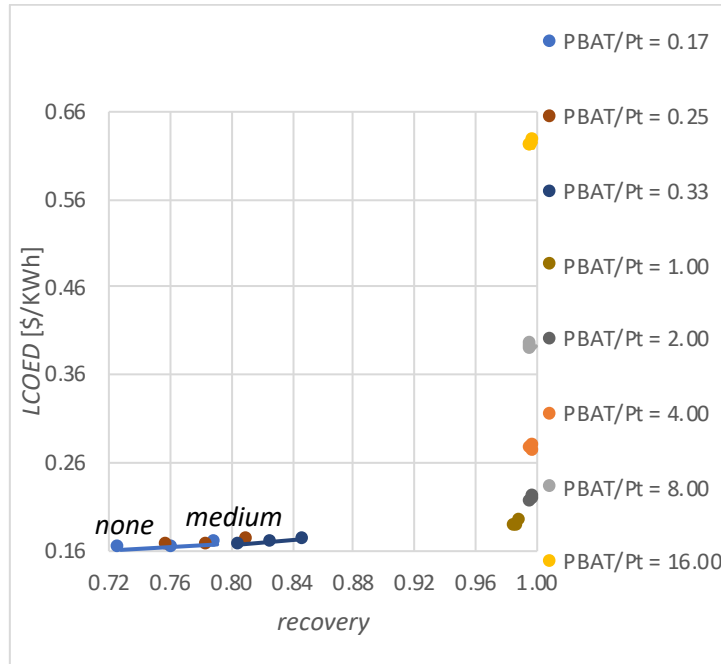


Figure 103. The effects of storage on *LCOED* and *recovery*.

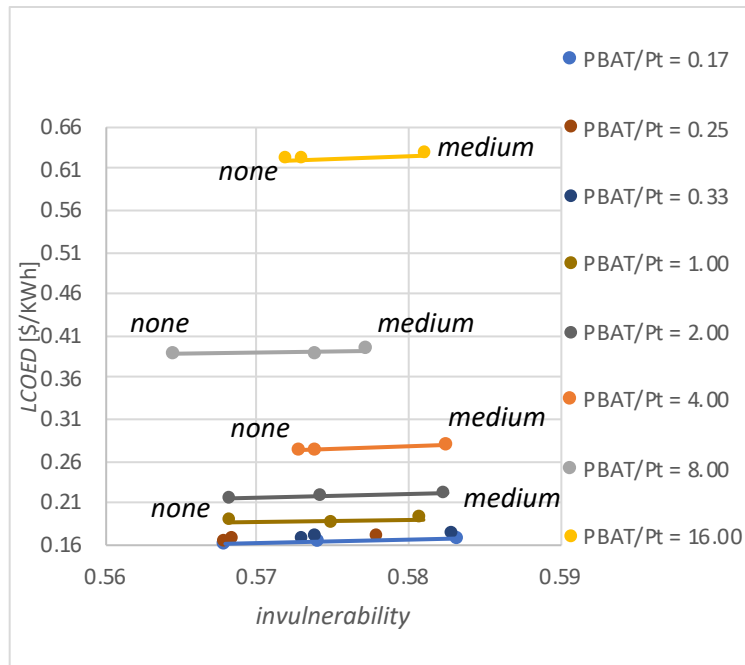


Figure 104. The effects of storage on *LCOED* and *invulnerability*.

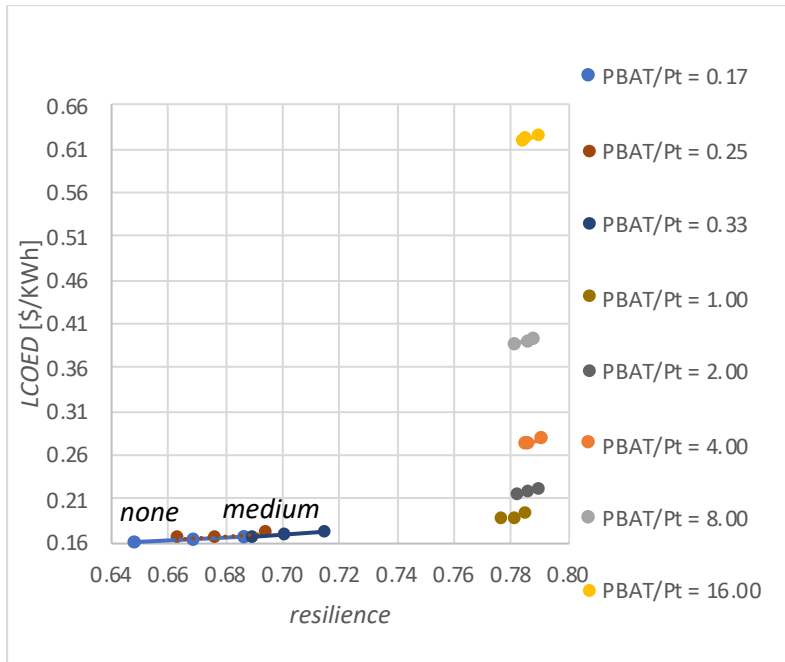


Figure 105. The effects of storage on *LCOED* and *resilience*.

B. ALTERING REDUNDANCY LEVELS

The 2D Figures 106–114 augment the redundancy experiments previously presented.

1. Redundancy and Maintenance Levels Impact on Resilience and Costs

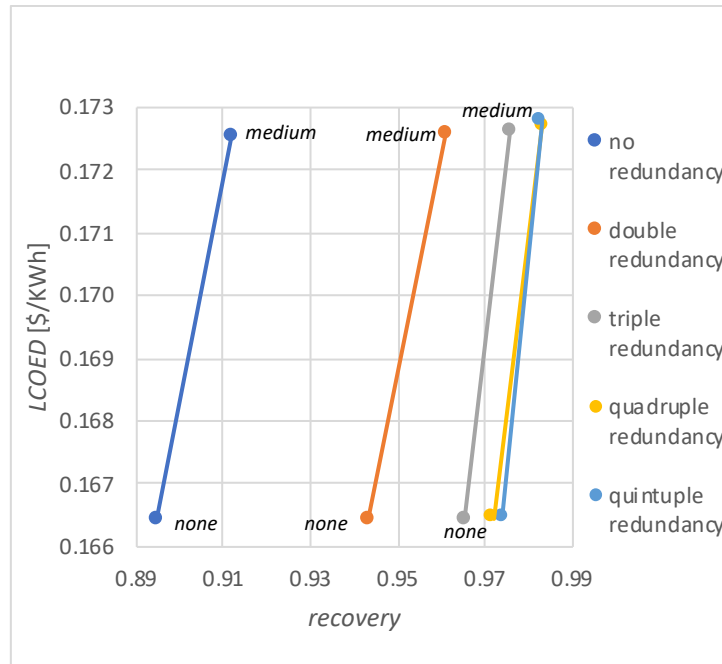


Figure 106. The effects of maintenance level and redundancy on *LCOED* and *recovery*.

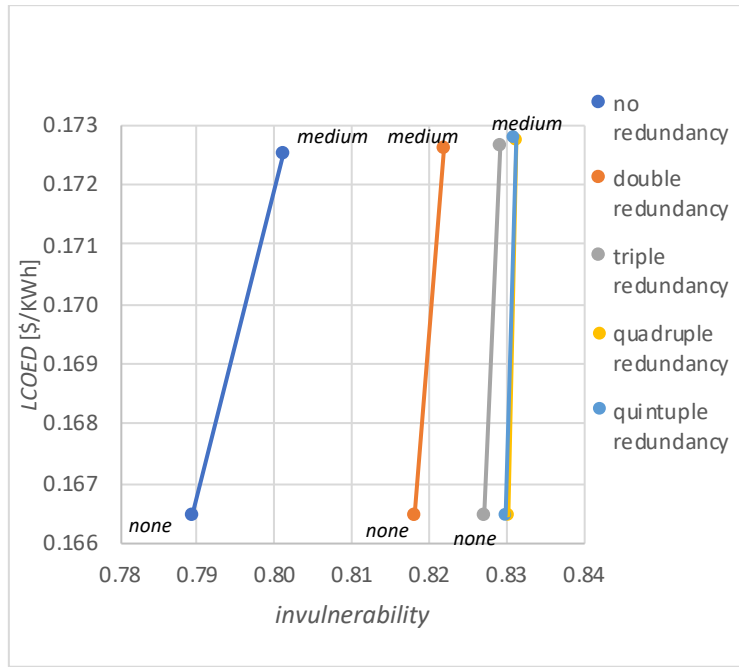


Figure 107. The effects of maintenance level and redundancy on *LCOE* and *invulnerability*.

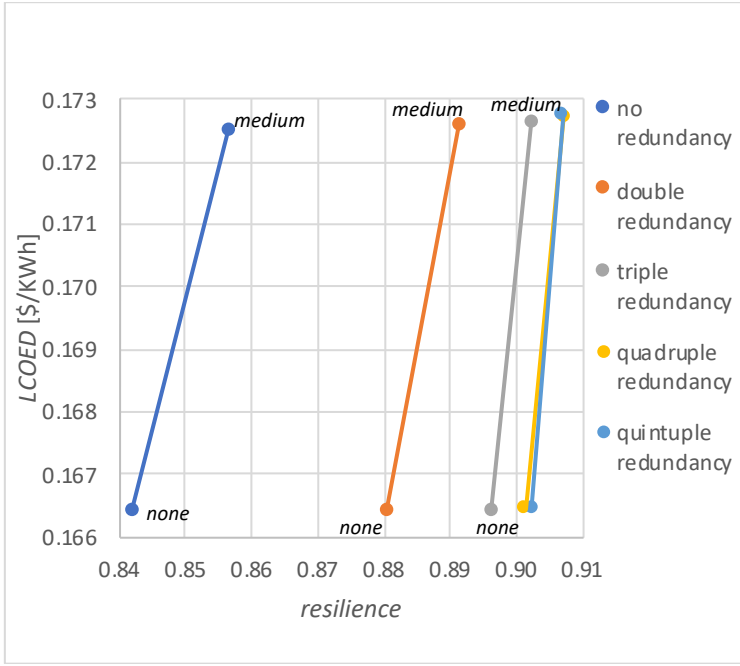


Figure 108. The effects of maintenance level and redundancy on *LCOE* and *resilience*.

2. Functional Redundancy and Maintenance Levels Impact on Resilience and Costs

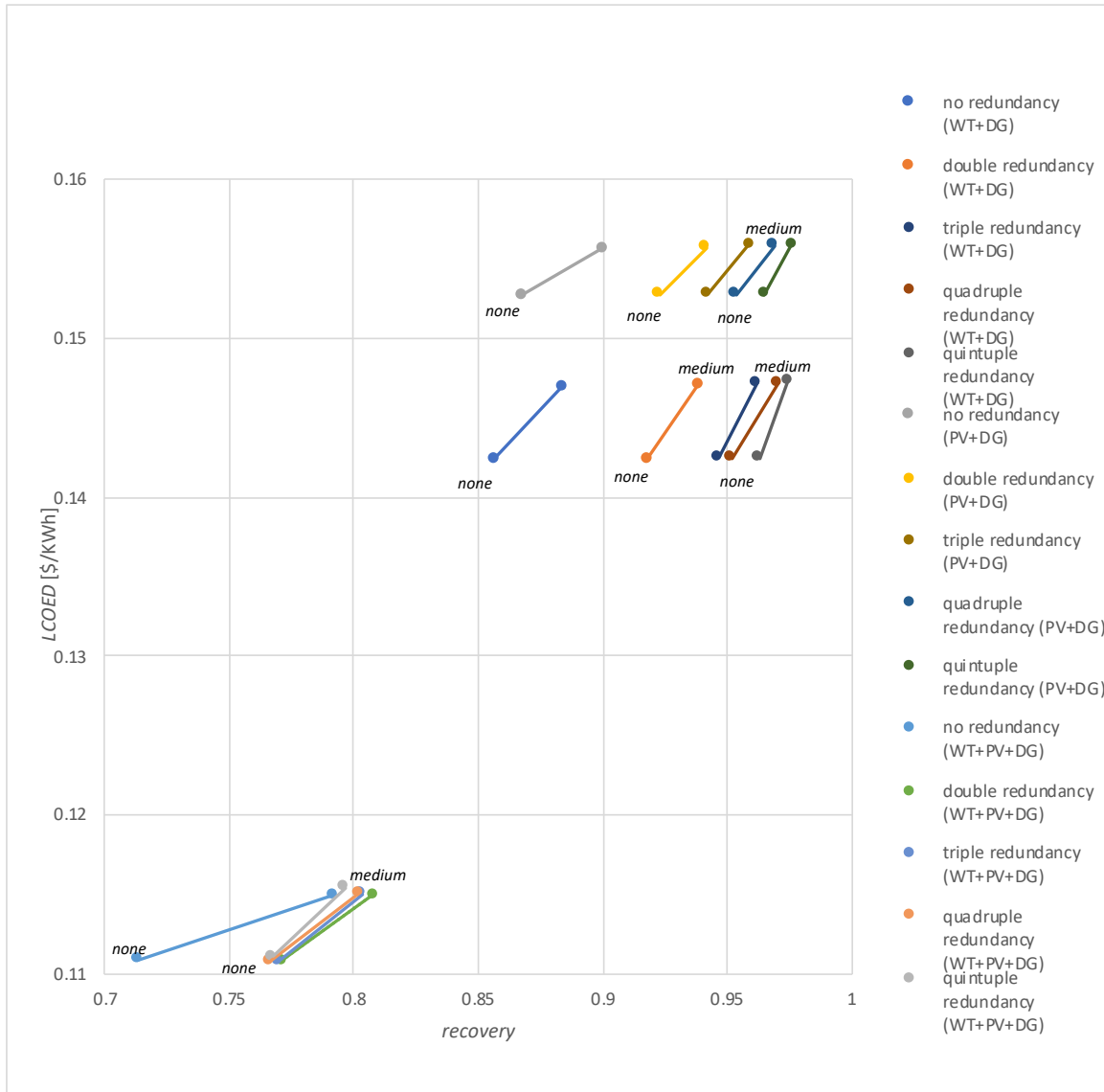


Figure 109. The effects of functional redundancy on *LCOED* and *recovery*.

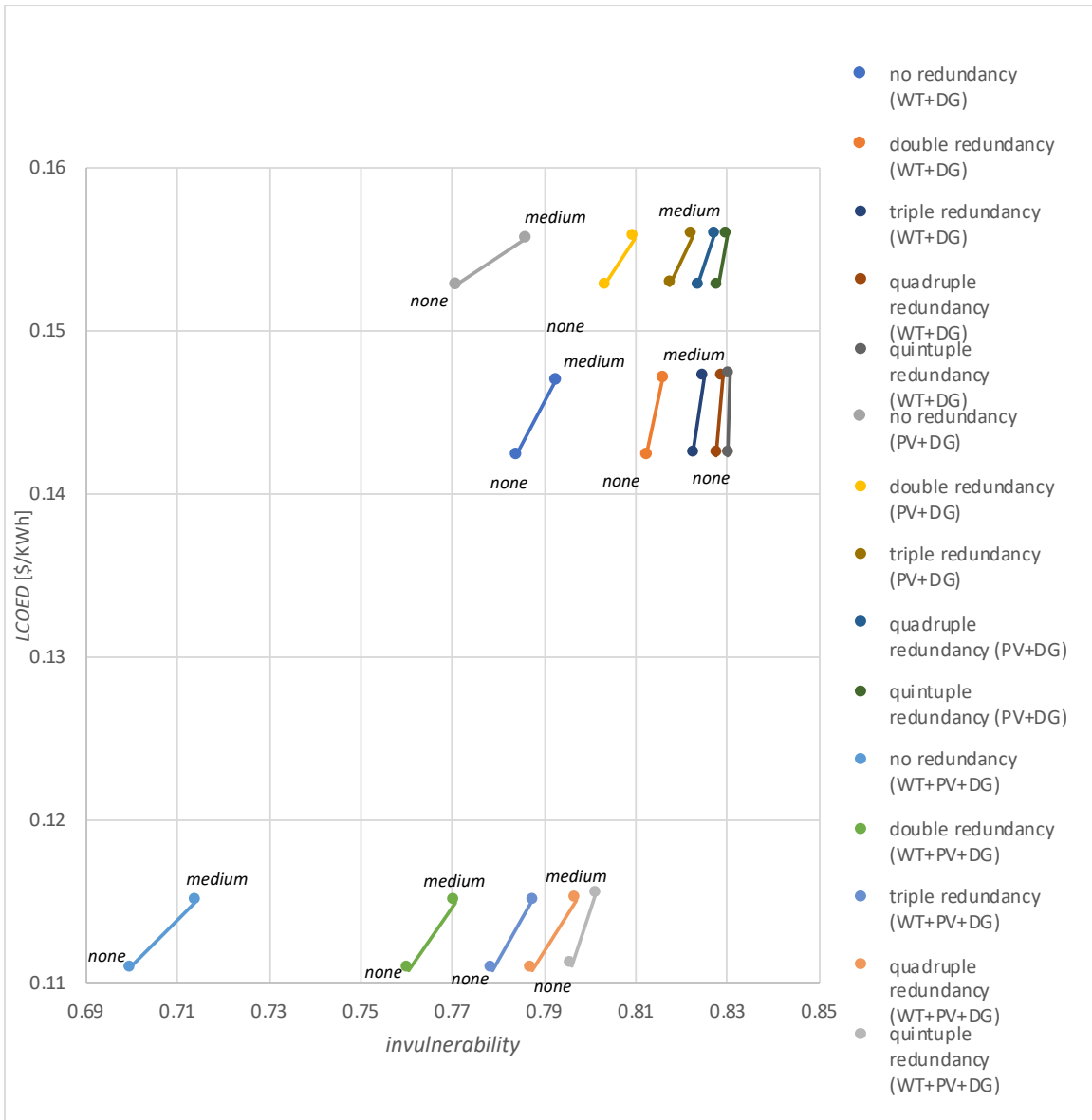


Figure 110. The effects of functional redundancy on *LCOED* and *invulnerability*.

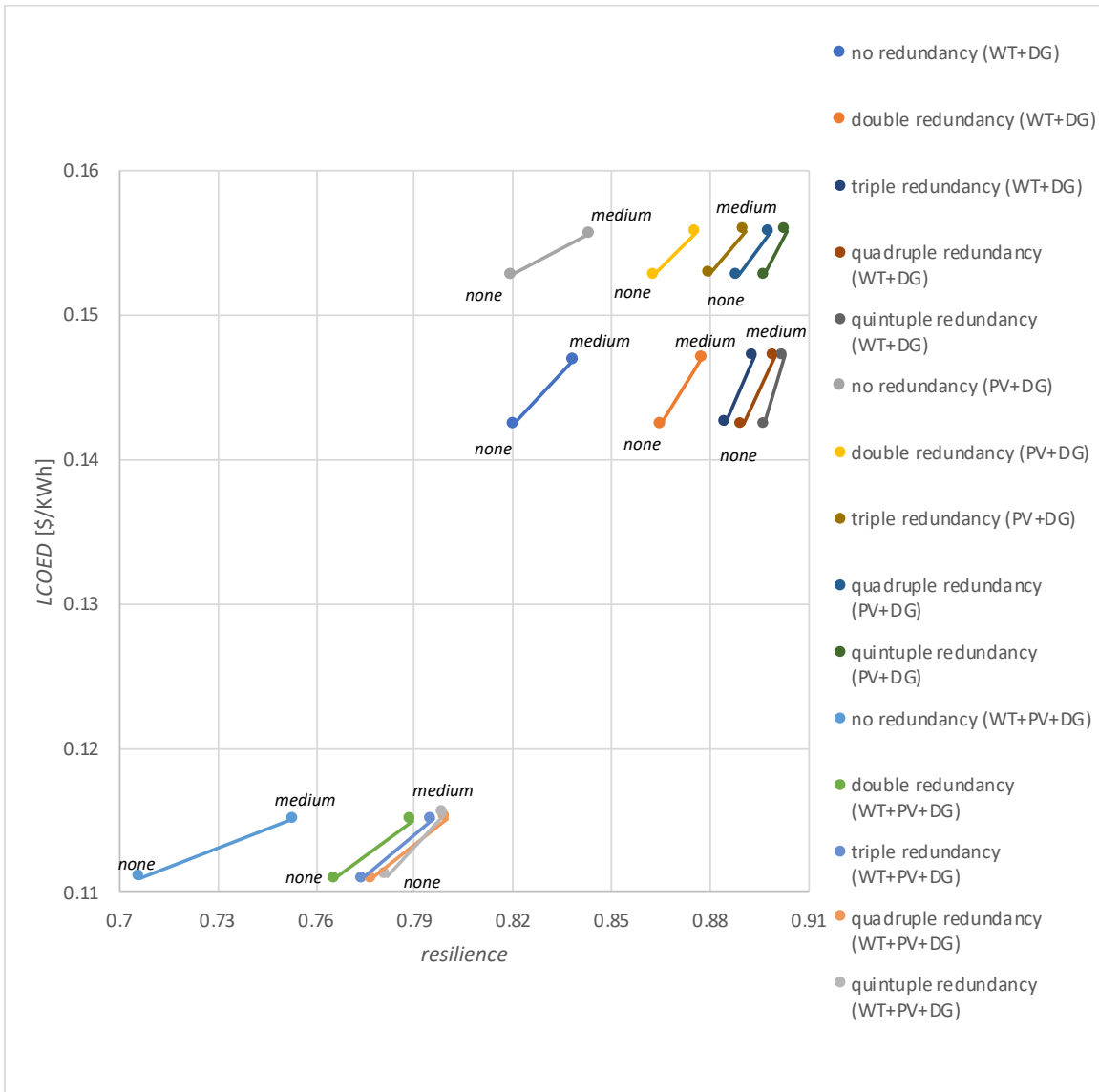


Figure 111. The effects of functional redundancy on *LCOED* and *resilience*.

3. RE Redundancy and Maintenance Levels Impact on Resilience and Costs

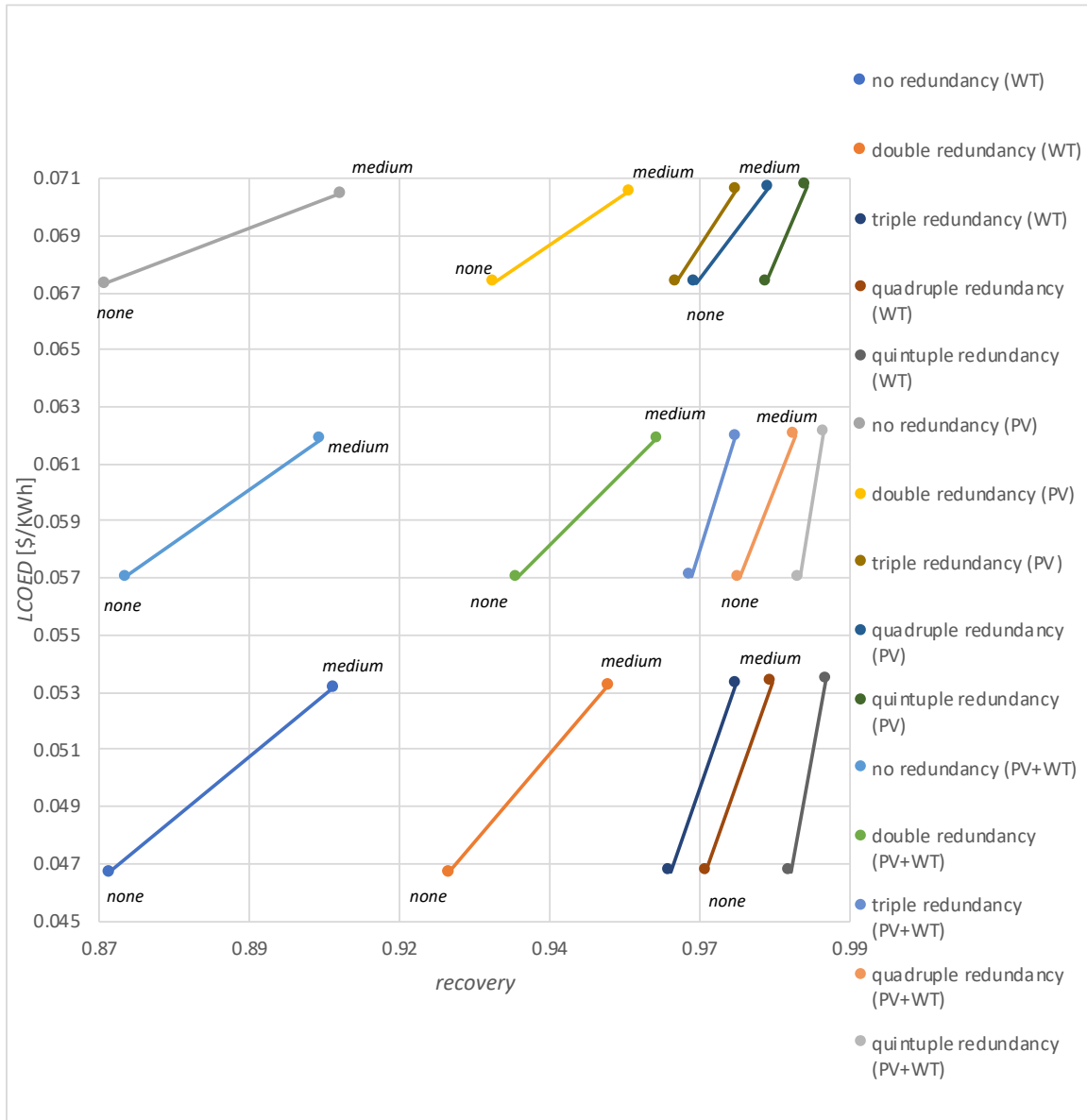


Figure 112. The effects of PV and WT redundancy on *LCOED* and *recovery*.

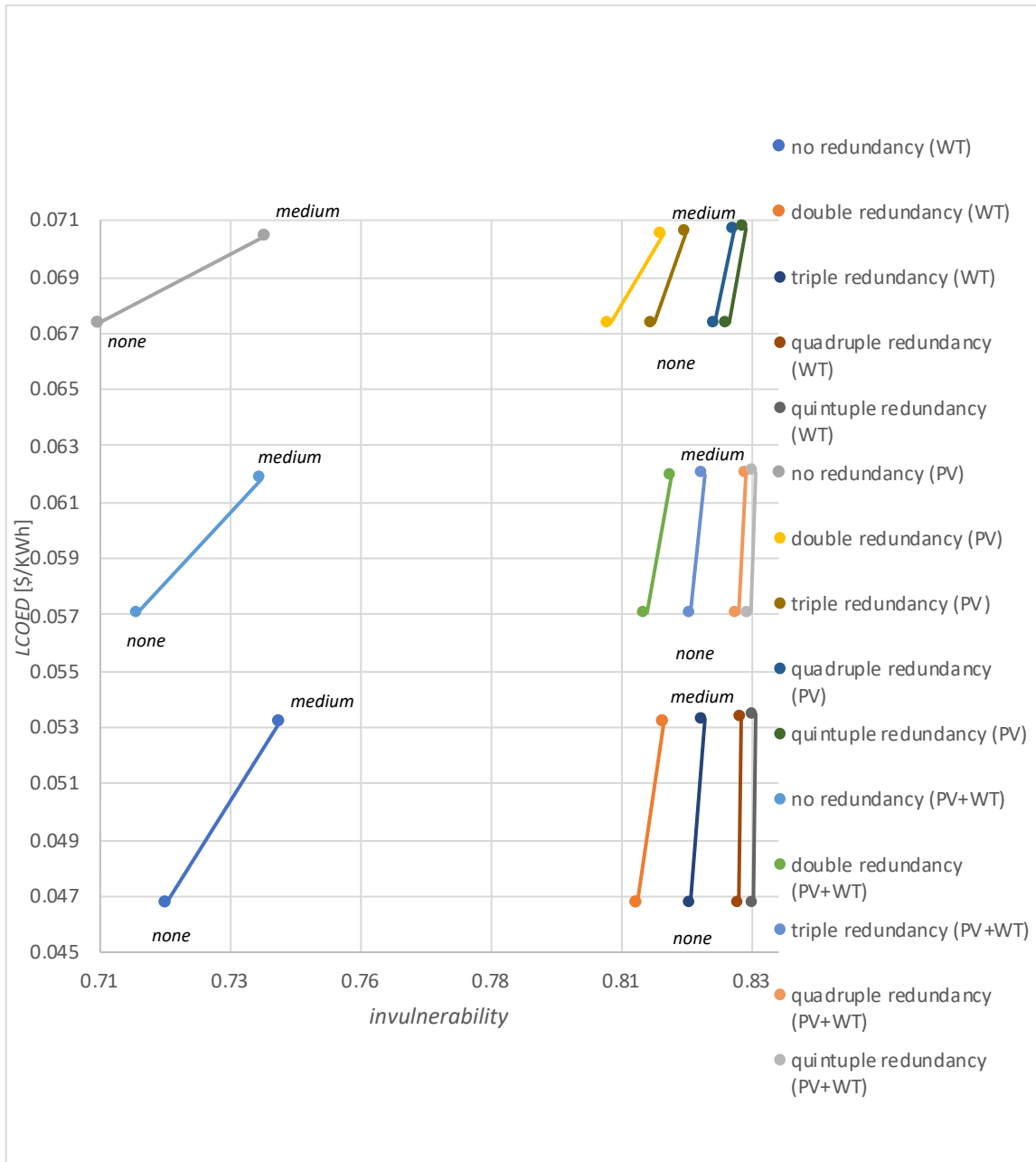


Figure 113. The effects of PV and WT redundancy on *LCOED* and *invulnerability*.

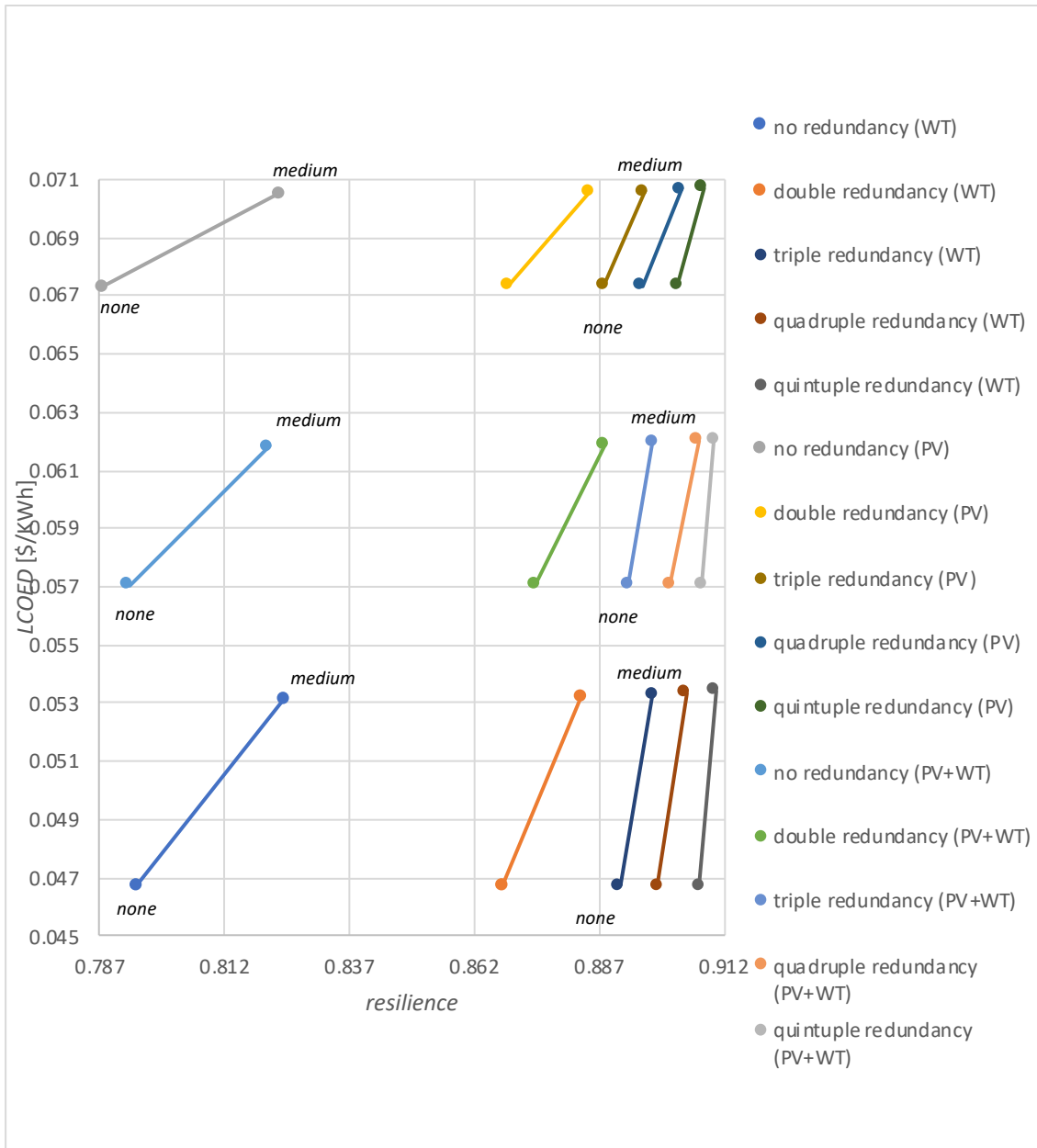


Figure 114. The effects of PV and WT redundancy on *LCOED* and *resilience*.

C. ALTERING REDUNDANCY LEVELS AT ROTA

The 2D Figures 115—123 augment the redundancy experiments at Rota previously presented.

1. **Base Case Impact of Redundancy, and Maintenance on Resilience and Costs**

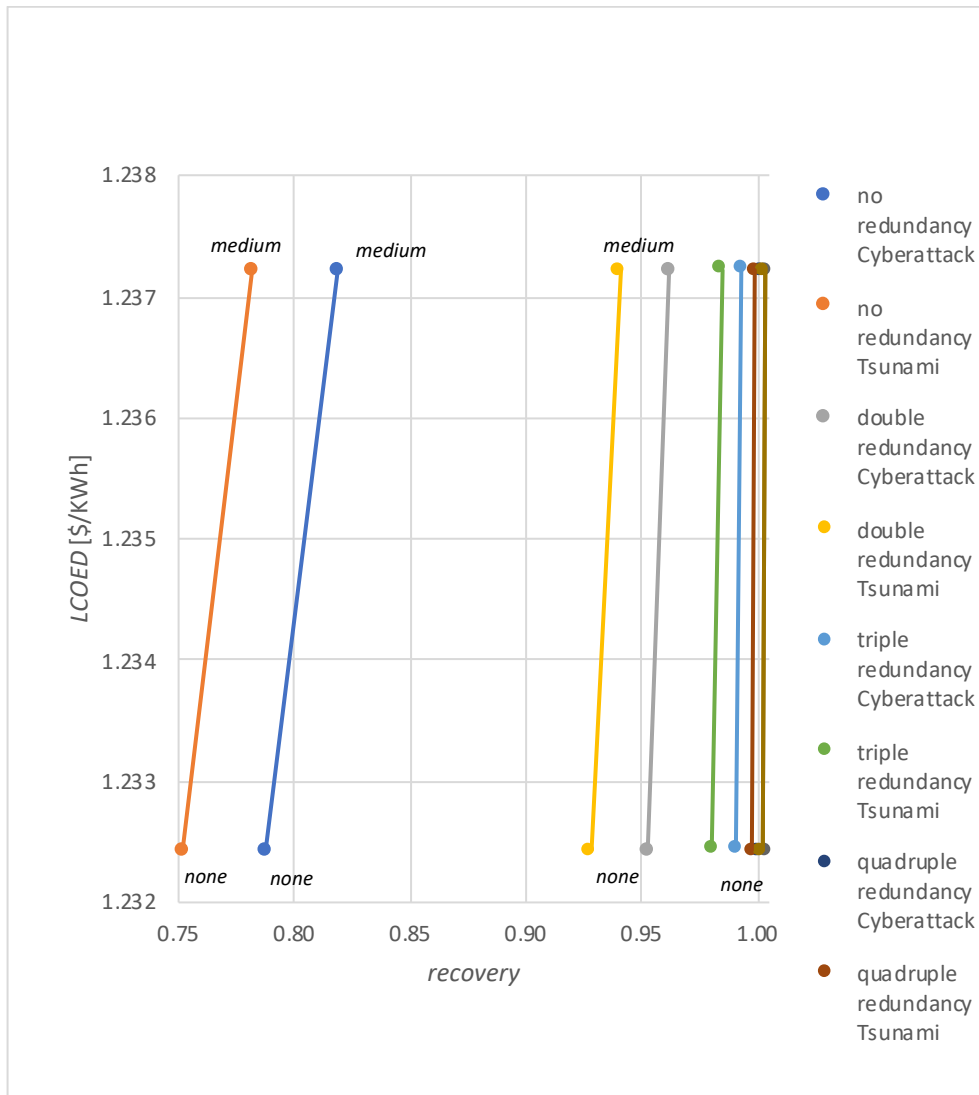


Figure 115. The effects of redundancy level on *LCOED* and *recovery*.

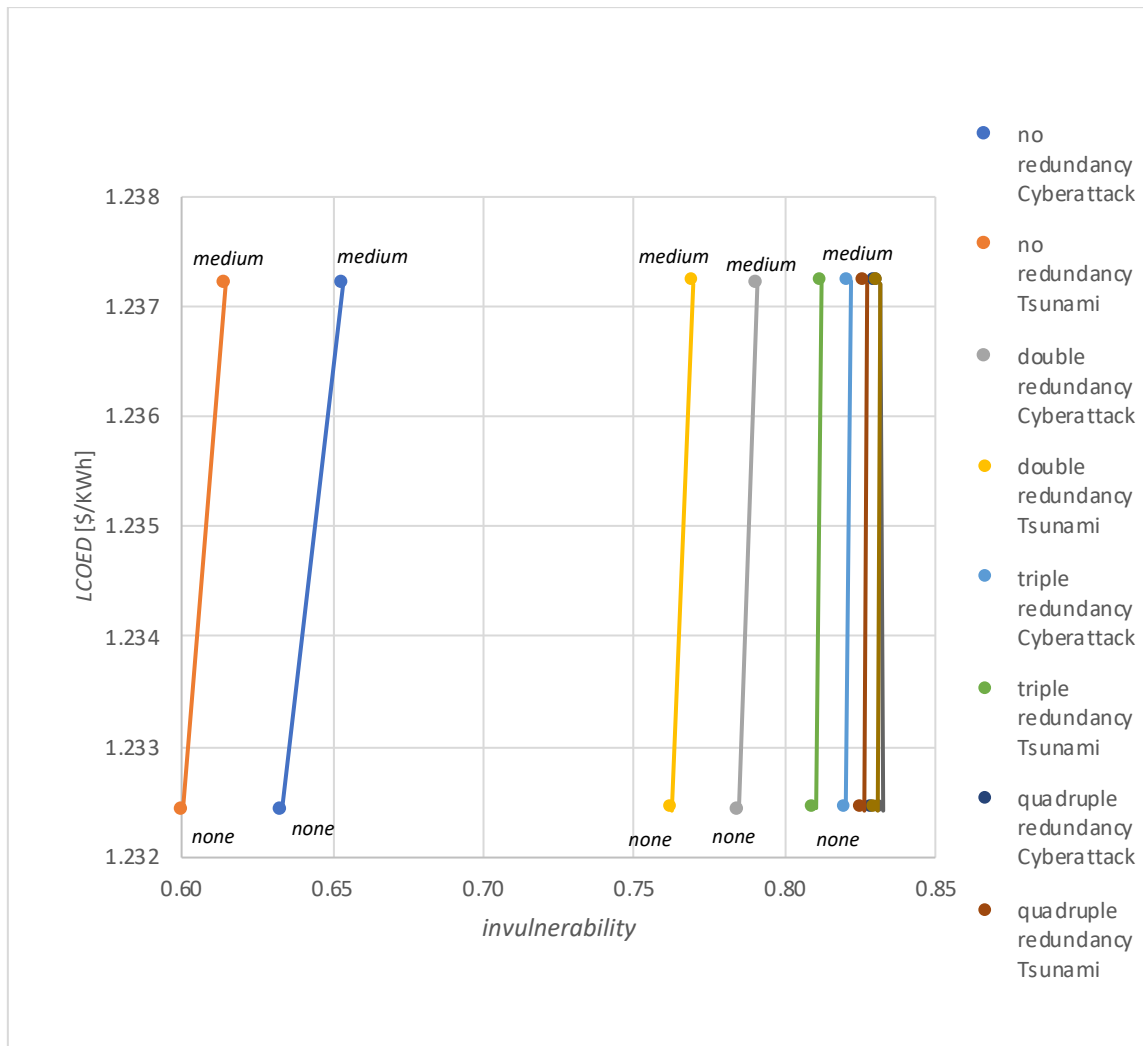


Figure 116. The effects of redundancy level on *LCOED* and *invulnerability*.

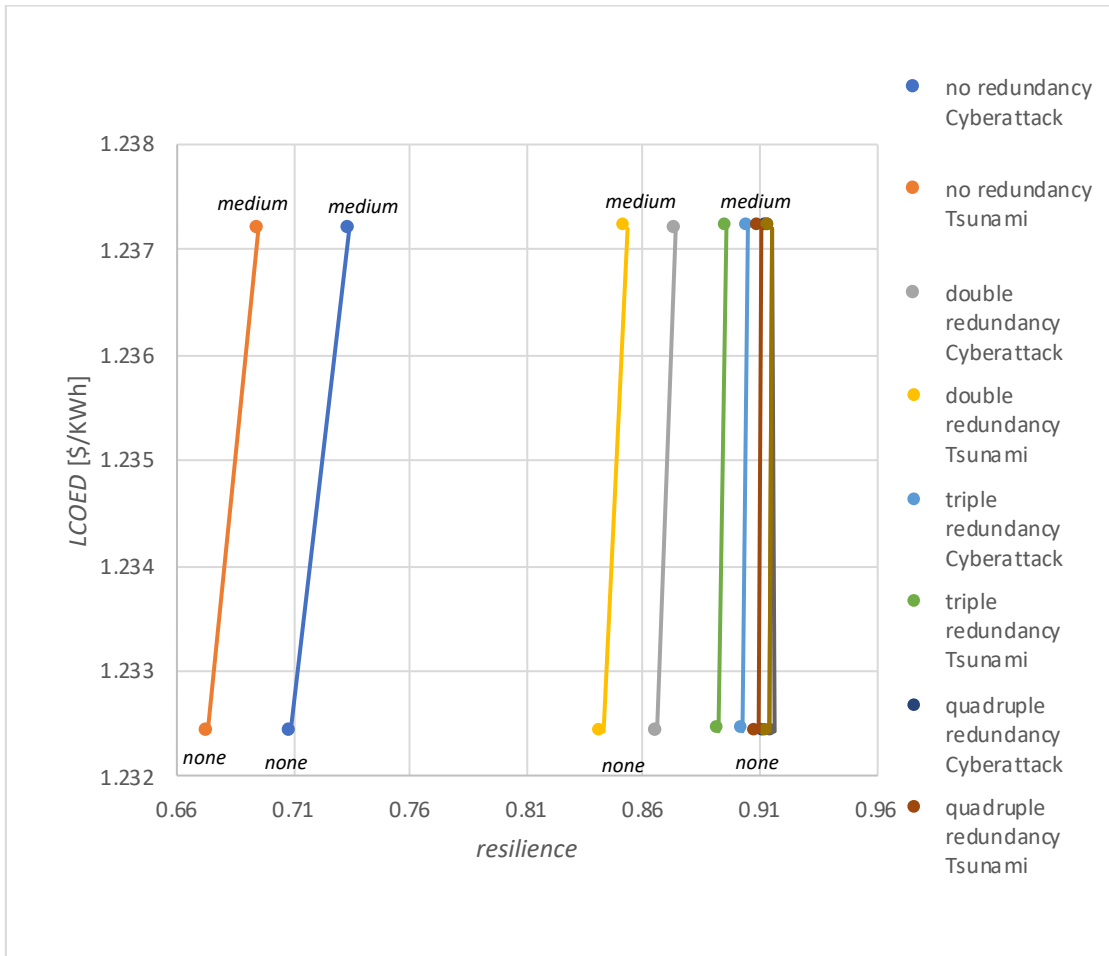


Figure 117. The effects of redundancy level on *LCOED* and *resilience*.

2. **Optimized Microgrid's Impact of Redundancy, and Maintenance on Resilience and Costs for a Morning Tsunami**

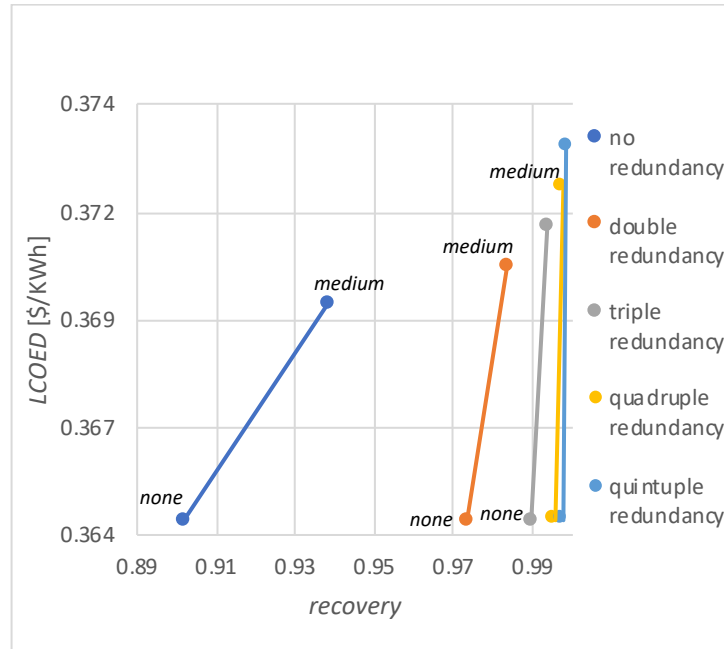


Figure 118. The effects of redundancy level on *LCOED* and *recovery*.

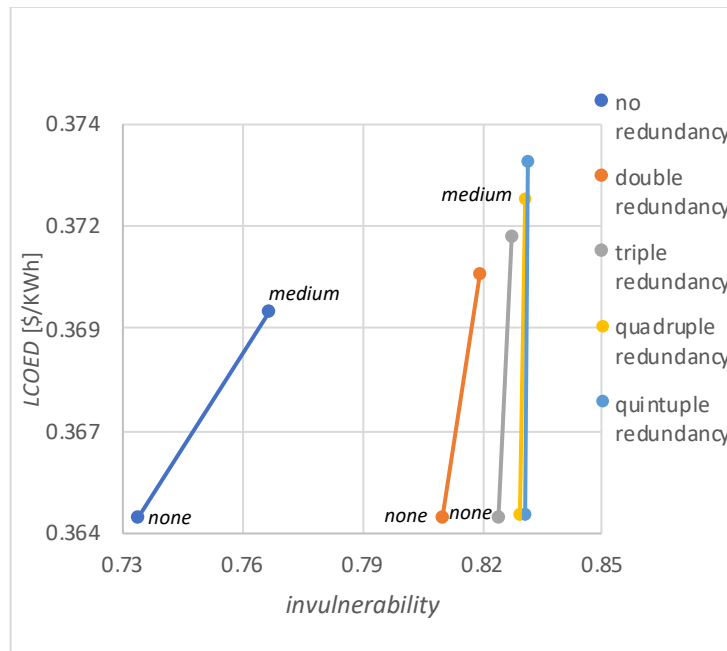


Figure 119. The effects of redundancy level on *LCOED* and *invulnerability*.

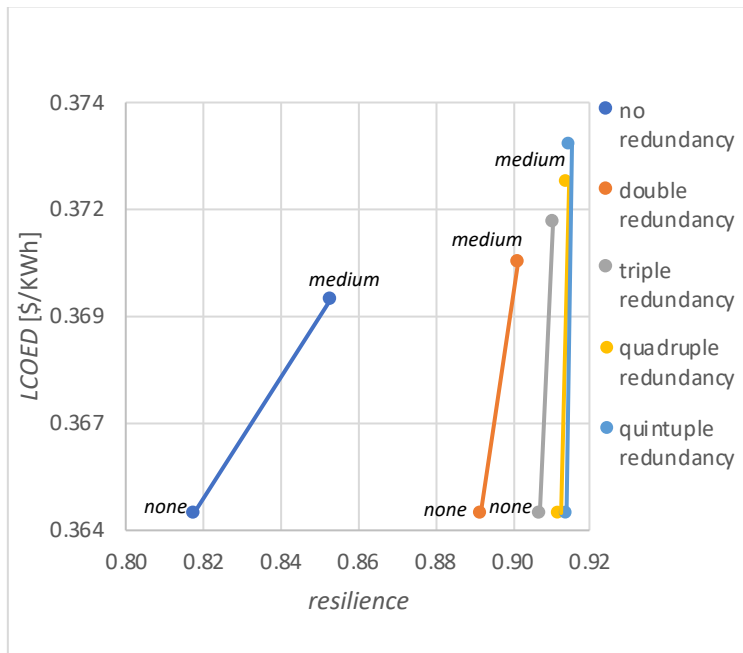


Figure 120. The effects of redundancy level on *LCOED* and *resilience*.

3. **Optimized Microgrid's Impact of Redundancy, and Maintenance on Resilience and Costs for a Midnight Tsunami**

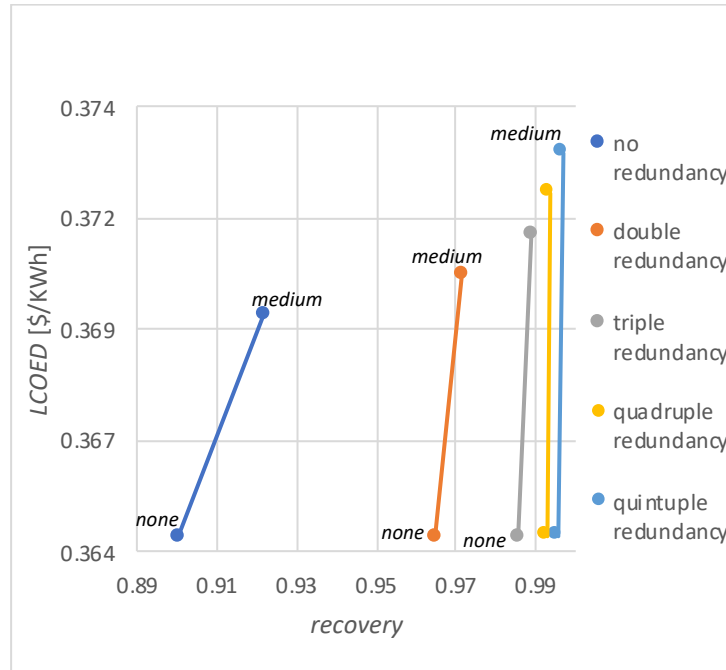


Figure 121. The effects of redundancy and maintenance level on *LCOED* and *recovery*.

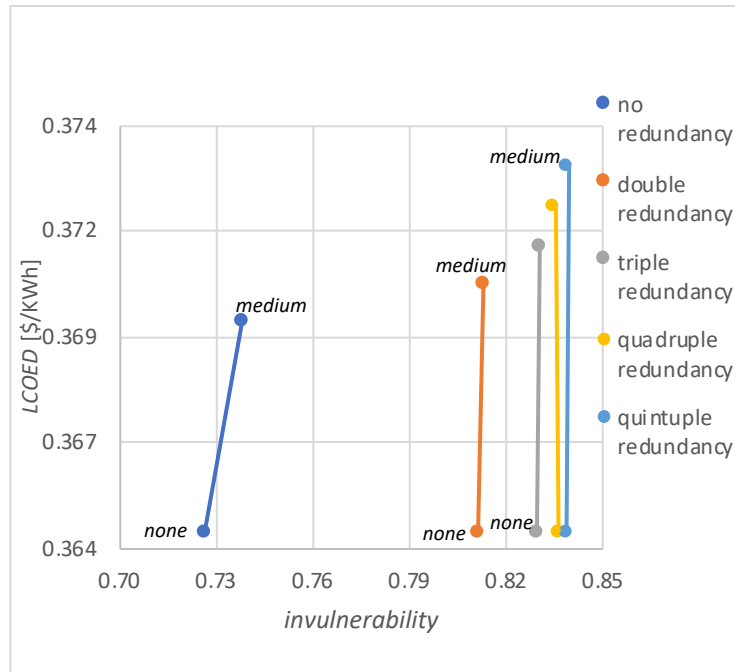


Figure 122. The effects of redundancy and maintenance level on *LCOED* and *invulnerability*.

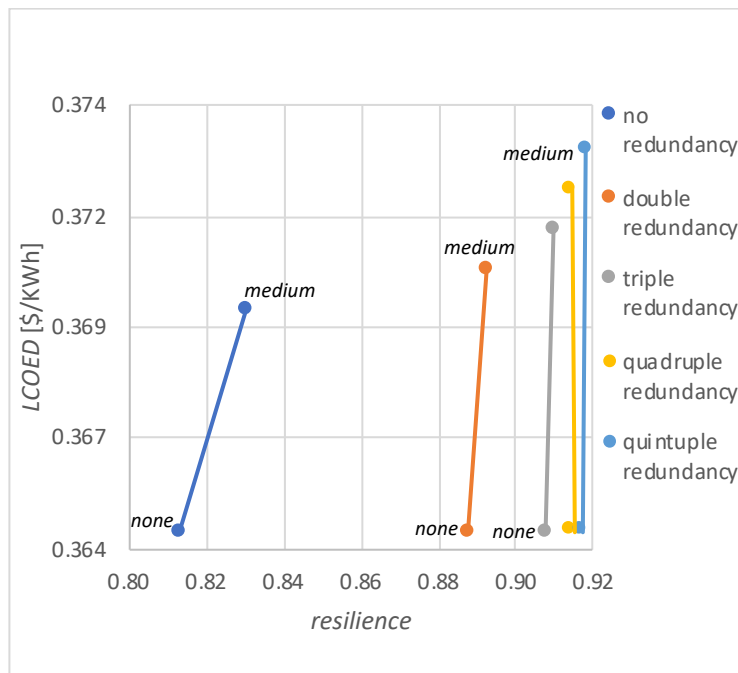


Figure 123. The effects of redundancy and maintenance level on *LCOED* and *resilience*.

THIS PAGE INTENTIONALLY LEFT BLANK

APPENDIX B. MICROSOFT EXCEL TOOL DEVELOPED FOR MODELS

A. RESILIENCE MODEL

1. Input Variables

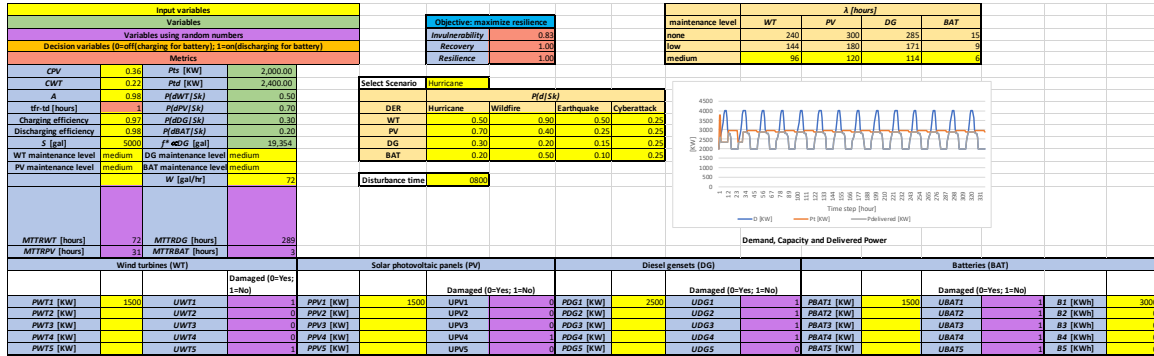


Figure 124. Resilience model variables. Measures are in red.

Table 36. Demand profile for each time step.

Day	Time [hour]	D [KW]	Pt [KW]	Pdelivered [KW]	T [KW]
1	0	2000	2000.00	2000.00	0.00
	1	2400	2314.04	2314.04	870.94
	2	2600	2314.04	2314.04	1070.94
	3	2800	2314.04	2314.04	1270.94
	4	3000	2314.04	2314.04	1470.94
	5	3400	2314.04	2314.04	1870.94
	6	3800	2314.04	2314.04	2270.94
	7	4000	2314.04	2314.04	2470.94
	8	4000	2314.04	2314.04	2470.94
	9	4000	2314.04	2314.04	2470.94
	10	3600	2314.04	2314.04	2070.94
	11	3000	2314.04	2314.04	1470.94
	12	2800	2371.07	2371.07	1213.91
	13	2800	2371.07	2371.07	1213.91
	14	2800	2371.07	2371.07	1213.91
	15	2600	2894.39	2600.00	1013.91
	16	2000	2894.39	2000.00	413.91
	17	2000	2894.39	2000.00	413.91
	18	2000	2894.39	2000.00	413.91
	19	2000	2894.39	2000.00	413.91
	20	2000	2894.39	2000.00	413.91
	21	2000	2894.39	2000.00	413.91
	22	2000	2894.39	2000.00	413.91
	23	2000	2894.39	2000.00	413.91


```

Do While counter < 44 + x
shRead.Calculate
shRead.Range("I5").Copy
shWrite.Cells(counter, "B").PasteSpecial xlPasteValues
shRead.Range("I4").Copy
shWrite.Cells(counter, "F").PasteSpecial xlPasteValues
shRead.Range("I6").Copy
shWrite.Cells(counter, "I").PasteSpecial xlPasteValues
shRead.Range("C10").Copy
shWrite.Cells(counter, "K").PasteSpecial xlPasteValues
shLCAE.Calculate
shLCAE.Range("G3").Copy
shWrite.Cells(counter, "O").PasteSpecial xlPasteValues
counter = counter + 1
Loop
Application.Calculation = xlCalculationAutomatic
Application.DisplayStatusBar = True
Application.EnableEvents = True
Application.ScreenUpdating = True
End Sub

```

APPENDIX C. CONFIDENCE INTERVAL CALCULATIONS

$$\text{Confidence Interval} = \left(\bar{x} - z \frac{s}{\sqrt{n}}, z \frac{s}{\sqrt{n}} \right) \quad (\text{AC.1})$$

where

n denotes the number of simulations

z = z-statistic

s = standard deviation

Level of precision is the width of the confidence interval. A confidence interval of two minutes per each time step is used for time to recover. This calculation is two minutes per hour, or 0.0333. Monte Carlo simulations were averaged for 7,500 simulations so as to satisfy the Central Limit Theorem's requirements for this confidence level and level of precision. The amount of simulations is determined to be 7,500 by first running the simulation 500 times and calculating the standard deviation as 1.753 for time to recover. Using a 90% confidence interval with a 1.645 z-statistic, the Equation AC.1 is solved for n as shown in Equation AC.2.

$$n = \left(\frac{zs}{P} \right)^2 \quad (\text{AC.2})$$

where

n = number of simulations

P = desired level of precision

z = z-statistic

s = standard deviation from 500 simulations

Equation AC.2 is then solved as shown in Equation AC.3.

$$n = \left(\frac{1.645(1.753)}{0.0333} \right)^2 \quad (\text{AC.3})$$

$n = 7,499$ simulations.

THIS PAGE INTENTIONALLY LEFT BLANK

LIST OF REFERENCES

- Abdulkarim, A., S. Abdelkader, D. Morrow, A. Falade, A. Lawan, and H. Iswadi. 2016. "Effect of Weather and the Hybrid Energy Storage on the Availability of Standalone Microgrid." *International Journal of Renewable Energy Research* 6 (1) (February): 189–98. https://pureadmin.qub.ac.uk/ws/portalfiles/portal/133935943/3319_14196_1_PB.pdf.
- Adhikari, Sushil, Nidara Mithulanathan, Animesh Dutta, and A. Mathias. 2008. "Potential of Sustainable Energy Technologies Under CDM in Thailand: Opportunities and Barriers." *Renewable Energy* 33 (9) (September): 2122–33. <https://www.sciencedirect.com/science/article/abs/pii/S0960148107004065>.
- Aalborg University. "Analysis Computer Model EnergyPLAN." Accessed July 5, 2017. www.energyplan.eu.
- Ainuddin, Syed, and Jayant Routray. 2012. "Community Resilience Framework for an Earthquake Prone Area in Baluchistan." *International Journal of Disaster Risk Reduction* 2 (July): 25–36. <https://www.infona.pl/resource/bwmeta1.element.elsevier-ecfd319a-bdc7-38bc-bd6f-d617886e58d8>.
- Akikur, Kazi, Rahman Saidur, Hew Ping, and K. Ullah. 2013. "Comparative Study of Stand-Alone and Hybrid Solar Energy Systems Suitable for Off-Grid Rural Electrification: A Review." *Renewable and Sustainable Energy Reviews* 27 (November): 738–52. <https://www.sciencedirect.com/science/article/abs/pii/S1364032113004346>.
- Aldersey-Williams, J, and Tim Rubert. 2019. "Levelised Cost of Energy – A Theoretical Justification and Critical Assessment." *Energy Policy* 124 (January): 169–179. <https://doi.org/10.1016/j.enpol.2018.10.004>.
- Amirioun, M., Farrokh Aminifar, Asgar Lesani, and Mohammad Shahidehpour. 2019. "Metrics and Quantitative Framework for Assessing Microgrid Resilience Against Windstorms." *International Journal of Electrical Power & Energy Systems* 104 (January): 716–23. <https://www.sciencedirect.com/science/article/abs/pii/S0142061518300097>.
- Alzahrani, Ahmad, Mehdi Ferdowsi, Pourya Shamsi, and Cihan H. Dagli. 2017. "Modeling and Simulation of Microgrid." *Procedia Computer Science* 114 (October-November): 292–400.
- Anderson, Bill, Michael Cruz, Nicholas DeMarco, Bruce Garrett, and Nathanael Royer. 2017. *A Microgrid Analysis of San Nicolas Island Using HOMER*. Port Hueneme, CA: Naval Facilities Engineering Command (NAVFAC) Engineering and Expeditionary Warfare Center (EXWC).

- Anderson, Kate, Nick DiOrio, Bob Butt, Dylan Cutler, and Allison Richards. 2020. "Resilient Renewable Energy Microgrids." *Paper Presented at the SCTE ISBE Energy 2020 Expo*. <https://www.nrel.gov/docs/fy18osti/70033.pdf>.
- Anderson, Kate, Nicholas Laws, Spencer Marr, Lars Lisell, Tria Case, Xiangkun Li, Dag Lohmann, and Dylan Cutler. 2018. "Quantifying and Monetizing Renewable Energy Resiliency." *Sustainability* 10 (4) (March): 933. <https://doi.org/10.3390/su10040933>.
- Anderson, William, and Oleg Yakimenko. 2017. "Comparative Analysis of Two Microgrid Solutions for Island Green Energy Supply Sustainability." In *Proceedings of the 6th International Conference on Renewable Energy Research and Applications*: 245–250. 10.1109/ICRERA.2017.8191274.
- Annaswamy, A., T. Nudell, M. Allais, A. Bonfiglio, M. Brignone, C. Cancemi, F. Delfino, R. Procopio, and M. Robba. 2016. "Experimental Validation of PV Model Uncertainties Impact on Microgrid EMS Performances." In *Proceedings of the Power and Energy Society General Meeting (PESGM)*: 1–5. <https://ieeexplore-ieee-org.libproxy.nps.edu/document/7741709>.
- Appalachian State University. 2007. "Utility Scale Wind Energy." Accessed June 19, 2020. <http://www.appvoices.org/ftp/wind/Wind-Energy-Fact-Sheet-WNCREI-Feb07.pdf>.
- Arctic Council. 2016. *Arctic Resilience Report*. Report No. 11374/1838. <https://oaarchive.arctic-council.org/handle/11374/1838>.
- Arghandeh, Reza, Alexandra von Meier, Laura Mehrmanesh, and Lamine Mili. 2016. "On the Definition of Cyber-Physical Resilience in Power Systems." *Renewable and Sustainable Energy Reviews* 58 (May):1060–1069. 10.1016/j.rser.2015.12.193.
- Arriaga, Mariano. 2016. "Long-Term Renewable Energy Planning Model for Remote Communities." *IEEE Transactions on Sustainable Energy* 7 (1) (January): 221–231. 10.1109/TSTE.2015.2483489.
- Aven, Terje. 2011 "On Some Recent Definitions and Analysis Frameworks for Risk, Vulnerability, and Resilience." *Risk Analysis* 31 (4) (November): 515–522. <https://onlinelibrary.wiley.com/doi/abs/10.1111/j.1539-6924.2010.01528.x>.
- Avossa, Alberto, Cristoforo Demartino, Pasquale Contestabile, Francesco Ricciardelli, and Diego Vicinanza. 2017. "Some Results on the Vulnerability Assessment of HAWTs Subjected to Wind and Seismic Actions." *Sustainability* 9 (9) (August): 1525. <https://www.mdpi.com/2071-1050/9/9/1525>.

- Ayyub, Bilal. 2013. "Systems Resilience for Multihazard Environments: Definition, Metrics, and Valuation for Decision Making." *Risk Analysis* 34 (2) (July): 340–55. https://www.researchgate.net/publication/251232911_Systems_Resilience_for_Multihazard_Environments_Definition_Metrics_and_Valuation_for_Decision_Making.
- Azim, Mohammed. 2016. "An Inverter Control Technique for an RES-based Islanded Microgrid." *International Journal of Renewable Energy Research (IJRER)* 6 (2) (January): 580–84. <https://www.ijrer.org/ijrer/index.php/ijrer/article/view/3531/pdf>.
- Bale, Catherine, Liz Varga, and Timothy Foxon. 2015. "Energy and Complexity: New Ways Forward." *Applied Energy* 138 (January): 150–159.
- Baroud, Hiba, Kash Barker, Jose Ramirez-Marquez, and Claudio Rocco. 2014. "Importance Measures for Inland Waterway Network Resilience." *Transportation Research Part E* 62 (February): 55–67. <http://dx.doi.org/10.1016/j.tre.2013.11.010>.
- Baschel, Stefan, Elena Koubli, Jyotirmoy Roy, and Ralph Gottschalg. 2018. "Impact of Component Reliability on Large Scale Photovoltaic Systems' Performance." *Energies* 11, no. 6 (June): 1579. <https://doi.org/10.3390/en11061579>.
- Bates, Gavin. 2011. *Lord Howe Island Renewable Operations*. <https://www.lhib.nsw.gov.au/sites/lordhowe/files/public/images/documents/lhib/Infrastructure/lhi%20energy%20supply%20road%20map%20-%20november%202011.pdf>.
- Baxter, John. 2018. "The Current Threat Environment." Presentation at Federal Utility Partnership Working Group Seminar, April 20, 2018. https://www.energy.gov/sites/prod/files/2018/04/f51/fupwg_spring_2018_20-baxter.pdf.
- Belderbos, Andreas, Erik Delarue, and William D'haeseleer. 2016. "Calculating the Levelized Cost of Energy Storage?" *In Proceedings of the 39th IAEE International Conference*: 19–22. <https://www.semanticscholar.org/paper/Calculating-the-Levelized-Cost-of-Electricity-Belderbos-Delarue/d240795ba137f004b963feb8b3eeac9210612c52?p2df>.
- Berkeley, Alfred, and Mike Wallace. 2010. *A Framework for Establishing Critical Infrastructure Resilience Goals*. National Infrastructure Advisory Council. <https://www.dhs.gov/xlibrary/assets/niac/niac-a-framework-for-establishing-critical-infrastructure-resilience-goals-2010-10-19.pdf>.
- Bhattacharyya, Subhes. 2012. "Review of Alternative Methodologies for Analyzing off-Grid Electricity Supply." *Renewable and Sustainable Energy Reviews* 16 (1) (January): 677–94. <https://www.sciencedirect.com/science/article/abs/pii/S1364032111004436>.

- Biello, David. 2010. "100 Percent Renewable? One Danish Island Experiments with Clean Power." *Scientific American*, January 19. www.scientificamerican.com/article/samso-attempts-100-percent-renewable-power/.
- Birkman, J., K. Teichman, T. Welle, M. González, and M. Olabarrieta. 2010. "The Unperceived Risk to Europe's Coasts: Tsunamis and the Vulnerability of Cadiz, Spain." *Natural Hazards and Earth System Sciences* 10 (December): 2659–2675. <http://www.proteccioncivil.es/documents/20486/25b1de87-e5eb-4c04-a9e4-0372e03a6208>.
- Borisoglesky, Dmitry, and Liz Varga. "A Resilience Toolbox and Research Design for Black Sky Hazards to Power Grids." *Complexity* 2019 (June): 1–15. <https://doi.org/10.1155/2019/1065419>.
- Branker, K., M. Pathak, and J. Pearce. 2011. "A Review of Solar Photovoltaic Levelized Cost of Electricity." *Renewable and Sustainable Energy Reviews* 15 (9) (December): 4470–82. <https://doi.org/10.1016/j.rser.2011.07.104>.
- Breen, Lewis. 2015. "Modelling, Optimisation and the Lessons Learned of a Renewable Based Electrical Network – The Isle of Eigg." Master's thesis, University of Strathclyde.
- Brtis, John, and Michael McEvelley. 2019. "Systems Engineering for Resilience." Report No. MP 190495. <https://www.researchgate.net/publication/334549424>.
- Bruneau, Michael, Stephanie Chang, Ronald Eguchi, George Lee, Thomas O'Rourke, Andrei Reinhorn, Kathleen Tierney, William Wallace, and Detlof Winterfeldt. 2003. "A Framework to Quantitatively Assess and Enhance the Science of the Seismic Resilience of Communities." *Earthquake Spectra* 19 (4) (November): 733–52. <http://courses.washington.edu/cee518/Bruneauetal.pdf>.
- Bruyelle, Jean-Luc, Conor O'Neill, EI-Miloudi El-Koursi, Fabrice Hamelin, Nicolo Sartori, and Louahdi Khoudour. 2014. "Improving the Resilience of Metro Vehicle and Passengers for an Effective Emergency Response to Terrorist Attacks." *Safety Science* 62 (February):37–45. <https://www.sciencedirect.com/science/article/pii/S0925753513001720>.
- Bunker, Kaitlyn, Kate Hawley, and Jesse Morris. 2015. *Renewable Microgrids: Profiles from Islands and Remote Communities Across the Globe*. Boulder, CO: Rocky Mountain Institute. http://www.rmi.org/islands_renewable_microgrids.
- Organization of American States. 2001. *Hurricane Procedures Manual*. <https://www.oas.org/cdmp/document/chaman/chasect4.html>.
- Chanda, Sayansom, and Manish Mohankpurkar. 2018. "Quantifying Power Distribution System Resiliency Using Code-Based Metric." *IEEE Transactions on Industry Applications* 54 (4) (July/August): 3676–3686. 10.1109/TIA.2018.2808483.

- Chanda, Sayonsom, and Anurag Srivastava. 2015. "Quantifying Resiliency of Smart Power Distribution Systems with Distributed Energy Resources." *In Proceedings of the 2015 IEEE 24th International Symposium on Industrial Electronics (ISIE)* 766–771. 10.1109/ISIE.2015.7281565.
- Chang, Stephanie, and Masanobu Shinozuka. 2004. "Measuring Improvements in the Disaster Resilience of Communities." *Earthquake Spectra* 20 (3) (August): 739–55. https://www.researchgate.net/publication/249873318_Measuring_Improvements_in_the_Disaster_Resilience_of_Communities.
- Chatterjee, Abhi, Daniel Burmester, Alan Brent, and Ramesh Rayudu. 2019. "Research Insights and Knowledge Headways for Developing Remote, Off-Grid Microgrids in Developing Countries." *Energies* 12 (2008) (May): 1–19. doi:10.3390/en12102008.
- Chaudry, Modassar, Paul Ekins, Kannan Ramachandran, Anser Shakoor, Jim Skea, Goran Strbac, Xinxin Wang, and Jeanette Whitaker. 2009. *Building a Resilient UK Energy System: Research Report*. London, UK: UK Energy Research Centre. <http://www.ukerc.ac.uk/publications/building-a-resilient-uk-energy-system-research-report.html>.
- Clavier, Juan, Géza Joós, and Steve Wong. 2013. "Economic Assessment of the Remote Community Microgrid: PV-ESS-Diesel Study Case." *In Proceedings of the 26th IEEE Canadian Conference of Electrical and Computer Engineering (CCECE)* 1–5. 10.1109/CCECE.2013.6567694.
- Connolly, David, Henrik Lund, Brian Vad Mathiesen, and Martin Leahy. 2010. "A Review of Computer Tools for Analysing the Integration of Renewable Energy into Various Energy Systems." *Applied Energy* 87 (4) (April):1059–82. <https://www.sciencedirect.com/science/article/abs/pii/S0306261909004188?via%3Dihub>.
- Cugini, John, Laurie Damianos, Lynette Hirschman, Robyn Kozierok, Jeff Kurtz, Sharon Laskowski, and Jean Scholtz. 1997. *Methodology for Evaluation of Collaboration Systems*. The Evaluation Working Group of The DARPA Intelligent Collaboration and Visualization Program. <https://pdfs.semanticscholar.org/f785/c1f2866b359114da719224a9b3c29b6b8cb7.pdf>.
- Curfman, David. 2020. "NAVFAC Design and Construction Programs." Presentation made at SAME conference, March 17, 2020. http://www.ncmbc.us/wp-content/uploads/13301430_NAVFACDesignConstruction.pdf.
- Cutter, Susan, Melissa Berry, Christopher Burton, Elijah Evans, Eric Tate, and Jennifer Webb. 2008. "A Place-Based Model for Understanding Community Resilience to Natural Disasters." *Global Environmental Change* 18 (4) (October): 598–606. <https://www.sciencedirect.com/science/article/abs/pii/S0959378008000666>.

- Davis, William, and David Yen. 1999. "Pseudocode." In *The Information System Consultant's Handbook: Systems Analysis and Design*, 465–471. London: CRC Press. <https://www-taylorfrancis-com.libproxy.nps.edu/books/e/9781315219745/chapters/10.1201/9781420049107-59>.
- Department of Defense. 2019. *Unified Facilities Criteria. Engine-Driven Generator Systems for Prime and Standby Power Applications*. UFC 3–540-01. Change 2. Washington, DC: Department of Defense.
- Department of Defense. 2020a. *Fiscal Years 2022 and 2023 Energy Resilience and Conservation Investment Program Guidance*. Washington, DC: Office of the Assistant Secretary of Defense.
- Department of Defense. 2020b. *Fiscal Year (FY) 2020 Fuel Price Change*. Washington, DC: Office of the Assistant Secretary of Defense, Pentagon, D.C. https://www.dla.mil/Portals/104/Documents/Energy/Standard%20Prices/Petroleum%20Prices/E_2020Jun1PetroleumStandardPrices_200529.pdf?ver=2020-05-29-153633-207.
- Department of Defense. 2020c. *Metrics and Standards for Energy Resilience at Military Installations*. Washington, DC: Office of the Assistant Secretary of Defense.
- Department of Energy. n.d. "Levelized Cost of Energy (LCOE)." Presentation. Accessed July 4, 2020. <https://www.energy.gov/sites/prod/files/2015/08/f25/LCOE.pdf>.
- Department of the Navy. 2013a. *Navy Net Zero/Energy Security Assessment for Diego Garcia (DG), Site Assessment*. NREL & NAVFAC.
- Department of the Navy. 2013b. *NAVFAC P-442 Economic Analysis Handbook*. Washington Navy Yard, DC. <https://www.wbdg.org/FFC/NAVFAC/PPUBB/p442.pdf>.
- Department of the Navy. 2015. *San Nicolas Island Microgrid Control Strategy*.
- Department of the Navy. 2017a. *Energy Security Assessment Tool*. NAVFAC.
- Department of the Navy. 2017b. *NAVFAC P-602 3-Pillars of Energy Security (Reliability, Resiliency, and Efficiency)*. Washington Navy Yard, DC: NAVFC HQ.
- Department of the Navy. 2018. *Navy FY 2017 AEMR Supplemental Workbook*. Washington Navy Yard, D.C: NAVFC HQ.
- Diesel Service & Supply. n.d. "Approximate Fuel Consumption Chart." Accessed June 19, 2020. https://www.generatorsource.com/temp/Fuel_Consumption_Chart.pdf.

- D’Lima, Minette, and Francesca Medda. 2015. “A New Measure of Resilience: An Application to the London Underground Part A: Policy and Practice.” *Transportation Research* 81 (November): 35–46.
- Department of Energy. “Energy Infrastructure Resilience.” 2015. <https://www.energy.gov/sites/prod/files/2015/01/f19/SNLResilienceApril29.pdf>.
- Etienne, Elius, Naresh Devineni, Reza Khanbilvardi, and Upmanu Lall. 2016. “Development of a Demand Sensitive Drought Index and its Application for Agriculture over the Conterminous United States.” *Journal of Hydrology* 534 (March): 216–229. <http://dx.doi.org/10.1016/j.jhydrol.2015.12.060>.
- Faraji, Jamal, Masoud Babaei, Navid Bayati, and Maryam Hejazi. 2019. “A Comparative Study between Traditional Backup Generator Systems and Renewable Energy Based Microgrids for Power Resilience Enhancement of a Local Clinic.” *Electronics* 8, no. 12: 1485. <https://doi.org/10.3390/electronics8121485>.
- Fathi, Hazem, Eman Beshr, and Magdy Eteiba. 2015. “Multi-Objective Optimization of Islanded Microgrids.” In *Proceedings of the 2015 IEEE International Conference on Electrical, Computer and Communication Technologies (ICECCT)* 1–7. 10.1109/ICECCT.2015.7225988.
- Faturechi, Reza, Eyal Levenberg, and Elise Miller-Hooks. 2014. “Evaluating and Optimizing Resilience of Airport Pavement Networks.” *Computers & Operations Research* 43 (March): 335–348.
- Fauziah, Siti. 2010. “International Study of Renewable Energy Regions.” Center for Renewable Energy, University of Freiburg. reregions.blogspot.com/2010/03/isle-of-eigg-scotland.html.
- Field, Christopher, Vicente Barros, Thomas Stocker, and Qin Dahe. 2012. “Managing the Risks of Extreme Events and Disasters to Advance Climate Change Adaptation: Special Report of the Intergovernmental Panel on Climate Change.” Cambridge, U.K.: Cambridge University Press. https://www.ipcc.ch/site/assets/uploads/2018/03/SREX_Full_Report-1.pdf.
- Fitch, Anna, Julie Lundquist, and Joseph Olson. 2013. “Mesoscale Influences of Wind Farms throughout a Diurnal Cycle.” *Monthly Weather Review* 141 (July): 2173–2918. <https://doi.org/10.1175/MWR-D-12-00185.1>.
- Francis, Royce, and Behailu Bekera. 2014. “A Metric and Frameworks for Resilience Analysis of Engineered and Infrastructure Systems.” *Reliability Engineering & System Safety* 121 (January): 90–103. <https://www.sciencedirect.com/science/article/abs/pii/S0951832013002147>.
- Garcia, Kevin. 2017. “Optimization of Microgrids at Military Remote Base Camps.” PhD diss., Naval Postgraduate School. <https://calhoun.nps.edu/handle/10945/56923>.

- Giachetti, Ron, Luis Martinez, Oscar Sáenz, and Chin Chen. 2003. "Analysis of the Structural Measures of Flexibility and Agility using a Measurement Theoretical Framework." *International Journal of Production Economics* 86 (October): 47–62. [https://doi.org/10.1016/S0925-5273\(03\)00004-5](https://doi.org/10.1016/S0925-5273(03)00004-5).
- GlobalSecurity.org. n.d. "Naval Station Rota." Accessed September 6, 2020. <https://www.globalsecurity.org/military/facility/rota.htm>.
- Goel, Sonali, and Renu Sharma. 2017. "Performance Evaluation of Stand Alone, Grid Connected and Hybrid Renewable Energy Systems for Rural Application: A Comparative Review." *Renewable and Sustainable Energy Reviews* 78 (October): 1378–89. <https://www.sciencedirect.com/science/article/abs/pii/S1364032117308365>.
- Guevara-Stone, Laurie. 2015. "An Alaskan Island Goes 100% Renewable." *RMI Outlet Blog*. May 19, 2015. https://rmi.org/blog_2015_05_19_an_alaskan_island_goes_one_hundred_percent_renewable/.
- Haimes, Yacov. 2018. "On the Definition of Resilience in Systems." *Risk Analysis* 29, no. 4 (March): 498–501. <https://onlinelibrary.wiley.com/doi/abs/10.1111/j.1539-6924.2009.01216.x>.
- Han, Zhang, Hanjie Yuan, Gengfeng Li, and Yanling Lin. "Quantitative Resilience Assessment under a Tri-Stage Framework for Power Systems." *Energies* 11, no.1427 (June): 1–23. https://www.google.com/url?sa=t&rct=j&q=&esrc=s&source=web&cd=1&ved=2ahUKEwiY9oqS9pLnAhV6GTQIHWpzBcEQFjAAegQIAhAB&url=https%3A%2F%2Fwww.mdpi.com%2F1996-1073%2F11%2F6%2F1427%2Fpdf&usq=AOvVaw3L4e_IVJmml1iE1PNCUhow.
- Hamilton, Michelle, James Lambert, Elizabeth Connelly, and Kash Barker. 2016. "Resilience Analytics with Disruption of Preferences and Life cycle Cost Analysis for Energy Microgrids." *Reliability Engineering and System Safety* 150 (June): 11–21. <http://dx.doi.org/10.1016/j.res.2016.01.005>.
- Hashimoto, Tsuyoshi, Jerry Stedinger, and Pete Loucks. 1982. "Reliability, Resiliency, and Vulnerability Criteria for Water Resource System Performance Evaluation." *Water Resources Research* 18 (1) (February): 14–20. https://www.researchgate.net/publication/248804973_Reliability_Resiliency_and_Vulnerability_Criteria_For_Water_Resource_System_Performance_Evaluation.
- Hazelton, James, Anna Bruce, and Iain MacGill. 2014. "A Review of the Potential Benefits and Risks of Photovoltaic Hybrid Mini-Grid Systems." *Renewable Energy* 67 (July): 222–29. <https://www.sciencedirect.com/science/article/abs/pii/S0960148113006046>.

- Henry, Devanandham, and Jose Ramirez-Marquez. 2012. “Generic Metrics and Quantitative Approaches for System Resilience as a Function of Time.” *Reliability Engineering and System Safety* 99 (March): 114–22. <https://www.sciencedirect.com/science/article/abs/pii/S0951832011001748>.
- Hill, Roger, Jennifer Stinebaugh, Daniel Briand, Allan Benjamin, and James Linsday. 2008. *Wind Turbine Reliability: A Database and Analysis Approach*. Sandia Report SAND2008-0983. <https://pdfs.semanticscholar.org/b44a/4e1c0cf908badc1009e6864438888f0e6302.pdf>.
- Hollnagel, Erik, David Woods, and Nancy Leveson. 2006. *Resilience Engineering Concepts and Precepts*. Aldershot, U.K. Crc Press.
- Hossain, Eklas, Ron Perez, and Ramazan Bayindir. 2016. “Implementation of Hybrid Energy Storage Systems to Compensate Microgrid Instability in the Constant Power Loads.” *In Proceedings of the 5th International Conference on Renewable Energy Research and Applications (ICRERA)*: 1068–1073. 10.1109/ICRERA.2016.7884498.
- Hossain, Mohammed, Nazmus Sakib, Eklas Hossain, and R. Bayindir. 2017. “Modeling and Simulation of Solar Plant and Storage System: A Step to Microgrid Technology.” *IJREER* 7 (2) (June): 723–37. https://www.researchgate.net/publication/317662517_Modelling_and_Simulation_of_Solar_Plant_and_Storage_System_A_Step_to_Microgrid_Technology.
- Hosseini, Seyedmohsen, Kash Barker, and Jose Ramirez-Marquez. 2016. “A Review of Definitions and Measures of System Resilience.” *Reliability Engineering and System Safety* 145 (January): 47–61.
- Hussain, Akhtar, Van-Hai Bui, and Hak-Man Kim. 2019. “Microgrids as a Resilience Resource and Strategies Used by Microgrids for Enhancing Resilience.” *Applied Energy* 240 (April): 56–72. <https://doi.org/10.1016/j.apenergy.2019.02.055>.
- Ibrahaim, Mariam, and Asma Alkhraibat. 2020. “Resiliency Assessment of Microgrid Systems.” *Applied Sciences* 10 (5) (March): 1824. <https://doi.org/10.3390/app10051824>.
- Islam, F., Kabir Mamun, and Maung Amanullah. 2017. *Smart Energy Grid Design for Island Countries*. Springer International Publishing.
- INCOSE. 2010. *Systems Engineering Measurement Primer*. INCOSE-TP-2010-005-02. <https://www.incose.org/docs/default-source/ProductsPublications/systems-engineering-measurement-primer---december-2010.pdf>.
- International Energy Agency. 2019. *Results of IEA Wind TCP Workshop on a Grand Vision for Wind Energy Technology*. <https://www.nrel.gov/docs/fy19osti/72437.pdf>.

- International Renewable Energy Agency. 2020. *Renewable Power Generation Costs in 2019*. <https://www.irena.org/publications/2020/Jun/Renewable-Power-Costs-in-2019>.
- Jantzen, Jan. 2014. *Appraisal of Renewable Energy Projects with Cases from Samsø*. Samsø Energy Agency: TikiWiki. <http://seacourse.dk/wiki/tiki-index.php?page=Samsø%2C+a+Renewable+Energy+Island>.
- Judson, Nicholas, Alex Pina, E. Dydek, S. Van Broekhoven, and A. Castillo. 2016. *Application of a Resilience Framework to Military Installations: A Methodology for Energy Resilience Business Case Decisions*. Technical report 1216. <https://apps.dtic.mil/dtic/tr/fulltext/u2/1032242.pdf>.
- Judson, Nicholas, Alex Pina, and A. Whitehead. 2018. “Energy Resilience Analysis.” Presentation on April 12, 2018.
- Junior, Milton, Ubirtatan Bezerra, Jandecy Leite, and Jorge Rodriguez. 2017. “Maintenance Tools Applied to Electric Generators to Improve Energy Efficiency and Power Quality of Thermoelectric Power Plants.” *Energies* 10 (July):1091. <https://www.mdpi.com/1996-1073/10/8/1091>.
- Kahan, Jerome, Andrew Allen, and Justin George. 2009. “An Operational Framework for Resilience.” *Journal of Homeland Security and Emergency Management* 6 (1):1–48. <https://pdfs.semanticscholar.org/6848/7d0ec33d8d36b7f1a21f4181cc286afc506f.pdf>.
- Kandt, Alicen, and Andy Walker. 2008. *San Nicolas Island, CA: Renewable Community Plan Outline, Baseline Development, and Initial Renewable Assessment*. National Renewable Energy Laboratory.
- Karimi, Elham, and Mehrdad Kaserani. 2017. “Impact of Renewable Energy Deployment in Canada’s Remote Communities on Diesel Generation Carbon Footprint Reduction.” *In Proceedings of the 30th Canadian Conference on Electrical and Computer Engineering (CCECE)*: 1–5. <https://doi.org/10.1109/CCECE.2017.7946740>.
- Katsigiannis, Yiannis, Pavlos Georgilakis, and Emmanuel Karapidakis. 2012. “Hybrid Simulated Annealing–Tabu Search Method for Optimal Sizing of Autonomous Power Systems with Renewables.” *IEEE Transactions on Sustainable Energy* 3 (3) (July): 330–338. <https://doi.org/10.1109/TSTE.2012.2184840>.
- Kaur, Rajvir, Vijayakumar Krishnasamy, and Nandha Kandasamy. 2018. “Optimal Sizing of Wind–PV-based DC microgrid for Telecom Power Supply in Remote Areas.” *IET Renewable Power Generation* 12 (7) (May): 859–866. [10.1049/iet-rpg.2017.0480](https://doi.org/10.1049/iet-rpg.2017.0480).

- Keogh, Miles, and Christina Cody. 2013. *Resilience in Regulated Utilities*.
<https://pubs.naruc.org/pub/536F07E4-2354-D714-5153-7A80198A436D>.
- Kim, Sung Woo. 2015. “Clean Energy + Technology = Resilient Energy Infrastructure.” *Engineering the Next 100 years*. April 7, 2015. <https://www.devex.com/news/clean-energy-technologyresilient-energy-infrastructure-85860>.
- Kobold, Kyle. 2017. “Modeling and Optimizing Green Microgrids at Remote U.S. Navy Islands.” Master’s thesis, Naval Postgraduate School. Monterey, California.
<https://apps.dtic.mil/dtic/tr/fulltext/u2/1053336.pdf>.
- Konschnik, Kate, and Brian Murray. 2018. “FERC’s Resilience Order May Suggest Reliability Tweaks, Rather Than Novel Solutions.” *Utility Dive*. February 2, 2018.
<https://www.utilitydive.com/news/fercs-resilience-order-may-suggest-reliability-tweaks-rather-than-novel-s/515944/>.
- Korjani, Saman, Mario Porru, Allesandro Serpi, and Alfonso Damiano. 2016. “A Genetic Algorithm for the Definition of Nodal Load Time Evolutions in Micro Grids Assessment.” *In Proceedings of the 5th ICRERA*: 633–638. <https://doi.org/10.1109/ICRERA.2016.7884412>.
- Kremers, Enrique. 2013. “Modelling and Simulation of Electrical Energy Systems Through a Complex Systems Approach using Agent-Based Models.” PhD diss., Universidad del País Vasco. https://www.researchgate.net/publication/259739043_Modelling_and_Simulation_of_Electrical_Energy_Systems_through_a_Complex_Systems_Approach_using_Agent-Based_Models/citation/download.
- Labaka, Leire, Josune Hernantes, and Jose Sarriegi. 2015. “Resilience Framework for Critical Infrastructures: An Empirical Study in a Nuclear Plant.” *Reliability Engineering & System Safety* 141 (September): 92–105. <https://doi.org/10.1016/j.res.2015.03.009>.
- Lawton, Leora, Michael Sullivan, Kent Van Liere, Aaron Katz, and Joseph Eto. 2003. *A Framework and Review of Customer Outage Costs: Integration and Analysis of Electric Utility Outage Cost Surveys*. Technical Report LBNL 54365.
<https://emp.lbl.gov/sites/all/files/lbnl-54365.pdf>.
- Lazard. 2017. *Lazard’s Levelized Cost of Energy Analysis*. Version 11.0.
<https://www.lazard.com/media/450337/lazard-levelized-cost-of-energy-version-110.pdf>.
- Leonardo Martinez-Diaz. 2018. “Investing in Resilience Today to Prepare for Tomorrow’s Climate Change.” *Bulletin of the Atomic Scientists* 74 (2) (February): 66–72. <https://doi.org/10.1080/00963402.2018.1436805>.

- Li, Kaiyuan, and King Jet Tseng. 2015. "Energy Efficiency of Lithium-ion Battery Used as Energy Storage Devices in Micro-grid." *In Proceedings of the IECON2015 41st Annual Conference of the IEEE Industrial Electronics Society*: 5235–5240. <https://ieeexplore-ieee-org.libproxy.nps.edu/stamp/stamp.jsp?tp=&arnumber=7392923>.
- Li, Zhiyi, Mohammad Shahidehpour, Farrokh Aminifar, and Yusuf Al-Turki. "Networked Microgrids for Enhancing the Power System Resilience." 2017. *In Proceedings of the IEEE* 105(7): 1289–1310. <https://doi.org/10.1109/JPROC.2017.2685558>.
- Liu, Jianzhe, Xiaonon Lu, and Jianhui Wang. 2019. "Resilience Analysis of DC Microgrids under Denial of Service Threats." *IEEE Transactions on Power Systems* 34 (4) (July): 3199–3208. <https://ieeexplore.ieee.org/document/8633969>.
- Liu, Marco. 2020. *Optimal Number of Trials for Monte Carlo Simulation*. ValuationResearch.com. https://www.valuationresearch.com/wp-content/uploads/kb/SpecialReport_MonteCarloSimulationTrials.pdf.
- Lloret-Gallego, Pau; Mònica Aragües-Peñalba, Lien VanSchepdael, Eduard Bullich-Massague, and Pol Olivella-Rosell. 2017. "Methodology for the Evaluation of Resilience of ICT Systems for Smart Distribution Grids." *Energies* 10 (9) (August): 1287. <https://doi.org/10.3390/en10091287>.
- Lotfi, Hossein, and Amin Khodaei. 2016. "Levelized Cost of Energy Calculations for Microgrids." *In Proceedings of the 2016 IEEE Power and Energy Society General Meeting (PESGM)*: 1–5. <https://doi.org/10.1109/PESGM.2016.7741379>.
- Madni, Azad, and Scott Jackson, 2009. "Towards a Conceptual Framework for Resilience Engineering." *IEEE Systems Journal* 3(2) (June): 181–191. [10.1109/JSYST.2009.2017397](https://doi.org/10.1109/JSYST.2009.2017397).
- Mandelli, Stefano, Jacopi Barbieri, Riccardo Mereu, and Emanuela Colombo. 2016. "Off-Grid Systems for Rural Electrification in Developing Countries: Definitions, Classification and a Comprehensive Literature Review." *Renewable and Sustainable Energy Reviews* 58 (May): 1621–46. <https://www.sciencedirect.com/science/article/abs/pii/S1364032115017219>.
- Markovic, Mark, Zorica Nedic, and Andrew Nafalski. 2016. "Comparison of Microgrid Solutions for Remote Areas." *In Proceedings of the 2016 IEEE Electrical Power and Energy Conference (EPEC)*: 1–5. [10.1109/EPEC.2016.7771680](https://doi.org/10.1109/EPEC.2016.7771680).
- Mathew, Rohit, Ashok S., and Kumaravel S. 2016. "Resilience Assessment Using Microgrids in Radial Distribution Network." *In Proceedings of the 7th Power India International Conference (PIICON:)* 1–4. <https://doi.org/10.1109/POWERI.2016.8077250>.

- Mathiesen, Brian, Kenneth Hansen, Iva Ridhebn, Henrik Lund, and Steffen Nielsen. 2015. "Samsø Energy Vision 2030." https://vbn.aau.dk/ws/portalfiles/portal/220291121/Sams_report_20151012.pdf.
- Mishra, Sakshi, Kate Anderson, Brian Miller, and Kyle Boyer. 2020. "Microgrid Resilience: A Holistic Approach for Assessing Threats, Identifying Vulnerabilities, and Designing Corresponding Mitigation Strategies." *Applied Energy*: 264(April). <https://doi.org/10.1016/j.apenergy.2020.114726>.
- Mittal, Saurabh, Mark Ruth, Annabelle Pratt, Monte Lunacek, Dheepak Krishnamurthy, and Wesley Jones. 2015. "A System-of-Systems Approach for Integrated Energy Systems Modeling and Simulation." *In Proceedings of the Society of Computer Simulation International Conference*: 1–10. <https://dl.acm.org/doi/abs/10.5555/2874916.2874975>.
- Mizani, Shervin, and Amirnaser Yazdani. 2009. "Design and Operation of a Remote Microgrid." *In Proceedings of the 35th Annual Conference of IEEE Industrial Electronics*: 4299–4304. [10.1109/IECON.2009.5414925](https://doi.org/10.1109/IECON.2009.5414925).
- Mohamed, Mohamed, and Wencong Su. 2019. "Proactive Resilience of Power Systems Against Natural Disasters: A Literature Review." *IEEE Access* 7 (November): 163778–163795. <https://ieeexplore.ieee.org/stamp/stamp.jsp?arnumber=8894433>.
- Mongird, K., V. Viswanathan, P. Balducci, J. Alam, V. Fotedar, V. Koritarov, and B. Hadjerioua. 2019. *Energy Storage Technology and Cost Characterization Report*. PNNL-28866. https://www.energy.gov/sites/prod/files/2019/07/f65/Storage%20Cost%20and%20Performance%20Characterization%20Report_Final.pdf.
- Muller, George. 2012. "Fuzzy Architecture Assessment for Critical Infrastructure Resilience." *Procedia Computer Science* 12 (November): 367–372. <https://doi.org/10.1016/j.procs.2012.09.086>
- Munoz, Albert, and Michelle Dunbar. 2015. "On the Quantification of Operational Supply Chain Resilience." *International Journal of Production Research* 53 (22) (November): 6736–6751. <https://doi.org/10.1080/00207543.2015.1057296>.
- Nadimi, Ashkan, and Farid Adabi. 2016. "Optimized Planning for Hybrid Microgrid in Grid-Connected Mode." *IJRER* 6 (2) (April): 494–503. <https://www.ijrer.org/ijrer/index.php/ijrer/article/view/3586>.
- Narayanan, Anu, and Debra Knopman, Kristin Van Abel, Benjamin Miller, Nicholas Burger, Martha V. Merrill, Alexander D. Rothenberg, Luke Muggy, and Patrick Mills. 2019. *Valuing Air Force Electric Power Resilience: A Framework for Mission-Level Investment Prioritization*. RR2771. https://www.rand.org/pubs/research_reports/RR2771.html.

- National Infrastructure Advisory Council. 2009. *Critical Infrastructure Resilience Final Report and Recommendations*. Report No. 59972.000117 EMF_US 28318682v2 <https://www.cisa.gov/sites/default/files/publications/niac-critical-infrastructure-resilience-final-report-09-08-09-508.pdf>.
- National Renewable Energy Laboratory. 2019a. *Increasing Energy Resilience at Tyndall Air Force Base*. Report No. NREL/FS-7A40-74847. <https://www.nrel.gov/docs/fy20osti/74847.pdf>.
- National Renewable Energy Laboratory. 2019b. *Valuing Resilience in Electricity Systems*. Report No. NREL/FS-7A40-74673. <https://www.nrel.gov/docs/fy19osti/74673.pdf>.
- National Solar Radiation Database Data Viewer (accessed August 3, 2017). maps.nrel.gov/nsrdb-viewer/?aL=8VWYIh%255Bv%255D%3Dt%268VWYIh%255Bd%255D%3D1&bL=groad&cE=0&lR=0&mC=31.98944183792288%2C-105.99609375&zL=4.
- Nejabatkhah, Farzam, Yun Lei, Alexandre Nassif, and Taeho Kang. 2018. “Optimal Design and Operation of a Remote Hybrid Microgrid.” *CPSS Transactions on Power Electronics and Applications* 3 (1) (March):3–13. <https://doi.org/10.24295/CPSSSTPEA.2018.00001>.
- Nicolas, Claire, Jun Rentschler, Albertine Potter van Loon, Sam Oguah, Amy Schweikert, Mark Deinert, Elco Koks, Christopher Arderne, Diana Cubas, Jie Li, and Eriko Ichikawa. 2019. *Stronger Power: Improving Power Sector Resilience to Natural Hazards*. LIFELINES: The Resilient Infrastructure Opportunity, World Bank, Washington, DC. <http://documents.worldbank.org/curated/en/200771560790885170/pdf/Stronger-Power-Improving-Power-Sector-Resilience-to-Natural-Hazards.pdf>.
- Ojala, Dan, and Steve Drouilhet. 2016. *Dynamic Stability Modeling of the San Nicolas Island Power System*. Rev 3. Boulder, CO: Sustainable Power Systems.
- Olsen, Timothy, and Ed McKenna. 1996. *Hybrid Energy System Cost Analysis: San Nicolas Island, California*. Report No. NREL/TP-440-21120. Golden, CO: National Renewable Energy Laboratory.
- Orwin, Kate, and David Wardle. 2004. “New Indices for Quantifying the Resistances and Resilience of Soil Biota to Exogenous Disturbances.” *Soil Biology and Biochemistry* 36 (11) (November): 1907–12. <https://www.sciencedirect.com/science/article/abs/pii/S0038071704001658>.
- Ouyang, Min, Leonardo Duenas-Osorio, and Xing Min. 2012. “A Three-Stage Resilience Analysis Framework for Urban Infrastructure Systems.” *Structural Safety* 36–37 (May-July): 23–31. <https://www.sciencedirect.com/science/article/abs/pii/S0167473011000956>.

- Overbye, Thomas, Vijay Vittal, and Ian Dobson. 2012. "Engineering Resilient Cyber-Physical Systems." *In Proceedings of the IEEE Power and Energy Society General Meeting*: 1. <https://doi.org/10.1109/PESGM.2012.6344943>.
- Oviroh, Peter, and Tien-Chien Jen. 2018. "The Energy Cost Analysis of Hybrid Systems and Diesel Generators in Powering Selected Base Transceiver Station Locations in Nigeria." *Energies* 11: 687. <https://www.mdpi.com/1996-1073/11/3/687>.
- Paasch, Kasper. 2016. "Power Electronic System for Multi-MW PV Sites." PhD diss., University of Southern Denmark. https://www.researchgate.net/publication/303909878_Power_Electronic_System_for_Multi-MW_PV_Sites_PhD-thesis.
- Panteli, Mathaios, and Pierluigi Mancarella. 2015. "Influence of Extreme Weather and Climate Change on the Resilience of Power Systems: Impacts and Possible Mitigation Strategies." *Electric Power Systems Research* 127: 259–70. https://www.researchgate.net/publication/279313514_10.
- Panteli, Mathaios, Dimitris Trakas, Pierluigi Mancarella, and Nikos Hatziagyriou. 2017a. "Power Systems Resilience Assessment: Hardening and Smart Operational Enhancement Strategies." *In Proceedings of the IEEE* 105, no. 7 (July): 1202–13. <https://ieeexplore.ieee.org/document/7922545>.
- Panteli, Mathaios, Cassandra Pickering, Sean Wilkinson, Richard Dawson, and Pierluigi Mancarella. 2017b. "Power System Resilience to Extreme Weather: Fragility Modeling, Probabilistic Impact Assessment, and Adaptation Measures." *IEEE Transactions on Power Systems*. 32 (5) (September): 3747–3757. <https://doi.org/10.1109/TPWRS.2016.2641463>.
- Patel, Sandip, and Jigish Zaveri. 2010. "A Risk-Assessment Model for Cyber Attacks on Information Systems." *Journal of Computers* 5 (3) (March). <https://pdfs.semanticscholar.org/8a41/a48819b6ecf62424bb4d6041a8a31a630cfe.pdf>.
- Patterson, Emily, David Woods, Emile Roth, Richard Cook, Robert Wears RL, and Marta Render. 2006. "Three Key Levers for Achieving Resilience in Medication Delivery with Information Technology." *Journal of Patient Safety* 2 (1) (March): 33–8. <https://pdfs.semanticscholar.org/f09e/0d9600464182e291d2a538bef2d0d9227f37.pdf>.
- Perdue, Michael, and Ralph Gottschalg. 2015. "Energy Yields of Small Grid Connected Photovoltaic System: Effects of Component Reliability and Maintenance." *IET Renewable Power Generation* 9 (5): 432–437. <https://core.ac.uk/download/pdf/288375782.pdf>.
- Peterson, Chris. 2019. "Systems Architecture Design and Validation Methods for Microgrid Systems." Master's thesis, Naval Postgraduate School. <https://calhoun.nps.edu/handle/10945/63493>.

- Pettit, Timothy, Joseph Fiksel, and Keely Croxton. 2010. "Ensuring Supply Chain Resilience: Development of a Conceptual Framework." *Journal of Business Logistics* 31 (1):1–21. https://www.researchgate.net/publication/229897011_Ensuring_Supply_Chain_Resilience_Development_of_a_Conceptual_Framework.
- Pfaffel, Sebastian, Stefan Falstich, and Kurt Rohrig. 2017. "Performance and Reliability of Wind Turbines: A Review." *Energies*. <https://doi.org/10.3390/en10111904>.
- Phattanasak, Matheepot. 2015. "Switching Command Based on Lyapunov Function for a Boost Converter with an LC Input Filter in DC Microgrid Application." In *Proceedings of the International Conference on Renewable Energy Research and Applications (ICRERA)*: 1296–1300. <https://doi.org/10.1109/ICRERA.2015.7418617>.
- Okinawa Electric Power Company. 2012. "Renewable Energy Integration to Remote Islands – Miyako Island." Presentation May 26, 2012. https://www.irena.org/-/media/Files/IRENA/Agency/Articles/2012/May/11_Shinji-Uehara_Okiden.pdf?la=en&hash=EC4BCD1FC217E99A7C29BB5BBBCBB5EEB441C61A.
- Renewable Energy Research Laboratory, University of Massachusetts. n.d. *Community Wind Power Fact Sheet #2a*. Amherst, MA.
- Renschler, Chris, Amy Fraizer, Lucy Arendt, Gian-Paolo Cimellaro, Andrei Reinhorn, and Michel Bruneau. 2010. *A Framework for Defining and Measuring Resilience at the Community Scale: The PEOPLES Resilience Framework*. NIST GCR 10–930. Gaithersburg, MD: National Institute of Standards and Technology. <https://www.researchgate.net/publication/284507306>.
- Resilience Engineering Institute. 2017. "Resilience Library." Accessed August 6, 2019. <http://resilienceengineeringinstitute.org/resilience-library/>.
- Rimatrix5. 2020. *Reliability of Uninterruptable Power Supplies PMC*. NW/MTBF Calculus-VX-190903. <https://pdfs.semanticscholar.org/9daf/bbff888d23d90d20b2c485b99fbf98bc5ef6.pdf>.
- Rose, Adam. 2007. "Economic Resilience to Natural and Man-Made Disasters: Multidisciplinary Origins and Contextual Dimensions." *Environmental Hazards* 7 (4): 383–98. <https://www.sciencedirect.com/science/article/abs/pii/S1747789107000555>.
- Rose, Stephen, Paulina Jaramillo, Mitchell Small, Iris Grossman, and Jay Apt. 2012. "Quantifying the Hurricane Risk to Offshore Wind Turbines." In *Proceedings of the National Academy of Sciences of the United States of America* 109, no. 9: 3247–3252. <https://www.pnas.org/content/pnas/109/9/3247.full.pdf>.

- Ross, Michael. 2018. "Modeling and Control of a Microgrid Using a Hybrid Energy Storage System with Supercapacitors." Master's thesis, Naval Postgraduate School. <https://apps.dtic.mil/sti/citations/AD1060044>.
- Roth, John. 2017. "Fiscal Year (FY) 2018 Fuel Price Change." Official Memorandum. Washington, DC: Department of Defense.
- Rozenblat, Lazar. n.d. *Your Guide to Renewable Energy*. <http://www.renewable-energysources.com>.
- San Nicolas Island, CA. (accessed July 19, 2017). www.wunderground.com/history/airport/KNSI/2017/1/1/CustomHistory.html?dayend=19&monthend=7&yearend=2017&req_city=&req_state=&req_statename=&reqdb.zip=&reqdb.magic=&reqdb.wmo=.
- Sawle, Yashwant, Shivcharan Gupta, and Aashish Bohre. 2018. "Review of Hybrid Renewable Energy Systems with Comparative Analysis of Off-Grid Hybrid System." *Renewable and Sustainable Energy Reviews* 81 (2) (January): 2217–35. <https://www.sciencedirect.com/science/article/abs/pii/S1364032117309735>.
- Scioletti, Michael, Alexandra Newman, Johanna Goodman, Alexander Zolan, and Sven Leyffer. 2017. "Optimal Design and Dispatch of a System of Diesel Generators, Photovoltaics and Batteries for Remote Locations." *Optimization and Engineering* 18 (May): 755–792. <https://www.osti.gov/pages/biblio/1393847>.
- Sepanski, Annet, Florian Reil, Willi Vaaßen, Eckart Janknecht, Uwe Hupach, Nicolas Bogdanski, Bettina van Heeckeren et al. 2018. *Assessing Fire Risks in Photovoltaic Systems and Developing Safety Concepts for Risk Minimization*. https://www.energy.gov/sites/prod/files/2018/10/f56/PV%20Fire%20Safety%20Fire%20Guideline_Translation_V04%2020180614_FINAL.pdf.
- Shirali, Gholam, Majid Motamedzade, Iraj Mohammadfam, Vahid Ebrahimipour, and Abbas Moghimbeigi. 2012a. "Challenges in Building Resilience Engineering (RE) and Adaptive Capacity: A Field Study in a Chemical Plant." *Process Safety and Environmental Protection* 90 (2) (March):83–90. <https://www.sciencedirect.com/science/article/pii/S0957582011000784>.
- Shirali, Gholam, Iraj Mohammadfam, Majid Motamedzade, Vahid Ebrahimipour, and Abbas Moghimbeigi. 2012b. "Assessing Resilience Engineering Based on Safety Culture and Managerial Factors." *Process Safety Progress* 30 (September) (1):17–8. <https://aiche.onlinelibrary.wiley.com/doi/full/10.1002/prs.10485>.

- Shirali, Gholam, Iraj Mohammadfam, and Vahid Ebrahimpour. 2013. "A New Method for Quantitative Assessment of Resilience Engineering by PCA and NT Approach: a Case Study in a Process Industry." *Reliability Engineering & System Safety* 119 (November): 88–94. <https://www.sciencedirect.com/science/article/abs/pii/S0951832013001282>.
- Shortridge, Julie, Terje Aven, and Seth Guikema. 2017. "Risk Assessment Under Deep Uncertainty: A Methodological Comparison." *Reliability Engineering & System Safety* 159 (March): 12–23. <http://dx.doi.org/10.1016/j.res.2016.10.017>.
- Singh, Ranjeeta, Andrew Nafalski, Ozdemir Gol, and Zorica Nedic. 2015. "Enhancement of an Insular Power System in the Outback of South Australia." *In Proceedings of the TENCON 2015 IEEE Region 10 Conference* 1–3. <https://doi.org/10.1109/TENCON.2015.7372874>.
- Sinha, Sundada, and S. Chandel. 2014. "Review of Software Tools for Hybrid Renewable Energy Systems." *Renewable Sustainable Energy Reviews* 32 (April): 192–205. <https://www.sciencedirect.com/science/article/abs/pii/S136403211400046X>.
- Smith, Colin. 2014. "Fires are Major Cause of Wind Farm Failure, According to New Research." *Imperial College of London News*. July 17, 2014. <https://www.imperial.ac.uk/news/153886/fires-major-cause-wind-farm-failure/>.
- Smith, Kandler, Aron Saxon, Matthew Keyser, Blake Lundstrom, Ziwei Cao, and Albert Roc. 2017. "Life Prediction Model for Grid-Connected Li-ion Battery Energy Storage System." *In Proceedings of the American Control Conference* 4062–4068. <https://doi.org/10.23919/ACC.2017.7963578>.
- Spear, Stefanie. 2014. "Samsø: World's First 100% Renewable Energy-Powered Island is a Beacon for Sustainable Communities." *EcoWatch*. May 1, 2014. www.ecowatch.com/Samsø-worlds-first-100-renewable-energy-powered-island-is-a-beacon-for-1881905310.html.
- Sterbenz, James, Egemen Cetinkaya, Mahmood Hameed, Abdul Jabbar, and Justin Rohrer. 2011. "Modeling and Analysis of Network Resilience." *In Proceedings of the IEEE COMSNETS*, 978–987. https://www.researchgate.net/publication/220990821_Modelling_and_analysis_of_network_resilience.
- Sullivan, James. 2018. "Command Brief – PWD." Presentation at Naval Station Rota, Spain.
- Swathika, Gnana, and S. Hemamalini. 2016. "Review on Microgrid and its Protection," *IJRER* 6 (4) (June). <https://www.ijrer.com/index.php/ijrer/article/view/4353/pdf>.
- Teague, Brendan, T Goss, and Mark Weiss. 2015. *Applying Risk and Resilience Metrics to Energy Investments*. An MBA Professional Report. Monterey, CA: Naval Postgraduate School.

- Terrapon-Pfaff, Julia, Carmen Dienst, Julian König, and Willington Ortiz. 2014. “A Cross-Sectional Review: Impacts and Sustainability of Small-Scale Renewable Energy Projects in Developing Countries.” *Renewable Sustainable Energy Reviews* 40 (December): 1–10. <https://www.sciencedirect.com/science/article/pii/S1364032114006133>.
- “The Isle of Eigg.” n.d. Eigg Electric Limited. Accessed June 17, 2019. www.isleofeigg.org/eigg-electric/.
- The United Nations International Strategy for Disaster Reduction. *Hyogo Framework for Action 2005–2015: Building the Resilience of Nations and Communities to Disasters* 380. https://www.unisdr.org/files/1037_hyogoframeworkforactionenglish.pdf.
- Thomsen, Jan, Raymond Levitt, John Kunz, Clifford Nass, and Douglas B. Fridsma. 1999. “A Trajectory for Validating Computational Emulation Models of Organizations.” *Computational & Mathematical Organization Theory* 5 (4) (December): 385–401.
- Thompson, C., D. Gao, and P. Hale. 2018. An Evaluation of HVAC Failure and Maintenance Equipment Data for Facility Resiliency and Reliability. 124 (2). <https://go.gale.com/ps/anonymou?id=GALE%7CA559357532&sid=googleScholar&v=2.1&it=r&linkaccess=abs&issn=00012505&p=AONE&sw=w>.
- Ton, Dan, and W-T. Paul Wang. 2015. “A More Resilient Grid.” *IEEE Power and Energy Magazine*. May/June 2015. <https://doi.org/10.1109/MPE.2015.2397337>.
- Ton, Dan, and Merrill Smith. 2012. “The U.S. Department of Energy’s Microgrid Initiative.” *The Electricity Journal*, 25 (October): 84–94. <https://www.energy.gov/sites/prod/files/2016/06/f32/The%20US%20Department%20of%20Energy%27s%20Microgrid%20Initiative.pdf>.
- Trout, Jonathan. 2020. “MTTR Explained.” *RELIABLEPLANT*. <https://www.reliableplant.com/mttr-31713>.
- Tucker, Samuel, and Michael Negnevitsky. 2011. “Renewable Energy Micro-Grid Power System for Isolated Communities.” *In Proceedings of the 21st Australasian Universities Power Engineering Conference* 1–7. <https://ieeexplore.ieee.org/document/6102550>.
- Uday, Payuna, and Karen Marais. 2015. “Designing Resilient Systems-of-Systems: A Survey of Metrics, Methods, and Challenges.” *Systems Engineering* 18 (5) (November): 491–510. <https://doi.org/10.1002/sys.21325>
- Sustainable Power Systems. n.d. “Universal Microgrid Controller.” Accessed May 17, 2019. <http://www.sustainablepowersystems.com/wp-content/uploads/2016/07/UMC-Specifications-Rev-0.pdf>.

- U.K. Cabinet Office. 2011. *Keeping the Country Running: Natural Hazards and Infrastructure*. London, UK: https://assets.publishing.service.gov.uk/government/uploads/system/uploads/attachment_data/file/61342/natural-hazards-infrastructure.pdf.
- U. S. Energy Information Administration. n.d. Accessed July 18, 2017. <https://eia.gov>.
- Vlacheas, Panagiotis, Vera Stavroulaki, Panagiotis Demestichas, Scott Cadzow, Demosthenes Ikonomou, and Slawomir Gorniak. 2013. "Towards End-to-End Network Resilience." *International Journal of Critical Infrastructure Protection* 6 (3 and 4) (December): 159–78. <https://www.sciencedirect.com/science/article/pii/S1874548213000449>.
- Vugrin, Eric, Drake Warren, Mark Ehlen, and Chris Camphouse. 2010. "A Framework for Assessing the Resilience of Infrastructure and Economic Systems." In *Sustainable and Resilient Critical Infrastructure Systems*. 77–116. Berlin, Germany: Springer. https://link.springer.com/chapter/10.1007/978-3-642-11405-2_3.
- Vugrin, Eric, Drake Warren, and Mark Ehlen. 2011. "A Resilience Assessment Framework for Infrastructure and Economic Systems: Quantitative and Qualitative Resilience Analysis of Petrochemical Supply Chains to a Hurricane." *Process Safety Progress* 30 (3) (March), 280–90. <https://aiche.onlinelibrary.wiley.com/doi/pdf/10.1002/prs.10437>.
- Vugrin, Eric, Mark Turnquist, and Nathaniel Brown. 2014. "Optimal Recovery Sequencing for Enhanced Resilience Service Restoration in Transportation Networks." *International Journal of Critical Infrastructure* 10 (3/4): 218–246. https://www.sandia.gov/CasosEngineering/_assets/documents/Recovery_Optimization_2013_4852J.pdf.
- Vugrin, Eric, Anya Castillo, and Cesar Silva-Monroy. 2017. *Resilience Metrics for the Electric Power System: A Performance-Based Approach*. Sandia National Laboratories.
- Walsh, Connor. 2014. "Microgrid Regulatory Policy in the U.S." *CivicSolar*. December 2014. <https://www.civicsolar.com/article/microgrid-regulatory-policy-us>.
- Wang, Cao, Hao Zhang, Kairu Feng, and Quanwang Li. 2017. "Assessing Hurricane Damage Costs in the Presence of Vulnerability and Model Uncertainty." *Natural Hazards* 85 (3) (February): 1621–35. https://ideas.repec.org/a/spr/nathaz/v85y2017i3d10.1007_s11069-016-2651-z.html.

- Wang, Yezhou, Chen Chen, Jianhui Wang, and R. Baldick. 2015. "Research on Resilience of Power Systems Under Natural Disasters—A Review." *IEEE Transactions on Power Systems* 31 (2) (May): 1604–13. https://www.researchgate.net/publication/276466423_Research_on_Resilience_of_Power_Systems_Under_Natural_Disasters-A_Review.
- Wang, Yifei, Liping Huang, Lo Lei Lai, and Ya Zhou. 2020. "Impact of Cascading and Common-Cause Outages on Resilience-Constrained Optimal Economic Operation of Power Systems." *IEEE Transactions on Smart Grid* 11 (1) (January): 590–601. <https://ieeexplore-ieee-org.libproxy.nps.edu/stamp/stamp.jsp?tp=&arnumber=8752426>.
- Wattjes, F., and J. Slootweg. 2013. "Design considerations for smart microgrids." In *Proceedings of the 48th International Universities' Power Engineering Conference (UPEC)* 1–6. doi: 10.1109/UPEC.2013.6714879.
- Wen, Huiqing, and Huan Yu. 2016. "Modeling and Analysis of Coordinated Control Strategies in AC Microgrid." In *Proceedings of the 5th International Conference on Renewable Energy Research and Applications (ICRERA)*, 702–707. <https://doi.org/10.1109/ICRERA.2016.7884424>.
- Wheeler, Kaitlyn. 2017. "Efficient Operation of Diesel Generator Sets in Remote Environments." Master's thesis, Virginia Polytechnic Institute and State University. https://vtechworks.lib.vt.edu/bitstream/handle/10919/78374/Wheeler_KR_T_2017.pdf?sequence=1.
- Willis, Henry, and Kathleen Loa. 2015. *Measuring the Resilience of Energy Distribution Systems*. RAND Corporation. Accessed December 8, 2019. <https://www.jstor.org/stable/10.7249/j.ctt19w72pw.6>.
- Won, Jongnam, Wookyu Chae, Hakju Lee, Jungsung Park, Junbo Sim, and Changhoon Shin. 2017. "Demonstration of Remote Microgrid System in Korean Island." *CIRE Open Access Proceedings Journal* 2017 (1) (October): 2212–2214. <https://doi.org/10.1049/oap-cired.2017.0683>.
- World Weather and Climate Information. Accessed June 1, 2018. <https://weather-and-climate.com>.
- Yodo, Nita, and Pingfeng Wang. 2016. "Engineering Resilience Quantification and System Design Implications: A Literature Survey." *Journal of Mechanical Design* 138 (November). <https://asmedigitalcollection.asme.org/mechanicaldesign>.
- Youn, Byeng, Chao Hu, and Pingfeng Wang. 2011. "Resilience-Driven System Design of Complex Engineered Systems." *Journal of Mechanical Design* 133 (10) (October). <https://asmedigitalcollection.asme.org/mechanicaldesign/article-abstract/133/10/101011/467326/Resilience-Driven-System-Design-of-Complex?redirectedFrom=fulltext>.

- Zhao, Jie, Tian Liu, Yu Zhao, Dichen Liu, Xiaodong Yang, Yi Lin, Zhangsui Lin et al. 2016. "Reliability Evaluation of NPP's Power Supply System Based on Improved GO-FLOW Method." *Science and Technology of Nuclear Installations* (September): 1–10. <http://dx.doi.org/10.1155/2016/1245387>.
- Zobel, Christopher. 2011. "Representing Perceived Tradeoffs in Defining Disaster Resilience." *Decision Support Systems* 50 (2) (January): 394–403. <https://www.sciencedirect.com/science/article/pii/S0167923610001764>.
- Zobel, Christopher, and Lara Khansa. 2014. "Characterizing Multi-Event Disaster Resilience." *Computers & Operations Research* 42 (February): 83–94. <https://doi.org/10.1016/j.cor.2011.09.024>.

INITIAL DISTRIBUTION LIST

1. Defense Technical Information Center
Ft. Belvoir, Virginia
2. Dudley Knox Library
Naval Postgraduate School
Monterey, California